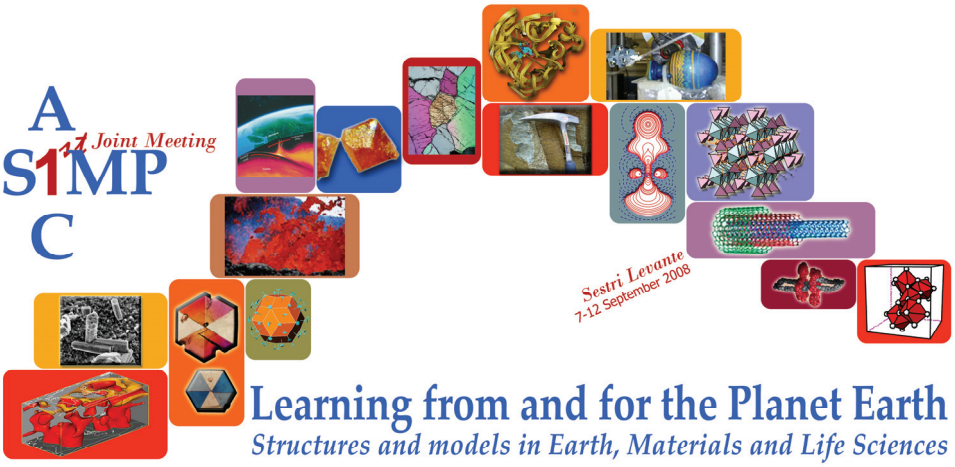

Learning from and for the Planet Earth

Structures and models in Earth, Materials and Life Sciences

under the patronage

pianetaterra®
Le Scienze della Terra per la Società
Commissione Italiana

website: http://simp.dst.unipi.it/SIMP-AIC2008

Welcome

On behalf of the Councils of the Società Italiana di Mineralogia e Petrologia and the Associazione Italiana di Cristallografia, we are pleased to welcome all participants to the first joint meeting of the two societies.

This joint meeting aims at tightening the relationships among the petrological, mineralogical and crystallographic communities, showing new points of contact and stimulating further synergies. Following the spirit of the International Year for the Planet Earth, we have decided to put particular emphasis on the still unexploited contributions that an atomistic perspective may give to the study of geo-materials, in particular to what concerns both their stability and systematics and their role in natural and anthropogenic processes, with a special focus on the interactions between the geo- and the bio-sphere. As a consequence, we have tried to involve Italian and foreign scientists from many allied disciplines, such as Cultural Heritage, Physics, Organic and Inorganic Chemistry, Biochemistry, Biomimetic Materials and Materials Sciences.

The rationale of the meeting is a journey from the inner of the planet Earth towards its surface, starting from the present knowledge of mantle processes, focusing on reaction surfaces in minerals and in geo- and nano-materials and ending with the characterization, synthesis and engineering of materials relevant for Earth, Materials and Life Sciences. Various scientific sessions summarize the state of the art of the researches in mineralogy, petrology and crystallography, and highlight recent improvements in our knowledge of the planet Earth and in the mastering of structure-properties relationships for a sustainable progress in environmental and technological issues. The central day of the meeting is focused on the core issue of the relations between surface properties, stability and reactivity.

A lot of people contributed to the success of this scientific project. First of all, we want to thank the many outstanding scientists from different countries and disciplines who have accepted to give plenary talks. We are sure that they will provide an interesting and stimulating melting pot for future research. We gratefully acknowledge the many ideas and continuous efforts provided by all the colleagues and friends of the Scientific and Organizing Committees, as well as of the Congress Secretariat. Finally, we express our gratitude to all the institutions and companies who financially supported the meeting.

To all contributing authors and participants, we warmly wish a fruitful and pleasant staying in Sestri Levante.

Simona Quartieri	Roberta Oberti	Gabriella Lucchetti
SIMP President	AIC President	Chair of the Meeting Committees

Sestri Levante, September 2008

Organizing Committee

President
Gabriella Lucchetti

Secretariat
Pietro Marescotti (Secretary for SIMP)
Michele Zema (Secretary for AIC)

Elena Bonaccorsi
Roberto Cabella
Fernando Cámara
Doretta Capsoni
Maria Luisa Fornasini
Laura Gaggero
Roberta Oberti
Marcella Pani
Simona Quartieri
Elisabetta Rampone
Livio Zefiro

Scientific Committees

SIMP

Simona Quartieri
Roberta Oberti,
Riccardo Basso
Pierfranco Lattanzi
Gabriella Lucchetti
Isa Memmi
Giovanni B. Piccardo

AIC

Roberta Oberti
Simona Quartieri
Dino Aquilano
Adriana Bigi
Vincenzo Massarotti
Lucio Randaccio
Menico Rizzi
Roberto Zamboni

Sponsoring and Supporting Institutions

Università degli Studi di Genova
Facoltà di Scienze M.F.N.

Dip.Te.Ris.
Dipartimento per lo Studio del Territorio e delle sue Risorse dell'Università di Genova

Dipartimento di Chimica e Chimica Industriale dell'Università di Genova

CNR - Istituto di Geoscienze e Georisorse

European Crystallographic Association
Special Interest Group #5

Università degli Studi di Parma

Provincia di Genova

Fondazione Mediaterraneo
Sestri Levante (GE)

Sponsors and exhibitors

Ente Parco Naturale Regionale dell'Aveto

Ente Parco Naturale Regionale del Beigua

Internet Point provided by:

Raffo Linea Ufficio s.n.c. - Apple Premium Reseller

Meeting Programme

Sunday, 7th September
Pre-congress field trip

Monday, 8th September
PETROLOGIC PROCESSES AND GEODYNAMICS

10.00 – 10.30 **86° SIMP Meeting opening ceremony**

Plenary Session 1. Mantle processes and geodynamics
Convenors: Giovanni B. Piccardo and Angelo Peccerillo

10.30 – 11.20 PL **Martin Menzies** (Dept. Earth Sciences, Royal Holloway, London)
Earth's lithosphere in 3D and 4D

11.20 – 11.50 KN **Giovanni B. Piccardo** (DipTeRiS, Genova)
Lithosphere/asthenosphere interaction at extensional settings: constraints to geodynamics

11.50 – 12.20 KN **Giacomo Corti** (IGG-CNR, Firenze)
Modelling extension of the continental lithosphere: rheological modifications in the mantle lithosphere and geodynamical effects

12.20 – 12.50 KN **Massimo Coltorti** (Dip. Scienze della Terra, Ferrara)
Metasomatism in mantle xenoliths from intraplate and suprasubduction settings

12.50 – 14.30 Lunch

Plenary Session 2. Petrology and Volcanology
Convenors: Giovanni B. Piccardo and Angelo Peccerillo

14.30 – 14.45 Introduction by **Angelo Peccerillo** (Dip. Scienze della Terra, Perugia)
Understanding how active volcanoes work: a petrological and geochemical perspective

14.45 – 15.30 PL **Roberto Santacroce** (Dip. Scienze della Terra, Pisa)
Geochemistry and petrography of pyroclastic deposits as keys for understanding how active volcanoes work

15.30 – 16.00 KN **Diego Perugini** (Dip. Scienze della Terra, Perugia)
Time-scales of volcanic processes: constraints from rock textures, trace element diffusivity and modelling

16.00 – 16.30 KN **Lorella Francalanci** (Dip. Scienze della Terra, Firenze)
Revealing macro-scale volcanic processes by micro-scale chemical and isotopic investigations

16.30 – 16.40 Coffee Break

16.40 – 18.40 Parallel scientific sessions

Scientific Session 3. Magmatic Processes
Convenor: Angelo Peccerillo

16.40 – 17.00 **Alba P. Santo** (Dip. Scienze della Terra, Firenze)
Geochemical and petrological evolution of Barren Island (Andaman Sea, Indian Ocean)

17.00 – 17.20 **Sonia La Felice** (Dip. Chimica e Fisica della Terra, Palermo)
Tephrocronology with ^{40}Ar-^{39}Ar dating of recent (<20 kyrs) silicic volcanism at Pantelleria Island: implications on magmatic system

17.20 – 17.40 **Ida Di Carlo** (Dip. Chimica e Fisica della Terra, Palermo)
Constraints on pre-eruptive conditions of recent felsic explosive volcanism at Pantelleria: an experimental approach

17.40 – 18.00 **Marcella Davì** (Dip. Scienze della Terra, Università della Calabria)
The recent latites of Lipari and Vulcano: evidence for a common origin

18.00 – 18.20 **Donatella Barca** (Dip. Scienze della Terra, Università della Calabria)
A combined SEM-EDX and LA-ICP-MS study of the Marsili seamount basic lavas, southern Tyrrhenian back-arc basin: preliminary results

18.20 – 18.40 **Silvio Ferrero** (Dip. Geoscienze, Padova)
Anatectic melt trapped in garnet from migmatites of Kerala Khondalite Belt, southern India: evidence from crystallized and glassy inclusions

Scientific Session 4. Metamorphic Processes
Convenor: Giovanni B. Piccardo

16.40 – 17.00 **Patrizia Fumagalli** (Dip Scienze della Terra, Milano)
Phase relations in K-doped lherzolites up to 6.0 GPa: the relevance of amphibole and phlogopite for ight elements recycling

17.00 – 17.20 **Bernardo Cesare** (Dip. Geoscienze, Padova)
Retrograde diffusion of hydrogen in biotite from metapelitic granulites of the Kerala Khondalite Belt (S. India)

17.20 – 17.40 **Alberto Zanetti** (IGG-CNR, Pavia)
Evidence for different styles of alkaline metasomatism during continental rifting as recorded by the mantle column beneath the Mid Atlas (Morocco)

17.40 – 18.00 **Nadia Malaspina** (Dip. Scienze della Terra, Milano)
The oxidation state of metasomatised mantle wedge: insights from hydrate-carbonate-bearing peridotite

18.00 – 18.20 **Simona Ferrando** (Dip. Scienze Mineralogiche e Petrologiche, Torino)
The Dora-Maira whiteschists (western Alps) re-examined: new data from mineral assemblage and UHP multiphase solid inclusions in pyrope

18.20 – 18.40 **Fabio Garzetti** (Dip. Scienze della Terra, Pavia)
Structure, chemistry and U-Pb geochronology of zircons from albitites of internal Ligurides ophiolites

18.40 – 19.30 **Meetings of GNM, GNP, GABEC**

Tuesday, 9th September
GEOMATERIALS

08.00 – 09.00 Posters mounting

09.00 – 11.00 Parallel scientific sessions

Scientific Session 5. Minerals
Convenor: Gabriella Lucchetti

09.00 – 09.20 **Ernesto Mesto** (Dip. Geomineralogico, Bari)
Appraisal of Ti speciation in trioctahedral micas by means of XPS investigation: recent improvements and applications

09.20 – 09.40 **Giancarlo Capitani** (Dip. Geomineralogico, Bari)
Total energies of different antigorite structure models: A DFT study

09.40 – 10.00 **Cecilia Viti** (Dip. Scienze della Terra, Siena)
Dehydration reactions and micro/nanostructures in experimentally-deformed serpentinites

10.00 – 10.20 **Nicola Rotiroti** (Dip. Scienze della Terra, Milano)
New insight into the extra-framework content of zeolite levyne

10.20 – 10.40 **Laura Chelazzi** (Dip. Scienze della Terra, Firenze)
High-pressure structural behavior of ingersonite, $Ca_3Mn^{2+}Sb_4^{5+}O_{14}$: an in situ single-crystal X-ray study

10.40 – 11.00 **Marco Ferrari** (Dip. Scienze della Terra, Siena)
Retrograde hydration mechanism of amphibole at the TEM scale

Scientific Session 6. Applications and models for Mineralogy, Petrology and Geochemistry
Convenor: Piero Lattanzi

09.00 – 09.20 **Fabrizio Nestola** (Dip. Geoscienze, Padova)
The effect of non-stoichiometry at high-pressure and high-temperature: implications for the Earth's mantle mineralogy

09.20 – 09.40 **Matteo Alvaro** (Dip. Scienze della Terra, Pavia)
High-temperature $P2_1/c - C2/c$ phase transition of $LiFe^{3+}Ge_2O_6$

09.40 – 10.00 **Gabriele Giuli** (Dip. Scienze della Terra, Camerino)
The effect of Fe oxidation state on the viscosity of silicate melts: Fe structural role in phonolitic glasses by XAS

10.00 – 10.20 **Sabrina Nazzareni** (Dip. Scienze della Terra, Perugia)
Water content of pyroxenes from Etna and Aeolian volcanoes: implications for the hazards of the active Italian volcanoes

10.20 – 10.50 KN **Luca Bindi** (Museo di Storia Naturale, Firenze)
Can clinopyroxene be a leading host of potassium in the Earth's upper mantle? Evidences from crystal chemistry and thermodynamic modelling

11.00 – 11.20 Coffee Break

11.20 – 13.20 Parallel scientific sessions

Scientific Session 7. Cultural Heritages

Convenor: Isabella Memmi

11.20 – 11.40 **Federico Bernardini** (Dip. Scienze dell'Antichità, Trieste)
Shaft-holed axes from Slovenia and North Western Croatia: an archaeometric study on artefacts manufactured from Doleritic basalts

11.40 – 12.00 **Ilaria Giunti** (Dip. Geoscienze, Padova)
Chemical and isotopic tracers in copper deposits and ancient artefacts: a geochemical database of copper mines to estabilish the provenance of materials

12.00 – 12.20 **Roberto Giustetto** (Dip. Scienze Mineraloogiche e Petrologiche, Torino)
Crystal structure refinement of sepiolite/indigo pigment using synchrotron radiation

12.20 – 12.40 **Serena Tonietto** (Dip. Geoscienze, Padova)
Gold tesserae from the paleo-christian glass mosaic of St. Prosdocimus (Padua, Italy): an archeometric study

12.40 – 13.00 **Rossella Arletti** (Dip. Scienze delle Terra, Modena e Reggio Emilia)
Eleventh century Byzantine mosaic tesserae from the Greek monasteries of Daphni and Hosios Loukas

13.00 – 13.20 **Isabella Memmi** (Dip. Scienze della Terra, Siena)
Sienese "archaic" majolica: characterization of coatings by transmission electron microscopy

Scientific Session 8. Geomaterials at large-scale facilities

Convenor: G. Diego Gatta

11.20 – 11.40 **Lara Leardin**i (Dip. Scienze della Terra, Ferrara)
"Nano reactors" under high pressure: the influence of the framework/extraframework composition in CHA topology

11.40 – 12.00 **Mario Tribaudino** (Dip. Scienze della Terra, Parma)
Synthesis, TEM characterization and high temperature behaviour of $LiNiSi_2O_6$ pyroxene

12.00 – 12.20 **Pilario Costagliola** (Dip. Scienze della Terra, Firenze)
Arsenic uptake by natural calcite: a XAS study

12.20 – 12.40 **Eleonora Paris** (Dip. Scienze della Terra, Camerino)
North-american microtektites are more oxidized compared to tektites

12.40 – 13.00 **Davide Levy** (Dip. Scienze Mineralogiche e Petrologiche, Torino)
A combined in situ X-ray powder diffraction and in situ neutron diffraction on $MgFe^{3+}AlO_4$ spinel

13.00 – 13.20 **G. Diego Gatta** (Dip. Scienze della Terra, Milano)
New insights into the crystal-chemistry of epididymite and eudidymite: a single-crystal neutron diffraction study

13.20 – 14.45 Lunch

14.45 – 17.30 **SIMP Poster session** with coffee and drinks (from 17.00)

17.30 – 19.30 **SIMP General Assembly**

20.30 **SIMP Social dinner**

Wednesday, 10th September

STRUCTURES, SURFACES, REACTIVITY (co-organised by SIMP and AIC)

09.00 – 09.30 **37° AIC Meeting opening ceremony and presentation of the joint session**

Joint Plenary Session 9. Structures, Surfaces, Reactivity

09.30 – 10.15 PL **Roy A. Wogelius** (School of Earth, Atmospheric and Environmental Sciences, Manchester)
Mineral surfaces, chelates, and radionuclides: il buono, il brutto, il cattivo

10.15 – 11.00 PL **Frank C. Hawthorne** (Dept. Geological Sciences, Winnipeg)
Characterizing the thin and the tiny: thin films and micro-particles of environmental importance

11.00 – 11.40 PL **Koen Janssens** (Dept. Chemistry, Antwerp)
Obtaining information on surface alteration of archaeological and cultural heritage materials by means of non-destructive X-ray based methods

11.40 – 12.00 Coffee Break

12.00 – 12.40 PL **Stefano Zanardi** (ENI SpA, R&M Division, Milano)
Interactions among CO_2, brine and minerals during greenhouse gas geological storage

12.40 – 13.20 PL **Giovanni Valdrè** (Dip. Scienze della Terra e Geologico Ambientali, Bologna)
Interactions between crystals and organic molecules

13.20 – 15.00 Lunch

15.00 – 15.40 PL **Elisa Boanini** (Dip. Chimica, Bologna)
Biomimetic materials: from Nature's structural materials to biomaterials

15.40 – 16.20 PL **Andrea Mattevi** (Dip. Genetica e Microbiologia, Pavia)
Biotechnological potential of structural enzymology

16.20 – 17.00 PL **Gianluca Calestani** (Dip. Chimica, Parma)
Nanomorphogenesis of inorganic materials: from nanoparticles to nanostructured threedimensional structures

17.00 – 17.20 Coffee Break

17.20 – 18.00 PL **Paola Paoli** (Dip. Energetica, Firenze)
Supramolecular structures: underlying philosophy and recent outcomes

18.00 – 18.45 Presentations by the sponsors

18.00 – 18.15 **PANalytical**

18.15 – 18.30 **Bruker AXS** (Frank van Meurs)
SMART X2S automated bench top system for chemical crystallography

18.30 – 18.45 **Oxford Diffraction Ltd.** (Andy Dorn)
New high intensity X-ray sources from Oxford Diffraction

18.45 – 18.55 **2008 AIC prizes**: presentation of recipients

18.55 – 19.35 **AIC Mario Nardelli prize**: acceptance speeches

18.55 – 19.15 **Serena C. Tarantino** (Dip. Scienze della Terra, Pavia)
Average structure and local distortions in minerals solid solutions

19.15 – 19.35 **Michele Cianci** (European Molecular Biology Laboratory, Hamburg)
Cracking lobster shell protein structures and explaining the colour shift

Thursday, 11th September
MATERIALS, FROM EARTH AND LAB TO LIFE -1

08.00 – 09.00 Posters mounting

09.00 – 09.50 PL **Elena Sokolova** (Dept. Geological Sciences, Winnipeg)
A topological algorithm: from chemistry to structure in titanosilicates

09.50 – 13.25 Parallel scientific sessions

Scientific Session 10. Crystal-chemical models for mineral families
Convenors: R. Oberti and S. Quartieri

09.50 – 10.20 KN **Paola Bonazzi** (Dip. Scienze della Terra, Firenze)
Crystal-chemical models to describe the molecular structure of arsenic sulphides and their changes induced by exposure to light

10.20 – 10.50 KN **Michele Zema** (Dip. Scienze della Terra, Pavia)
Cation ordering and microstructures in columbite

10.50 – 11.10 Coffee Break

11.10 – 11.40 KN **Giovanna Vezzalini** (Dip. Scienze della Terra, Modena e Reggio Emilia)
Pressure-induced over-hydration of zeolites: a review and new insights from gismondine

11.40 – 12.10 KN **Paola Comodi** (Dip. Scienze della Terra, Perugia)
HP-HT phase stability of sulphates

12.10 – 12.30 **Gennaro Ventruti** (Dip. Geomineralogico, Bari)
OD character and structural features of sideronatrite, $Na_2Fe(SO_4)_2(OH)\cdot 3H_2O$

12.30 – 12.50 **Marcella Cadoni** (Dip. Scienze Mineralogiche e Petrologiche, Torino)
OD-character and twinning in the structure of a new synthetic titanosilicate: $(Ba,Sr)_4Ti_6Si_4O_{24}\cdot H_2O$

12.50 – 13.10 **Fernando Cámara** (IGG-CNR, Pavia)
The crystal structure and crystal chemistry of jinshajiangite, a group-II Ti disilicate mineral

13.10 – 13.30 **Matteo Ardit** (Dip. Scienza della Terra, Ferrara)
The monoclinic polymorph of $Ba_2MgSi_2O_7$ and its relationships to the melilite-type structure

Scientific Session 11a. The polarity in mineral surfaces: fundamental and applied aspects
Convenor: Dino Aquilano

09.50 – 10.20 KN **Marco Bruno** (Dip. Scienze Geologiche e Petrologiche, Torino)
The energies of reconstructed crystal surfaces: an ab initio quantum-mechanical and thermodynamical study on NaCl, LiF and $CaCO_3$

10.20 – 10.50 KN **Giovanni De Giudici** (Dip. Scienze della Terra, Cagliari)
Hydrozincite crystal growth under cyanobacteria control: an investigation on lattice microstructural properties

10.50 – 11.10 Coffee Break

11.10 – 11.40 KN **Massimo Moret** (Dip. Scienze dei Materiali, Milano Bicocca)
Study of crystalline organic semiconductors: from the structure to the theoretical crystal morphology

11.40 – 12.10 KN **Gérard Pèpe** (Lab. Chimie Théorique e Modelisation Moléculaire, Aix-Marseille III)
From molecular structure to crystal polymorphs: a predictive genetic algorithm

Scientific Session 11b. From surface interactions to bulk crystal growth
Convenor: Dino Aquilano

12.10 – 12.30 **Daniele Malferrari** (Dip. Scienze della Terra, Modena e Reggio Emilia)
Effect of temperature on Hg- and Hg-cysteine complexes in vermiculite and montmorillonite

12.30 – 12.50 **Angelo Agostino** (Centro di Eccellenza NIS, Dip. Chimica Generale e Inorganica, Torino)
Growth of detective YBCO whiskers

12.50 – 13-10 **Andrea Zappettini** (IMEM-CNR, Parma)
Boron oxide encapsulated vertical Bridgman CdZnTe crystals for X-ray detector applications

13.10 – 13.30 **Davide Calestani** (IMEM-CNR, Parma)
Growth and characterization of ZnO nanostructures by a self-catalytic CVD process

13.30 – 14.45 Lunch

14.45 – 16.45 **AIC Poster Session** with coffee and drinks (from 16.15)

17.00 – 20.00 **AIC General Assembly and elections of the 2009-2011 Council**

20.30 **AIC Social dinner**

Friday, 12th September
MATERIALS, FROM EARTH AND LAB TO LIFE -2

Scientific Session 12. Building-up organic-based nanodevices
Convenor: Roberto Zamboni

09.00 – 09.50 PL **Salvatore Iannotta** (CNR-IMEM and CNR-IFN, Trento)
A jet approach to the growth of organic, cluster assembled and nano-hybrid materials to control properties at the different length-scales

09.50 – 10.20 KN **Michele Muccini** (CNR-ISMN - Dip. Progettazione Molecolare, Bologna)
Multiphoton Laser Scanning Confocal Spectro-Miscroscopy for advanced molecular based optoelectronic and photonic nanodevices

10.20 – 10.50 KN **Michele Maggini** (Dip. Scienze Chimiche, Università di Padova)
Functional surfaces with special wettability for new materials and devices

10.50 – 11.10 Coffee Break

11.10 – 11.40 KN **Mauro Causà** (Dip. Chimica, Università Federico II, Napoli)
Computational modelling of layered materials for advanced applications

11.40 – 12.00 **Nicola Coppedè** (IFN-CNR Trento)
Codeposition of hybrid nanostructured materials by Supersonic Beams for photovoltaic applications

12.00 – 12.20 **Adele Sassella** (Dip. Scienza dei Materiali, Milano Bicocca)
Homo- and hetero-epitaxial growth of thin films and nanostructures by organic molecular beam epitaxy

Scientific session 13. Structural characterization of nano-crystalline materials
Convenor: Vincenzo Massarotti

12.20 – 12.40 **Mauro Gemmi** (Dip. Scienze della Terra, Milano)
Structure solution of a novel Li-Ni-Ti oxide with precession electron diffraction data

12.40 – 13.00 **Monica Dapiaggi** (Dip. Scienze della Terra, Milano)
Local and average behaviour of size-stabilized nano-crystalline zirconia by Pair Distribution Function and Rietveld analysis

13.00 – 14.00 Lunch

Scientific Session 14. Biological and synthetic supramolecular systems

Convenors: Adriana Bigi, Lucio Randaccio, Menico Rizzi

14.00 – 14.30	KN **Gianluca Croce** (DISTA, Università del Piemonte Orientale, Alessandria) A mesoporous pattern created by Nature
14.30 – 15.00	KN **Massimo Degano** (Unità di Biocristallografia, Fondazione Centro San Raffaele, Milano) Structural enzymology in drug design and cancer gene therapy
15.00 – 15.30	KN **Silvano Geremia** (Centro di Eccellenza in Biocristallogafia, Dip. Scienze Chimiche, Trieste) From structural biology to supramolecular chemistry
15.30 – 15.50	Coffee Break
15.50 – 16.20	KN **Alessia Bacchi** (Dip. Chimica Generale ed Inorganica, Chimica Analitica e Chimica Fisica, Parma) Inclusion of volatile guests in organic-inorganic systems
16.20 – 16.50	KN **Piero Macchi** (Dip. Chimica Strutturale e Stereochimica Inorganica, Milano) Polarizing microscopy analysis of metal organic frameworks: solid state behavior of Rh(0)/Rh(I) bisphosphine and M(II) benzenetricarboxylates polymers
16.50 – 17.10	**Marco Milanesio** (Dip. Scienze eTecnologie Avanzate, Alessandria) Full implementation of the in situ simultaneous Raman/ X-ray Powder Diffraction setup: methods and applications
17.10 – 17.30	**Massimo Gazzano** (ISOF-CNR, Bologna) Strontium-substituted hydroxyapatite nanocrystals
17.30 – 17.50	**Antonietta Guagliardi** (IC-CNR, Bari) Nano-crystalline bone formation and bioceramic scaffold resorption: a microdiffraction-based study
17.50 – 18.10	**Michele Saviano** (IBB-CNR, Napoli) Monofunctionalized β-cyclodestrins: a molecular dynamics study of the self-inclusion process
18.10 – 18.30	**Silvio Cerrini** (IC-CNR, Sede di Monterotondo, Roma) Invariant characterization and recognition of the point group symmetries using high order moments
18.30	**Closing Ceremony**

Field trip

Conservation and reuse of mining heritage: the Val Graveglia manganese mines and the Val Fontanabuona slate quarries

Destination: Val Graveglia and Val Fontanabuona valleys (Lavagna, Genova)
Leaders: Pietro Marescotti (marescot@dipteris.unige.it), Laura Gaggero (gaggero@dipteris.unige.it)
Associate Leader: Laura Crispini (crispini@dipteris.unige.it)
Min / Max enrolment: 10/25
Short description of outcrops/sites: different types of manganese mineralisations and their relationships with adjoining and host Monte Alpe Cherts; Pillow lavas; stratigraphic and structural setting of underground slate outcrops and their relationships with adjoining rocks.
Departure / date: Sestri Levante, about 9 a.m.
Arrival / date: Sestri Levante, about 7 p.m.

Visit to the slate quarry in Val Fontanabuona courtesy of **Rosasco Lino e Figli s.n.c.** company which is kindly acknowledged.

Index

PLENARY LECTURES

3D & 4D ARCHITECTURE OF THE EARTH'S CONTINENTAL LITHOSPHERE: EVIDENCE FROM VOLCANOES, DIAMONDS & HIGH PRESSURE ROCKS

M. Menzies

Department of Earth Sciences, Royal Holloway University of London, UK
menzies@es.rhul.ac.uk

Continental lithosphere makes up 33% of the Earth's surface, and has an average age of 2500 Ma, ten times older than the oceanic lithosphere which covers twice as much of the Earth's surface. Since time began continents have formed by terrane accretion around pre-existent crustal core(s), some retaining evidence of the oldest crust (4400 Ma). A unique insight into the nature of the continental lithosphere is forthcoming from continental volcanoes, a very effective transport mechanism for high pressure rocks, diamonds and other minerals from depths of up to 660 km. The geology, geochemistry & geophysics of these materials help us re-construct the 3D architecture of the Earth's continental lithosphere and allow us to compare lithospheres of different ages and origin(s). The oldest, most inert parts of the continents (cratons) have been stable for 2500 Ma (*e.g.* Fennoscandia, Greenland, Kaapvaal) with cold, refractory, dry keels rich in diamonds. The opposite is found in the tectonically active parts of the continents (*e.g.* western USA, eastern China) which are thin, relatively hot and volcanically/seismically active. These regions have 3D architectures more akin to ocean basins. In some cases, like eastern China, episodic volcanic activity has sampled the continental lithosphere allowing us to re-construct the 4D evolution of a craton over 400 Ma and to evaluate the causes. It appears that subduction-related recycling processes (that help form continents) have destroyed the North China Craton and transformed it in part into an ocean basin.

GEOCHEMISTRY AND PETROGRAPHY OF PYROCLASTIC DEPOSITS AS KEYS FOR UNDERSTANDING HOW ACTIVE VOLCANOES WORK

R. Santacroce

Dipartimento di Scienze della Terra, Università di Pisa, Italy
santac@dst.unipi.it

Volcanoes are great chemical separators of fluids from a partially melted source whose continuous activity allowed the formation of the different portions of the Earth. Their structure can be schematically retraced to five different zones (magma generation and segregation, deep storage, feeding, shallow differentiation, eruption) that can be investigated through different instruments belonging to various branches of the Earth Sciences. Having Vesuvius as reference, the talk focuses on the upper zones, discussing processes leading to the formation, evolution and emptying of shallow magma chambers. It will not include the early stages of melt generation and segregation as well as deep storage and upward ascent of magma. Major and trace element data on whole rock, glass shards and minerals from pyroclastic fall deposits (greatly preferred because of their quenched nature) provide information on the compositional variations during magma withdrawal. These allow the reconstruction of the pre-eruptive inner (absent, continuous or two fold zoning) and outer (layered carapace) arrangement of the magma chamber as well as the estimate of the extent of sin-eruptive magma mixing. Melt and fluid inclusions on crystals, juvenile or cognate (MI), are useful in indicating the P-T conditions of the formation and growth of the host mineral (and hence inform on their depth of provenance) and, in propitious cases, contribute to the recognition of the modalities of feeding shallow magma reservoirs. The Vesuvius magma chambers were periodically supplied by discrete, deep, slightly evolved mafic magma bodies, whose composition (revealed by melt inclusions in high-T crystals) changed from K-basalt to K-tephrite around 3000 years B.P.. Under open conduit conditions these chambers (< 3 km depth) are small, and each magma pulse induces thermal and compositional variations recorded by oscillatory zoned pyroxenes (Fs_{4-15}). The deposits of the explosive eruptions which reopen the Vesuvius conduit reflect variable mixing during magma withdrawal from zoned reservoirs, whose layering was deciphered through MI in salite (Fs_{15-30}). These suggest that the magma chambers evolve from prolate toward subequant, changing their layering with increasing volume and age: (1) initial stage, high aspect ratio chamber, homogeneous mafic melt (T ~ 1100°C) crystal enriched downward; (2) young stage, medium aspect ratio, continuous gradation from mildly evolved (T ~ 1050°C) to felsic melt (T ~ 850-900°C); and (3) mature stage, low aspect ratio, twofold chamber with stepwise gradient separating lower, convective, mildly evolved portion (T ~ 1050°C) from upper, stratified, felsic portion (T ~ 800-950°C).

MINERAL SURFACES, CHELATES, AND RADIONUCLIDES: IL BUONO, IL BRUTTO, IL CATTIVO

R.A. Wogelius

Williamson Research Centre for Molecular Environmental Science & School of Earth, Atmospheric, and Environmental Sciences, University of Manchester, UK
roy.wogelius@manchester.ac.uk

Interest in nuclear power as an important part of the 21st century energy mix has been rekindled. However, there are still significant gaps in our knowledge relating to radioactive waste disposal. In the event of a breach of the primary waste container, complexation reactions with surfaces and solution phase molecules are postulated to have an enormous affect on the mobility of radionuclides through the engineered barrier, the geological barrier, and ultimately into the biosphere. Therefore, an understanding of complexation with solid surfaces (both natural minerals and synthetic substrates) and with organic ligands is fundamental to making useful predictions about repository safety. The study of complex formation is made even more difficult due to the formation of ternary complexes involving the surface (*il buono*), the organic ligand (*il brutto*), and the radionuclide (*il cattivo*). Recent work on this and related problems in geochemistry and environmental mineralogy will be discussed and presented with particular emphasis on how new developments in surface analysis will have an impact on this critical research area. Presented work will be organized into two parts as given below.

I. *Advances in surface sensitive spectroscopic studies of organic ligand attachment at mineral surfaces* involving EXAFS, X-ray scattering, surface diffraction, ESEM, AFM, and *in situ* FTIR. The stability of minerals and other solid phases is strongly affected by chelation reactions, and in turn the mobility of organic pollutants can be drastically decreased due to bonding with solid surfaces, and therefore considerable effort has been focussed on understanding the kinetics and structure of organic complexation reactions in the natural environment. These reactions have been recognized as important not only in the context of radionuclide mobility, but also with respect to scale formation in oilfields [1], PAH mobility in groundwaters [2], and weathering reactions in the presence of background organic acids [3]. Conceptual and analytical progress from a range of various research strands will be outlined and key points pertinent to radwaste disposal highlighted.

II. *Radionuclide surface chemistry and release mechanisms from sludge, crystalline solids, and from waste glass* involving organic ligands will be constrained as ligand-exchange reactions within the context of recent research [4,5]. Explicit information about surface evolution during reaction with fluids can now be combined with information about the actinide coordination environment and changes in organic functional groups to give a dynamic picture of how radionuclides are released, how this changes the solid/liquid interface, what controls electron transfer, and the structural details of how various chelate complexes bind up the radionuclide. These advances will allow us to refine our fundamental understanding of how key contaminants will be released and migrate in both the engineered portion of the system as well as in the geological barrier.

References. [1] R.A. Wogelius, P.M. Morris, M.A. Kertesz, E. Chardon, A.I.R. Stark, M. Warren, J.R. Brydie, *Eur. J. Mineral.*, **19**, 297-307, 2007; [2] D. Zhu, B.E. Herbert, M.A. Schlautman, E.R. Carraway, J. Hur, *J. Environ. Qual.*, **33**, 1322-1330, 2004; [3] P.M. Morris, R.A. Wogelius, *Geoch. Cosmoch. Ac.*, **72**, 1970-1985, 2008; [4] M.A. Denecke, *Coordin. Chem. Rev.*, **250**, 730-754, 2006; [5] M.I. Boyanov, E.J. O'Loughlin, E.E. Roden, J.B. Fein, K.M. Kemner, *Geoch. Cosmoch. Ac.,* **71***,* 1898-1912, 2007.

CHARACTERIZING THE THIN AND THE TINY: THIN FILMS AND MICRO-PARTICLES OF ENVIRONMENTAL IMPORTANCE

F.C. Hawthorne, M. Schindler

Department of Geological Sciences, University of Manitoba, Canada
frank_hawthorne@umanitoba.ca

Dissolution and precipitation of uranyl minerals are important processes in the behaviour of uranium in the near-surface environment. It is important to be able to identify what minerals precipitate as a function of the pH and composition of the nascent aqueous solution. However, the characterization of thin films and minute particles is very difficult as there is often insufficient material for standard identification methods. XPS (X-ray Photoelectron Spectroscopy) provides direct information on valence state and local environment for both cations and anions. Examination of single crystals of uranyl minerals by XPS (X-ray Photoelectron Spectroscopy) shows that the valence states of uranium can be determined *in situ*. The results suggest that these minerals can be divided into the following four groups: (1) Uranyl-hydroxy-hydrate compounds with no or monovalent interstitial cations; (2) Uranyl-hydroxy-hydrate minerals with divalent interstitial cations; (3) Uranyl-oxysalt minerals with (TO_n) groups (T = Si, P, and C) in which all equatorial O-atoms of the uranyl-polyhyedra are shared with (TO_n) groups; (4) Uranyl-oxysalt minerals with (TO_n) groups (T = S and Se), in which some equatorial O-atoms are shared only between uranyl polyhedra. The average binding energies of the U^{6+}, U^{5+} and U^{4+} bands shift to lower values with (1) incorporation of divalent cations, and (2) increase in the Lewis basicity of the anion group bonded to U. The latter trend correlates with an increase in the covalency of the U-O bonds with increase in Lewis basicity of the anion group, which results in a shift of the electron density from O to U. The presence of U^{4+} and U^{5+} on the surface of uranyl minerals can be detected by the shape of the U $4f_{7/2}$ peak, and the occurrence of the U 5*f* peak and satellite peaks belonging to the U $4f_{5/2}$ peak. The fine structure of the O 1*s* spectrum allows identification of specific oxygen-cation linkages. The resolution of the O 1*s* spectra includes for the first time different O^{2-} bands, which are assigned to O atoms linking uranyl- with uranyl polyhedra (*U-O-U*) and O atoms of uranyl groups which do (*O=U=O-M*) and do not (*O=U=O*) bond to interstitial cations (*M*). The resolved bands in the O 1s spectrum occur at distinct ranges in binding energy: bands for (*U-O-U*) occur at 529.4-530.5 eV, bands for (*O=U=O*) and (*O=U=O-M*) at 530.5-531.4 eV, bands for O^{2-} in the equatorial plane of the uranyl polyhedra linking uranyl polyhedra with (TO_n) groups (T = Si, S, C, P, Se) (*T-O*) occur at 531.1-532.2 eV, bands for (OH) groups in the equatorial plane of the uranyl polyhedra (*OH*) occur at 531.9-532.4 eV, bands of (H_2O) groups in the interstitial complex of the uranyl-minerals ($H_2O_{interst}$) occur at 533.0-533.8 eV and bands of physisorbed (H_2O) groups on the surface of uranyl minerals (H_2O_{adsorb}) occur at 533.6-535.5 eV. Combination of information on U and O speciation can provide sufficient chemical and bond-topological constraints for precipitates to be identified. XPS has considerable potential for characterizing the mineralogy of thin films and microparticles of environmental importance.

OBTAINING INFORMATION ON SURFACE ALTERATION OF ARCHAEOLOGICAL AND CULTURAL HERITAGE MATERIALS BY MEANS OF NON-DESTRUCTIVE X-RAY BASED METHODS

K. Janssens, S. Bugani, S. Cagno, G. Van Der Snickt, W. De Nolf, J. Jaroszewics, O. Schalm

Departement of Chemistry, University of Antwerp, Belgium
koen.janssens@ua.ac.be

Among the analytical methods that are employed for (almost) non-destructive characterization of cultural heritage materials such as glass, metals, ceramics, etc., X-ray based techniques take an important position. It concerns X-ray fluorescence analysis (XRF) for elemental analysis of materials, X-ray diffraction (XRD) for structural identification of crystalline materials and X-ray absorption spectroscopy (XAS) for obtaining information on the chemical state of specific constituents.

Since the 1970's, X-ray fluorescence analysis (XRF) has been used extensively for the characterization of inorganic components in archaeological artefacts and in works of art. Several technological advances during the last decade have made it possible to develop user-friendly portable XRF units which can be used for *in-situ* analysis, *e.g.*, of work of arts in musea and galleries or of archaeological finds at excavation sites. In the laboratory, next to conventional bulk-XRF units, open-beam units, optionally mounted on moveable stages with many degrees of freedom, allow to perform analysis of (small areas of) macroscopic artifacts such as statues and large paintings. In some cases such instruments are equipped with focussing X-ray optics, allowing to confine the analyzed area to typically 20 x 20 μm^2.

On the other end of the technological spectrum, (sub)microscopic X-ray beams generated at synchrotron radiation facilities allow to employ a combination of XRF, XRD and XAS for a multi-modal characterization of alternation layers and original parts of (partially) weathered cultural heritage materials. For obtaining information on the macroscopic structure and the microscopic distribution of elements and compounds, various types of tomography can now be employed: next to conventional X-ray transmission tomography, which can also be performed by means of table-top equipment, at synchrotron facilities, also phase-contrast transmission tomography, X-ray fluorescence tomography and X-ray diffraction tomography are now coming into use.

A combination of the above-mentioned methods can either be used for characterization of small samples (often in cross-section) or may also be employed to obtain elemental, chemical or structural information about specific microvolumes of material, *e.g.*, in virtual planes that are situated deep inside a macroscopic specimen or artifact.

The possibilities of the above-mentioned methods will be outlined by means of examples taken from the following case studies:

- gaining insight in the degradation processes of cellulose-based documents by historic and modern ferro-gallic inks via Fe-K microscopic X-ray absorption near-edge spectroscopy (μ-XANES) and X-ray micro diffraction (μ-XRD)
- monitoring changes in the porosity of Lecce sandstone during preventive conservation by means of X-ray micro- and nanotomography
- understanding color alteration in 17th and 20th century painters' pigments such as smalt and cadmium-yellow via combined μ-XRF, μ-XANES and μ-XRD.

INTERACTIONS AMONG CO_2, BRINE AND MINERALS DURING GREENHOUSE GAS GEOLOGICAL STORAGE

S. Zanardi

Eni S.p.A. Refining & Marketing Division, San Donato Milanese (MI), Italy
Stefano.Zanardi@eni.it

One of the possible options for confining CO_2 produced in power plants by burning fossil fuels and reducing its content in the atmosphere is to sequester it in geological formations, including saline aquifer, coal deposition and depleted reservoirs. In order to guarantee the long-term and safe storage of large CO_2 volumes in depleted oil and gas fields, the sealing efficiency of the overlying geological strata (cap-rock) must be careful checked. In fact, even though the cap-rock sealing can trap natural gas for ages, possible transformation due to injection of acid gas can compromise its efficiency. Moreover, in depleted hydrocarbon fields the sealing efficiency could be lost by the presence of plugged, abandoned or still working monitoring wells. As a matter of fact the cement constituting them can be a possible pathway for the CO_2 to travels back to the surface (*e.g.* through the primary well cement, along the interfaces between the primary well cement and the geologic formation or through the cement plug [1]).

Eni has promoted a multidisciplinary research project to assess the feasibility of a pilot CO_2 injection test in an exploited gas field in Italy. The cap-rock and wellbore cement alterations were addressed combining experiments and numerical modelling [2,3]. Laboratory experiments involved samples of cap-rock and cement aged with CO_2 and brine, at different time and under reservoir conditions. The samples before and after testing were characterized by using different physico-chemical techniques such as X-Ray Powder Diffraction (XRD), Scanning Electron Microscopy (SEM) coupled to the Energy Dispersive Spectroscopy (EDX), Optical Microscopy (OM) and permeability measurements.

The results of this experimental study will be presented giving emphasis to the mineralogical transformations occurred in the cap-rock and wellbore cement.

References. [1] A. Duguid, M. Radonjic, G. Scherer, *Proceedings 4th Annual Conference on Carbon Capture and Sequestration*, Alexandria (Virginia), 2005; [2] S. Carminati, E. Previde Massara, S. Zanardi, M. Bartosek, M. Favaretto, A. Battistelli, M. Guidi, S. Biagi, N. Moroni, M. Brignoli, *Proceedings of the 8th International Conference of Greenhouse Gas Control Technologies*, 2006; [3] S. Biagi, C. Geloni, E. Previde Massara, S. Zanardi, G. Granelli, F. Gherardi, A. Battistelli, S. Carminati, N. Moroni, *Proceedings of the International School of Geophysics, 30th Course: CO_2 Capture & Storage*, 2007.

INTERACTIONS BETWEEN CRYSTALS AND ORGANIC MOLECULES

G. Valdré

Dipartimento di Scienze della Terra e Geologico Ambientali, Università di Bologna, Italy
giovanni.valdre@unibo.it

The ability to control the binding of biological and organic molecules to a crystal surface is central to several research areas and technological applications such as biotechnology, catalysis, molecular microarrays, biosensors and environmental sciences. Furthermore, investigating the way mineral surfaces interact with biomolecules has fundamental implications considering that these substrates may have played an important role as catalysts for the polymerization of biomolecules in the prebiotic environment. Here we deal with our recent achievements in the field of the interaction between mineral surfaces and bio-organic molecules: DNA molecules have different binding affinities and assume different conformations when adsorbed on different layered silicate surfaces, as we regularly observed on *Chlorite* isolated DNA molecules that became stretched bridging adjacent brucite-like surface regions. On these crystals the surface potential anisotropy is able to order and stretch the DNA filament thus inducing a natural change in its conformation. All the experimental results are in good agreement with modelling. Then, the active stretching of DNA on *Chlorite* is a clear indication of the basic and technological potential carried by these minerals when used as substrates for biomolecules.

BIOMIMETIC MATERIALS: FROM NATURE'S STRUCTURAL MATERIALS TO BIOMATERIALS

E. Boanini

Guppo di Biomimetica e Chimica dei Materiali, Dipartimento di Chimica "G. Ciamician", Università di Bologna, Italy
elisa.boanini@unibo.it

Nature has developed - with comparatively a small number of low cost raw substances, and through not expensive processes - a range of materials with remarkable functional properties. In particular, biomineralized tissues often display unique and desirable morphological, structural and mechanical properties, and represent informative models for the development of complex functional materials.

Biomimetics exploits the strategies adopted by living organisms to produce biomineralized tissues for the design and synthesis of innovative materials. As a consequence, biomimetic materials research starts with the study of structure-function relationships in biological materials. The biological tools include chemical and interfacial regulation of precipitation, matrix induced or matrix-mediated nucleation and crystal growth, inhibition by binding of molecules to specific faces of the crystals, and involve complex events, such as hierarchical structuring, adaptive growth, and constant remodelling. It follows that the reproduction of the whole biomineral assembly mechanism by non-biological methods cannot be regarded as an affordable goal. A more realistic approach is to develop bio-inspired processes for obtaining tailored functions using cheap base materials. This is true in different materials science and engineering fields, such as in electronics and optics, as well as in the fabrication of laminated ceramics or biomimetic coatings.

The basic knowledge on biomineralization fundamentals and a biomimetic approach are particularly relevant in the biomedical field, where they might play a key role on the development of materials suitable to interact well with mineralized tissues and will allow tailoring the properties of composite particles aimed at being used in controlled release of drugs or other bioactive molecules. Novel methodologies are presented to process bulk bioactive biomaterials or to induce a bioactive behaviour in biomaterials' surface. In particular, in the last years many efforts have been made to develop innovative compact or porous materials aimed at being used on bone replacement or regeneration applications.

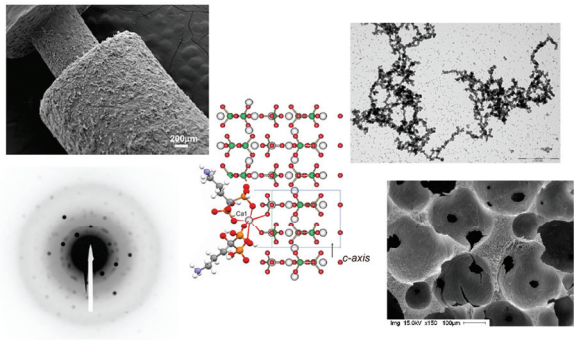

BIOTECHNOLOGICAL POTENTIAL OF STRUCTURAL ENZYMOLOGY

A. Mattevi

Dipartimento di Genetica e Microbiologia, Università di Pavia, Italy
mattevi@ipvgen.unipv.it

Enzymes are extremely powerful natural catalysts able to perform almost any type of chemical reaction while being mild by nature and highly specific. In fact, the delicate functioning of enzymes forms the basis of every living creature. The catalytic potential of enzymes is more and more appreciated by the industry as many industrial processes rely on these sophisticated bio-catalysts. However, the number of reactions catalyzed by enzymes is restricted as enzymes only have evolved to catalyze reactions that are physiologically relevant. Furthermore, enzymes have adapted to the cellular environment in which they have to function (*e.g.* operative at ambient temperature, turnover rate fits with metabolic partners, resilient towards proteolysis). This excludes the existence of enzymes that do not fit within the boundaries set by nature. It is a great challenge to go beyond these natural boundaries and develop methodologies to design "unnatural" tailor-made enzymes. Ideally it should become possible to (re)design enzymes to convert pre-defined substrates. Such designer enzymes could theoretically exhibit unsurpassed catalytic properties and, obviously, will be of significant interest for industrial biotechnology and life sciences. The role of crystallography in this type of research activities will be discussed.

NANOMORPHOGENESIS OF INORGANIC MATERIALS: FROM NANOPARTICLES TO NANOSTRUCTURED THREEDIMENSIONAL STRUCTURES

G. Calestani

Dipartimento di Chimica Generale ed Inorganica, Chimica Analitica e Chimica Fisica, Università di Parma e CNR-IMEM, Parma, Italy
calestg@unipr.it

In case of organic materials, finite molecules can often be considered as nanometric building units able to self-assemble in supramolecular aggregates. On the contrary, the preparation of inorganic nanomaterials, whose structure is based on an "infinite" three-dimensional framework of chemical bonds, implies an effective control of the dimensionality of the system just in the early stages of the process leading to nanometric units. Moreover, since quantum size effects are expected to modify the properties of such systems, when the dimension are reduced on a nanometric scale, the requirement of monodispersity is in most cases imperative.

The thermodynamic and kinetic control of the growth process leading to the formation of monodisperse nanoparticles will be discussed in the lecture, as well as synthetic strategies dealing with solution growth and the use of microemulsions.

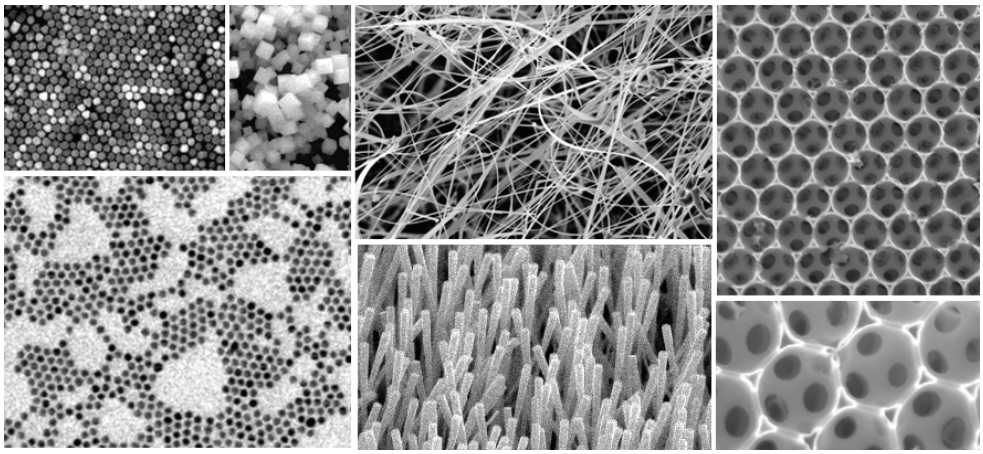

The attention will be then focused on the increase of the system dimensionality, passing from zero-dimensional (nanoparticles), to one-dimensional (nanowires, nanotubes and nanobelts) systems, up to three-dimensional nanostructured architectures produced whether by physical methods or by self-assembly of elementary units. Different examples will be discussed, covering a wide range of materials and applications.

SUPRAMOLECULAR STRUCTURES: UNDERLYING PHILOSOPHY AND RECENT OUTCOMES

P. Paoli

Dipartimento di Energetica "Sergio Stecco", Università di Firenze, Italy
paolapaoli@unifi.it

In 1967 the Journal of the American Chemical Society published the first article by Charles J. Pedersen on the synthesis and cation binding properties of crown ethers [1]. 20 years later the pioneering work in the supramolecular chemistry field by Donald J. Cram, Jean-Marie Lehn and Charles J. Pedersen were recognized by the award of the Nobel Prize in Chemistry. From the discovery, about forty years ago, of the macrocyclic ligands as synthetic and selective alkali metal cations binders, the area of supramolecular chemistry (the term was coined by Jean-Marie Lehn in 1969) has expanded enormously from pure chemistry to biology, physics, material science etc., as indicated by the ever increasing number of scientific papers featuring the word "supramolecular".

Supramolecular chemistry is often referred to as "the chemistry beyond the molecule" or "the chemistry of the non-covalent bond" alluding to the fact that molecules held together by intermolecular forces constitute supramolecular structures as well as atoms linked by covalent bonds form molecules. The intrinsic weakness of such non-covalent interactions makes the supramolecular aggregates by nature dynamic. Hence the difficulty in predicting supramolecular structures, but at the same time their intrinsic lability opens the way to a huge variety in terms of resulting structures, properties and functions, giving that supramolecular entities can reversibly associate, rearrange, etc. (dynamic non-covalent chemistry) [2].

Today, thanks to an improved comprehension of the molecular recognition principles which drive host-guest complexation, self-assembly and crystal packing, a plethora of diverse, beautiful and fascinating supramolecular structures have been obtained.

Examples from recent literature of hosts suitable for the selective binding of almost any conceivable guest, to be used in a variety of applications, including sensing, biological modeling and drug delivery, are presented.

The basic concepts of self-assembly which, besides constructing complex functional structures in nature (DNA, proteins, viruses), is also a powerful tool to produce synthetic intriguing molecular architecture (ladders, helices, rotaxanes, knots, Borromean rings, capsules etc.), are demonstrated by selected examples.

Finally a quick look at the enlarged scene: the crystal resulting from the ordered array of many single supramolecular assemblies held together by non-covalent forces, that is, a supermolecule par excellence [3].

References. [1] C.J. Pedersen, *J. Am. Chem. Soc.*, **89**, 7017-7036, 1967; [2] J.-M. Lehn, *Chem. Soc. Rev.*, **36**, 151-160, 2007; [3] J.D. Dunitz, *Pure Appl. Chem.*, **63**, 177-185, 1991.

A TOPOLOGICAL ALGORITHM: FROM CHEMISTRY TO STRUCTURE IN Ti-SILICATES

E. Sokolova

Department of Geological Sciences, University of Manitoba, Winnipeg, Canada
elena_sokolova@umanitoba.ca

Currently, the crystal structures of about 120 Ti-O compounds minerals are known, half of them Ti silicates and half of them Ti oxides. Titanium silicate minerals are common as accessory minerals in alkaline and peralkaline rocks. A prominent feature of such rocks is their extraordinary variety of minerals, many of which are readily soluble in water or are altered under atmospheric conditions. In a group of minerals of fixed structure topology, the relation between structure and chemical composition is usually straightforward: the sum of the sites in the structure gives the stoichiometry of all minerals in that group. However, in a group of minerals of reasonable complexity in which the structure topology is related but not identical, the general relation between structure topology and chemical composition is not known. This problem is of major theoretical significance in terms of the relation between structure and chemical composition. It is simple to go from structure topology to chemical composition. However, what one wants to do is to go in the inverse direction: from chemical composition to structure topology. A major component of my talk addresses this very fundamental problem. Here, I consider structural hierarchy and stereochemistry for titanium disilicate minerals containing the TS (titanium-silicate) block and establish the relation between structure topology and chemical composition for those minerals.

There are twenty five titanium disilicate minerals that contain the TS (Titanium-Silicate) block, a central trioctahedral (O) sheet and two adjacent (H) sheets of [5]- and [6]-coordinated polyhedra and (Si_2O_7) groups. The TS block is characterized by a planar cell based on translation vectors, $\mathbf{t_1}$ and $\mathbf{t_2}$, with $t_1 \sim 5.5$ and $t_2 \sim 7$ Δ and $\mathbf{t_1} \wedge \mathbf{t_2}$ close to 90°. The general formula of the TS block is $A^P{}_2\ B^P{}_2\ M^H{}_2\ M^O{}_4\ (Si_2O_7)_2\ X_{4+n}$, where $M^H{}_2$ and $M^O{}_4$ are cations of the H and O sheets; M^H = Ti (= Ti + Nb), Zr, Mn^{2+}, Ca; M^O = Ti, Zr, Mn^{2+}, Ca, Na; A^P and B^P = cations at the peripheral (*P*) sites = Na, Ca, Ba; X = anions = O, OH, F; n = 0, 2, 4. Cations in each sheet of the TS block form a close-packed layer and the three layers are cubic close packed. There are three topologically distinct TS blocks, depending on the type of linkage of two H sheets and the central O sheet. The H sheets of one TS block attach to the O sheet in the same way. All structures consist of a TS block and an **I** (intermediate) block that comprises atoms between two TS blocks. Usually, the **I** block consists of alkali and alkaline-earth cations, (H_2O) groups and oxyanions $(PO_4)^{3-}$, $(SO_4)^{2-}$ and $(CO_3)^{2-}$. These structures naturally fall into four groups, based on differences in topology and stereochemistry of the TS block. In Group I, Ti = 1 *apfu*, Ti occurs in the O sheet, and (Si_2O_7) groups link to a Na polyhedron of the O sheet (linkage 1). In Group II, Ti = 2 *apfu*, Ti occurs in the H sheet, and (Si_2O_7) groups link to two M^{2+} octahedra of the O sheet adjacent along $\mathbf{t_2}$ (linkage 2). In Group III, Ti = 3 *apfu*, Ti occurs in the O and H sheets, and (Si_2O_7) groups link to the Ti octahedron of the O sheet (linkage 1). In Group IV, Ti = 4 *apfu* (the maximum possible content of Ti in the TS block), Ti occurs in the O and H sheets, and (Si_2O_7) groups link to two Ti octahedra of the O sheet adjacent along $\mathbf{t_1}$ (linkage 3). The stability of the TS block is due to an extremely wide range in Ti (Nb)-O bond lengths, 1.68-2.30 Å, which allows the chemical composition of the TS block to vary widely. In a specific crystal structure, only one type of TS block occurs. The TS block propagates close-packing of cations into the **I** block. General structural principles have been developed for these twenty five titanium disilicates, and the relation between structure topology and chemical composition has been established for minerals based on the TS block.

A general algorithm is as follows:

O (octahedral) sheet composition ⇒ TS (titanium silicate) block composition ⇒ O–H (heteropolyhedral) sheets linkage ⇒ TS block propagates close packing of cations onto the I (intermediate) block [composition varies].

A JET APPROACH TO THE GROWTH OF ORGANIC, CLUSTER ASSEMBLED AND NANO-HYBRID MATERIALS TO CONTROL PROPERTIES AT THE DIFFERENT LENGTH-SCALES

S. Iannotta

CNR-IMEM e CNR-IFN, Trento, Italy
iannotta@imem.cnr.it

The ability to control structure, morphology, chemical and functional properties during growth is an aim that becomes particularly critical when dealing with organic and hybrid materials, the final (multi-)functional properties of which are designed for devices including electronics and nano-technologies. The jet-approach that we have proposed and explored allows unprecedented control on the growth process of organics allowing very different regimes up to preparation of films with single crystal like properties. Furthermore kinetically activated processes based on organic supersonic beams allow the synthesis of both hybrid structures and of refractory materials such as microcrystalline SiC. Finally jet co-deposition of organic molecules and inorganic clusters allows the synthesis of nanohybrids and of sensitized materials that could be uniquely suitable for the fabrication of novel classes of devices including sensors and solar cells. An overview of the perspectives opened by this approach will be given in view of the attractive performances achieved in prototype devices such as OFET and gas sensing devices.

COMMERCIAL PRESENTATIONS BY THE SPONSORS

SMART X2S AUTOMATED BENCH TOP SYSTEM FOR CHEMICAL CRYSTALLOGRAPHY

F. van Meurs

Bruker AXS BV, The Netherlands
frank.vanmeurs@bruker-nonius.com

SP

SMART X2S system offers truly automated single crystal structure determination at virtually no maintenance cost; an ideal solution for every synthetic chemistry laboratory. *The **SMART X2S** has been awarded the Editor's Choice Gold Award at 2008 Pittcon.*

It is a true bench top system, which can be placed anywhere in your laboratory. It is extremely compact, lightweight and completely air-cooled. It requires only a standard AC power line to operate and draws ten times less power than a conventional diffractometer. It has a fully enclosed internal radiation shield (no exposure to X-rays possible) and makes radiation badges redundant. There is no exposure of user(s) to mechanical components. The operation is completely automated and the output is fully compatible with Bruker's APEX2 software suite for crystallography.

The **SMART X2S** features a user-friendly Touch Screen interface. No crystallographic knowledge is required to operate it; an intelligent accelerator platform (automation layer) controls the flow of the experiment and makes all necessary decisions. It combines an expert knowledge of structural chemistry with the power of industry-standard SHELXTL data processing engines for structure solution and refinement. It uses the well-tested AUTOSTRUCTURE software package, which has been developed in collaboration with the University of Durham and is widely used in laboratories world-wide. When applied to an extensive library of over 2,000 real-world samples compiled at the University of Durham, the structure solution and refinement software automatically determined the correct structure in well over 90% of the cases.

In the unlikely case of failure to produce the structure, the **X2S software** performs an error analysis to determine the most likely cause of failure. Problem data sets that can not be solved automatically can be processed off-line using standard APEX software programs or the data can be sent to an expert crystallographer for manual processing.

NEW HIGH INTENSITY X-RAY SOURCES FROM OXFORD DIFFRACTION

A. Dorn

Oxford Diffraction Ltd., Abingdon, Oxfordshire, UK
andy.dorn@oxford-diffraction.com

Oxford Diffraction is synonymous with the pioneering of novel and innovative instrumentation for both small molecule and protein crystallography. Founded in 2001, the company has experienced rapid growth, and now has an install base of more than 200 systems in 29 countries worldwide. This success has led to the recent acquisition of Oxford Diffraction by Varian Inc., a major provider of scientific instrumentation.

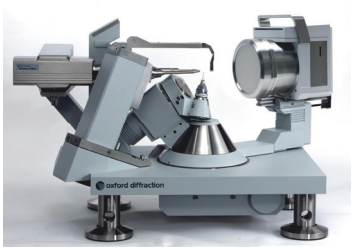

Fig. 1 - Gemini A Ultra

Oxford Diffraction developed the world's first dual-source diffractometer with production of the Gemini (Fig. 1) in 2005. This combines both Cu and Mo wavelengths, and is the best-selling dual wavelength diffractometer in the marketplace. In keeping with our reputation for innovation, this presentation will focus on a new philosophy for dual-source diffractometers, combining high intensity X-ray sources in a revolutionary new design.

The presentation will also concentrate on our new range of CCD detectors including the Eos and Atlas cameras (Fig. 2a and 2b). These detectors offer true 18-bit dynamic range, the fastest read-out times at 0.22 seconds, and they are the highest gain, highest sensitivity CCD's available today.

Fig. 2a - Eos

Fig. 2b - Atlas

AIC “MARIO NARDELLI” PRIZE

Acceptance speeches

AVERAGE STRUCTURE AND LOCAL DISTORTIONS IN MINERALS SOLID SOLUTIONS

S.C. Tarantino

Dipartimento di Scienze della Terra, Università di Pavia, Italy
tarantino@crystal.unipv.it

Natural minerals are typically binary or multicomponent solid solutions. As a consequence, many of the physical and thermodynamic properties of the bulk Earth depend on the effects of chemical mixing in crystals. When one atom is replaced by another with different size, the surrounding framework relaxes around it and accommodates the size difference by the development of a local strain field. Strain effects can be on a local scale giving rise to excess enthalpies of mixing, or they can be on a macroscopic scale giving the spontaneous strains which accompany phase transitions. Significant advances have been made in the last few year in the context of characterising such strain fields and their variations by using diffraction and spectroscopic techniques.

The response of the $(Fe,Mn)Nb_2O_6$ columbite structure to intrasite Fe^{2+}–Mn^{2+} and intersite Mn^{2+}–Nb^{5+} exchanges has been characterised at different length scales. Strain fields associated with the substitution of Fe for Mn across the solid solution are quite localised. The distortions appear to be fairly weak and fade away over a length scale of few unit cells. Variations in the average structure from refinements of X-ray diffraction data are consistent with linear variations of structural parameters with composition [1]. On the other hand, spectroscopic studies (IR, Mössbauer and XAS) reveal a complex but systematic response of the columbite structure type to Mn-Fe substitution on the A octahedral site. In ferrocolumbite, all the Fe octahedra are close to being identical, while there are local structural heterogeneities at a longer length scale, presumably in ordering the precise topology of polyhedra immediately adjacent to the octahedron. By contrast, the manganocolumbite seems to have some diversity in the precise coordination at the MnO_6 octahedra but a greater uniformity in how the adjacent polyhedra are configured around them [2,3].

The intracrystalline cation exchange reaction of divalent and pentavalent cations proceeds through the formation of nanosized domains with rhombic shape, as evidenced by TEM analysis. Diffraction contrast images and high resolution images clearly show that rhombic domains are ordered and dispersed in a disordered matrix. *In situ* high temperature synchrotron-radiation powder diffraction data show that a biphasic system composed of two distinct columbite phases with different degrees of order develops after short time of annealing. Rietveld and PDF analyses indicate two stages for the cation ordering mechanism: a first stage in which the degree of order increases and the domains size remains nearly constant and a second one in which the growth of the domains accompanies the achievement of the complete cation order.

References: [1] S.C. Tarantino, M. Zema, *Am. Mineral.*, **90**, 1291-1300, 2005; [2] S.C. Tarantino, P. Ghigna, C. McCammon, R. Amantea, M.A. Carpenter, *Acta Crystallogr. B***61**, 250-257, 2005; [3] S.C. Tarantino, M. Zema, F. Maglia, M.C. Domeneghetti, M.A. Carpenter, *Phys. Chem. Miner.*, **32**, 568-577, 2005.

CRACKING LOBSTER SHELL PROTEIN STRUCTURES AND EXPLAINING THE COLOUR SHIFT

M. Cianci

European Molecular Biology Laboratory, Hamburg, Germany
michele.cianci@embl-hamburg.de

The coloration of the lobster shell, famously known from its colour change on cooking, derives from a complicated mix of astaxanthin carotenoid molecules and several proteins in complex. The 1.4 Å resolution of apo A1 protein structure [1] was used to get a molecular replacement solution for the β-crustacyanin 'A1+A3' dimer complex at 3.2 Å [2].

At present the molecular tuning parameters causing the 100 nm bathochromic shift of the astaxanthin in the β-crustacyanin, versus free astaxanthin, are known from our work and have stimulated research in theoretical and carotenoid chemistry. The end rings coplanarisation, a conformation of the astaxanthin fixed by the protein, extends the polyene chain alternating single and double bond effect to give ~ 30 nm to the UV/Vis spectral absorption shift.

Two theories have been advanced to explain the remaining 70 nm bathochromic shift; one involves an exciton interaction between the two bound astaxanthins *i.e.* that are held in close proximity and the second involves two interestingly positioned histidines and, if protonated, could create a sufficient electronic polarisation of each carotenoid and also affect the 'HOMO-LUMO' energy gap.

Preliminary expression of one of the two subunits is already in progress in Prof. Berni's Lab. (University of Parma) (unpublished results).

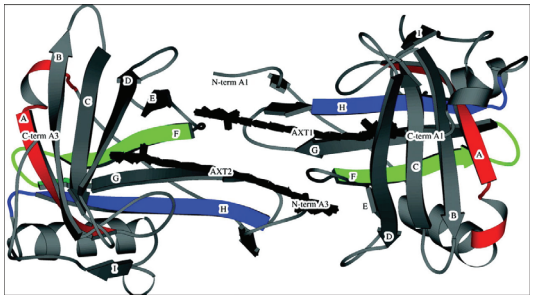

The health and commercial implications are for production of food colorants, including production of safer food colorants and development of means to determine if fast food is sufficiently cooked in order to prevent poisoning. Moreover this type of protein may, in the future, also be designed to act as a carrier of water insoluble drugs such as astaxanthin, for prevention of many diseases.

Public interest in the crustacyanin studies via the media has been especially strong not least because "the" question: *Why does a lobster change colour on cooking?* is known to nearly everyone. The PNAS 2002 paper was downloaded over 600 times in the first 6 months, for example. The protein protonation determination methods developments have also attracted wide attention, at this stage mainly from academe and industry, and featured in "The Scientist" magazine as well as being an "Institut Laue Langevin Highlight 2005".

References.[1] M. Cianci, P.J. Rizkallah, A. Olczak, J. Raftery, N.E. Chayen, P.F. Zagalsky, J.R. Helliwell. *Acta Crystallogr. D***57**, 1219-1229, 2001; [2] M. Cianci, P.J. Rizkallah, A. Olczak, J. Raftery, N.E. Chayen, P.F. Zagalsky, J.R. Helliwell, *PNAS,* **99**, 15, 9795-9800, 2002.

PETROLOGIC PROCESSES AND GEODYNAMICS

Session 1
Mantle processes and geodynamics

LITHOSPHERE/ASTHENOSPHERE INTERACTION AT EXTENSIONAL SETTINGS: CONSTRAINTS TO GEODYNAMICS

G.B. Piccardo

Dip.Te.Ris., Università di Genova, Italy
piccardo@dipteris.unige.it

Mesozoic continental rifting and break-up of the Ligurian-Piemontese (Ligurian Tethys) ocean, whose remnants are now preserved in the ophiolites of the Alpine-Apennine (AA) orogenic belt, are generally considered a case of passive, hence cold extension and stretching of the Europe-Adria lithosphere, driven by far-field tectonic forces. Sections of the subcontinental mantle were exhumed from lithospheric levels and were exposed to the sea-floor of the basin after complete tectonic removal of the continental crust. The Ligurian Tethys basin was, thus, floored by a peridotite basement discontinuously covered by basaltic lava flows underlying the oceanic sediments. The AA ophiolitic peridotites derive from both Ocean-Continent Transition (OCT) zones and More Internal Oceanic (MIO) settings of the ancient basin. Peridotites exposed at OCT settings consist of fertile, sub-continental lithospheric lherzolites, recording the tectonic-metamorphic processes that led to their exhumation to the sea-floor. Peridotites exposed at MIO settings show an extreme compositional heterogeneity, caused by variable interaction (depletion/ enrichment) with fractional MORB-type melts percolating via diffuse porous flow mechanisms.

Available geological, petrologic and geochemical data on the AA ophiolitic peridotites provide relevant information on the thermo-mechanical history of the upper mantle and the geodynamic evolution of the the Ligurian-Piemontese realm. Lithosphere extension was driven by whole-lithosphere, km-scale extensional shear zones that caused stretching and thinning of the lithosphere and passive uprising of the asthenosphere. The adiabatically upwelling asthenosphere underwent decompressional melting along the axial zone of the extensional system. MORB-type asthenospheric melts percolated through the extending mantle lithosphere exploiting the network of extensional shear zones and infiltrating the host mantle lithosphere.

Available isotope data on AA ophiolitic mantle and intrusive rocks, describe the evolution steps of the sub-continental mantle. AA peridotites from OCT settings record: 1) early Proterozoic ages of lithosphere accretion, 2) Late Triassic ages of exhumation (220-225 Ma), and 3) Early Jurassic ages of MORB melt percolation and intrusion (170-180 Ma), evidencing the minimum age of inception of asthenosphere partial melting. AA peridotites from MIO settings record Middle-Late Jurassic ages of MORB melt percolation and intrusion (163-150 Ma).

Significant melt/peridotite interaction caused the thermochemical/mechanical erosion the lithospheric mantle which attained asthenospheric rheological characteristics. This process resulted in a significant decrease in Total Lithospheric Strength (TLS), achieved in a relatively short time (< 5 Ma) by most part of the mantle lithosphere along the axial zone. The relatively rapid TLS decrease associated with softening of the lithospheric mantle is potentially sufficient to cause whole lithosphere failure under appropriate far-field tectonic forces.

Present knowledge on ophiolitic peridotites from the lithosphere of the Jurassic Ligurian Tethys evidences the close relationships between geodynamics and mantle processes during pre-oceanic rifting. In fact: (1) passive extension of the lithosphere induced decompression partial melting of the underlying mantle asthenosphere; (2) melt percolation through the extending mantle lithosphere caused their rheological modification (*i.e.* softening); (3) melt-induced thermo-mechanical erosion of the mantle lithosphere was a controlling factor in the transition from distributed continental deformation to localized rifting, drifting and spreading.

The tectonic processes (lithosphere extension) induced magmatic processes (asthenosphere partial melting and lithosphere melt percolation), and the magmatic processes enhanced the geodynamic evolution of the continental extensional system towards the oceanic spreading.

MODELLING EXTENSION OF THE CONTINENTAL LITHOSPHERE AND THE DEVELOPMENT OF PASSIVE MARGINS: RHEOLOGICAL MODIFICATIONS IN THE LITHOSPHERE AND GEODYNAMICAL EFFECTS

G. Corti[1], G.B. Piccardo[2], G. Ranalli[3], P. Manetti[1]

[1]*Istituto di Geoscienze e Georisorse, CNR, Italy*
[2]*Dip.Te.Ris., Università di Genova, Italy*
[3]*Department of Earth Sciences and Ottawa-Carleton Geoscience Centre, Carleton University, Canada*
giacomo.corti@unifi.it

The thermo-mechanical process of continental break-up and the transition to oceanic spreading represent some of the most important aspects of plate tectonics. Yet, the mechanics and evolution of continental rifting and the dynamics by which distributed continental deformation is progressively focused at oceanic spreading centres remain unclear. Two examples (one fossil, one active) and thermal/rheological and analogue modelling suggest that weakening due to magma intrusion in the lithosphere may be a controlling factor on continental break-up and oceanization.

The Western Alpine - Northern Apennine ophiolitic peridotites represent portions of subcontinental lithospheric mantle, which underwent progressive exhumation related to lithospheric extension between Europe and Adria, and were exposed at the sea-floor of the Mesozoic Ligurian Tethys. Field work evidences that, when residing in the mantle lithosphere, the peridotites were diffusely percolated by melts generated by decompressional melting of the asthenosphere which was adiabatically upwelling in response to lithospheric extension and thinning. This percolation was accompanied by significant heating of the subcontinental mantle to asthenospheric conditions, which resulted in the thermo-chemical erosion ("asthenospherisation") of the mantle lithosphere. Distribution and abundance of these "modified" peridotites within the ophiolitic peridotites from the Ligurian Tethys suggest that substantial volumes of the lithospheric mantle along the axial zone of the future basin underwent these melt-related processes and were asthenospherised, pointing to a major role played by magmatism on break-up and oceanization.

Massive magma intrusion within the continental lithosphere has been recently imaged in the Main Ethiopian Rift, East Africa, which is is an active rift in the break-up stage that marks the incipient boundary between the Nubia and Somalia plates. This rift is characterized by the occurrence of tectono-magmatic segments of focused deformation and volcanism affecting the rift depression; addition of voluminous magmatic material has been imaged below these segments in the upper 75 km of the continental lithosphere in the form of cooled mafic magma intrusion, melt-filled cracks or dykes, magma chambers. The tectono-magmatic segments are currently acting as a slow-spreading ridge mid ocean ridge; continental break-up occurs for a limited amount of extension-related lithospheric thinning, indicating that magma penetration of the lithosphere strongly facilitates rupture of continental plates.

Both examples suggest that the thermal and rheological consequences of magma intrusion in the lithosphere may weaken the continental lithosphere to the point of its rupture. Thermal and rheological models confirm that the strength of the continental lithosphere may be reduced up to one order of magnitude, provided that a significant thickness of the lithosphere is weakened. Following this strength reduction, strong localization of the extensional strain may occur in the intruded region. Small-scale analogue models support this conclusion and show strong localised thinning of the continental lithosphere when the lithosphere is characterised by significant weakening within a narrow region. In these conditions, continental break-up may be achieved very rapidly, supporting a major role played by magma in the transition to localised oceanic spreading.

METASOMATISM IN MANTLE XENOLITHS FROM INTRAPLATE AND SUPRASUBDUCTION SETTINGS

M. Coltorti

Dipartimento di Scienze della Terra, Università di Ferrara, Italy
clt@unife.it

Chemical composition of minerals and glasses in mantle xenoliths in alkaline basalts from intraplate (Cape Verde, Antarctica, Gran Comore, Lessini) and in calc-alkaline basalts from suprasubduction settings (Kamchatcka, Japan, Philippine, Grenada) are summarized, with the aim of highlighting the petrological features of the metasomatizing melts in the two environments. Two peridotites complexes (Finero and Val d'Ultimo) believed to represent subduction-metasomatized bodies are also included in the comparison.

It appears that, at comparable SiO_2, subduction-related glasses are characterized by lower alkalies contents than glasses from intra-plate settings. The more SiO_2-saturated character of the metasomatizing melts in this environament is also evidenced by the widespread presence of secondary orthopyroxene. Subduction-related glasses may have Na_2O content similar to carbonatite-metasomatised intra-plate glasses, but the latter presents consistently higher CaO and Nb abundances. Subduction-related glasses have also lower Rb, Ba, Zr, Ti and HREE contents than alkali-silicate intra-plate glasses, bearing some analogies with slab-derived melt. Chemical features of erupted adakites are however unable to take into account the whole compositional range of minerals and glasses in subduction zone. Irrespective of textural positions, amphiboles in mantle xenoliths from intra-plate settings present much higher Nb and, to a lesser extent, Zr and Ti contents than amphiboles found in xenoliths from suprasubduction setting. Similar indications, although less robust for crystallographic and statistical reasons, can be found for clinopyroxene and orthopyroxene. These data strongly suggest that metasomatizing agents in the mantle wedge above a subduction zone are richer in SiO_2 and depleted in Nb, Zr and Ti with respect to fluids migrating in intra-plate setting. The presence of accessory phases such as rutile and zircon in the downgoing slab, retaining HFSE during dehydration and/or melting and producing HFSE-depleted fluids seems to account for the observed geochemical features. The commonly observed occurrence of "plume-related" alkaline magmatism which follows in a time span of few to ten millions of years a subduction process, together with the position of the major volcanic province within Europe which seems to be correlated with the presence of a zone of high-velocity, presumed subducted slab material, at the base of the upper mantle point toward a link between subduction processes and alkaline basalts petrogenesis.

PETROLOGIC PROCESSES AND GEODYNAMICS

Session 2
Petrology and vulcanology

UNDERSTANDING HOW ACTIVE VOLCANOES WORK: A PETROLOGICAL AND GEOCHEMICAL PERSPECTIVE

A. Peccerillo

Dipartimento di Scienze della Terra, Università di Perugia, Italy
pecceang@unipg.it

The understanding of the physical conditions of magma storage and crystallisation, of the nature and timing of magmatic processes in crustal reservoirs is relevant for the aim of working out reliable models of the internal structure of volcanoes. This is an essential preliminary step for getting a better understanding of causes of volcanic phenomena occurring at the surface and for establishing more reliable criteria for monitoring active volcanoes.

Petrological and geochemical studies on volcanic rocks and minerals, along with studies on fluid inclusions, can contribute substantially to this objective [1-3]. Major, trace element and isotopic studies of volcanic rocks, single mineral phases and fluid inclusions entrapped into igneous mineral have been used to work out models of the plumbing system of several active volcanoes in several tectonic environments. Textural features of volcanic rocks, such as crystal size distribution, have helped substantially to shed light on timing of magma ascent and eruption [4]. Crystal chemistry data on mineral phases are also helpful to elucidate conditions of magma ponding and crystallisations [5].

Vesuvius, Vulcano and Stromboli represent three active volcanic centres in southern Italy. Petrological, geochemical and isotopic studies of volcanic rocks and minerals from these centres, along with fluid inclusion studies, have allowed to work out models of their plumbing systems and the way magmas behave during ascent to the surface. It has been demonstrated that several levels of magma ponding occur beneath these volcanoes and that much of the behaviour of magmas during eruptions are closely related to evolution processes occurring within the magmatic chambers at various depths [6,7]. Its has been demonstrated that the role of magmas stored in deep reservoirs is much more important than believed in the past, opening new ways to establishing better strategy of monitoring and forecasting of volcanic eruptions.

References. [1] M.L. Frezzotti, A. Peccerillo, *Eos*, **85**, 157-163, 100-110, 2004; [2] L. Francalanci, S. Tommasini, S. Conticelli, G.R. Davies, *Earth Planet. Sc. Lett.*, **167**, 61-69, 1999; [3] A. Peccerillo, *Acta Vulcanol.*, **17**, 43-52, 2005; [4] D. Perugini, G. Ventura, M. Petrelli, G. Poli, *Earth Planet. Sc. Lett.*, **222**, 1051-1066 , 2004; [5] S. Nazzareni, M. Molin, A. Peccerillo, P.F. Zanazzi, *B. Volcanol*., **63**, 73-82. 2001; [6] R. Cioni, P. Marianelli, R. Santacroce, *J. Geophys. Res*., **103**, 18227-18294, 1997; [7] A. Peccerillo, M.L. Frezzotti, G. De Astis, G. Ventura, *Geology*, **34**, 17-20, 2006.

TIME-SCALES OF VOLCANIC PROCESSES: CONSTRAINTS FROM ROCK TEXTURES, TRACE ELEMENT DIFFUSIVITY AND MODELLING

D. Perugini

Dipartimento di Scienze della Terra, Università di Perugia, Italy
diegop@unipg.it

Recent researches on magma interaction systems have shown that, during the mixing process, different fluid dynamic domains can be generated in which chemical exchanges between magmas can be strongly modulated, depending on the ability of the two melts to spread across the magmatic system [1-3]. These structural domains, tightly linked to the chaotic nature of the magma mixing process, are preserved in igneous rocks as fractal structures, which can be recognized from the meter to the micrometer length-scale.

Detailed petrological studies of lava microstructures generated by magma mixing revealed the presence, in the same system, of highly heterogeneous volumes of melts in which both depletion and enrichment of trace elements occurred, depending on the values of their chemical diffusion coefficients, triggering a "diffusive fractionation" process [4].

Numerical simulations in which mixing process was induced by applying a chaotic advection numerical scheme and a chemical diffusion model, revealed that the "diffusive fractionation" of trace elements, analogous to that observed in lava flows, can be readily achieved and that the extent of this process depends upon the mixing time.

Chaotic magma mixing experiments were performed experimentally in a Taylor-Couette-like experimental setting by mixing natural magmatic compositions from Phlegrean Fields. Experiments were carried out at different mixing times. Micro-analysis of experimental runs confirmed a very variable mobility for the different trace elements, depending on diffusion coefficients. Equations relating the degree of "diffusive fractionation" of trace elements to the time-scales of mixing have been derived from experimental data.

Application of the "diffusive fractionation" conceptual model to two pyroclastic sequences from Phlegrean Fields (Astroni 6 and Averno) allowed us to apply the relationships derived from numerical and experimental petrology experiments to estimate mixing time-scales for these two magmatic systems. Results indicate that mixing processes in Astroni 6 and Averno systems lasted for ca. two and eight days, respectively. These short time-scales for the mixing process argue in favor of the hypothesis that refilling of magma chambers and magma mixing processes likely represent the key processes that triggered eruptions of the two volcanic systems.

In conclusion, combination of Chaos theory, classic petrology, microtextural evidence, numerical simulations and experimental petrology is a highly effective and much needed approach to increase our knowledge on the behavior of volcanic systems, especially for the key issue of constraining time-scales of volcanic eruptions and hazard assessment at active volcanic centres.

References. [1] D. Perugini, G. Poli, R. Mazzuoli, *J. Volcanol. Geoth. Res.*, **124**, 255-279, 2003; [2] D. Perugini, G. Ventura, M. Petrelli, G. Poli, *Earth Planet Sc. Lett.*, **222**, 1051-1066, 2004; [3] D. Perugini, M. Petrelli, G. Poli, *Physica A*, **370**, 741-746, 2006; [4] D. Perugini, M. Petrelli, G. Poli, *Earth Planet. Sc. Lett.*, **243**, 669-680, 2006.

REVEALING MACRO-SCALE VOLCANIC PROCESSES BY MICRO-SCALE CHEMICAL AND ISOTOPIC ANALYSES

L. Francalanci

Dipartimento di Scienze della Terra, Università di Firenze, Italy
lorella.francalanci@unifi.it

Mineral/liquid elemental and isotopic disequilibria occur in many volcanic systems and are often key factors in revealing pre-eruptive magmatic processes. Indeed, bulk rock compositions often represent a mechanical mixture of various phases with possible different origin. Mineral phases retain the history of changing physical and chemical conditions during their growth and therefore record more information on processes occurring during the magma ascent to the surface than the whole-rock. Accordingly, *in situ* mineral determinations of $^{87}Sr/^{86}Sr$ values, associated with major and trace element analyses on core-rim traverses, give us the opportunity to understand the configurations of the volcanic plumbing systems and the timescales through which magmas are assembled, differentiated and delivered to sites of eruptions. Examples on active volcanoes will be reported.

The present-day activity of Stromboli volcano will be considered as main case study. This persistent activity, which mainly consists of moderate explosions ejecting scoria bombs, lapilli and ash, is sometime broken either by effusive events or by more violent explosions. The latter paroxysms also erupt a variable volume of light pumice. A volatile poor and highly porphyritic magma (HP magma) with about 50 vol% of olivine, clinopyroxene and plagioclase phenocrysts, is erupted by effusive and normal Strombolian eruptions, whereas a volatile rich magma with very low phenocryst contents (LP magma; usually < 5 vol% of crystals) of olivine and clinopyroxene ± plagioclase, is only outpoured as pumice by paroxysms. The LP magma is slightly less evolved and has a distinct composition of groundmass and Sr isotope ratios than the HP magma. The different petrographic, mineralogical, geochemical and isotopic characteristics provide evidence that the LP and HP magmas are characterised by sharply distinct physical-chemical conditions.

In situ geochemical and Sr isotope analyses on plagioclase and clinopyroxene significantly contributed to the knowledge of the configuration of the present day plumbing system. They clearly define the process of mixing between HP and LP magmas + crystallisation of clinopyroxene, plagioclase and olivine, occurring in the shallow reservoir (probably at around 100 MPa) feeding the present day Strombolian activity. The LP magma is deep sited (probably at about 300 MPa) and represents the refreshing magma of the shallow reservoir. Its fast arrival at very shallow level causes the paroxysmal eruptions. Integrated *in situ* Sr isotope and major element data of xenocryst cores in pumice demonstrate that the HP magma in the shallow reservoir is not fully degassed when interacting with the LP magma, making possible an efficient mixing process that often produces a well overturned homogeneous reservoir.

A third component in the plumbing system of Stromboli, together with the HP and LP magmas, has been moreover found by the fundamental contribution of the isotopic micro-Sr analyses. This component is represented by more Sr-radiogenic re-cycled minerals, found as resorbed cores of large phenocrysts, and deriving from an older (up to 10 ka ago) cumulus crystal-mush zone, which is periodically disrupted and sampled by the LP ascending magmas, thus possibly interfering with the mechanisms of the paroxysmal explosions. An increased volume of LP magma entering into the shallow reservoir before the lava effusions has been also pointed out by detailed micro-analytical studies on the last lavas (2002-2003 and 2007).

PETROLOGIC PROCESSES AND GEODYNAMICS

Session 3
Magmatic processes

GEOCHEMICAL AND PETROLOGICAL EVOLUTION OF BARREN ISLAND (ANDAMAN SEA, INDIAN OCEAN)

A.P. Santo[1,2], B. Capaccioni[3], D. Chandrasekharam[4], O. Vaselli[1,2], M.A. Alam[1], P. Manetti[1], F. Tassi[1]

[1]*Dipartimento di Scienze della Terra, Università di Firenze, Italy*
[2]*CNR-IGG, Firenze, Italy*
[3]*Dipartimento di Scienze della Terra e Geologico-Ambientali, Università di Bologna, Italy*
[4]*Department of Earth Sciences, Indian Institute of Technology, Bombay, India*
alba.santo@unifi.it

Barren (12.29°N, 93.85°E, Andaman Sea, Indian Ocean) is a subduction-related volcanic island, located at about 135 km NE of Port Blair, the capital of the Andaman and Nicobar Archipelago, to which it belongs to. Barren Island (BI) is unmanned and represents the only active volcanic system in the Indian subcontinent. The BI rises for about 2300 m from the sea floor, with an elevation of 355 m a.s.l. and consists of a 2-km-wide caldera, open to the sea on the West, which could have formed by either a giant, non-eruptive lateral landslide of the original volcanic cone or vertical collapse of a shallow magma chamber as a result of a paroxysmal eruption. However, there is no conclusive evidence for any of the two mechanisms of formation. The oldest rocks are apparently related to the Late Pleistocene, although no radiometric dating is presently available. The morphology of a fresh pyroclastic cone that was built up in the centre of the caldera has changed during historical eruptions which have also frequently produced lava flows. These effusive events have partly filled the caldera floor and have occasionally reached the sea along the western coast. The last strombolian eruption started on May 2005 and apparently has continued through September 2007. In this work we present two new geological maps prior and after the 2005 eruption of the Barren Island together with new petrological, geochemical and isotopic data of the pre- and post-calderic volcanic products, which display some significative differences. The transition from the pre- to post-caldera formations is marked by the presence of hydromagmatic deposits, firstly described in this study.

The volcanic products show a small compositional variation: from low-K basalts to basaltic andesites. Pre-caldera magmas display a general less evolved composition (*i.e.* higher Mg#, higher Ni and Cr content), scattering of major and trace element abundances and a relatively high variability of the Sr isotopic ratios; on the contrary, post-caldera magmas, basalts in particular, have a more homogeneous composition with almost constant Sr isotopic ratios, corresponding to the highest values measured in the pre-caldera magmas. Petrographic and geochemical features indicate that crystal-liquid fractionation processes have played a key role for the BI magmas. However, the presence of megacrysts (plagioclase, clinopyroxene and olivine) of possible xenocrystic origin, the small but significant variations of the Sr isotopic ratios in the pre-caldera magmas, the relationships between $^{87}Sr/^{86}Sr$ and abundances and ratios of trace elements and the variability of incompatible trace element ratios in the basaltic rocks point to either the occurrence of additional evolutionary processes and/or a role of a heterogeneous magma source. The most primitive BI magma (Mg# = 71, Ni = 218 ppm, Cr = 557 ppm), displaying the lowest Th contents in the arc, recognized in the present work, represents an important reference composition for the Andaman - Indonesian Arc study.

TEPHROCRONOLOGY WITH ^{40}Ar–^{39}Ar DATING OF RECENT (< 20 KYRS) SILICIC VOLCANISM AT PANTELLERIA ISLAND: IMPLICATIONS ON MAGMATIC SYSTEM

S. La Felice[1], S. Rotolo[1], S. Scaillet[2], G. Vita[2]

[1]*Dipartimento C.F.T.A., Università di Palermo, Italy*
[2]*LSCE, CNRS/CEA, Gif-sur-Yvette, France*
s.lafelice@unipa.it

The recent eruptive history of felsic volcanism at Pantelleria island is characterized by an intricate tephrostratigraphy, reflecting the complex volcanologic evolution of the last 20 kyrs. Silicic volcanism during this period was centred within of the most recent caldera, the "Cinque Denti" caldera. The magmatic activity has been characterized by strombolian to sub-plinian eruptions and pantelleritic lava flows, produced by several eruptive centers and results in complex interfingered tephra sequences.

The principal aim of this study is to reconstruct the recent volcanological *scenario* and the stratigraphy with particular attention to the petrological implications on space-time evolution of the magmatic system. Therefore, it was essential to combine the field observations, the petrochemical study and the $^{40}Ar/^{39}Ar$ dating.

Ten eruptive units of pantelleritic pumice air-fall deposits and pantelleritic lava flows have been recognized, mapped and petrographically characterized.

All the analysed rocks are peralkaline in composition (from trachyte to rhyolite) and the agpaitic index (*i.e.* the $Na_2O + K_2O/Al_2O_3$ molar ratio) ranges from 1.3 to 1.8.

We have selected the most representative eruptions for $^{40}Ar/^{39}Ar$ laser dating, on anorthoclases collected from the 0.5-1.0 mm or from the 1.0-1.6 mm grain size fractions.

The possibility to decipher some relevant age-related volcano tectonic features was severely limited in previous K/Ar ages by the large quoted errors, in full reciprocal overlap amongst the different deposits. As a whole, our ages range from 16 kyrs to 6 kyrs; the youngest eruption occurred on the N slopes of M. Grande, and was related to the initial explosive phases of the Cuddia Gallo pantelleritic lava dome. The relatively older activity (almost 14 kyrs ago) occurred above the buried Cinque Denti caldera rim in South sector of the island, almost contemporaneous with Cuddia Mueggen and M. Gelfiser shield volcanoes.

The existing ages are variably affected by incorporation of $^{40}Ar_{xs}$, resulting in variably older ages with respect to $^{40}Ar/^{39}Ar$ ages. We envisage in the presence of anorthoclase xenocrysts, the major source of inherited argon. The similarity between the magmas that fed the Mueggen and Patite eruptions strongly suggests that considerable amounts of the same pantelleritic magma were ponding below Montagna Grande in recent times, and that an active role was played by the caldera-related fracture system in draining volatile-rich magma in the south sector (Patite) or outgassed magma in the east sector (Mueggen).

CONSTRAINTS ON PRE-ERUPTIVE CONDITIONS OF RECENT FELSIC EXPLOSIVE VOLCANISM AT PANTELLERIA: AN EXPERIMENTAL APPROACH

I. Di Carlo[1], S. Rotolo[1], B. Scaillet[2], M. Pichavant[2]

[1]*Dipartimento di Chimica e Fisica della Terra, Università di Palermo, Italy*
[2]*Institut des Sciences de la Terre d'Orléans (ISTO), CNRS - Université d'Orléans, France*
di.carlo@unipa.it

Pantelleria island (Sicily Channel) was characterized during the last 50 ka by the emission of abundant peralkaline rhyolites and minor amounts of alkali basalts. Peralkaline magma (*i.e.* pantellerites) may have elevated pre-eruptive melt H_2O contents, but chlorine can also represent an important volatile constituent. Chlorine behaviour during magma degassing is more complex than water because of the existence of solid-liquid-gas immiscibility in the H_2O-$NaCl_{eq}$ system at low pressures (< 2 kbar) and also because chlorine solubility seems to be strongly dependent on fO_2.

In the framework of an INGV-DPC project (V3-07, Pantelleria), we pursued an experimental petrology study aimed at: 1) constraining the pre-eruptive T, P, melt H_2O content of pantelleritic magmas, when matched with natural phase equilibria (phase equilibrium experiments); 2) evaluating the solubility of chlorine *vs.* pressure at different fO_2 (chlorine solubility experiments).

We selected a recent pantelleritic pumiceous agglutinate (agpaitic index = 1.68 − $[Cl]_m$ = 0.4 wt.%) as starting material. Phenocryst (kfs, Na-cpx, Fa, aenig, ilm, +/− amph +/− qz) content is 20 vol%, and the natural sample is also characterized by late halite occurrence.

The starting pantellerite was fused at 1200°C, 1 atm, and the resulting glass was used as starting material. Phase equilibrium experiments (from nominally dry up to water saturation conditions) were performed over a pressure range corresponding to expected storage conditions of felsic magmas at Pantelleria (P = 1.5-0.25 kb, T = 800-680°C) in an Internally Heated Pressure Vessel (IHPV). Redox conditions were imposed close to, or below, the QFM buffer. Chlorine solubility experiments were performed over the pressure range 1.5-0.25 kb at T = 800°C, and at two fO_2 conditions: NNO-2 (IHPV) and NNO+2 (CSPV, cold seal pressure vessel) with variable amounts of aqueous solutions containing both NaCl and KCl (five solutions containing from 1 to 30% eq NaCl).

Ti-magnetite is the first phase to crystallise followed by clinopyroxene, then K- feldspar and later quartz. Aenigmatite crystallisation is inhibited for pressure < 1.0 kb. At 1.5 kb and 680°C the dominant phenocryst assemblage in the natural sample (cpx, aenig, kfs, ox) is produced for melt H_2O content of 3-4 wt.%. Amphibole, the last phase to crystallise, appears at 680°C either at 1.5 or at 1 kb. The presence of aenigmatite +/− amphibole in the natural sample sets a minimum P of 1 kb, since lower pressure experiments crystallize neither amphibole nor aenigmatite.

At 1.5 kb, oxidizing and reducing conditions impose the same chlorine concentrations when saturated with a brine. Generally, however, at the same P, more oxidizing experimental conditions give rise to lower chlorine contents in the melt than those reducing: the possibility that Cl complexes with Fe^{2+} and/or Na^+ in silicate melts can explain higher Cl solubility in more reducing experiments. Our results suggest that the pre-eruptive Cl content of melt inclusions, if brine-saturated, requires a trapping pressure of ca 1 kb, in good agreement with phase equilibrium constraints.

THE RECENT LATITES OF LIPARI AND VULCANO: EVIDENCE FOR A COMMON ORIGIN

D. Barca, M. Davì, R. De Rosa, P. Donato

Dipartimento di Scienze della Terra, Università della Calabria, Italy
davi@unical.it

Lipari and Vulcano islands belong to the central sector of the Aeolian Arc. Since the last 50 ka southern Lipari and northern Vulcano are considered as a single volcanic complex (LVVC) on the base of petrographic, geochemical and structural studies [1]. A common feature of the historical Lipari and Vulcano eruptions is the emission of intermediate latitic products associated with mafic or salic rocks. In particular at Rocche Rosse (Lipari; 1230±40 A.D.) and Commenda (Vulcano; 1200 A.D.) latite was erupted as enclaves in obsidianaceous rhyolitic lava flows. Instead, at Palizzi (Vulcano; 1200 A.D.) and Vulcanello (Punta del Roveto; Vulcano, 1600 A.D.) they gave lava flows associated with rhyolitic pyroclastites and shoshonitic products, respectively.

Despite their different occurrence and association, latites show similar petrographic and geochemical features.

Bulk rock from different eruptions show similar major (XRF) element contents, falling in the same compositional field of the Peccerillo and Taylor [2] classificative diagram. Spider diagrams of the incompatible elements (XRF) and REE (ICPMS) patterns are also superimposed for all products.

In order to better investigate similarities among the several latites, a major (SEM-EDS) and trace (LA-ICPMS) elements investigation has been carried out on their main mineral phases (*i.e.* clinopyroxene, plagioclase and K-feldspar).

Clinopyroxene ($Wo_{43-46}En_{39-44}Fs_{13-15}$, Mg# = 0.72-0.76) is the most abundant phase of all latites and its trace element composition is strongly similar among the different products. REE patterns are coincident and show an Eu negative anomaly (average value 0.65) which is inversely correlated with Mg#.

K-feldspar ($An_{0-3.50}Ab_{37-39}Or_{60-61}$) crystals have been analyzed only in Rocche Rosse and Palizzi products. They show superimposed incompatible trace element and LREE patterns with Eu positive anomaly up to 41 while HREE are below the detection limit.

Plagioclase ($An_{38-49}Ab_{50-42}Or_{12-9}$) phenocrysts composition has been determined at Commenda, Palizzi and Vulcanello. Spider diagrams of incompatible trace elements are very similar showing a strong positive anomaly of Sr and very low HFSE contents often close to detection limit. LREE patterns are also nearly coincident (Eu/Eu* in the range 6-10).

Similarities among major and trace element of both bulk rock and mineral phases strongly suggest that all latites are probably related to a similar parental magma. Geochemical models have been drawn to test the origin of latite of the different eruptions. Results show an origin by AFC (Fractional Crystallization plus Assimilation) starting from the shoshonitic basalt found in the olivine melt inclusion of La Fossa cone 1888-1890 products [3]. Available isotopic data and geochemical signatures seem to indicate low crustal assimilation rates.

References. [1] A. Gioncada, R. Mazzuoli, M. Bisson, M.T. Pareschi, *J. Volcanol. Geoth. Res*., **122**, 191-220, 2003; [2] A. Peccerillo, S.R. Taylor, *Contrib. Mineral. Petr*., **58**, 63-81, 1976; [3] A. Gioncada, R. Clocchiatti, A. Sbrana, P. Bottazzi, D. Massare, L. Ottolini, *B. Volcanol*., **60**, 286-306, 1998.

A COMBINED SEM-EDX AND LA-ICP-MS STUDY OF THE MARSILI SEAMOUNT BASIC LAVAS, SOUTHERN TYRRHENIAN BACK-ARC BASIN: PRELIMINARY RESULTS

D. Barca[1], E. De Vuono[1], T. Trua[2]

[1]*Dipartimento di Scienze della Terra, Università della Calabria, Rende (CS), Italy*
[2]*Dipartimento di Scienze della Terra, Università di Parma, Italy*
d.barca@unical.it

The southern Tyrrhenian back-arc basin (BAB), the youngest (< 7 Ma) volcanically active BAB of the Western Mediterranean area, is distinctive in having in its axial zone a well developed, magmatically inflated, morphology represented by the Marsili volcano.

Previous petrological studies on the more primitive Marsili samples indicate that two distinct island arc basalt (IAB)-like magmas contributed to the Marsili petrogenesis; but, the involvement of an OIB-like mantle component is also required to explain the genesis of the OIB-like magmas erupted during the latest stage of Marsili magmatism.

In order to better investigate the processes involved in the origin of the different Marsili basic magmas, a combined SEM-EDX and LA-ICP-MS study has been carried out on the mineral phases and glass of four Marsili samples (*i.e.*, D6: OIB-like; MRS3E2 and MRS3F1: IAB-like type 1; D12: IAB-like type 2), representative of the Marsili basic lavas spectrum and showing specific petrologic, geochemical and isotopic signatures.

This study shows that significant geochemical differences do exist in the mineral phases, *i.e.,* olivine (ol), clinopyroxene (cpx), and plagioclase (pl), as well as in the glass of the analysed samples. Indeed, ol (Fo) shows narrow, but distinct, compositional ranges for the IAB-like samples, whereas ol from the OIB-like sample displays a wider compositional range, with one end overlapping the whole compositional range observed for the IAB ol. Only IAB-like type 2 and OIB-like samples have cpx phenocrysts. Compared to the cpx in the IAB-like type 2 sample, cpx phenocrysts in the OIB-like sample result to be enriched in light and middle REE. The range in the An content of the pl phenocrysts results to be the same for the IAB- and OIB-like samples, although it is related to a wider variation of Ba and Sr concentrations in the pl of the OIB-like sample. Finally, the *in situ* trace element composition of the analysed glasses of each sample shows a clear resemblance to that of the whole rocks, confirming that the variety of magmas types (*i.e.*, IAB- and OIB-like) coexist in the Marsili magmatic system.

The observed geochemical differences suggest that the Marsili IAB magmas migrated and differentiated beneath the volcano, without mixing each other. This could be possible if the magmatic plumbing system beneath Marsili seamount was made of small conduits at the time of the Marsili IAB magmatism. Instead, the geochemical features observed for the phenocrysts of the OIB-like sample suggest that, during the latest stage of Marsili magmatism, the Marsili magmatic plumbing system changed permitting the encountering of the intruding OIB-like magma with the older IAB magmas.

ANATECTIC MELT TRAPPED IN GARNET FROM MIGMATITES OF KERALA KHONDALITE BELT, SOUTHERN INDIA: EVIDENCE FROM CRYSTALLIZED AND GLASSY INCLUSIONS

S. Ferrero[1], B. Cesare[1], E. Salvioli Mariani[2], D. Pedron[3], A. Cavallo[4]

[1]*Dipartimento di Geoscienze, Università di Padova, Italy*
[2]*Dipartimento di Scienze della Terra, Università di Parma, Italy*
[3]*Dipartimento di Scienze Chimiche, Università di Padova, Italy*
[4]*Istituto Nazionale di Geofisica e Vulcanologia - Sezione Roma1, Italy*
silvio.ferrero@unipd.it

Primary melt inclusions have been found in garnets from metapelitic migmatites of the Kerala Khondalite Belt, southern India. Host rocks are 521-535 Ma in age and underwent UHT metamorphism and partial melting at ≈ 900°C and ≈ 8 kbar, with development of a Crd-Grt-Sil-Qtz-Kfs-Bt-Ilm-melt assemblage. Garnet is abundant and sized up to 1 cm. Clusters of preserved melt inclusions are up to 500 microns wide and localised randomly within the host phase. Clusters contain two different types of melt inclusions: 1) crystallised melt inclusions and 2) glassy inclusions. The crystallised inclusions are rounded in shape, locally with incipient negative crystals shape, and up to 20 micron in size. They are holocrystalline (no visible shrinkage bubble) and contain the assemblage Qtz + Kfs + Ab + Bt + Fe-oxide ± Rt ± Ap ± Zrn with a grain size from 100 nanometres up to 2 microns. By these features we can call such a composite solid inclusion a "nanogranite". The glassy inclusions are smaller, sizing less than 5 microns. The shape is similar to previous inclusions, even if more spherical. Every glassy inclusions is composed by glass (> 70% volume) + crystals such as Rt, Zr and Ap. These minerals seem to be solid inclusions that were trapped together with melt in the inclusions. The nature of the glass is supported by microscopic evidence, EMP data and Raman Spectroscopy analyses. Particularly, the EMP analyses provide an ultrapotassic rhyolitic composition (SiO_2 = 68-73 %).Based on mode of occurrence, modal and chemical composition, we infer that these inclusions represent the evidence of the anatectic melt produced by the partial melting of the migmatite.

This is the first case of preserved – either glassy or crystallized – melt inclusions found within a regional migmatite, that underwent a complex post-peak history, with slow cooling and exhumation lasting tens of m.y. Until now only volcanic rocks showed inclusions like these. Moreover the coexistence of two different types of preserved melt inclusions in the same cluster is a remarkable feature. This fact can be explained by the different kinetic behaviour: since the fully crystallized inclusions are the biggest in size, it is possible to imagine that volume/surface ratio has a key-role in the preservation of glass *versus* total crystallization. Alternatively, the volatile contents may have had an influence on the internal diffusivity of the cooling melt entrapped within the inclusion.

PETROGRAPHY AND GEOCHEMISTRY OF TRACHILAS AND FYRIPLAKA (MILOS ISLAND, GREECE) PRODUCTS: A PRELIMINARY STUDY

V. Azzaro[1], R. De Rosa[1], P. Donato[1], K. Kyriakopoulos[2], M. Lupo[1], G. Niceforo[1]

[1]*Dipartimento di Scienze della Terra, Università della Calabria, Italy*
[2]*Departement of Geology and Geoenvironment, University of Athens, Greece*
donatop@unical.it

In this work we present a preliminary study on the deposits of Trachilas and Fyriplaka, two Pleistocenic eruptive centres on the island of Milos (Cyclades, Southern Aegean Sea). Both centres were built by alternating effusive and explosive phases, these lasts leading to the formation of tuff rings. The composition of erupted products is mainly rhyolitic [1].

Trachilas and Fyriplaka rocks show differences both in the petrography and geochemistry: biotite, plagioclase and quartz are present in both products even if with different compositions and percentages, while K-feldspar is present only in Trachilas. Besides, in Trachilas the opaques are represented only by Fe-Ti oxides, while in Firyplaka both Fe and Fe-Ti oxides occur. The differences in the petrography also reflect in the chemical composition: Trachilas whole rock and glasses are more K-rich than Fyriplaka ones; in these lasts the Na_2O/K_2O ratio is always > 1.

Some preliminary consideration can be done on the pre-eruptive conditions of the two magmas:

1) the simultaneous occurrence of two different oxides (ilmenite and magnetite) in the Fyriplaka products allowed us to obtain a pre-eruptive temperature of about 740°C, and a $-\log fO_2$ of 14;

2) in the Trachilas samples, the presence of two feldspars (sanidine and plagioclase) allowed us to apply the Stormer geothermometer [2]. For a depth of 5-6 km (P = 2 kbars) we obtained a pre-eruptive temperature of 690°C, while in the hypothesis of a deeper magma chamber (15 km, about 5 kbars) we obtained a slightly higher temperature (730°C).

3) indication on the oxygen fugacity for Trachilas comes from the biotite composition, less Mg-rich than that of Fyriplaka: this suggests that the Trachilas magma was in relatively less oxidizing conditions before the eruption [3].

Preliminary data collected in this work thus suggest that the pre-eruptive conditions of the two magmas can be different and that this can account for their differences.

References. [1] M. Fytikas, F. Innocenti, N. Kolios, P. Manetti, R. Mazzuoli, G. Poli, F. Rita, L.Villari, *J. Volcanol. Geoth. Res.*, **28**, 297-317, 1986; [2] J.C. Stormer, *Am. Mineral*., **60**, 667-674, 1975. [3] J. Berndt, F. Holtz, J. Koepke, *Contrib. Mineral. Petr.*, **140**, 469-486, 2001.

U-Pb SHRIMP II GEOCHRONOLOGY OF THE MAGMATIC ENCLAVES OCCURRING IN THE EUGANEAN HILLS MAGMATIC COMPLEX

O. Bartoli[1], S. Meli[1], M. Bergomi[2], D. Magaraci[3], R. Sassi[3], D.-Y Liu[4]

[1]*Dipartimento di Scienze della Terra, Università di Parma, Italy*
[2]*Dipartimento di Scienze Geologiche e Geotecnologie, Università di Milano-Bicocca, Italy*
[3]*Dipartimento di Geoscienze, Università di Padova, Italy*
[4]*SHRIMP CENTER, Chinese Academy of Geological Sciences, Beijing, China*
sandrom@unipr.it

Many of the Euganean trachytes bear igneous enclaves of different nature and composition. Five different types of enclaves have been recognized: (i) blobs of mafic magmas quenched within the trachyte: they belong to the transitional series and are classified as trachybasalts, basaltic trachyandesites and trachyandesites; phenocrysts are Cpx, Pl and, in more evolved enclaves, Amph, Bt and Kfs; (ii) dioritic to granitic enclaves, which display typical hypidiomorphic textures; (iii) highly porphyritic enclaves ("crystal mushes"): the glomerocrysts are composed by the same minerals occurring as phenocrysts in the host trachyte; (iv) partially molten granitoids; (v) cumulitic enclaves: mainly heteradcumulates, where Cpx, Amph and Pl are the common cumulus minerals, and Amph, Pl, Ilm, Bt, Ap are the intercumulus phases.

U-Th-Pb analyses were performed on two enclaves at the Beijing SHRIMP Center, employing a sensitive high-resolution ion microprobe (SHRIMP II). Data processing was carried out using the Squid 1.08 and Isoplot/Ex3 add-in programs [1,2]. The $^{206}Pb/^{238}U$ ratios and ages were corrected on the basis of the ^{207}Pb common lead [3,4]. Since some samples show a high proportion of common Pb, the age calculations were conducted by regressing uncorrected ratios in a Tera-Wasserburg concordia diagram [5]. The data from each sample are dispersed along a mixing line between common Pb and a single radiogenic end member, and whose intersection with the concordia line defines the age of the samples [6].

The $^{206}Pb/^{238}U$ ages obtained from MM28 zircon grains scatter from 31.3 ± 0.8 to 34.8 ± 1.2 Ma. Fourteen analyses give a weighted average $^{206}Pb/^{238}U$ age of 32.94 ± 0.59 Ma (MSWD = 0.94, probability of fit = 0.51), whereas on Tera-Wasserburg diagram they define an intercept age of 32.76 ± 0.66 Ma (MSWD = 0.78, probability = 0.67).

Nine SHRIMP U-Th-Pb analyses on zircons from ML19 yield $^{206}Pb/^{238}U$ ages ranging between 29.4 ± 1.3 and 32.3 ± 1.3 Ma with a weighted average $^{206}Pb/^{238}U$ age of 30.83 ± 0.68 Ma. The MSWD of 1.5 (probability of fit = 0.13) appears in excess of scatter attributable to experimental error of a population of only nine points. On Tera-Wasserburg diagram they define an intercept age of 30.9 ± 1.6 Ma (MSWD = 1.8, probability of fit = 0.07).

The Early Oligocene age of 31 ± 1 Ma (Rupelian) is interpreted as the crystallization age of the enclaves under investigation. These enclaves are coeval with the volcanics which host them [7]. Taking also into account Sr isotopic data, which suggest that very little crustal contamination took place in this volcanic district [8], we can strengthen the hypothesis that the magmatic enclaves hosted in the Euganean Hills lavas are cogenetic with their hosts: they represent different stages of fractional crystallization of a system of magmatic chambers.

References. [1] K.R. Ludwig, *Berkeley Geochron. Center, Sp. Publ.,* **1a**, 2001; [2] K.R. Ludwig, *Berkeley Geochron. Center, Sp. Publ.,* **2**, 2001; [3] W. Compston, I.S. Williams, J.L. Kirschvink, Z. Zhang, G. Ma, *J. Geol. Soc. London*, **149**, 171-184, 1992; [4] I.S. Williams, *Rev. Econ. Geol*., **7**, 1-35, 1998; [5] F. Tera, G. Wasserburg, *Earth Planet. Sc. Lett.*, **14**, 281-304, 1972; [6] K.R. Ludwig, *Geochim. Cosmochim. Ac.,* **62**, 665-676, 1998; [7] S. Borsi, G. Ferrara, G. Piccoli, *Rend. Soc. It. Miner. Petrol.*, **25**, 27-34, 1969; [8] L. Milani, L. Beccaluva, M. Coltorti, *Eur. J. Mineral*., **11**, 379-399, 1999.

EVOLUTION OF THE EUGANEAN HILLS MAGMATIC DISTRICT: A MODEL BASED ON MAGMATIC ENCLAVES

O. Bartoli[1], S. Meli[1], D. Magaraci[2], R. Sassi[2]

[1]*Dipartimento di Scienze della Terra, Università di Parma, Italy*
[2]*Dipartimento di Geoscienze, Università di Padova, Italy*
sandrom@unipr.it

In the Veneto region extensive volcanic activity took place from Late Paleocene to Late Oligocene and gave rise to four volcanic districts: Marostica Hills, Berici Mts., Lessini Mts., and Euganean Hills. On the basis of petrological and geochemical data, three main volcanic series were identified: alkaline, transitional and tholeiitic. The geochemistry of the volcanic districts points to intraplate geodynamic system were magmas originated in the spinel peridotite lithospheric mantle, from progressively deeper sources [1]. The most widespread rocks are alkali basalts, basanites and transitional basalts; more evolved trachytes occur only in the Euganean center. The geochemical features point to a within-plate tectonic setting, where a metasomatized Amph-bearing astenosphere underwent partial melting [2].

Five different types of igneous enclaves have been recognized in the Euganean Hills trachites and rhyolites [3]: (i) blobs of mafic magmas quenched within the trachyte, belonging to the transitional series: trachybasalts, basaltic trachyandesites and trachyandesites; (ii) dioritic to granitic enclaves; (iii) highly porphyritic enclaves, *i.e.*, crystal mushes; (iv) partially molten granitoids; (v) cumulitic enclaves: mainly heteradcumulates, where Cpx, Amph and Pl are the common cumulus minerals, and Amph, Pl, Ilm, Bt, Ap are the intercumulus phases.

We modelled the magmatic evolution considering the magmatic enclaves we found hosted in trachitic and rhyolitic lavas in the Monte Merlo center. We think that all kind of magmatic enclaves found in the Euganean Hills lavas are good proxies of the fractionating phases during the magmatic evolution of this center. The calculations for major elements are made employing XlFrac [4], Melts [5], whereas the calculations for trace elements were made employing programs which consider both partitioning coefficients and the possibility of assimilating crustal material. We employed Sr isotope data to monitor the contribution of crustal assimilation, which is yet considered to be a minor process [2]. We modelled the magmatic evolution of the transitional serie, starting from transitional basalt to rhyolite. As fractionating material, we considered the phases occurring in the cumulates, in the crystal mushes and in the enclaves showing granitic textures. We found that cumulates and gabbroic enclaves fit the evolutionary trend of the lavas, and can be formed directly by fractionating and cumulating of the crystallizing phases during the evolution from trachiandesite to trachite, through fractionation of Amph, Cpx, Pl, Bt, Ilm, Mt, Ap in different stages. The magmatic evolution of the Euganean Hills lavas is consistent with the fractionation of Kfs, Pl, Bt, Amph, Mt, Ap, occurring in the crystal mushes and in the granitoid enclaves with granitic and granodioritic bulk composition. This model is in accordance with a previous one, already proposed [2], but it is more detailed and links the hypothesized magmatic evolution of the center to something really detectable, and suggests fractionation of phases which are consistent with the geodynamic environment suggested [1] for the Euganean Hills magmatic center.

References. [1] L. Beccaluva, G. Bianchini, C. Bonadiman, M. Coltorti, L. Milani, L. Salvini, F. Siena, R. Tassinari, *Geol. Soc. Am. Spec. Paper*, **418**, 131-152; [2] L. Milani, L. Beccaluva, M. Coltorti, *Eur. J. Mineral*., **11**, 379-399, 1999; [3] D. Magaraci, S. Meli, R. Sassi, *Int. Geol. Congress, Florence, 20-28 Aug. 2004*, 1297, 2004; [4] J.C. Stormer, J. Nicholls, *Comput. Geosci*., **4**, 143-159, 1978; [5] M.S. Ghiorso, R.O. Sack, *Contrib. Mineral. Petr*., **119**, 197-212, 1995.

PLEISTOCENE VOLCANISM OF LINOSA ISLAND (SICILY CHANNEL, ITALY): PETROGENESIS AND GEODYNAMIC IMPLICATIONS

M. Di Bella[1], S. Russo[1], A. Peccerillo[2], M. Petrelli[2]

[1]*Dipartimento di Scienze della Terra, Università di Messina, Italy*
[2]*Dipartimento di Scienze della Terra, Università di Perugia, Italy*
mdibella@unime.it

The Linosa Island represents the emergent portion of a wide submarine volcanic complex placed on the SW edge of the Linosa graben, along the Sicily Channel rift zone, Pelagian Block. The island was formed between 1.06±0.10 and 0.53±0.07 Ma, through three main stages of volcanic activity: Paleolinosa, Arena Bianca and Monte Bandiera [1]. The volcanic rocks from Linosa Island exhibit a transitional to mildly Na-alkaline affinity and are mainly mafic in composition (alkali basalt to hawaiite); benmoreitic to trachytic lithic clasts occur in the lowest exposed pyroclastic deposits [1]. The aim of this study is to provide petrological and geochemical information able to constrain the origin and geodynamic significance of the volcanism in the Sicily Channel.

Major and trace elements of the studied volcanics show curved variation trends typical of magmatic series evolved through fractional crystallization processes. Mass balance calculations [2], MELTS thermodynamic modelling [3] and trace element modelling suggest an evolution by dominant fractional crystallisation, with separation of different proportions of the main minerals at variable pressures. Crustal assimilation played a very minor role during fractionation.

The Linosa rocks have similar Sr-Nd-Pb isotope signatures to the Iblei and other volcanics of the Pelagian block, falling close to the so-called FOZO (Focus Zone; [4]) mantle composition, with a small trend toward DMM (*e.g.* [5]). This composition has been found in many anorogenic volcanic rocks in Europe, including the Mediterranean area [6] and has been indicated as representing an European Asthenospheric Reservoir (EAR) [7]. The occurrence of these compositions at volcanoes on the Pelagian Block, *i.e.* south of the contact zone between African and European plates, supports the idea that the FOZO composition represents a common asthenospheric layer, which extends over wide areas below the sectors of the upper mantle whose composition is directly affected by recent and active subduction processes. The trend toward DMM could testify interaction between deep asthenospheric and lithospheric components, as suggested by several authors.

References. [1] G. Rossi, C.A. Tranne, N. Calanchi, E. Lanti, *Acta Vulcanol*., **8**, 73-90, 1996; [2] J.C. Stormer, J. Nicholls, *Computat. Geosci*., **4**, 143-159, 1978; [3] P.D. Asimow, M.S. Ghiorso, *Am. Mineral.*, **83**, 1127-1132, 1998; [4] S.R. Hart, E.H. Hauri, L.A. Oschmann, J.A. Whitehead, *Science*, **256**, 517-520, 1992; [5] T. Trua, S. Esperança, R. Mazzuoli, *Contrib. Mineral. Petr*., **13**, 307-322, 1998; [6] M. Lustrino, M. Wilson, *Earth Sci. Rev*., **81**, 1-65, 2007; [7] M. Wilson, R. Patterson, *Geol. Soc. Am. Spec. Publ*., **352**, 37-58, 2001.

U-Pb GEOCHRONOLOGY OF PRE-VARISCAN METARHYOLITES IN THE PRE-PIEDMONT BASEMENT (LIGURIAN ALPS)

L. Gaggero[1], L. Buzzi[1], M. Tiepolo[2]

[1]*Dip.Te.Ris., Università di Genova, Italy*
[2]*IGG - CNR, Pavia, Italy*
buzzi_laura@dipteris.unige.it

A Mid Ordovician calc-alkalic rhyolitic magmatism is reported in several domains of Gondwana-derived terranes from southern Europe (*e.g.* Sardinia, French Central Massif, Central and Southern Alps, Peloritan Mountains). Its widespread occurrence within lower Palaeozoic basements makes it a prominent geodynamic tracer of the Ordovician evolution at the northern Gondwana margin. Lithostratigraphic correlations between Southalpine, Sardinia and Ligurian Alps have been evidenced [1], but radiometric age determinations of some sequences assumed as pre-Variscan in the Ligurian Alps were lacking.

In the innermost Pre-Piedmont Unit (T. Visone) of the Ligurian Alps [1,2], the Palaeozoic basement comprises: 1) a gneiss complex of augen orthogneisses and paragneisses grading into quartzitic schists and 2) a silicate marble complex [1]. The metasedimentary host of orthogneisses derives from continental clastic deposits likely pre-dating the carbonatic - metapelitic sequence. Metamorphosed MORB-type tholeiites and subordinate ultramafic rocks occur within both complexes as former dykes. The protolith of orthogneisses has rhyolitic composition; K-feldspar and quartz phenoclast relics are preserved in the blastoporphyritic texture.

In situ U-Pb radiometric dating carried out by LA-ICP-MS on zircon separates from orthogneisses yielded a protolith age of about 461.8 Ma. The morphological characteristics and oscillatory zoning of zircon grains are consistent with a single-stage magmatic crystallization. The overall low trace elements content suggests unaltered isotope compositions. The inherited zircons yielded a Late Neoproterozoic age (626 Ma) supporting a Gondwana crustal source region.

This result is in good agreement with the data obtained for metarhyolites from adjacent areas: *e.g.* 473-459 Ma in the Ligurian Briançonnais [3], ~ 465 Ma in Sardinia [4], 465-450 Ma in the Montagne Noire (French Central Massif) [5,6], 456-452 Ma in the Peloritan Mountains (Sicily) [7].

Therefore, lithostratigraphic and radiometric investigations support the existence of a short-lived Ordovician orogenic cycle, that corresponds to a probable ocean-continent collision, associated with the subduction of the embryonic Rheic ocean [8].

The age of Mid-Ordovician intrusive orthogneisses (470-460 Ma, [3]) in the Ligurian basement is consistent with the regional frame.

References. [1] R. Cabella, L. Cortesogno, L. Gaggero, *Rend. Soc. Geol. It.*, **14**, 29-33, 1991; [2] F. Forcella, A. Mottana, G. Pasquaré, *Mem. Soc. Geol. It.*, **XII**, 485-528, 1973; [3] L. Gaggero, L. Cortesogno, J.M. Bertrand, *Per. Min.*, **LXXIII**, 2, 85-96, 2004; [4] L. Buzzi, A. Funedda, L. Gaggero, G. Oggiano, M. Tiepolo, *Geophys. Res. Abs.*, **9**, 03789, 2007; [5] M. Robardet, J. Verniers, Feist R., F. Paris, *Géologique France*, **3**, 3-31, 1994; [6] F. Roger, J.-P. Respaut, M. Brunel, P. Matte, J.-L. Paquette, *C. R. Geoscience*, **336**, 19-28, 2004; [7] A. Trombetta, R. Cirrincione, F. Corfu, P. Mazzoleni, A. Pezzino, *J. Geol. Soc., London*, **161**, 265-276, 2004; [8] J.F. von Raumer, G.M. Stampfli, G. Borel, F. Bussy, *Int. J. Earth Sci.*, **91**, 35-52, 2002.

THE TZONTEHUITZ DOME COMPLEX, CHIAPANECAN VOLCANIC ARC (CHIAPAS, MEXICO): GEOCHEMICAL AND PETROLOGICAL INSIGHTS

M.C. Jaimes-Viera[1], J.C. Mora[2], A.P. Santo[3], O. Vaselli[3]

[1]*Posgrado en Ciencias de la Tierra, Instituto de Geofísica, UNAM, Mexico*
[2]*Departamento de Vulcanología, Instituto de Geofísica, UNAM, Mexico*
[3]*Dipartimento di Scienze della Terra, Università di Firenze, Italy*
areivsemiaj@yahoo.com.mx

The Chiapanecan Volcanic Arc (CVA) is located in the central part of Chiapas State between 92°00' and 92°20' W and 17°00' and 16°15' N (UTM 15Q 500000 and 1880000; 15Q 571000 and 1797000). It lies in a tectonically complex region where three great plates interact: the North American Plate, the Caribbean Plate and the Cocos Plate. The CVA is located between two volcanic features: the Trans-Mexican Volcanic Belt (TMVB) to the northwest, and the Central American Volcanic Arc (CAVA) to the southeast. The central part of this arc is composed by at least NW-SE oriented 10 volcanic structures aligned, mainly dominated by volcanic domes and pyroclastic flow deposits. The oldest volcanic structure (2.14 ± 0.04 Ma, K-Ar) is represented by Tzontehuiz Dome Complex (TzDC), located 80 km SE of El Chichón volcano and 10 km NE of San Cristóbal de las Casas. The TzDC covers an area of about 16 km^2 and is composed by at least 3 N-S aligned dome and pyroclastic outflow sheets erupted along a ring fracture. The pyroclastic flow deposits have been emplaced to the SSE of TzDC, with a maximum length of 9.5 km, a mean thickness of 8 m and cover an area of approximately 73 km^2. The domes that composed this volcanic structure are: 1) El Calvario Dome (15Q 5433300E, 1857600N UTM), 80 m high and a mean diameter of 1 km. It is composed of a dark gray rock with porphyritic texture; 2) Tzontehuitz Dome 1 (15Q 544200E, 1859800N UTM), located north of El Calvario, ~ 200 m high and a mean diameter of 1 km. The volcanic rocks are light gray in color, with a massive and compact structure, and contain some isolated megacrystals of amphibole (2.5 cm) and some dark mafic enclaves with elongated shapes (< 1cm); 3) Tzontehuitz Dome 2 (15Q 543850E and 1861400N UTM), located to the north of Tzontehuitz 1. It shows a semicircular structure 180 m high and a mean diameter of 1.5 km. It is dark gray in color, with a massive and compact structure, and porphyritic texture. The juvenile fragments from both the domes and pyroclastic flow deposits have a porphyritic texture with phenocrysts of plagioclase ± amphibole ± clinopyroxene ± Fe-Ti oxides surrounded by a matrix composed by microlites of plagioclase and glass. The geochemical data obtained on representative samples from the deposits and domes indicate that these belong to the subalkaline rock series, and fall into the calc-alkaline field with medium to high content of potassium. They vary from trachybasalts, basaltic trachyandesite, basaltic andesite, and andesite (SiO_2 52-60 wt.%). The mineral chemistry shows that plagioclase varies from andesine to bytownite, pyroxene has a diopsidic-augitic composition, amphibole belongs to the calcic group, whereas opaque minerals pertain to the magnetite-ulvospinel group. Major elements abundances in the TzDC analyzed samples are similar to those found in the calc-alkaline rocks from the TMVB and CAVA. These petrographic and geochemical characteristics indicate that the studied rocks were generated in a typical subduction environment. The main purpose of this work is to know the volcanic activity of the TzDC, to understand the magma genesis processes and to find the relationships possibly existing between this and the other volcanic structures pertaining to the TMVB and CAVA.

CLINOPYROXENES STUDY FROM SOMMA-VESUVIO VOLCANO (ITALY)

S. Nazzareni, P.F. Zanazzi, A. Peccerillo

Dipartimento di Scienze della Terra, Università di Perugia, Italy
sabrina.nazzareni@unipg.it

Somma-Vesuvio volcano was built during three main stages of volcanic activity [1]. Stage-I (25-14 ka) and stage-II (14ka to 79 AD) built up the Somma volcano, whereas Vesuvio was constructed entirely during stage-III (79AD- 1944).

Petrological and geochemical studies have shown that rocks of the different stages define distinct variation trends for some major and trace elements [1-4], a feature that has been interpreted as an evidence of fractionation of different mineral assemblages during polybaric magma evolution [3,4]. In contrast, an increasing amount of carbonate assimilation with time has been suggested by Iacono Marziano *et al*. [5], on the basis of experimental evidence. These authors suggest that younger Vesuvius magmas assimilated larger amounts of carbonate wall rocks that the older ones, thus favouring heavy crystallisation of clinopyroxenes at expenses of plagioclase and olivine.

Crystal chemistry study of clinopyroxenes (Cpx) has been carried out in order to explore possible time-related variations of compositional and/or structural parameters, which may shed light on styles of magma evolution at Somma-Vesuvio.

Single crystals were picked up from thick sections and used for the SCXRD and EMPA study. The analysed Cpx crystals vary from $Wo_{48-50}En_{42-40}Fs_{9-10}$ in samples of the stage-I to $Wo_{48-54}En_{47-39}Fs_{5-7}$ in samples of stage-III. Cpx from stage-III samples showed strong compositional zoning; therefore, core and rim fragments were carefully selected and analysed.

In general, samples from stage-I (Somma) are poorly zoned with Ca around 0.873 a.f.u. and Mg around 0.692-0.749 a.f.u.; Cpxs from stage-III (Vesuvio) have a higher content of Ca always > 0.9 a.f.u. and a significant core-rim variation of Al (0.120-0.219 a.f.u.), Si (1.888-1.969 a.f.u.) and Mg (0.717-0.859 a.f.u.).

Cpxs from the stages I and III showed differences in most of the geometrical and crystal chemical parameters allowing to define two groups in many diagrams. Nevertheless, the volumes of unit cell and M1 octahedron give indications that the Cpxs from period I and period III of the Somma-Vesuvio volcano crystallised at a similar moderate depth (around 1-2 kbars). This indicates similar depth of magma ponding and crystallisation, supporting the hypothesis that the different elemental trends of the Somma-Vesuvio rocks represent variable amounts of carbonate assimilation rather than polybaric magma crystallisation.

References. [1] R.A Ayuso, B. De Vivo, G. Rolandi, R.R. Seal, A. Paone, *J. Volcanol. Geotherm. Res.*, **82**, 53-78, 1998; [2] R. Santacorce (ed), *Quad. Ric. Sci. CNR*, Roma, **114**, 8, 105-174, 1987; [3] A. Peccerillo, Springer, Berlin, 2005a; [4] A. Peccerillo, *Acta Vulc.*, **17**, 43-52, 2005b; [5] G. Iacono Marziano, F. Gaillard, M. Pichavant, *CMP*, **9**, 100-110, 2008;

ORIGIN AND EVOLUTION OF METABASITES FROM THE NORTHERN PART OF THE IZERA-KARKONOSZE BLOCK, WEST SUDETES, POLAND

I. Nowak

Institute of Geological Sciences, Polish Academy of Sciences, Poland
izanowak@twarda.pan.pl

The early Palaeozoic rift-related bimodal volcanism, with mafic products ranging from alkali WPB to N-MORB chemistry, is common in the Saxothuringian zone of the Variscides. In the northern part of the Izera-Karkonosze Block, representing the trailing edge of the Saxo-Thuringian terrane, the ca. 500 Ma granites were cut by a swarm of the WNW-trending subvertical basic dykes and then were jointly deformed and metamorphosed.

Geochemically, the metabasites represent 5 groups: I – alkali basalts, II – transitional basalts, III – N-MORB-like basalts, IV – WP tholeiites and V – calc-alkaline basalts similar to SSZ basites (Nowak, 2003). Ratios of incompatible elements and degree of fractionation of REE allow to infer that: (1) group I basalts originated from an enriched astenospheric mantle of OIB-type, (2) group II basalts were derived a slightly depleted source resulting from mixing of undepleted and depleted asthenospheric magmas, (3) group III basalts of N-MORB-type were released from a strongly depleted asthenospheric source with some contamination from the continental crust, (4) group IV came from a heterogeneously enriched mantle source with mixed E- and N-MORB compositions contaminated by the continental crust, and (5) group V developed from a lithospheric source.

Magmas I to III formed quite a consistent evolutionary trend A in which an enriched asthenospheric region was modified due to increasing flux of depleted material. The alkali basalts dominate in the trend A. Their affinity to HIMU-type mantle source are inferred from Sr and Nd isotopic signatures and trace element ratios (*e.g.* Nb/La, La/Ba, Th/Nb, Zr/Nb), which suggests that the origin of the Izera alkali basalts was connected with the mantle plume. Its presence controlled an early Palaeozoic extension of the Cadomian crust in the Saxothuringian zone, the process extensively recorded in the Izera section. As long as the extension went on, the Izera continental crust received, via plume, injections of basic magmas coming from enriched astenospheric source which was evolving and, with time, became more and more depleted producing transitional basalts and eventually N-MORB. Relatively high $\varepsilon Nd_{(500)}$ values (8.5-9.4) of the Izera N-MORB-like basalts are consistent with their derivation from the depleted mantle source. Significantly elevated $(^{87}Sr/^{86}Sr)_i$ ratios of the group II either reflect contamination by continental crust or, more likely secondary alternation. Two different populations of zircons from the Izera metabasites yielded U-Pb ages of ca. 500 Ma and ca. 400 Ma. The younger zircons probably crystallized during extensive hydrothermal metamorphism, which could effect high $(^{87}Sr/^{86}Sr)_i$ ratios.

Magmas IV and V formed an evolutionary trend B. The wide variations in Sr and Nd isotopic ratios ($\varepsilon Nd_{(500)}$ = 11.6-6.3; $(^{87}Sr/^{86}Sr)_i$ = 0.7037-0.7056) in the group IV together with negative correlations between Sr and Nd isotopic ratios confirm derivation of WP tholeiites from heterogeneously enriched mantle source and contamination with continental crust. The group V is characterized by negative $\varepsilon Nd_{(500)}$ values and high $(^{87}Sr/^{86}Sr)_i$ which indicate that the calc-alkaline basalts were derived from lithospheric mantle source and imply the significant involvement of a crustal component in their genesis. The trend A and B are interpreted to match two different geodynamic conditions, *i.e.* divergence and convergence, respectively. A switch from the trend A to B reflected the end of lithospheric extension and the onset of subduction. Alternatively, strong contamination might have occurred when magmas were passing through the continental lithosphere.

THE ORIGIN OF TRACHYTES AT PANTELLERIA: NEW INSIGHTS FROM BASALT-TRACHYTE MINGLED ROCKS

N. Romengo[1], P. Landi[2], S.G. Rotolo[1]

[1]*Dipartimento di Chimica e Fisica della Terra, Università di Palermo, Italy*
[2]*Istituto Nazionale di Geofisica e Vulcanologia - Sezione di Pisa, Italy*
capinera77@virgilio.it

The island of Pantelleria, the type locality of pantellerite (peralkaline rhyolite), is characterized by the bimodal association of mildly alkaline basalts and felsic volcanites (pantellerites and trachytes), with a large compositional gap (*e.g.* SiO_2 = 50-65 wt.%) between these two compositional poles.

The lack of rocks with intermediate compositions constitutes a primary feature of Pantelleria magmatism and has been explained either invoking a negative buoyancy for the intermediate rocks, or the absence of a petrogenetic link among mafic and felsic rocks.

The main morfhological feature of the island is the ~ 50 ka old Cinque Denti caldera, nested in the older "La Vecchia" caldera.

Voluminous ($\geq$ 3 km^3), slightly peralkine and highly porphyritic trachite lava flows were erupted within the Cinque Denti caldera, building up the resurgent block of Montagna Grande. Alkaline basalts have never erupted within the nested calderas.

Recent field surveys allowed us to recognize a short lava flow, benmoreitic in composition, close to the top of the trachyte lava pile. Textural and mineralogical characteristics indicate that these products with intermediate composition result from mingling processes between trachyte and less evolved magma. In particular they show sieved textured plagioclase An_{70-30}, anorthoclase Or_{15-22}, An_{50-70}, and crystals of olivines and clinopyroxenes with different composition, in the range Fo_{56-84} and Fs_{12-28} respectively, and frequent resorption textures. The rims of the phenocrysts and the microphenocrysts have intermediate composition. The mafic end member remains, at the present, the sole evidence of the rising of mafic magmas beneath the caldera.

We analyzed major and trace element contents in olivine and clinopyroxene (determined by electron microprobe and LA-ICP-MS), with the aim to (i) trace back the chemistry of the mafic component, (ii) explore its relationship with the basaltic rocks outcropping in the northernmost part of the island and (iii) investigate possible genetic correlations between basaltic and trachytic magmas.

PETROCHEMICAL AND GEODYNAMIC STUDY OF THE NYIRAGONGO VOLCANO (EAST AFRICAN RIFT SYSTEM)

A.P. Santo[1], A.R. Basu[2], R. Chakrabarti[2,3], O. Vaselli[1], D. Tedesco[4]

[1]*Dipartimento di Scienze della Terra, Università di Firenze, Italy*
[2]*University of Rochester, New York, USA*
[3]*Harvard University, Cambridge, USA*
[4]*Università di Napoli 2, Caserta, Italy*
alba.santo@unifi.it

The Nyiragongo volcano is located in the western branch of the East African Rift System about 18 km N of Lake Kivu in the Democratic Republic of Congo (DRC). It is best-known for the presence since 1894 of an active lava lake in the summit 1.3 km-wide and 800 m-deep crater. On January 2002 a series of fractures opened on Nyiragongo's upper southern flanks triggering drainage of magma stored in the crater lava lake, conduit and edifice and the emission of turbulent flows of highly fluid lava. The area includes almost one hundred phreatic, hydromagmatic and magmatic adventive cones aligned along three preferential orientations: NNW-SSE, NS and EW. Despite the area provides an ideal setting to study the interaction between plumes, continental lithosphere and asthenosphere, as well as the relation of mantle plumes and continental rifting, only a few studies of the Nyiragongo and its multiple eruption products, including the most recent eruption of 2002, have so far been undertaken. In this work we report major and trace element and isotopic studies of the most recent volcanic products of Nyiragongo and its associated satellite cones, plugs and flows of unknown age. The studied rocks are undersaturated and mainly represented by foidites and by tephrites and basanites (Fig.). They generally exhibit porphyritic textures with variable phenocryst content and glassy or microcrystalline groundmass; phenocrysts are represented by abundant feldspathoids (nepheline, melilite and/or leucite), clinopyroxene ($Wo_{46-56}En_{28-44}Fs_{7-20}$) ± olivine ($Fo_{83-89}$); kalsilite has been found in the lava samples from 2002 eruption; apatite and Fe-Ti oxides are the common accessory mineral phases. Calcite of probable magmatic origin is sometimes present in the groundmass. Chromite has been observed in some rock samples. Tephrites display subaphyric textures with small quantities of clinopyroxene ($Wo_{46-50}En_{38-43}Fs_{9-12}$) and minor olivine ($Fo_{80-82}$) enclosed in a glassy matrix containing Fe-Ti oxides and fine-grained aggregates of clinopyroxene, with cumulitic texture. Basanites are porphyritic and contain euhedral and subhedral phenocrysts of clinopyroxene ($Wo_{47-50}En_{36-44}Fs_{8-14}$) and olivine ($Fo_{74-85}$) set in a groundmass composed by glass, leucite and Fe-Ti oxides. Nyiragongo volcanics show low K/Rb ratios, indicative of phlogopite melting in the mantle source, enrichment in REE, highly fractionated La/Yb and high chondrite-normalised Dy/Yb, suggesting residual garnet in the source. In Nd-Sr-Pb isotope space they show correlations similar to ocean island basalts and a strong affinity for EM II. Our combined data (trace element and isotopic data were acquired at the University of Rochester) are discussed in order to investigate the composition of the magma source, the possible contributions from the sub-continental lithospheric mantle, astenospheric or sub-astenospheric mantle and the role of fluids in generating the distinctive characteristics of these unique magmas originated around the Tanzanian craton.

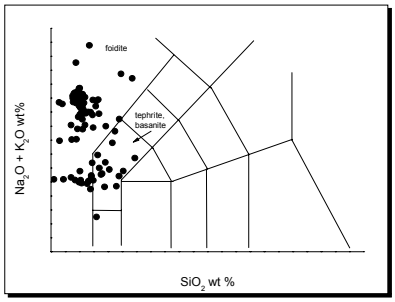

SPINEL LHERZOLITES XENOLITHS FROM HANNUOBA, NE CHINA: PERSPECTIVES ON CRUSTAL COMPONENTS IN THE MANTLE AND TIMING OF METASOMATISM

M. Scarbolo, A. De Min, F. Princivalle

Dipartimento di Scienze della Terra, Università di Trieste, Italy
mscarbolo@units.it

A suite of xenoliths from Hannuoba basaltic plateau (located in the North China Craton (NCC), Eastern China) has been studied by single crystal X-ray diffraction, EMPA and LA-ICP-MS. The xenoliths investigated are spinel lherzolites with protogranular texture whose mineralogical assemblages and chemical compositions reflect those of the upper mantle rocks and suggest the samples suffered a basaltic extraction. Crystal chemical studies reveal that structural parameters and cation distribution resemble those of mineral phases crystallizing in high pressure conditions. Chondrite-normalised REE abundances in clinopyroxenes show a wide range of patterns (depleted, enriched, U-shaped) confirming the origin of the studied xenoliths as peridotite restites. Moreover some of them, after melt depletion, experienced a metasomatic enrichment derived by the involvement of crustal melts. Many authors [1,2] agree on the timing of melt depletion (in the Paleoproterozoic), at the time of the final amalgamation of the NCC [3-5] and on the metasomatism related to a subductional event of crustal material, but the timing and the "velocity" of the metasomatic overprinting is still controversial. The metasomatism could be an ancient event related to the subduction that leaded to the amalgamation of the NCC or a recent event related to the Late Mesozoic reactivation. Moreover, the metasomatism could be a fast event (metasomatism due to diffusion along interfaces between grains) or a slow event (metasomatism due to diffusion through grain interiors).

The data collected in this work are favourable to an ancient and slow event, and this is evidenced by: 1) the coexisting phases in the xenoliths do not show any chemical variation between core and rim, 2) their crystal-chemical parameters suggest a P-T equilibrium stage in the mantle (15-20 kbar; 880-1050°C), 3) the REE distribution in cpx is homogeneous both for high diffusivity element (*e.g*. Sr) and low diffusivity element (La). Moreover, the NCC experienced a long period of magmatic and tectonic quiescence and this is a sufficient condition to justify the re-equilibration of all the elements in clinopyroxenes. So, the studied xenoliths are representative of a heterogeneous mantle which experienced a metasomatic overprinting related to crustal subduction at the time of the final amalgamation of the NCC and could represent an evidence of the statistical upper mantle assemblage (SUMA) [6].

In such a way the REE behaviours of Hannuoba xenoliths could be considered as representative of a lithospheric mantle source type for the genesis of the Neo Proterozoic tholeiitic Large Igneous Provinces (LIP) of cratonic areas.

References. [1] Y. Xu, *Chem. Geol*., **182**, 301-322, 2002; [2] R.L. Rudnick, S. Gao, W. Ling, Y.S. Liu, F. McDonough, *Lithos*, **77**, 609-637, 2004; [3] G. Zhao, P.A. Cawood, S.A. Wilde, M. Sun, L. Lu, *Precamb. Res*., **103**, 55-88, 2000; [4] G. Zhao, S.A. Wilde, P.A. Cawood, M. Sun, *Precamb. Res*., **107**, 45-73, 2001; [5] G. Zhao, M. Sun, S.A. Wilde, L. Sanzhong, *Precamb. Res*., **136**, 177-202, 2005; [6] A. Meibom, D.L. Anderson, *Earth Planet. Sc. Lett*., **217,** 123-139, 2003.

SOLIDIFICATION INDUCED BY COOLING OF ANDESITIC MELTS

G. Torresi[1], S. Mollo[2], G. Ventura[2], G. Iezzi[1,2], A. Cavallo[2], P. Scarlato[2], H. Behrens[3]

[1]*Università "G. d'Annunzio" di Chieti, Italy*
[2]*Istituto Nazionale di Geofisica e Vulcanologia, Roma, Italy*
[3]*Institute of Mineralogy, University of Hannover, Germany*
g.iezzi@unich.it

The solidification behaviour induced by cooling has been investigated on three andesitic melts (one Fe-free) in laboratory from super-*liquidus* (1300°C) to near-*solidus* (800°C) conditions. The glassy starting materials were prepared by repeated melting of natural volcanic rocks and/or synthetic reagent mixtures. Two experimental and complementary approaches were used to investigate the nucleation and crystallization parameters for all the starting compositions: 1) variation of different cooling rates of 25, 12.5, 3, 0.5 and 0.125°C/min and 2) adjustment of progressively lower quenching temperatures for a fixed cooling rate of 0.5°C/min.

The recovered run-products were analyzed by SEM-EDS, EPMA-WDS and XRPD. The andesitic melts nucleate much easier compared to their alkaline counterpart compositions, such as latititic and trachytic melts [1]. The two Fe-bearing andesites follow a similar crystallization path, with a significant crystal content even at the higher cooling rates or quenching temperatures. The run-products of the Fe-free andesite have instead always similar textural features, irrespectively of the applied cooling regime(s). All the crystalline phases appear to nucleate internally for all the starting compositions. The glass-forming ability (GFA) of andesitic melts is lower compared to those of latite and trachyte melts. This implies that a trachytic lava has a higher nucleation barrier and it can flow at metastable condition for a longer period compared to a latitic [1] or especially to an andesitic melt.

The crystal content of the Fe-bearing andesitic run-products is mainly composed by plagioclase. The composition of these crystal phases span a large range, virtually from anorthite to andesine. Interestingly, the latter plagioclase composition is found only at the higher cooling rates; these andesines are always surrounded by anorthite-rich compositions. The nucleation composition of plagioclase inferred from smaller crystals is invariably around $An_{90}Ab_{10}$ due to kinetic effects. On the contrary, the larger plagioclase crystals, dwelling in the cooling andesitic melts for longer periods, tend to re-equilibrate towards more Na- and Si-rich compositions. This effect is also prompt by the evolution of the liquid to more evolved dacitic and rhyolitic compositions, especially at 0.5 and 0.125°C/min, in response to the plagioclase crystallization. The combined effects of nucleation kinetic and melt evolution by crystallization, at least under these cooling conditions, determine the occurrence of textural/chemical heterogeneity of plagioclases. A similar situation is found for oxide crystals. The silicate melts surrounding these mineral phases also have an heterogeneous chemical composition. Therefore the presence of disequilibrium features in an andesitic lava are not necessarily indicative of open-system magmatic processes.

The crystal growth of the larger plagioclase and oxide crystals mainly occurs by coarsening, indicating that nucleation and crystal growth parameters recovered by CSD data on natural volcanic rocks could be underestimated.

References. [1] G. Iezzi, S. Mollo, G. Ventura, A. Cavallo, C. Romano, *Chem. Geol.*, 2008, in press.

PETROLOGIC PROCESSES AND GEODYNAMICS

Session 4
Metamorphic processes

PHASE RELATIONS IN K-DOPED LHERZOLITES UP TO 6.0 GPA: THE RELEVANCE OF AMPHIBOLE AND PHLOGOPITE FOR LIGHT ELEMENTS RECYCLING

P. Fumagalli[1], S. Zanchetta[2], S. Poli[1]

[1]*Dipartimento di Scienze della Terra, Università di Milano, Italy*
[2]*Dipartimento di Scienze Geologiche e Geotecnologie, Università di Milano-Bicocca, Italy*
patrizia.fumagalli@unimi.it

Metasomatic processes affect mantle wedge peridotites at subduction zones. Buoyancy forces acting at slab-mantle interface are responsible for peridotite emplacement in the subducted continental crust while devolatilization of felsic rocks and mass-transfer toward peridotite bodies are strongly enhanced. As a result, a variety of volatile-bearing phases develop in ultramafic bodies such as phlogopite and amphibole characterized by a peculiar "orogenic" geochemical signature.

Phase relations and the mineral chemistry variations of micas, amphiboles and other high pressure hydrates enable to interpret the metamorphic evolution of metasomatised peridotite bodies. Although K- and Ti-doped mantle compositions at near solidus temperature have been widely investigated, subsolidus phase relations, and the influence of pressure on mineral chemistry of amphibole and phlogopite are still barely known. The aim of this work is to investigate the effect of K and Ti on subsolidus phase relations in model systems approaching natural compositions, particularly focusing on the pressure controlled breakdown of amphibole, on the element partitioning between amphibole and coexisting phases, and on the crystal chemistry of high pressure phlogopites.

An experimental approach has been followed to investigate complex systems and composition approaching natural rocks, as required by the complexities related to the occurrence of continuous reactions involving both phlogopite and amphibole. Piston cylinder and multi anvil experiments have been performed from 1.5 to 6.0 GPa and from 800 to 1000°C. A slightly depleted lherzolite composition was considered in the NKCFMASH system, while a MORB pyrolite has been investigated in the TiNCFMASH system. Gels have been used as starting materials, added with garnet and pyroxene seeds to favor the crystals growth. Experiments were carried out at fluid saturated conditions. In piston cylinder experiments the oxygen fugacity was controlled using NNO buffer and employing the double capsule technique.

Amphibole and phlogopite coexist in the K-bearing lherzolite up to 3.2 GPa, 900°C. The stability of amphibole in alkali-bearing ultramafics, and its implication for recycling of light elements deep into the Earth mantle need to be re-evaluated. Phlogopite mineral chemistry shows a pressure dependent increase of talc component, suggested by a K deficiency coupled with enhanced Si and decreased Al. Such a behaviour is observed within the stability field of a Dense Hydrous Magnesium Silicate (DHMS), the 10 Å phase, suggesting both solid solutions and interlayering relations. The possibility of using phlogopite to estimate metamorphic pressure is evaluated as petrological consequence.

In the Ti-bearing system garnet and amphibole show an inverse correlation between xMg and Ti content: in amphibole Ti increases with T, while the $Mg/(Mg+Fe^{2+})$ ratio decreases; the opposite is shown in garnet. The Ti partitioning between garnet and amphibole has been shown to depend mainly on temperature, with only a minor influence of pressure. These results suggest the possible use of Ti content in amphibole coexisting with garnet as a geothermometer for amphibole-bearing ultramafics.

RETROGRADE DIFFUSION OF HYDROGEN IN BIOTITE FROM METAPELITIC GRANULITES OF THE KERALA KHONDALITE BELT (S INDIA)

B. Cesare[1], S. Meli[2], M. Satish-Kumar[3], G. Cruciani[4]

[1]*Dipartimento di Geoscienze, Università di Padova, Italy*
[2]*Dipartimento di Scienze della Terra, Università di Parma, Italy*
[3]*Institute of Geosciences, Shizuoka University, Japan*
[4]*Dipartimento di Scienze della Terra, Università di Ferrara, Italy*
bernardo.cesare@unipd.it

We have recently shown that biotite in contact with garnet from metapelitic granulites and migmatites exhibits a complex behaviour during retrograde exchange, involving Ti and F which add to the common $FeMg^{-1}$ substitution with garnet. We also suggested that this exchange also involves H.

Here we constrain the role of H in this process, by means of detailed analytical characterization. We have performed secondary ion mass spectrometry (SIMS) profiles at Bt-Grt, Bt-Sil and Bt-Kfs contacts, using a focused 1.8 μm beam and 2 μm steps.

Results indicate that there is an increase of H in biotite crystals in contact with garnet, whereas H is constant or slightly decreasing at the rims of biotite in contact with other phases. The positive variation (approximately 10% relative) of H is observed over a distance of 30-40 μm, similar to that over which variations in Ti and Fe (decreasing towards garnet) and F and Mg (increasing) are also observed by electron probe.

It follows that during cooling of high-grade rocks, retrograde exchange not only affects Fe-Mg diffusion with garnet, but a more complex substitution that is essentially a reverse Ti-oxy vector. This in turn requires chemical exchange with the surrounding rock matrix, and availability of elements not provided by garnet (H and F).

The time and temperature conditions at which these diffusional processes occur can be constrained by *in situ* analysis of stable isotopes.

EVIDENCE FOR DIFFERENT STYLES OF ALKALINE METASOMATISM DURING CONTINENTAL RIFTING AS RECORDED BY THE MANTLE COLUMN BENEATH THE MID ATLAS (MOROCCO)

A. Zanetti[1], N. Raffone[1], R. Vannucci[1,2], G. Chazot[3], C. Pin[3]

[1]*IGG-CNR, Pavia, Italy*
[2]*Dipartimento di Scienze della Terra, Università di Pavia, Italy*
[3]*Laboratoire de Geologie, Universitè Blaise Pascal, Clermont-Ferrand, France*
zanetti@crystal.unipv.it

Insights into the multistage metasomatic evolution of the subcontinental mantle beneath the Mid Atlas have been provided by the petrochemical characterisation of ultramafic xenoliths hosted in alkaline basalts from the Azrou-Timahdite volcanic district. Since Eocene, this area has been subjected to alkaline volcanism along fault systems developed in response to the collision between European and African plates. The lithospheric mantle established after the Pan-African orogenic cycle results to be formed by porphyroclastic to protogranular spinel-lherzolites associated with spinel-websterites, and, subordinately, by porphyroclastic to coarse-granular spinel-harzburgites. The websterites rarely contain secondary garnet, produced by subsolidus reaction at P of 2.5 GPa. Lherzolite and websterite minerals show major and trace elements, as well as isotopic signature, strictly consistent with those estimated for DM reservoir, showing only limited metasomatic enrichments in LILE. Cryptic metasomatic imprint is stronger in the spinel-harzbugites, according to a higher permeability with respect to the migration of small melt volumes. The widespread development of alkaline metasomatism is better recorded by the occurrence of several types of amphibole-bearing ultramafics. The early metasomatic event was related to pervasive porous-flow migration of alkaline liquids ubiquitously characterised by strong enrichments (in particular, larger than in the host basalts) in highly-incompatible elements such as LREE, U and Th, but with distinct LILE/HFSE fractionation. In particular, melts producing porphyroblastic (amphibole-rich) to coarse-granular (amphibole-poor) lherzolites were originally also enriched in Nb, Ta, Zr and Hf, but with negative Ti anomaly. Differently, melts producing porphyroblastic (amphibole-poor) lherzolites were dramatically impoverished in all the HFSE. Notwithstanding such differences, these LILE-enriched melts shared the same Nd and Sr isotopic composition of the host alkali basalts, indicating a derivation from a common mantle reservoir. A second style of alkaline metasomatism is characterised by the production of Fe-rich and Mg-rich wehrlites. Fe-rich wehrlites developed for the late crystallisation of mineral assemblages formed by clinopyroxene+spinel+amphibole in mantle sectors formerly strongly impoverished in modal pyroxene by interaction with porous-flow migrating melts. Fe-wehrlites sometimes show trace-element heterogeneity testifying for an early percolation of strongly LREE-enriched melts with large negative HFSE anomaly, followed by melts progressively more similar to the host alkali basalts. The geochemical variation of the metasomatic melts recorded by the Mid Atlas mantle is broadly consistent with the regional change of the alkaline volcanics, highlighting a progressive evolution of the melting process in the mantle source region.

THE OXIDATION STATE OF METASOMATISED MANTLE WEDGE: INSIGHTS FROM HYDRATE-CARBONATE-BEARING PERIDOTITE

N. Malaspina, S. Poli, P. Fumagalli

Dipartimento di Scienze della Terra, Università di Milano, Italy
Nadia.Malaspina@unimi.it

In subduction environments the fluid phases released by the subducting plates are vehicles for the slab-to-mantle element transfer, leading to the metasomatism, re-fertilisation and partial melting of the mantle. Occurrences of hydrous minerals coexisting with carbonates and C polypmorphs (*e.g.* phlogopite + magnesite + graphite/diamond) in mantle wedge peridotites evidence that such fluids are represented by C-O-H solutions, derived by dehydration reactions and decarbonation of the slab. The equilibria involving the volatile elements play an important role in controlling the iron oxidation state of mantle silicates and oxides by redox reactions. Alternatively, Fe^{3+}/Fe^{2+} equilibria between mantle minerals may buffer the fluid speciation, and therefore oxygen fugacities (fO_2). Despite a number of studies have been devoted to determine the redox state of the upper mantle, the fO_2 of supra-subduction mantle wedge, used as monitor of its oxidation state, is still poorly investigated.

An essential input for fO_2 estimates is represented by the determination of ferric-ferrous iron content of key mantle minerals such as garnet. $Fe^{3+}/\Sigma Fe$ in garnet can be measured by the "flank method" electron microprobe analyses [2]. The "flank method" has been calibrated on the JEOL 8200 Superprobe at the Dipartimento di Scienze della Terra (University of Milano) using almandine, andradite and skiagite standards with fixed $Fe^{3+}/\Sigma Fe$ (0, 1 and 0.4 respectively). We have synthesised the end-member skiagite in a multianvil apparatus at P = 10 GPa and 1100°C. The experiments were performed starting from a glass and slag produced in a vertical furnace. The correct $Fe^{3+}/\Sigma Fe$ was achieved by controlling the fO_2 of the furnace atmosphere using $CO\text{-}CO_2$ gas mixes.

As case studies, we selected samples of orogenic peridotites from the ultrahigh pressure Sulu belt (Eastern China) and from the Ulten Zone (Italian Alps), corresponding to slices of metasomatised mantle wedge sampled at different depths. The "flank method" measurements indicate that garnet from the Sulu peridotite contains significant amounts of $Fe^{3+}/\Sigma Fe$ (0.05-0.06), while garnet from the Ulten peridotite has $Fe^{3+}/\Sigma Fe$ below the detection limits. For peridotite mineral assemblages fO_2 can be evaluated from equilibria involving Fe^{3+}-garnet components, such as: 2 $Fe^{2+}{}_3Fe^{3+}{}_2Si_3O_{12}$ (skiagite) = 4 $Fe^{2+}{}_2SiO_4$ (fayalite) + 2 $Fe^{2+}{}_2Si_2O_6$ (ferrosilite) + O_2 [1]. Up to date, the lack of thermodynamic data for the Fe^{3+}-garnet component (skiagite), and of an appropriate solid solution model for this phase, limited the applicability of this equilibrium. We therefore modelled non-ideal mixing of Al and Fe^{3+} on the octahedral site for the almandine-skiagite join by a symmetric regular solution model, combining previous experimental and thermochemical data [3,4]. This enabled us to calculate garnet-peridotite fO_2, given the presence of Fe^{3+} in garnet. The determination of fO_2 of metasomatised garnet-peridotites is a powerful tool to estimate the speciation of C-O-H fluids. This permits to speculate on the devolatilisation processes in subduction zones and on the mechanism of C-O-H components transfer from the slab to the mantle wedge.

References. [1] G. Gudmundsson, B.J. Wood, *Contrib. Mineral. Petr.*, **119**, 56-67, 1995; [2] H. Höfer, G.P. Brey, B. Schulz-Dobrick, R. Oberhänsli, *Eur. J. Mineral.*, **6**, 407-418, 1994; [3] A.B. Woodland, H.S.C. O'Neill, *Am. Mineral.*, **78**, 1002-1015, 1993; [4] G. Ottonello, M. Bokreta, P.F. Sciuto, *Am. Mineral.*, **81**, 429-447, 1996.

THE DORA-MAIRA WHITESCHISTS (WESTERN ALPS) RE-EXAMINED: NEW DATA FROM MINERAL ASSEMBLAGE AND UHP MULTIPHASE SOLID INCLUSIONS IN PYROPE

S. Ferrando[1], M.L. Frezzotti[2], M. Petrelli[3], R. Compagnoni[1]

[1]*Dipartimento di Scienze Mineralogiche e Petrologiche, Università di Torino, Italy*
[2]*Dipartimento di Scienze della Terra, Università di Siena, Italy*
[3]*Dipartimento di Scienze della Terra, Università di Perugia, Italy*
simona.ferrando@unito.it

The new studies on ultrahigh-pressure (UHP) terranes are supported by published experimental petrologic works and by use of more sophisticated micro-analytical techniques. On this basis, we re-examined the whiteschists of the Brossasco-Isasca Unit (BIU) from the Dora-Maira Massif (Western Alps) in order to better constrain their origin and evolution.

We report the results of a petrological study on whiteschist minerals and fluid phase in equilibrium at the UHP peak from the Case Parigi whiteschist classic site and from a new site. The whiteschists consist of pyrope-rich garnet, quartz/coesite, phengite, kyanite, talc, chlorite, and minor unusual Mg-rich minerals. Three generations of garnet occur in both sites: 1) prograde reddish megablasts (pyrope 1) (10-20 cm across); 2) zoned porphyroblasts (2-10 cm across) with a prograde core (pyrope 1: $Prp_{69-81}Alm_{17-26}$) and a peak rim (pyrope 2: $Prp_{86-98}Alm_{2-11}$); 3) smaller peak crystals (pyrope 2) (< 2 cm across). Coesite inclusions occur only in Pyrope 2 suggesting UHP conditions. The UHP peak assemblage consisted of garnet (pyrope), coesite, phengite (Si = 3.548-3.580 a.p.f.u.), kyanite, talc, and accessory rutile, apatite, zircon and monazite. For a nominal T = 730°C, peak $P \leq 4$ GPa was estimated from the phengite geobarometer.

The peak fluid phase composition may be inferred from the primary Multiphase Solid (MS) inclusions within pyrope 2. The MS inclusions (10-30 microns across) are regularly distributed and may show evidence for post-entrapment decrepitation. Non decrepitated MS inclusions contain Mg-chlorite, Na-phlogopite, Cl-rich apatite, Zn-rich pyrite, and chlorides as daughter minerals, talc and magnesite as step-daughter minerals, and rutile, zircon and monazite as incidentally-trapped minerals. Although water has never been observed, IR-synchrotron-radiation mapping revealed significant water diffusion from MS inclusions to the hosting garnet. Trace element analyses show variable enrichments on LILE. Therefore, the inferred composition of the peak fluid was an aqueous fluid enriched in Si, Al, Mg, Na, and Ca, and containing significant amounts of Cl, P, S, and some LILE.

These data indicate that, at the UHP peak, in the Dora-Maira whiteschists a hydrous mineral assemblage developed in the presence of a fluid phase high in chlorine. This composition is significantly different from that estimated for UHP Toz-Ky quartzite from Sulu orogen, China, where the peak mineral assemblage was anhydrous and the UHP fluid composition, poor in chlorine, was internally derived.

Our results on the Dora-Maira whiteschists are in agreement with the model for whiteschist genesis envisaging metasomatism along shear zones of precursor granitoids/orthogneiss by influx of complex brines derived from prograde serpentinite dehydration.

STRUCTURE, CHEMISTRY AND U-Pb GEOCHRONOLOGY OF ZIRCONS FROM ALBITITES OF INTERNAL LIGURIDES OPHIOLITES

F. Garzetti[1], R. Tribuzio[1,2], M. Tiepolo[2]

[1]*Dipartimento di Scienze della Terra, Università di Pavia, Italy*
[2]*Istituto di Geoscienze e Georisorse, CNR, Pavia, Italy*
fabio.garzetti@manhattan.unipv.it

The Internal Ligurides ophiolites are remnants of the oceanic lithosphere of the Ligurian Tethys basin. These ophiolites include gabbroic plutons that are locally crosscut by elongated bodies of pegmatoid horneblende-albitites. These leucocratic bodies display irregular contacts against the host gabbro, thus indicating that the melt injections occurred when the gabbroic body was not completely solidified. The gabbroic complex subsequently underwent an event of high temperature shearing. The resulting foliation is locally crosscut at high angle by a second generation of albitite bodies showing sharp planar boundaries against the host gabbro. On the basis of field relations, this event is inferred to be nearly coeval with the onset of hydrothermal circulation, as indicated by the presence of horneblende-bearing veins parallel to the second generation of albitites

Two types of zircons occur in both generations of albitites. The first zircon type (1) is colorless to slightly pink, commonly anhedral, with oscillatory and sector zoning. The second type (2) shows a short prismatic morphology, the color is opaque-pink to brown. The internal structure of zircon (2) is essentially spongy with pores and inclusions of chlorite, prehnite, albite, apatite and, to a lesser extent, of xenotime and thorite. A third type (3) of zircon is only present in the second generation of albitite. These zircons are morphologically similar to (2) but their internal structure is characterized by oscillatory zoning at the core, in turn rimmed by a zircon portion with spongy texture.

Zircons (1) from the two types of albitites have similar trace element compositions, compatible with an igneous origin. The inner portion of zircon (3) with oscillatory zoning differs in the higher contents of Sr, Y, Th, U, and a more pronounced Eu anomaly. However, their internal structures and chemical compositions are consistent with a magmatic nature. Conversely a different behavior is shown by zircon (2). On the basis of structure, inclusions and preliminary chemical data, a hydrotermal origin can be inferred for these zircons.

U-Pb geochronology indicates that zircons (3) are significantly younger than zircon (1). This implies that the formation of Internal Ligurides igneous rocks cover a relatively long time span. Further U-Pb data are currently in progress to verify the timing of the hydrothermal event.

THE LANZO PERIDOTITE MASSIF (WESTERN ALPS) IN THE FRAME OF THE PRE-OCEANIC EVOLUTION IN THE LIGURIAN TETHYS

L. Guarnieri, G.B. Piccardo

Dip.Te.Ris., Università di Genova, Italy
Luisa.Guarnieri@unige.it

The Lanzo Peridotite Massif belongs to the internal part of the High-Pressure, Low-Temperature metamorphic belt of the Western Alps (NW Italy) and it is divided in Southern (~ 55 km^2), Central (~ 90 km^2) and Northern (~ 5 km^2) bodies. Recent investigations document that the Lanzo peridotites derived from the sub-continental lithospheric mantle of the Europe-Adria system. They were exhumed towards shallow levels during passive lithospheric extension driving pre-oceanic rifting of the Jurassic Ligurian-Piemontese basin.

The South Lanzo peridotite section was diffusely and reactively percolated by MORB-type fractional melts when it was still resident at P > 1 GPa (*i.e.*, spinel-peridotite facies conditions), it was later impregnated by MORB-type fractional melts when exhumed to P < 1 GPa (*i.e.*, plagioclase-peridotite facies conditions), and finally was focused percolated by aggregate MORB melts. The North Lanzo peridotites were solely impregnated by aggregate MORB melts when they were already exhumed to plagioclase-peridotite facies conditions (P < 1 GPa).

Accordingly, the evolution of the South and North Lanzo bodies was remarkably different. The North Lanzo peridotites solely record melt impregnation by variably evolved aggregate MORB melts which, most probably, are related to the aggregate MORB primary melts which migrated through the South Lanzo peridotites by focused percolation within replacive harzburgite-dunite channels and underwent variable crystal fractionation (mostly olivine) during reactive migration. This suggests that prior to inception of lithosphere extension the mantle protoliths of the two different sections of the Lanzo Massif were originally located at different levels in the sub-continental lithosphere within the spinel-peridotite facies zone (1 GPa < P < 2.5 GPa) *i.e.*, at deeper levels the South Lanzo protoliths and at shallower levels the North Lanzo protoliths.

The early MORB-type fractional melts infiltrated and transformed the deeper South Lanzo peridotite protoliths, forming firstly the depleted reactive spinel peridotites and, subsequently, the impregnated plagioclase peridotites (*impregnation by fractional MORB melts*). The shallower North Lanzo peridotite protoliths escaped these early melt-peridotite interaction events and preserved their pyroxenite banding and pristine fertile lherzolite composition. Later on, focused migration within harzburgite-dunite channels allowed aggregate MORB melts to pass through the deeper South Lanzo plagioclase peridotites and to percolate diffusely the shallower, more fertile North Lanzo peridotites, producing significant interstitial crystallization and impregnation by variably evolved aggregate MORB melts (*impregnation by aggregate MORB melts*) in the North Lanzo lherzolites.

Ongoing lithosphere extension and stretching caused the break-up of the continental crust and the sea-floor exposure of the sub-continental lithospheric mantle. The South Lanzo peridotites, deriving from originally deeper mantle levels, were exposed at the sea-floor at more Internal Oceanic (MIO) settings of the basin, whereas the North Lanzo peridotites, deriving from originally shallower mantle levels, were confined to more External Ocean-Continent Transition (OCT) zones of the basin, close to the Adria continental margin.

Field, petrographic-structural and petrologic-geochemical studies on the Lanzo mantle peridotites allow to constraint from a mantle perspective the geodynamic scenario for the evolution of the Europe-Adria extensional system towards the opening of the Jurassic Ligurian Tethys oceanic basin.

NEW DATA ON EET 90299 ENSTATITE CHONDRITE CHONDRULES

P. Manzari, N. Melone

Dipartimento Geomineralogico, Università di Bari, Italy
paola.manzari@geomin.uniba.it

Elephant Moraine 90299 (EET 90299) enstatite chondrite is an unequilibrated low-iron chondrite [1]. Enstatite chondrites contain mineral assemblages suggestive of very reducing environment [2]. Unlike the other chondrites classes it contains only enstatite, $(Mg,Fe)_2Si_2O_6$, as major phase in chondrules. Searching for the relationship between their composition and micro-nano structures would led to new clues on their formation context. Five chondrules with a porphiritic and non porphiritic textures had been selected in a polished thin section. Their dimensions range from 400 to 3000 μm circa. μXRD data were collected with the Rigaku micro-diffractometer at IMAA-CNR (staz. TITO, Potenza, Italy), operating with CuKα (λ = 1,541838 Å) at 40 kV and 30 mA. As a first step, data points were collected with a 100 μm diffraction beam, with fixed ψ, ω values. EET 90299 chondrite consists of enstatite chondrules in a troilite(FeS)-kamacite(Fe-Ni) as major phases in matrix [3]. Here we compare collected data on one chondrule by *in situ* micro X-ray diffraction (μXRD) and electron microprobe analysis (EMPA). μXRD spectrum of this non porphiritic chondrule, ETC1, showed partial diffraction streaks thus indicating a partial mosaicity of the enstatite-pigeonite, $(Ca,Mg,Fe)(Mg,Fe)Si_2O_6$, grains and so a policrystalline nature of this chondrule, while partial diffraction lines of Na-feldsphatic mesostasis indicate its poorly crystalline nature. On the other hand, these results were confirmed by EMPA spots on different parts in ETC1. We used pressure variable secondary electron (VPSE) images as map because of cathodoluminescence of VPSE provides further informations on the chondrule microstructure. Fayalite, Fe_2SiO_4, also occurs, but is difficult to resolve in the bulk chondrule due to low signal and peaks overlap. Troilite occurs as a more distinguishable phase in this chondrule. It is also present chromite, $(Fe,Mg)Cr_2O_4$, probably a Fe-chromite as indicated by SEM analysis. Phase identification made use of the ICDD database using Crystal Sleuth software. These results, with EMPA investigation, provide new data on EET 90299 chondrules mineralogy. In this respect, micro X-ray diffraction is a versatile complementary technique that allows to identify major phases *in situ* on a thin section and so it is useful in meteoritics for preliminary, non destructive, investigations.

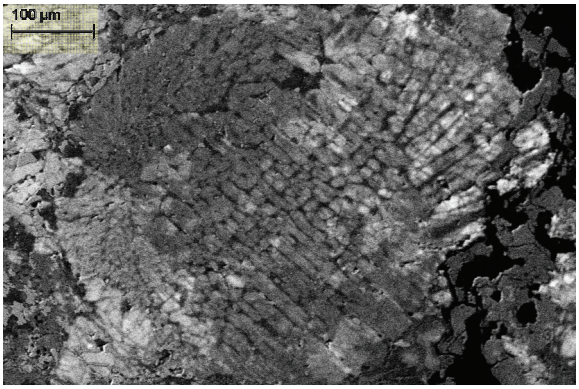

VPSE image of an EET 90299 chondrule

References [1] K. Keil, *Meteoritics*, **24**, 195-208, 1989; [2] D.M. Schneider, S.J.K. Symes, P.H. Benoit, D.W.G. Sears, *Meteor. Planet. Sci.*, **37**, 1401-1416, 2002, [3] W. Hsu, G. Crozaz, *Geochim. Cosmochim. Ac.*, **62**, 1993-2004, 1998.

GEOMATERIALS

Session 5
Minerals

APPRAISAL OF Ti SPECIATION IN TRIOCTAHEDRAL MICAS BY MEANS OF XPS INVESTIGATION: RECENT IMPROVEMENTS AND APPLICATIONS

E. Mesto[1], F. Scordari[1], M.R. Guascito[2], C. Malitesta[2]

[1]*Dipartimento Geomineralogico, Università di Bari, Italy*
[2]*Dipartimento di Scienza dei Materiali, Università del Salento, Italy*
mesto@geomin.uniba.it

The full characterization of transition elements (Ti, Fe) in mica, still today, is a not completely satisfied topic. Actually, the study is quite complicated because UV-VIS spectroscopy [1], EXAFS or XAS techniques [2] and EPR spectroscopy [3], that have been used to this end, gave ambiguous results. Differently, XPS technique proved to be a very useful tool in studying this kind of matrices, especially as to Ti and Fe, because the chemical shifts of these elements are related to their oxidation states and to their chemical environments. As it is well known, in the interpretation of XPS spectra, and particularly in terms of speciation, the "secondary structures" like shake-up, plasmon-loss, intrinsic and extrinsic losses (background), as well as the Auger parameter, play an important role. It is possible to obtain, in some cases, direct indications of bonding states and of the electronic structure of compounds, by means of the **κ** parameter, which gives a direct quantitative measure of intrinsic loss of energy [4]. The potentialities of the technique are particularly useful when also the Auger parameter is used in the interpretation of the spectra [5,6]. Such method, initially applied in order to characterize pure elements, has been extended to the characterization of a series of materials of technological interest, like oxides of transition metals [7], intermetallic compounds (special alloys of Al, Ti, V, Fe, silicides, etc.) [8], composite materials (interface silica/silica-modified with organic polymers) [9]. To test the possibility of using this method to improve the chemical characterization of Ti in complex materials like micas, we have systematically characterized a series of materials (single crystals) as "standard of references" in terms of BE, **κ** and Auger parameters. In particular, for Ti element the numerous XPS studies carried out in order to determine its speciation have given variegate results [10-12]. To provide accurate information from Ti signals it is necessary to use suitable standards in order to obtain guide parameters for the curve-fitting procedure. In this work, a very well characterized phologopite (SA1) from Monte Vulture (Potenza, Italy), with Ti^{4+} in octahedral site only [13], has been employed as Ti standard mica for XPS investigation. The curve fitting parameters of Ti*2p* spectrum obtained from SA1 sample were used to fit the XPS spectra of other mica samples from Black Hill (Australia) and Alto Paranaibo Presidente Olegairo (Brazil), in which octahedral Ti^{3+} and tetrahedral Ti^{4+} are detected. XPS results are in good agreement with SC-XRD, EPMA, SIMS and Mössbauer measurements, and show the great potentiality of XPS as a technique to get information on Ti speciation also from very small single crystals (100-200 μm).

References. [1] F.C. Hawyhorne, *Am. Mineral.*, **68**, 287-306, 1983; [2] G.A. Waychnas, *Acta Crystallogr. A***50**, 411-437, 1987; [3] H. Rager, C.A. Geiger, A Stall, *Eur. J. Mineral.*, **15**, 697-699, 2003; [4] J.E. Castle, A.M. Salvi, *J. Electron Spectrosc.*, **1103**, 114-116, 2001; [5] G. Moretti, *J. Electron Spectrosc.*, **95**, 95, 1998; [6] G. Moretti, A.M. Salvi, M.R. Guascito, F. Langerame, *Surf. Interface Anal.*, **36**, 1402, 2004; [7] A.M. Salvi, M.R. Guascito, A. BeBonis, F. Simone, F. Pennisi, Decker, *Surf. Interface Anal.*, **35**, 897, 2003; [8] J.E. Castle, A.M. Salvi, M.R. Guascito, *Surf. Interface Anal*., **31**, 881, 2001; [9] A.M. Salvi., R. Pucciariello, M.R. Guascito, V. Villani, L. Intermite, *Surf. Interface Anal*., **33**, 850-861, 2002; [10] C. Malitesta, I. Losito, F. Scordari, E. Schingaro, *Eur. J. Mineral*., **7**, 847-858, 1995; [11] F. Scordari, E. Schingaro, G. Pedrazzi, *Eur. J. Mineral*., **11**, 855-869, 1999; [12] E. Mesto, F. Scordari, C. Malitesta, P.M.A. Sherwood, *32nd International Geological Congress, Florence, Italy*, 2004; [13] F. Scordari, G. Ventruti, A. Sabato, F. Bellatreccia, G. Della Ventura, G. Pedrazzi, *Eur. J. Mineral.*, **18**, 379-391, 2006.

TOTAL ENERGIES OF DIFFERENT ANTIGORITE STRUCTURE MODELS: A DFT STUDY

G.C. Capitani[1], M. Mellini[2], L. Stixrude[3]

[1]*Dipartimento Geomineralogico, Università di Bari, Italy*
[2]*Dipartimento di Scienze della Terra, Università di Siena, Italy*
[3]*Department of Geological Sciences, University of Michigan, Ann Arbor, U.S.A.*
g.capitani@geomin.uniba.it

The serpentine mineral antigorite is known to be stable up to 6 GPa (200 km) at 620°C [1]. Under more extreme conditions, it breaks down to a dehydrated assemblage (Atg = Ol + Tlc (En) + H_2O). Earthquakes at intermediate mantle depth may be triggered by dehydration embrittlement caused by antigorite breakdown. In spite of the importance of antigorite at subduction zones, little is known of its properties at high pressures. Knowledge of the elasticity of antigorite is important for the interpretation of seismological observations at subduction zones and for the detection of antigorite in this and other geological settings.

This knowledge may be achieved, in principle, either experimentally or computationally. However, both routes are troublesome. Experimentally, one is faced with the high density of defects usually affecting single-crystal sized specimens, and with the difficulties in dealing with such a large unit cell and a DAC-shadowed reduced dataset. Computationally, the antigorite system is quite large and thus very costly. Moreover, a good guess of the crystal structure is mandatory to enhance the chances to successfully achieve any reliable result.

We report here the results of an *ab initio* quantum mechanical investigation of the antigorite structures proposed in the recent literature. The structures investigated are the m = 17 and the m = 16 polysomes, XRD refined by Capitani & Mellini [2,3] and a second m = 17 polysome proposed by Dòdony & co-workers [4]. Basically, the first two structure models differ from the last by the presence of tetrahedral 8-reversals and the absence of octahedral offsets.

The total free energy for the three models after structural relaxation are -6.983189, -6.986766, -6.977770 eV/atom, respectively. From these results it turns out that the models with tetrahedral 8-reversals and without octahedral offsets are energetically favoured with respect to the model excluding tetrahedral 8-reversals and including octahedral offsets. For comparison, the total energy difference between the two m = 17 antigorite models (5.42 meV/atom) is close to the energy difference between andalusite and kyanite. Moreover, has highlighted by the largest atomic displacements during relaxation, the energy excess is almost entirely due to the octahedral offsets, where Mg atoms at the centres of triangular prisms entail unfavourable crystal-chemical bonding.

Future calculations will be focused on the evaluation the antigorite compressibility.

References. [1] P. Ulmer, V. Trommsdorff, *Science*, **269**, 858-861, 1995; [2] G.C. Capitani, M. Mellini, *Am. Mineral*., **89**, 147-158, 2004; [3] G.C. Capitani, M. Mellini, *Am. Mineral.*, **91**, 394-399, 2006; [4] I. Dòdony, M. Postfai, P.R. Buseck, *Am. Mineral.*, **87**, 1443-1457, 2002.

DEHYDRATION REACTIONS AND MICRO/NANOSTRUCTURES IN EXPERIMENTALLY-DEFORMED SERPENTINITES

C. Viti[1], T. Hirose[2]

[1]*Dipartimento di Scienze della Terra, Università di Siena, Italy*
[2]*Kochi Institute for Core Sample Research, JAMSTEC, Kochi, Japan*
vitic@unisi.it

Serpentinites play a chief role in oceanic lithosphere dynamics, particularly in shear/fault and subduction zones. On one hand, serpentinites have peculiar mechanical properties (*e.g.*, low friction coefficient), strongly affecting fault behaviour and related seismicity. On the other hand, serpentine dehydration in subduction zones is responsible for fluid release, with implications in partial melting and subduction-related magmatism. Moreover, serpentinites show a transition from ductile to brittle under increasing T, following an opposite trend with respect to most rocks; this behaviour is related to dehydration processes, that give rise to pore overpressure and brittle failure (dehydration embrittlement; *e.g.*, [1,2]).

Mineralogical and micro/nanostructural changes in deformed lizardite + chrysotile serpentinites have been investigated by torsion experiments up to 650°C and 400 MPa [3]. High-resolution TEM showed that specimens underwent ductile (by microkinking and (001) interlayer glide) and brittle deformation (by microfracturing), together with dehydration and break-down reactions. Lizardite is affected by microkinking, with axial planes at high angle with respect to (001), and shows polytypic disorder, at difference from starting 1*T*-lizardite. Chrysotile fibres are deformed, with squeezed cross-sections and strong loss of interlayer cohesion.

Both lizardite and chrysotile break down to a fine intergrowth of olivine (up to 200 nm), talc (up to 30 nm) and poorly-crystalline material. Lizardite-out reaction preferentially occurs at kink axial planes, representing sites of preferential strain and enhanced reactivity; conversely, chrysotile break-down is a bulk process, resulting into large healed olivine aggregates. Overall observations suggest that dehydration and break-down reactions are more advanced in chrysotile than in lizardite.

References. [1] S.M. Peacock, *Geology*, **29**, 299-302, 2001; [2] H. Jung, H.W. Green, *Intern. Geol. Rev.*, **46**, 1089-1102, 2004; [3] C. Viti, T. Hirose, *Contrib. Mineral. Petr.*, 2008 (submitted).

NEW INSIGHT INTO THE EXTRA-FRAMEWORK CONTENT OF ZEOLITE LEVYNE

N. Rotiroti[1], G.D. Gatta[1], M. Petrelli[2]

[1]*Dipartimento di Scienze della Terra, Università di Milano, Italy*
[2]*Dipartimento di Scienze della Terra, Università di Perugia, Italy*
nicola.rotiroti@unimi.it

Levyne is a rare zeolite [ideal chemical formula $(Ca_{0.5},Na,K)_6(Al_6Si_{12}O_{36})\cdot 18H_2O$] discovered almost two centuries ago in the Fær Øer Islands by Brewster [1]. It is usually found as secondary mineral into cavities of andesitic and basaltic rocks. Merlino *et al*. [2] solved its crystal structure in the space group $R\bar{3}m$ from an untwined crystal. Later, Sacerdoti [3] reported new refinements of the crystal structure of two different levynes, Na and Ca-rich respectively. In all the aforementioned studies, all the extra framework cations (except the site C1 site), were described with isotropic thermal parameters [2,3]. The crystal chemistry of a large number of natural levynes was studied by Galli *et al*. [4]. The framework of this zeolite can be described as a sequence of six-membered rings (AABCCABBC…), which build up the so-called "levyne-cage" and is characterized by the presence of three equivalent channel systems perpendicular to the threefold axis, confined by eight-membered rings. The six-membered single ring represents the secondary building unit (SBU) of this framework type. The topological symmetry is $R\bar{3}m$ and corresponds to the general symmetry of the crystal structure.

In the present work we give new insights into the description of the extra framework population of two levynes, Ca-rich and Na-rich respectively, based on anisotropic structure refinement from single-crystal X-ray diffraction, wave-length dispersive electron microprobe analysis and Laser Ablation - Inductively Coupled Plasma - Mass Spectrometry (LA-ICP-MS). The chemical composition of our crystals slightly differs from those of Sacerdoti [3]. In order to describe the thermal behaviour of the extra framework content, we collected intensity data for both the levynes at 298 and 150 K.

The extra-framework content, represented by Ca, Na, K and water molecules, lies in the levyne-cages. At least five independent cation sites (C1, C2, C3, C4 and C5) have been located [2,3]. C1 is fully [2] or almost fully [3] occupied by Ca only. The C2, C3 and C4 sites are occupied by a mixture of Ca, Na and K. The C5 site is considered to be occupied by Ca, Na and K [2] or by K only [3].

Compared to previous studies, we observe different occupancies for the extra-framework sites that are in good agreement with the chemical analysis of the two samples. The high quality of the structural refinements allow a reliable description of the bonding environments based on a very good determination of bond-distances and bond-angles. Moreover, the low temperature data show that the thermo-elastic deformation of the structure is mainly accommodate by a re-arrangement of the extra-framework population.

LA-ICP-MS analyses show a high selection of trace elements with Ga, Rb, Sr, Ba and Mg detected in appreciable contents. As shown by LA-ICP-MS data, levyne behaves as a "geochemical trap" for Sr which displays different affinity (ratio of about 1:5) for Ca (~ 300 ppm) and Na-rich (~1500 ppm) levyne respectively.

References. [1] M. Brewster, *Edinb. J. Sci.*, **2**, 332-334, 1825; [2] S. Merlino, E. Galli, A. Alberti, *Tscher. Miner. Petrog.*, **22**, 117-129, 1975; [3] M. Sacerdoti, *Neues Jb. Miner. Monat.*, **3**, 114-124, 1996; [4] E. Galli, R. Rinaldi, C. Modena, *Zeolites*, **1**, 157-160, 1981.

HIGH-PRESSURE STRUCTURAL BEHAVIOR OF INGERSONITE, $Ca_3Mn^{2+}Sb^{5+}{}_4O_{14}$: AN *in situ* SINGLE-CRYSTAL X-RAY STUDY

L. Chelazzi[1], P.F. Zanazzi[2], P. Bonazzi[1], L. Bindi[3]

[1]*Dipartimento di Scienze della Terra, Università di Firenze, Italy*
[2]*Dipartimento di Scienze della Terra, Università di Perugia, Italy*
[3]*Museo di Storia Naturale, Università di Firenze, Italy*
laura.chelazzi@unifi.it

An *in situ* high-pressure single-crystal X-ray diffraction study has been carried out at room temperature up to 7.42 GPa on a crystal of ingersonite, ideally $Ca_3Mn^{2+}Sb^{5+}{}_4O_{14}$, from the type material. Unit-cell data were measured at 10 pressures, and intensity data were collected at 6 pressures. Ingersonite is isostructural with the synthetic weberite-3*T* polytype [1] and related to the pyrochlore structure-type. The structure of ingersonite can be described as a sequence of pairs of polyhedral layers (*M* and *N*) stacked along [001]. As far as the cation sites are concerned, *M* and *N* layers have general formula AB_3 and A_3B respectively, where B are octahedrally coordinated cations (B1, B2, and B3) which accommodate Sb^{5+} with very minor substitution by lighter divalent cations. The octahedral framework gives rise to three types of larger cavities, which host Ca (A1 and A3) and Mn^{2+} (A2). Owing to the P range investigated and the quality of data, a 2nd-order Birch-Murnaghan Equation of State (EoS) is the best approximation to describe the ingersonite volume evolution with P. The refined EoS parameters are V_0 = 810.6(1) Å^3 and K_0 = 154.5(2.4) GPa. To our knowledge, no compressibility data of fluorides and oxides with weberite-type structure have been reported in literature. However, the value of the bulk modulus found in ingersonite appears lower than those reported for cubic pyrochlore-like compounds with different composition, which are in the range 164.8(1.5) GPa ($Sm_2Ti_2O_7$; [2]) - 210(4) GPa (Tb_2SnTiO_7; [3]). The ingersonite behavior with pressure is almost isotropic and the decrease of the unit-cell volume is mainly due to the kinking of the polyhedra rather than their volume decrease. The overall mean <B-O> distance and the ^{VI}<A2-O> distance are quite constant, indicating a scarce compressibility of both the Sb^{5+} and Mn^{2+} octahedra. However, an increase of pressure induces marked variations in the pyrochlore-like *M* layer where A2 is located. The largest change is observed for *z* atomic coordinate of the O2 atom. As a first consequence of the shift of this atom, a dramatic lengthening of the A3-O2 distance is observed (from 2.710 to 3.20 Å), so that from 6.38 GPa the A3 cation is properly described as seven-fold coordinated. Using an anion-centered polyhedral description, O2 is the only oxygen atom which is asymmetrically located in an octahedral interstice, this feature being the most remarkable difference between the structure of ingersonite (*i.e.* weberite-3*T* type, space group $P3_121$) and that of zirconolite-3*T* (pyrochlore structure type, space group $P3_121$), where all the oxygen atoms occupy the tetrahedral interstices of a cubic A_2B_2 array. With the increase of pressure, O2 atom migrates from the A_4B_2 octahedral cavity towards the adjacent AB_3 tetrahedral cavity, suggesting that a transition from weberite-3*T* to zirconolite-3*T* structure type could occurs at pressures higher than 11 GPa.

References. [1] P. Bonazzi, L. Bindi, *Am. Mineral.*, **92**, 947-953, 2007; [2] F.X. Zhang, B. Manoun, S.K. Saxena, C.S. Zha, *Appl. Phys. Lett.*, **86**, 181906, 2005; [3] R.S. Kumar, A.L. Cornelius, M.F. Nicol, K.C. Kam, A.K. Cheetham, J.S. Gardner, *Appl. Phys. Lett.*, **88**, 031903, 2006.

RETROGRADE HYDRATION MECHANISM OF AMPHIBOLE AT THE TEM SCALE

M. Ferrari, C. Viti

Dipartimento di Scienze della Terra, Università di Siena, Italy
ferrari15@unisi.it

The Monte Capanne intrusion (Elba Island, Italy) induced thermal metamorphic reactions within pseudomorphic lizardite + chrysotile serpentinites, giving rise to amphibole (anthophyllite and/or tremolite) and olivine crystallization.

Anthophyllite grows both on bastites and mesh textures, producing elongated random crystals, commonly cut by late retrograde serpentine veins. TEM investigation revealed that anthophyllite may be locally ordered, with sharp and intense [001], [010], and [$0\bar{1}1$] SAED patterns, unaffected by streaking. However, in most cases, the amphibole structure is affected by several defects, resulting into evident streaking along **b*** (polysomatic disorder) and **c*** (polytypic disorder).

TEM images revealed that anthopyllite is affected by different retrograde hydration processes resulting into: 1) topotactic talc, 2) pyriboles and 3) serpentine inclusions. [001] HR-images show that anthopyllite have topotactic boundaries with talc and with talc + lizardite intergrowths; the characteristics of (010) and (210) reactions fronts are in agreement with previous papers [1,2].

Pyribole chains (triple and wider chains) occur in disordered sequences and are often associated to serpentine-bearing inclusions. Serpentine inclusions may be elongated, with planar $(001)_{liz}$ lattice fringes parallel to (100) of host anthophyllite; otherwise, they have a rounded to euhedral-rhombic shape (negative-crystals) and are filled by curved (001) lattice fringes, resulting into incomplete chrysotile half-fibres. Serpentine inclusions always cut the pyribole lamellae. These kinds of inclusions may recall the so-called "flying soucers", described by [3].

According the overall nanotextural evidences, the possible hydration sequence is 1) topotactic talc – 2) pyriboles – 3) serpentine inclusions.

References: [1] D.R. Veblen, *Am. Mineral.*, **65**, 1075-1086, 1980; [2] D.R. Veblen, P.R. Buseck, *Am. Mineral*., **66**, 1107-1134, 1981; [3] D.R. Veblen, P.R. Buseck, *Am. Mineral*., **65**, 599-623, 1980.

THE GEMMOLOGICAL CHARACTERIZATION OF PERIDOT FROM SARDINIA (ITALY)

I. Adamo[1], R. Bocchio[1], L. Prosperi[2]

[1]*Dipartimento di Scienze della Terra "A. Desio", Università di Milano, Italy*
[2]*Istituto Gemmologico Italiano, Milano, Italy*
ilaria.adamo@unimi.it

The green gem variety of olivine is today known by gemmologists as peridot. Compositionally, it belongs to the solid-solution series between forsterite [Fo: $Mg_2(SiO_4)$] and fayalite [Fa: $Fe_2(SiO_4)$], but most material falls within the range 80-90 % forsterite. Peridot has been reported from a number of sources worldwide, including some with past and present commercial significance, as Zabargad (Egypt), Arizona (United States), Myanmar, China and Pakistan.

A gem quality yellowish green olivine has been found also in Italy: it occurs in nodules of spinel-peridotites included in the Plio-Quaternary alkali basalts from Pozzomaggiore, north-western Sardinia [1]. Nodules range in dimension from 10 to 25 cm and contain a typical four-phase mineral assemblage of olivine, orthopyroxene, clinopyroxene and spinel, in varying modal proportion [2].

In the present work we have investigated six rough peridot fragments of about 0.5-1 cm, sampled in nodules occurring along the road from Padria to Pozzomaggiore, Sardinia. From this material, we have obtained ten faceted gems weighting from 0.14 to 0.66 ct. The gems and the rough grains have been characterized by traditional gemmological tests combined with advanced analytical techniques (X-ray powder diffraction, IR and UV-Vis-NIR spectroscopy, EMPA-WDS and LA-ICP-MS measurements) in order to determine their optical, physical and chemical properties.

All the examined gems are biaxial positive with refractive indices and birefringence ranging over 1.650-1.690 and 0.038-0.039, respectively; the density varies from 3.32 to 3.36 g/cm^3. When viewed with a gemmological microscope, all the specimens are characterized by few inclusions, mainly liquid veils and partially healed fractures. The crystallographic features [space group *Pbnm* with unit cell parameters a = 4.762(1) Å, b = 10.224(2) Å and c = 5.992(1) Å] and the mid-IR spectra are consistent with the obtained chemical composition of $Fo_{91}Fa_9$. They also contain appreciable NiO and MnO contents (average 0.56 and 0.13 wt.%, respectively), whereas the amounts of all the other trace elements (Li, B, Na, Ca, Sc, Ti, V, Cr, Co, Zn) are below 0.1 wt.%. The UV-Vis-NIR spectra are characterized by the absorption features of Fe^{2+}, which is the main responsible for the colour [3].

All the physical and chemical properties of the olivine from Pozzomaggiore, Sardinia, are in the range of those commonly reported in literature for peridot [4-6] and confirm that this material is potential as gem and could indeed have a definite economic interest [1].

References. [1] B. Bianchi Potenza, V. De Michele, G. Liborio, R. Rizzo, *La Gemmologia*, **XVI**, 17-28, 1991; [2] C. Dupuy, J. Dostal, J.L. Bodinier, *Mineral. Mag.*, **51**, 561-568, 1987; [3] R.G. Burns, *Mineralogical Applications of Crystal Field Theory*, 2nd ed., Cambridge University Press, UK, 1993; [4] W.A. Deer, R.A. Howie, J. Zussman, *Rock-forming Minerals*, Longman, 1982; [5] R. Webster, *Gems: Their sources, Description and Identification*, 6th ed., Butterworth-Heinemann, Oxford, 2006; [6] R.G. Burns, F.E. Huggins, *Am. Mineral*., **57**, 967-985, 1972.

A MULTI-METHODOLOGICAL STUDY OF A GEM-QUALITY SYNTHETIC DARK BLUE BERYL

I. Adamo[1,2], G.D. Gatta[1,2], N. Rotiroti[1,2], V. Diella[2], A. Pavese[1,2]

[1]*Dipartimento di Scienze della Terra "A. Desio", Università di Milano, Italy*
[2]*CNR - Istituto per la Dinamica dei Processi Ambientali, Milano, Italy*
ilaria.adamo@unimi.it

Beryl is an accessory mineral commonly found in pegmatitic rocks, with ideal chemical formula $Be_3Al_2Si_6O_{18}$ and crystal structure consisting of six-membered rings of Si-tetrahedra, linked by Al-octahedra and Be-tetrahedra, forming a three-dimensional framework. The "extra-framework" content (alkali cations, water and carbon dioxide molecules) lies within the six-membered ring channels parallel to [0001].

Because of the peculiar commercial value of beryl, a remarkable number of synthetic samples, emeralds and other various specimens with "exotic" colourations, are permanently present on the market [1].

In the present work a multi-methodological investigation of a synthetic Cu/Fe-bearing dark blue beryl [$^{IV}(Be_{2.86}Cu_{0.14})_{\Sigma=3.00}$ $^{VI}(Al_{1.83}Fe^{3+}_{0.14}Mn^{2+}_{0.03}Mg_{0.03})_{\Sigma=2.03}$ $^{IV}(Si_{5.97}Al_{0.03})_{6.00}$ O_{18} · $(Li_{0.12}Na_{0.04}$ · $0.40H_2O)$] has been performed by means of gemmological standard testing, combined with electron microprobe analysis, laser ablation inductively coupled plasma mass spectroscopy, thermogravimetric analysis, infrared spectroscopy and single-crystal X-ray diffraction. The aim of this work is to provide a full characterization of this material, covering gemmological properties, crystal structure and crystal chemistry.

The investigated 2.70 ct gem is uniaxial negative with refractive indices $\omega = 1.590$ and $\varepsilon = 1.582$ and birefringence 0.008; the measured density is 2.77 g/cm^3. These properties are the same reported for the natural aquamarine beryl [2]. Only the characteristic internal growth pattern can be useful for the separation of this gem material from its natural counterparts [3]. The chemical analyses reveal significant contents of iron and copper, the latter never found in any natural aquamarine beryl. The X-ray single-crystal structural refinements confirm that the gem maintains the space group *P*6/*mcc* and the general structural arrangement of the natural beryls, with unit-cell parameters: $a \sim 9.25$ and $c \sim 9.22$ Å. The analysis of the difference Fourier maps of the electron density suggests that Cu is located at the tetrahedral site (Wyckoff 6*f*-position), along with Be, whereas Fe shares the octahedral site with Al (4*c*-position). The channel content is distributed on two extra-framework sites: the first one occupied by water molecules (2*a*-position) and the second one (2*b*-position) mainly by alkali cations, in agreement with previous studies on beryls [4]. Infrared spectra show that the H_2O molecules in the channel are present with two different configurations: one with the H···H vector oriented //[0001] ("type I") and the other with H···H vector oriented ⊥[0001] ("type II") [5,6].

References. [1] J.I. Koivula, M. Tannous, K. Schmetzer, *Gems Gem.*, **36**, 360-379, 2000; [2] R. Webster, *Gems: Their sources, Description and Identification*, 6th ed., Butterworth-Heinemann, Oxford, 2006; [3] I. Adamo, A. Pavese, L. Prosperi, V. Diella, D. Ajò, G.D. Gatta, *Gems Gem.*, submitted; [4] G.D. Gatta, F. Nestola, G.D. Bromiley, S. Mattauch, *Am. Mineral.*, **91**, 29-34, 2006; [5] D.L. Wood, K. Nassau, *J. Chem. Phys.*, **42**, 2220-2228, 1967; [6] D.L. Wood, K. Nassau, *Am. Mineral.*, **53**, 777-800, 1968.

XRDT AND TEM STUDY OF THE STRIATIONS OF THE TOURMALINE PRISM FACES

G. Agrosì, G.C. Capitani, I. Pignatelli, E. Scandale

Dipartimento Geomineralogico, Università di Bari, Italy
scandale@geomin.uniba.it

Natural crystals of tourmaline are characterized by striations parallel to the **c** axis on prismatic faces. Crystals without striations are really rare, so it is important to understand the origin and the meaning of striations. Different hypotheses were made about the origin of the striations and the most important of which are: 1) juxtaposition of prismatic facets, that make curved prism surfaces, 2) multiple parallel twinning. A different conclusion was made in a study of tourmaline crystals from pegmatite pockets of island of Elba (Italy): the origin of striations was attributed to a particular type of growth mechanism [1]. Two growth stages were identified in the quoted study from both defect analysis and crystal-chemical characterization of the samples. The former stage was the pegmatitic, corresponding to the inner greenish-yellow region dislocation-free that was characterized by growth bands and growth sector boundaries. Therefore, 3D nucleation occurred and the bulk tourmaline crystals grew either by 2D mechanism or by direct adsorption of growth units, or both these mechanisms at once. The latter stage was hydrothermal and regarded the colourless overgrowth characterized by screw dislocations. During this last growth stage striations were formed. Small crystal grains, in fact, developed parallel to the *c* axis by spiral growth mechanism. The imperfect juxtaposition of prismatic facets of each crystal grain caused the striations.

Nevertheless, it should be emphasized that the absence of striations on prismatic facets of core during the pegmatitic growth stage has not been found yet.

In order to deeply investigate the origin of striations, in this study other samples of tourmaline from island of Elba with a greenish-yellow core and colourless overgrowth have been analyzed. In particular, sample fragments with missing external overgrowth have been investigated. Hence it has been possible to observe optically that the prismatic facets of inner core did not show striations. XRDT studies of basal slices confirm that the core is dislocation-free, while the colourless overgrowth is characterized by a high density of dislocations. Therefore these observations confirm the conclusions of Agrosì *et al.* [1].

In addition, to investigate the interface between core and rim, smaller fragments of tourmalines have been studied by TEM. Preliminary HRTEM results show a perfect structural continuity between inner core and external rim. Moreover, the interface does not correspond to an integer surface but correspond to a transition region characterized by a high concentration of impurities.

References. [1] G. Agrosì, F. Bosi, S. Lucchesi, G. Melchiorre, E. Scandale, *Am. Mineral.*, **91**, 944-952, 2006.

MINERALOGICAL AND CHEMICAL VARIATIONS IN A SULPHIDE WASTE-ROCK DUMP (LIBIOLA MINE, LIGURIA)

E. Azzali[1], P. Marescotti[1], C. Carbone[1], G. Lucchetti[1], D. Servida[2]

[1]*Dip.Te.Ris., Università di Genova, Italy*
[2]*Dipartimento di Scienze della Terra, Università di Milano, Italy*
marescot@dipteris.unige.it

In this work we have studied the mineralogical, chemical, and NAPP (Net Acid Producing Potential) variations occurring on a 3.5 ha sulphide waste-rock dump built over a period of about 100 years by the dumping, in a vertical sequence, of both non-valuable mineralisations and non-mineralised rocks coming from underground and open-pit excavations. This dump, as well as the overall Libiola mine area, is characterised by active AMD (Acid Mine Drainage) processes triggered by the diffuse oxidation of sulphide minerals [1 and references therein]. Twenty-one sampling sites were chosen by defining a grid throughout the overall dump surface and the sampling points were selected within every cell where well-exposed vertical cuts occur. Qualitative and quantitative mineralogical analyses were performed by transmitted- and reflected-light optical microscopy and by SEM-EDS. Bulk chemistry was assessed by ICP-AES and XRF analyses whereas the NAPP evaluation was based on the "AMIRA P387A" procedure [2].

The studied samples are generally incoherent or weakly cemented by Fe-oxide and -oxyhydroxides and vary from gravel-dominated to sandy-gravel sediments, with a uniform particle size distribution in the range 2-64 mm. They are composed by variable amount (10-26 wt.%) of sulphide mineralization fragments (pyrite ± chalcopyrite ± sphalerite) showing various degree of oxidation. Mafic and ultramafic clasts (basalt, serpentinite and ophiolitic breccias) vary from 35 to 80 wt.% and they are generally unaltered (serpentinite) or weakly altered. Secondary minerals are almost exclusively represented by Fe-oxyhydroxides (goethite) and -oxides (hematite) and they occur as cement filling interclast voids, homogeneous crusts (hardpan layers), and pseudomorphic replacement of sulphide mineralisation. They vary from 10 to 50 wt.% and their abundance is strictly correlated to the sulphides content of the sample.

The bulk chemistry (major, minor, and trace elements) appears to be controlled either by the primary unaltered minerals and by the different alteration products. In fact, as evidenced by several authors [3 and references therein], Fe-oxydes and -oxyhydroxides have a good affinity for several transition- and heavy-metals, that they effectively scavenge by the circulating solutions. The distribution of metals of environmental concern on the waste dump has been further plotted on contour maps. These statistical interpolations allow to evidence significant spatial variations throughout the dump that reflect either the composition of the dumped materials and the evolutive stage of the AMD processes.

With the exception of few sites, all sampling points evidenced positive NAPP values which mean that AMD processes are still active and presumably should persist for long time, due to the high sulphide contents and to the complete absence of potentially neutralising mineral phases.

References. [1] P. Marescotti, C. Carbone, L. De Capitani, G. Grieco, G. Lucchetti, D. Servida, *Environ. Geol.*, **53**, 1613-1626, 2008; [2] IWRI & EGI, *ARD test handbook - AMIRA P387A*, 2002; [3] R.M. Cornell, U. Schwertmann, *Iron Oxides, VCH - Weinheim*, 573 pp., 1996.

"ANOMALOUS RINKITE", A NEW MINERAL FROM AGPAITIC SYENITE OF ILES DE LOS (GUINEA)

C. Biagioni[1], E. Bonaccorsi[1], S. Merlino[1], G.C. Parodi[2], N. Perchiazzi[1], V. Chevrier[2]

[1]*Dipartimento di Scienze della Terra, Università di Pisa, Italy*
[2]*Muséum National d'Histoire Naturelle, Paris, France*
biagioni@dst.unipi.it

During a study of the complex Zr-Ti-Nb-REE minerals belonging to cuspidine and rinkite families, present in the cavities of nepheline syenites of Los Archipelago (Guinea, West Africa) [1], we investigated, with single crystal techniques, a sample tentatively identified as nacareniobsite-(Ce) by Parodi & Chevrier [2]. This mineral forms very small acicular crystals (up to 0.5 mm), colorless, elongated on [100]; it is a late-stage product of hydrothermal alteration of "eudialyte" and is associated with aegirine, analcime and sphalerite.

Oscillation and Weissenberg photographs showed a doubling of the *b* axis (11.3 Å instead of 5.6 Å) and possible space groups *C*2/*c* or *Cc* instead of $P2_1/c$ as in nacareniobsite-(Ce) [3]. We provisionally denoted this new phase "anomalous" rinkite, due to the differences in comparison with the other members of rinkite family (mosandrite, nacareniobsite-(Ce) and rinkite).

As in the case of rinkite, this "anomalous" rinkite shows an OD character: all the reflections with odd *k* values (and also with odd *h* values, due to the *C* centring) are very weak and display diffuseness along **c***. The 'family cell', corresponding to the strong reflections (even *k* and *h* values) displays orthorhombic symmetry: $a_F \sim 3.75$, $b_F \sim 5.65$, $c_F \sim 18.8$ Å, space group symmetry *Pmnn* (or *P*2*nn*).

The intensity data for structure determination have been collected at the synchrotron radiation source Elettra (Trieste). The structure was solved by direct methods in the space group *Cc*, cell parameters: $a = 7.473(2)$, $b = 11.294(2)$, $c = 18.778(4)$ Å, $\beta = 101.60(2)°$. The crystal structure was then refined to $R_1 = 0.106$ for 1793 independent reflections with $|F_o| \geq 4\sigma_F$. Following the description of the crystal structure of dovyrenite [4], "anomalous" rinkite can similarly be described in modular terms as composed by rosenbuschite-like "octahedral" sheets, tobermorite-like sheet and disilicate groups.

The rosenbuschite-like "octahedral" sheet is parallel to (001) and it is formed by two distinct columns running along **a**, formed by edge-sharing polyhedra; a first column is composed by Na(1) eight-fold polyhedra, alternating with small Nb octahedra; the other column is formed by alternating Na(2) and Na(3) octahedra. The structural study shows that the Nb site is actually occupied by Nb for 60% and Ti for 40%, in good agreement with chemical data, and that the Na sites are occupied by Na and Ca, with Na >> Ca.

The tobermorite-like sheet is formed by columns, running along **a**, of edge-sharing seven-fold coordinated Ca polyhedra connected along **b**, giving rise to an undulating **a**,**b** sheet. The results of the study indicate that the Ca sites are occupied by Ca and REE, with Ca > REE.

Disilicate groups are grasped on both sides of the Na(1) polyhedron in the rosenbuschite-like sheets; at the same time they are linked through edge sharing to the seven-fold coordinated polyhedra in the tobermorite-like sheets, thus firmly fixing the connection between the two types of sheets.

The simplified chemical formula of "anomalous" rinkite, obtained through chemical and structural investigations, is $(Ca,Na,REE,\square)_7(Nb,Ti)[Si_2O_7]_2OF_3$.

References. [1] C. Moreau, D. Ohnestetter, D. Demaiffe, B. Robineau, *Can. Mineral.*, **34**, 281-299, 1996; [2] G.C. Parodi, V. Chevrier, *Bull. Lias. Soc. Française Min. Crist.*, **16**(2), 2004; [3] O.V. Petersen, J.G. Rønsbo, E.S. Leonardsen, *N. Jb. Miner. Monat.*, **1989**, 84-96, 1989; [4] M. Kadiyski, T. Armbruster, E.V. Galuskin, N.N. Pertsev, A.E. Zadov, I.O. Galuskina, R. Wrzalik, P. Dzierzanowski, E.V. Kislov, *Am. Mineral.*, **93**, 456-462, 2008.

ANKANGITE FROM MONTE ARSICCIO MINE (APUAN ALPS, TUSCANY): THIRD WORLD OCCURRENCE

C. Biagioni, P. Orlandi, M. Pasero

Dipartimento di Scienze della Terra, Università di Pisa, Italy
biagioni@dst.unipi.it

Ankangite is a Ba-Ti oxide of the cryptomelane group, described in 1989 from the Ankang County, Shaanxi Province, China, in a quartz vein associated with baryte, barytocalcite, roscoelite, and diopside [1]. Ankangite was also reported as an accessory mineral in corundum-bearing hornfels in the Khibiny alkaline pluton, Kola Peninsula, Russia [2].

During a study of the mineralogy of the baryte-pyrite-Fe oxides deposit of Monte Arsiccio (Apuan Alps, Tuscany) we identified this rare species. Ankangite occurs in fractures of dolomitic marble as small prismatic crystals, up to 1 mm long, black in color, with submetallic luster. It is associated with "apatite", anatase, arsenopyrite, Ba-rich K-feldspar, baryte, dolomite, Pb-Sb sulfosalts, pyrite, quartz, sphalerite, stibnite, and valentinite.

A chemical analysis performed by EPMA points to the crystal-chemical formula $Ba_{0.93}(Ti_{5.93}V_{1.79}Cr_{0.32}Fe^{2+}_{0.05})_{\Sigma=8.08}O_{16}$.

The intensity data for the structure refinement have been collected with a Siemens P4 four-circle diffractometer; unit cell parameters were a = 10.142(1), c = 2.9533(3) Å. The structure was refined in the space group $I4/m$ to R_1 = 0.016 for 371 independent reflections with $|F_o| \geq 4\sigma_F$.

The crystal structure of ankangite is characterized, as all members of the cryptomelane group, by octahedra arranged in edge-sharing columns, which in turn link together, again by edge-sharing, forming ribbons, with width of two octahedra; cross-linking of ribbons by corner sharing gives rise to a square 2x2 tunnel structure [3].

Ba cations are located inside the tunnels; the introduction of Ba in the structure requires the partial substitution of Ti by trivalent or divalent cations. In ankangite, Ti is predominantly substituted by V^{3+}. The structural refinement shows that Ba is statistically distributed between two distinct sites, the former at (0,0,½), the latter at (0,0,z); it is likely that this statistical occupancy reflects an incommensurate distribution of Ba cations along the tunnels.

References. [1] X. Ming, M. Zhesheng, P. Zhizhong, *Chinese Sci. Bull.*, **34**, 592-596, 1989; [2] Y.A. Mikhailova, N.G. Konopleva, V.N. Yakovenchuk, G.Y. Ivanyuk, Y.P. Men'shikov, Y.A. Pakhomovsky, *Geol. Ore Dep.*, **49**, 590-598, 2007; [3] M. Pasero, *Rev. Min. Geochem.,* **57**, 291-305, 2005.

GOING INSIDE THE POLYBASITE STRUCTURE: THE ROLE OF SILVER IN THE *B* LAYER OF THE -*M*2*a*2*b*2*c* POLYTYPE

L. Bindi[1], S. Menchetti[2]

[1]*Museo di Storia Naturale, Università di Firenze, Italy*
[2]*Dipartimento di Scienze della Terra, Università di Firenze, Italy*
crystal@unifi.it

The minerals of the pearceite-polybasite group exhibit the general formula $[M_6T_2S_7][Ag_9CuS_4]$ with M = Ag, Cu and T = As, Sb, and their crystal structure can be described as the succession, along the *c* axis, of two pseudo-layer modules: a $[M_6T_2S_7]^{2-}$ *A* module layer and a $[Ag_9CuS_4]^{2+}$ *B* module layer ([1] and references therein). From a chemical point of view, the members of this group are generally pure, only containing minor amounts of Bi, Pb, Zn, and Fe. Nonetheless, the recent discovery of three new mineral species belonging to this group (*i.e.*, selenopolybasite [2], cupropearceite and cupropolybasite [3]) expands the range of chemical compositions reported to date. In the course of a study dealing with the characterization of structurally complex silver-bearing minerals of mineralogical collections from various museums, we recovered a sample of polybasite (polytype -*M*2*a*2*b*2*c*) with the highest silver content (> 15 a.p.f.u.) and the lowest Cu content (< 1 a.p.f.u.) yet discovered in nature. Indeed, the chemical range reported up to date (in atoms per formula unit) for polybasite-*M*2*a*2*b*2*c* samples was 13.62-14.98 for Ag and 1.01-2.42 for Cu [1-4]. The sample containing the polybasite crystal used in the present study (Royal Ontario Museum, Canada - cat. number M27183) is from Gowganda, Timiskaming District, Ontario, Canada, a well-known source of silver-bearing minerals. Electron microprobe analysis gave the following chemical formula (on the basis of 29 atoms): $[Ag_6(Sb_{1.78}As_{0.18})_{\Sigma=1.96}S_7][Ag_9(Ag_{0.63}Cu_{0.43})_{\Sigma=1.06}S_4]$. The structural study ($R$ = 0.0574) showed that in the $[Ag_9CuS_4]^{2+}$ *B* (or *B*') module layer the B3 structural position is dominated by silver. This result is new because the B positions [B1, B2 (Wyckoff 4*e*), and B3 (Wyckoff 8*f*)] are occupied by copper only and exhibit a nearly perfect linear coordination in all the members belonging to the pearceite-polybasite group. In the sample studied here B1 and B2 are occupied by copper (bond distances: 2.16 Å), whereas B3 (fully occupied by silver) shows a larger distance of 2.39 Å. This value is close to those observed for the linearly-coordinated Ag atoms of the *B* module layer (range: 2.39-2.49 Å). All the <B1,B2,B3>-S bond distances are mainly lined along the **c**-axis. This means that when Ag substitutes for Cu in one of these structural positions we should observe an increase in the *c* parameter and a consequent increase in the volume of the unit-cell. Such an increase in cell volume for the Ag-rich polybasite studied here was observed. It exhibits a unit-cell volume (9599 $Å^3$) which exceeds by far the range of values reported in the literature (9242-9504 $Å^3$; [1]). The increase in the unit-cell volume is principally related to the increase of the **c**-axis which jumps to 24.1061 Å in the present sample. Remarks on the possibility that the polybasite here studied deserves or not its own name are discussed.

References. [1] L. Bindi, M. Evain, P.G. Spry, S. Menchetti, *Am. Mineral.*, **92**, 918-925, 2007; [2] L. Bindi, M. Evain, S. Menchetti, *Can. Mineral.*, **45**, 1525-1528, 2007; [3] L. Bindi, M. Evain, P.G. Spry, K.T. Tait, S. Menchetti, *Mineral. Mag.*, **71**, in press, 2007; [4] H.T. Hall, *Am. Mineral.*, **52**, 1311-1321, 1967.

ASCHAMALMITE ($Pb_6Bi_2S_9$): CRYSTAL STRUCTURE REFINEMENT AND ORDERING SCHEME FOR Pb AND Bi ATOMS

M. Boiocchi[1], A. Callegari[2]

[1]*Centro Grandi Strumenti, Università di Pavia, Italy*
[2]*Diparimento di Scienze della Terra, Università di Pavia, Italy*
massimo.boiocchi@cgs.unipv.it

Aschamalmite is a rare sulfosalt with the ideal formula $Pb_6Bi_2S_9$. It is reported as a monoclinic form of heyrovskyite, the orthorhombic (*Cmcm*) modification of the $Pb_6Bi_2S_9$ compound [1]. This study, performed on a single crystal with a Bruker-Axs CCD-based diffractometer, reports the first structure refinement [R_{obs} 6.54% for 2141 reflections with $I_{obs} > 3\sigma(I_{obs})$ and $2\theta_{max} = 60°$ Mo-Kα] of a pure stoichiometric aschamalmite crystal, with the aim of clarifying the crystal-chemical reasons that lead to the lowering of symmetry.

S5

Aschamalmite is monoclinic, *C*2/*m*, with $a = 13.719(1)$ Å, $b = 4.132(1)$ Å, $c = 31.419(3)$ Å, $\beta = 90.94(1)°$, $V = 1780.8(4)$ Å^3. The unit cell edges are similar to heyrovskyite but, lacking the mirror plane parallel to (001), the four independent octahedra of heyrovskyite (M2, M3, M4, M5) become eight independent octahedra in aschamalmite (M2A, M2B, M3A, M3B, M4A, M4B, M5A, M5B). An independent eight-fold coordinated M1 site (filled by Pb) is present in both structures. Occupancy refinement for the octahedral sites does not allow to detect significant differences among the mean atomic numbers, because Pb^{2+} and Bi^{3+} cations are isoelectronic. The comparison of the mean bond lengths between couples of octahedral sites with A and B suffix (that in the orthorhombic phase are symmetrically related) shows that the M4A-M4B couple, as well as the M5A-M5B couple, exhibit significant differences.

It is well known that no direct relation exists between the mean dimension of Me-S polyhedra (Me = Tl^+, Pb^{2+}, Bi^{3+}) and the site population, because of the variable influence of the lone electron pairs that often induces the formation of highly distorted polyhedra. Better comparisons can be obtained by using the mean value of the three shortest Me-S distances, that are more suitable to discriminate Me-S polyhedra differently populated [2]. In the case of aschamalmite, comparison among the mean value of the three shortest bond distances emphasizes that the most different couples are M4A-M4B and M5A-M5B and that M4A and M5B have the shortest mean bond lengths among all the M sites. Therefore, the monoclinic symmetry of aschamalmite is due to the preferred ordering of the smaller Bi^{3+} cations at M4A and M5B sites. However, it is not ascertained that these sites (corresponding to 2 apfu) are only Bi^{3+} populated, because other sites (in particular the M4B and M5A) have crystallographic features suggesting a mixed population with $Pb^{2+} >> Bi^{3+}$. A minor presence of Bi^{3+} also in other octahedra is supported by the bond valence analysis. The valences are in the range 2.0-2.1 v.u. for M2A, M2B, M3A, M3B atom sites, 2.2 v.u. for M4B, 2.4 v.u. for M5A, 2.6 v.u. for M4A and 2.7 v.u. for M5B. Considering the results of the bond valence analysis, the crystal chemical formula of aschamalmite is: $^{[M1]}Pb^{2+}{}_2{}^{[M2A]}(Pb^{2+}{}_{0.90}Bi^{3+}{}_{0.10})_{\Sigma1}{}^{[M2B]}(Pb^{2+}{}_{0.94}Bi^{3+}{}_{0.06})_{\Sigma1}{}^{[M3A]}Pb^{2+}{}_2{}^{[M3B]}Pb^{2+}{}_2{}^{[M4A]}(Bi^{3+}{}_{1.28}Pb^{2+}{}_{0.72})_{\Sigma2}$ $^{[M4B]}(Pb^{2+}{}_{1.68}Bi^{3+}{}_{0.32})_{\Sigma2}{}^{[M5A]}(Pb^{2+}{}_{1.24}Bi^{3+}{}_{0.76})_{\Sigma2}{}^{[M5B]}(Bi^{3+}{}_{1.40}Pb^{2+}{}_{0.60})_{\Sigma2}S_{18}$, that corresponds to $Pb_{12.08}Bi_{3.92}S_{18}$, in good agreement with the unit formula $Pb_6Bi_2S_9$ ($Z = 2$).

References. [1] W.G. Mumme, G. Niedermayr, P.R. Kelly, W.H. Paar, *N. Jb. Miner. Monat.,* **H.10,** 433-444, 1983; [2] T. Armbruster, W. Hummel, *Am. Mineral.*, **72,** 821-831, 1987.

IRON SULPHIDE MINERALIZATION IN THE "ARGILLE SCAGLIOSE" UNIT IN SICILY

G. Caruso, M. Di Bella, G. Sabatino, M. Triscari

Dipartimento di Scienze della Terra, Università di Messina, Italy
mtriscari@unime.it

In the Peloritani Mts. the "Argille Scagliose *Auct.*" formation outcrops in the northern portion of the Etna volcano, next to the village of Mojo Alcantara. These scaly shales are dated to upper Cretaceous and are characterized by clay and silty clays brownish to greenish and/or variously coloured with interbedded sandy clay levels [1]. Carbonates in decimetres levels with quartzarenites are occasionally found.

These clayey formations have locally been used as a preferred site for an urban waste disposal area that nowadays has completely covered the previously outcropping diffused levels rich in iron sulphides.

So far it seems to be the only known occurrence of this type of mineralization in the entire Etna volcano region.

Interbedded into the scaly shales are levels - up to 15-20 cm thick - characterized by a deep red-brownish colour. On the upper surface of these levels, diffusely scattered sulphide "rosette" are discernible, up to 1-2 cm in diameter large. A mineralogical-petrological study has been carried on with RLPM, XRD and SEM-EDX techniques.

The sulphide mineralization proved to be all pyrite in perfect stoichiometric ratio. Reflected light microscopy showed that a sulphide deposition in typical anoxic environments with Fe and Mn carbonates led to the primary simple sulphide deposition that later evolved into the present pyrite "rosettes". SEM observations have revealed diffused "framboydal pyrite" pointing to the original bacterial deposition in anoxic environments. A later remobilization of this last, has originated the pyrite rosette crystallization process. The growing substratum is characterized by massive silica and iron, often in the form of quartz and Mn and Fe carbonated and oxides. The framboydal pyrite points to a precise reducing environment with biogenic involvement.

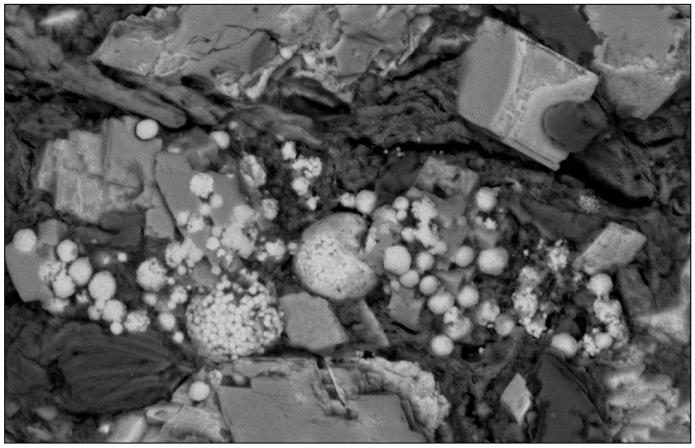

SEM-BSE image, 7000 X – Mojo Alcantara scaly shales. Framboydal pyrite.

References. [1] F. Lentini, S. Catalano, S. Carbone, *Carta geologica della Provincia di Messina: scala 1:50.000*. Prov. Regionale di Messina. Assessorato al Territorio, Servizio geologico. Ed. S.E.L.C.A., Firenze, 70 pp., 2000.

SINGLE-CRYSTAL POLARIZED FTIR SPECTROSCOPY AND NEUTRON DIFFRACTION REFINEMENT OF CANCRINITE

G. Della Ventura[1], G.D. Gatta[2], G.J. Redhammer[3], F. Bellatreccia[1], A. Loose[4], G.C. Parodi[5]

[1]*Dipartimento di Scienze Geologiche, Università Roma Tre, Italy*
[2]*Dipartimento di Scienze della Terra, Università di Milano, Italy*
[3]*Department of Materials Engineering & Physics, Division of Mineralogy, University of Salzburg, Austria*
[4]*Forschungszentrum Jülich, Institute of Solid State Research (IFF), Jülich, Germany*
[5]*Laboratoire de Minéralogie, Museum National d'Histoire Naturelle, Paris, France*
dellaven@uniroma3.it

We relate here a combined single-crystal polarized-light FTIR (Fourier Transform Infrared) and neutron diffraction study of two natural cancrinites from Cameroun and Canada, respectively. Electron microprobe analyses show both samples to be almost end-member carbonate-cancrinites [ideal chemical formula $Na_6Ca_2(Si_6Al_6O_{24})(CO_3)_2 \cdot 2H_2O$].

The structure refinements show that the extra-framework content in the large 12-membered rings channels is represented by one independent Na-site (Na2) and two independent, and statistically distributed, CO_3 groups. The geometry of the CO_3 groups appears to be almost regular, with C1-O_{C1} ~ 1.298(7) Å and C2-O_{C2} ~ 1.300(5) Å, in agreement with previous studies [1-3]. The atoms of the carbonate-groups are not perfectly coplanar, being $z(C1) \neq z(O_{C1})$ and $z(C2) \neq z(O_{C2})$. The H_2O molecules and a further Na-site (Na1) lie in the cancrinite-cage; the H_2O oxygen site (O_W) lies off from the triad axis, giving rise to a statistical configuration with three equivalent and mutually exclusive water molecules, as already suggested [1,2]. The high-quality neutron data show that the water molecule is almost symmetric, with very similar Ow-H1 and Ow-H2 bond distances, and is slightly tilted from the (0001) plane. It is involved in bifurcated hydrogen bridges, with two possible bonds for H1 (*i.e.* O_W-H1···O2 and O_W-H1···O4) and two for H2 (*i.e.* O_W-H2···O3 and O_W-H2···O2). The Ow···O donor-acceptor distances are all > 2.7 Å.

The polarised-light FTIR spectra show two main absorptions, at 3602 and 3531 cm^{-1}, respectively. The former is polarised for $\mathbf{E} \perp \boldsymbol{c}$, while the latter is polarized for $\mathbf{E} \perp \boldsymbol{c}$. On the basis of the neutron diffraction data, the 3602 cm^{-1} band is assigned to the anti-symmetric stretching mode (ν_3), while the 3531 cm^{-1} band is assigned to the symmetric stretching mode (ν_1) of the same water molecule, in agreement with the presence of a single bending mode at 1630 cm^{-1}. One additional weak component at 4108 cm^{-1} could possibly indicate the presence of low amounts of additional OH groups in the structure of cancrinite. Several overlapping bands in the 1300-1500 cm^{-1} range are strongly polarized for $\mathbf{E} \perp \boldsymbol{c}$, and are assigned to the vibrations of the CO_3 group.

References. [1] H.D. Grundy, I. Hassan, *Can. Mineral*., **20,** 239-251, 1982; [2] P. Ballirano, A. Maras, *Eur. J. Mineral*., **16**, 135-141, 2004; [3] I. Hassan, S.M. Antao, J.B. Parise, *Am. Mineral*., **91**, 1117-1124, 2006.

NEW INSIGHTS INTO THE CRYSTAL STRUCTURE AND CRYSTAL CHEMISTRY OF THE ZEOLITE PHILLIPSITE-Na

G.D. Gatta[1], P. Cappelletti[2], N. Rotiroti[1], R. Rinaldi[3], C. Slebodnick[4]

[1]*Dipartimento di Scienze della Terra, Università di Milano, Italy*
[2]*Dipartimento di Scienze della Terra, Università "Federico II", Napoli, Italy*
[3]*Dipartimento di Scienze della Terra, Università di Perugia, Italy*
[4]*Crystallography Laboratory, Virginia Polytechnic Institute, Blacksburg, VA-USA*
diego.gatta@unimi.it

Phillipsite, a common natural zeolite with ideal composition $K_2(Na,Ca_{0.5})_3[Al_5Si_{11}O_{32}]\cdot 12H_2O$, is typically found in amygdaloidal vugs of massive volcanic rocks (*e.g.* basalt, leucitites), in palagonitic basalts and tuffs as an alteration product of volcanic glass, or in diagenetically altered sediments in "closed hydrologic systems" (*e.g.* saline lake and hot spring deposits) and "open hydrologic systems" (*e.g.* soils and land surface deposits, burial diagenetic environments, deep-sea sediments). Phillipsite is isotypic with harmotone $[Ba_2(Na,Ca_{0.5})Al_5Si_{11}O_{32}\cdot 12H_2O]$, forming a continuous series with no compositional gap. Crystals of natural phillipsite are often found in spherical radial aggregates and ubiquitously twinned (cruciform single and double penetration twins on {001}, {021} and {110}). Intergrowths with several other zeolites (*e.g.* faujasite, offretite, gismondine, garronite and gobbinsite) have been reported The crystal structure, crystal chemistry and low-temperature behavior of a natural phillipsite-Na from the "Newer Volcanic Suite", Richmond, Melbourne district, Victoria, Australia $[K_{0.75}(Na_{0.88}Ca_{0.57})_{\Sigma=1.45}(Al_{2.96}Ti_{0.01}Si_{5.07})_{\Sigma=8.04}O_{16}\cdot 6.2H_2O$ (Z = 2), a = 9.9238(6), b = 14.3145(5), c = 8.7416(5) Å, β = 124.920(9)° and V = 1018.20(9) Å^3, space group $P2_1/m$], have been investigated by means of *in situ* single-crystal X-ray diffraction, thermogravimetric analysis and electron microprobe analysis in the wavelength dispersive mode. Two accurate structural refinements have been obtained on the basis of single-crystal X-ray diffraction data collected at 298 and 100 K, with: $R_1(F)_{298K}$ = 0.035, 3678 unique reflections with $F_o > 4\sigma(F_o)$ and 195 parameters, and $R_1(F)_{100K}$ = 0.035, 3855 unique reflections, $F_o > 4\sigma(F_o)$ and 195 parameters. In both refinements the residuals in the final difference Fourier maps are less than $1e^-$Å^{-3}. A configuration of the extra-framework population different from that reported in previous studies is found at room temperature, with two possible sites for potassium (K1 and K2), one sodium/calcium-site (Ca) and seven independent sites partially occupied by water molecules (W1, W2, W3, W4, W4', W5 and W6). The low-temperature refinement shows that the framework component of the phillipsite structure is maintained within the T-range investigated. However, a change in the configuration of the extra-framework content occurs at low temperature: the occupancy of site K2 drastically decreases, while that of site K1 increases, the Ca-site is split into two sub-sites (Ca1 and Ca2) and the number of water molecule sites decreases to six (W1, W2, W3, W4, W5 and W6). The evolution of the unit-cell parameters with T (measured at 298, 250, 200, 150 and 100 K) shows a continuous and linear trend, without evident thermo-elastic anomalies. The axial and volume thermal expansion coefficients ($\alpha_j = l_j^{-1}\cdot\partial l_j/\partial T$, $\alpha_V = V^{-1}\cdot\partial V/\partial T$) between 100 and 298 K, calculated by weighted linear regression, yield the following values: $\alpha_a = 1.8(1)\cdot 10^{-5}$, $\alpha_b = 1.2(1)\cdot 10^{-5}$, $\alpha_c = 1.1(1)\cdot 10^{-5}$ and $\alpha_V = 3.7(1)\cdot 10^{-5}$K^{-1}. The thermal expansion of phillipsite is significantly anisotropic (α_a:α_b:α_c = 1.64:1.09:1).

KINETICS OF Fe-OXYDATION/DEPROTONATION PROCESS IN A Fe-RICH PHLOGOPITE BY *in situ* XRD

M. Lacalamita[1], M. Zema[2], F. Scordari[1], G. Ventruti[1]

[1]*Dipartimento Geomineralogico, Università di Bari, Italy*
[2]*Dipartimento di Scienze della Terra, Università di Pavia, Italy*
f.scordari@geomin.uniba.it

The kinetics of the Fe-oxidation/deprotonation process in a natural Fe-rich phlogopite from Mt. Vulture (Potenza, Italy) has been studied by *in situ* high temperature X-ray single-crystal diffraction. The thermal behaviour of the same phlogopite sample up to 750°C was recently characterized by Ventruti *et al.* [1], who observed that the Fe-oxidation/deprotonation process takes place starting from T > 550°C and causes a decrease of all unit-cell dimensions and, consequently, of cell volume. In that work, it was demonstrated too, that the process is not reversible but whether it is a one-step or a multi-step reaction remained questionable.

In the present study, isothermal annealing experiments were performed in air at 600 and 700°C until equilibrium was reached. Two crystals characterized by very similar chemical composition and lattice parameters, were used. For each crystal, unit-cell parameters were firstly measured from RT up to 500°C at regular intervals to determine linear thermal expansion coefficients of the sample before Fe-oxidation/deprotonation process starts. Hence, temperature was quickly (~ 10°C/s) increased up to the selected set-point (600 and 700°C for the two crystals, respectively) and maintained constant until the achievement of the equilibrium conditions. Under isothermal conditions, unit-cell parameters were measured at regular intervals (every 5 minutes in the first stages of the experiment, longer time-steps as reaction rate slowed down) by centring 15-25 reflections in the range $\sim 7.7° \leq \theta \leq 15.4°$ to monitor the rate of the temperature-induced Fe-oxidation/deprotonation process. Some reflections, representative of different classes, were also scanned periodically ($\omega/2\theta$ scan mode; 2.4°θ scan width; 0.8°θ/s scan speed) to check for the crystallinity of the sample.

Equilibrium was reached in a time scale of ~ 10^4 min and ~ 10^3 min at 600 and 700°C, respectively. Analyses of the evolutions of unit-cell parameters as a function of time revealed that they all decrease following an exponential law. As expected, the most pronounced variations occur along the *c* axis. Exponential fits for normalized cell volumes are as follows:

T = 600°C: $V/V_0 = 0.9898(2) + 1.00(2)\cdot10^{-2}\ \exp[-7.94(4)\cdot10^{-4}\cdot t(\text{min})]$

T = 700°C: $V/V_0 = 0.9906(1) + 9.3(2)\cdot10^{-3}\ \exp[-7.6(4)\cdot10^{-3}\cdot t(\text{min})]$.

After completion of the deprotonation process, thermal expansions of both the crystals were measured in the temperature range 25 - 950°C and resulted to be linear, even if a general worsening of diffraction profiles and the appearance of broad satellite reflections were observed starting from ~ 800°C. This confirms the irreversibility of the process, and the stronger anisotropy of the thermal expansion behaviour of the Fe^{3+}-bearing phase. It is worth noting that such expansion curves obtained for the two crystals are almost superimposable, thus demonstrating that the same degree of deprotonation was achieved at the two temperatures.

References: [1] G. Ventruti, M. Zema, F. Scordari, G. Pedrazzi, *Am. Mineral.*, **93**, 632-643, 2008.

MINERALOGICAL AND CHEMICAL EVOLUTION OF OCHREOUS STREAM SEDIMENTS FROM THE LIBIOLA Fe-Cu-SULPHIDES MINE (EASTERN LIGURIA, ITALY)

P. Marescotti[1], C. Carbone[1], P. Comodi[2], F. Frondini[2], G. Lucchetti[1]

[1]*Dip.Te.Ris., Università di Genova, Italy*
[2]*Dipartimento di Scienze della Terra, Università di Perugia, Italy*
marescot@dipteris.unige.it

Underground and superficial waters of Libiola Mine area are mostly ASW (Acid Sulfate Waters) due to active AMD (Acid Mine Drainage) processes triggered by oxidation of pyrite and chalcopyrite mineralizations [1-4]. These mineralizations are still abundant as relics within the underground excavations and outcropping rocks and as non-economic pyrite-rich clasts within subaerial waste rock dumps [5]. ASW cause precipitation of large quantities of iron-rich ochreous stream sediments that occur both as soft crusts inside the mine adits and as loose suspensions associated with overland flow of mine drainage.

The aim of this study is to evaluate the genesis and the seasonal mineralogical and chemical evolution, of the amorphous, nano- and micro-crystalline Fe-oxyhydroxides that represent the main or the exclusive constituents of these stream sediments.

Stream sediments vary in colour from ochre to yellowish-red to brown and directly precipitate from solutions characterized by strong acidity ($2.4 < pH < 4.5$) and Eh value between 300 and 670 mV. Their mineralogy has been characterized by X-ray powder diffraction (XRPD) and transmission electron microscopy (TEM), whereas the bulk-element composition was obtained by ICP-MS analysis.

ASW and stream waters were sampled for chemical analyses. Water temperature, electrical conductivity, alkalinity by acidimetric titration, pH, and Eh were determined in the field during sampling. In the laboratory, waters were analysed for: Mg, and Ca by AAS, Na and K by AES Cl, SO_4, and NO_3 by ion-chromatography, Si, Fe, minor and trace elements by ICP-OES.

The results show that the mineralogy and the chemistry of stream sediments occurring in different sites and different seasons are mainly controlled by the pH, Eh, and SO_4 concentration of the circulating solutions. We have distinguished 5 stream sediments (SS) groups on the basis of their mineral assemblages: jarosite-bearing SS precipitate only from extremely acid (pH = 2-2.5) and SO_4-rich solutions; schwertmannite- and goethite-bearing SS form in a wide range of pH (2-4.5) and SO_4 concentration; ferrihydrites- and amorphous-bearing SS only form at $pH > 3$ and at the lowest SO_4 concentration. Many micro- and nano-textural features observed by HR-TEM suggest that these low-crystalline minerals rapidly evolve toward more stable species (mostly goethite) or underwent dissolution as a consequence of ageing and seasonal variation of physico-chemical parameters of the circulating waters.

The bulk chemistry, and in particular the concentration of minor and trace elements, of the stream sediments varies significantly among the different 5 groups. In particular, low crystallinity- (schwertmannite and ferryhydrites) and amorphous-phases efficiently scavenge many metals of environmental concern (such as Cu, Pb, Zn, Ni, As, Cd, and Ag) due to their high surface area and adsorption capacity. Nevertheless these elements, are mainly scavenged by the ASW through absorption and co-precipitation mechanisms and can be easily desorbed during seasonal transformation and dissolution processes.

References. [1] P. Marescotti, C. Carbone, *GEAM*, **3**, 45-51, 2003; [2] C. Carbone, F. Di Benedetto, P. Marescotti, A. Martinelli, C. Sangregorio, C. Cipriani, G. Lucchetti, M. Romanelli, *Eur. J. Mineral.*, **17**, 785-795, 2005; [3] E. Dinelli, F. Tateo, *Appl. Geochem.*, **17**, 1081-1092, 2002; [4] L. Marini, G. Saldi, F. Cipolli, G. Ottonello, M. Vetuschi Zuccolini, *Geochem. J.*, **37(2)**, 199-216, 2003; [5] P. Marescotti, C. Carbone, L. De Capitani, G. Grieco, G. Lucchetti, D. Servida, *Environ. Geol.*, **53**, 1613-1626, 2008.

X-RAY MICRODIFFRACTION AS A TOOL FOR SINGLE CRYSTAL STRUCTURE REFINEMENT: A STUDY ON APATITE CRYSTALS

L. Medici[1], M.F. Brigatti[2], D. Malferrari[2]

[1]*Istituto di Metodologie per l'Analisi Ambientale, CNR, Potenza, Italy*
[2]*Dipartimento di Scienze della Terra, Università di Modena e Reggio Emilia, Italy*
medici@imaa.cnr.it

The aim of this work is to verify if data obtained via laboratory-based X-ray microdiffraction are suitable to give reliable atomic coordinates, bond distances and bond angles. A further aim is to carefully compare values obtained using microdiffractometer and single crystal data to establish if microdiffraction technique can be used as routine technique to obtain structural information on very dispersed phases or on zoned crystals in thin section, or on crystals in bulk matrices.

Three crystals of hydroxyl fluorapatite were thus analyzed by single crystal X-ray diffraction (Siemens P4P rotating-anode four-circle diffractometer operating at 50 kV and 140 mA with graphite-monochromatized MoKα radiation) and by X-ray microdiffraction (Rigaku D-Max Rapid microdiffractometer) equipped with an image plate detector, a flat graphite monochromator, a microscope for the positioning of the sample in the path of the X-ray beam, operating at 40 kV and 30 mA with CuKα radiation. Crystal structure refinements were carried out in space group $P6_3/m$ using SHELXL-97 and GSAS software. Unit cell parameters, obtained via microdiffraction for sample Tas22-1 (a = 9.404(1), c =6.901(2) Å) well agree with those determined by single crystal (a = 9.411(1), c = 6.899(1) Å); furthermore, significant differences are not highlighted when different beam diameters are used on the same crystal, *e.g.* for sample Tae23-1 unit cell parameters resulted: a = 9.443(1), c =6.917(2) Å with 0.1 mm beam diameter, a = 9.438(1), c =6.916(1) Å with 0.3 mm beam diameter, a = 9.436(1), c =6.916(2) Å for a beam diameter of 0.8 mm. This feature implies that results obtained from a part of the sampling volume are reliable, and this technique suitable to analyse zoned crystals or samples folded, such as metamorphic micas. On the contrary microdiffraction gives a higher uncertainty on atomic coordinates and consequently on bond distances and angles.

MINERALOGY OF ACTUALLY FORMING SUBLIMATES AT ELDFELL VOLCANO (HEIMAEY ISLAND, VESTMANNAEYJAR ARCHIPELAGO, ICELAND)

D. Mitolo[1], A. Garavelli[1], L. Pedersen[2], T. Balić-Žunić[2], S.P. Jakobsson[3], F. Vurro[1]

[1]*Dipartimento Geomineralogico, Università di Bari, Italy*
[2]*Department of Geography and Geology, University of Copenhagen, Denmark*
[3]*Icelandic Institute of Natural History, Hlemmur 3, Reykjavik, Iceland*
d.mitolo@geomin.uniba.it

Eldfell is a cinder cone volcano just over 200 metres (650 feet) high on the Icelandic island of Heimaey (Vestmannaeyjar archipelago). It formed in a volcanic eruption which began without warning just outside the town of Heimaey on January 23, 1973. During and after the eruption a large amount of gases were released, leading to the formation of extensive fumarole deposition on the surface of the andesitic new-born cone [1]. Minerals formed in the area immediately after the last eruption, were extensively collected and investigated but for long time the results of investigations remained unpublished. The fumarole minerals formed in the area mainly consist of of variously hydrated sulfates, chlorides and fluorides, as well as a number of potentially new mineralogical phases [2]. Among them, the new mineral phase eldfellite, $NaFe(SO_4)_2$, has been recently discovered [3] and approved by the special IMA commission (IMA2007-051).

A new sublimate collection from the Eldfell crateric area was organized in August 2007. Temperature registered on the ground was not higher than 200°C, but the temperature of the formation of fumaroles exceeded at a recent time 240°C, as testified by the presence of the high-temperature phase metathenardite. In laboratory, the different phases were separated by hand-picking and analyzed by SEM-EDS technique and X-ray powder diffraction (XRPD).

Our investigations indicate that presently the fumarole encrustations from Eldfell volcano mainly consist of anhydrous or variously hydrated sulphates (anhydrite, gypsum and bassanite, but also jarosite, chessexite, vanthoffite, thenardite, glauberite, aphtitalite, etc.) and halogenides (ralstonite, sal ammoniac, halite, sylvine, meniaylovite, thomsenolite and others). Iron oxides are also present, mainly as a substrate.

This mineralogical association is typical of fumarole fields associated to the rise of volcanic fluids diluted with surficial acquifer and interacting with lava rocks. No indications of the presence of elements directly coming from the magma degassing in the fluid phase, could be found from the study of the mineral association actually forming in the area.

References. [1] S. Thorarinsson, S. Steinthorsson, T. Einarsson, H. Kristmannsdottir, N. Oskarsson, *Nature*, **241**, 372-375, 1973; [2] S.P. Jakobsson, E. Leonardsen, T. Balić-Žunić, S.S. Jónsson, in preparation; [3] T. Balić-Žunić, P. Acquafredda, A. Garavelli, E. Leonardsen, S.P. Jakobsson, in preparation.

THE CRYSTAL STRUCTURE OF CHALLACOLLOITE, KPb_2Cl_5, AND HEPHAISTOSITE, $TlPb_2Cl_5$, FROM LA FOSSA CRATER, VULCANO, AEOLIAN ISLANDS, ITALY

D. Mitolo[1], D. Pinto[1], A. Garavelli[1], L. Bindi[2], F. Vurro[1]

[1]*Dipartimento Geomineralogico, Università di Bari, Italy*
[2]*Museo di Storia Naturale, Sezione di Mineralogia e Litologia, Università di Firenze, Italy*
a.garavelli@geomin.uniba.it

This work deals with the first structure investigation on natural K- and Tl-end members of the challacolloite, KPb_2Cl_5, and hephaistosite, $TlPb_2Cl_5$, series. The crystals investigated were found among volcanic sublimates directly collected on the crater rim of the "La Fossa Crater" at Vulcano, Aeolian Archipelago, Italy. EDS qualitative chemical analyses showed almost pure compositions for both the phases, with exceptions of minor K-Tl and Br-Cl substitutions. Challacolloite and hephaistosite are monoclinic, space group $P2_1/c$, with unit-cell parameters a = 8.8989(4) Å, b = 7.9717(5) Å, c = 12.5624(8) Å, β = 90.022(4)°, V = 891.2(1) Å^3, Z = 4 and a = 9.0026(6) Å, b = 7.9723(6) Å, c = 12.5693(9) Å, β = 90.046(4)°, V = 902.1(1) Å^3, Z = 4, respectively. Owing to the high R values (R_1 = 13.28% and R_1 = 5.91% for challacolloite and hephaistosite, respectively) and the pseudo-orthorhombic crystal lattice of these minerals which provides a basis for likely twinning on either {100}or {001}, or both of them, the possibility of twinning was taken into account during the structure refinement. Twin refinement improved the final R values from 13.28% to 2.72% in challacolloite and from 5.91% to 2.92% in hephaistosite, thus confirming the presence of twinning. The challacolloite-hephaistosite structure framework may be described as (100) layers of M atoms (M = K, Tl) alternating with layers which accommodate the Pb atoms. Two symmetry independent Pb atoms are present. The first one (Pb1) shows an almost distorted bi-capped trigonal prismatic coordination. It forms [100] columns of prisms by sharing their bases with the adjacent prism centered by M (K, Tl). The Pb2 coordination may be described as a split octahedron. According to our structure refinements, the two natural crystals investigated here show Tl/K ratios of 96/4 (hephaistosite) and 6/94 (challacolloite). The total amounts of Br obtained from the refinement were 0.18 *apfu* and 0.13 *apfu* for hephaistosite and challacolloite, respectively. This study allowed to point out the influence of Br-for-Cl and K-for-Tl substitutions on the structure framework of the compounds with general formula MPb_2X_5, with M = K, Tl and X = Cl, Br. As a matter of fact, the K for Tl substitution in the trigonal prismatic coordinated M atoms, which are concentrated into structural planes perpendicular to [100] direction, with the basis of the prisms standing the (100) planes, causes a general stretching of the interatomic distances along [100]. This increases the distances between the bases of the prisms leading to an anisotropic stretching of the unit-cell along [100]. We estimated that the complete K-for-Tl substitution increases the a parameter by 1%. No significant increase was observed for b and c. Structure refinements showed that Br appears to prefer those anion sites located in the almost expanded portion of the structure around the (100) chains of M atoms (*i.e.* Cl3, Cl4 and Cl5). Instead, the anion sites Cl1 and Cl2, which lie in the more compact portion of the structure closer to the Pb rows, remain free of Br. Cross comparison between unit-cell parameters of the natural phases investigated in this work and those of the synthetic phases KPb_2Cl_5, KPb_2Br_5, $TlPb_2Cl_5$ and $TlPb_2Br_5$ showed that the cell expands in all directions with the increase of Br. We estimated the complete Br-for-Cl replacement leads to an increase of 4.5%, 5.5% and 4.3% in parameters a, b, c respectively, and an increase of 15.1% in cell volume for $KPb_2(Cl,Br)_5$ compounds, and an increase of 4.0%, 5.7% and 3.5% in parameters a, b, c respectively, and an increase of 13.7% in cell volume of $TlPb_2(Cl,Br)_5$ compounds.

HIGH-PRESSURE BEHAVIOUR OF A Li-BEARING ORTHOPYROXENE

F. Nestola[1], F. Cámara[2], M. Alvaro[3], M.C. Domeneghetti[3], V. Tazzoli[3], H. Ohashi[4]

[1]*Dipartimento di Geoscienze, Università di Padova, Italy*
[2]*C.N.R. - I.G.G., Unità di Pavia, Italy*
[3]*Dipartimento di Scienze della Terra, Università di Pavia, Italy*
[4]*Hashi Institute for Silicate Science, Tokyo, Japan*
matteo_alvaro@manhattan.unipv.it

A synthetic orthopyroxene with composition $(Li_{0.5}Zn_{0.5})(Sc_{0.5}Zn_{0.5})Si_2O_6$ and space group *Pbca* was investigated by *in situ* high-pressure single-crystal X-ray diffraction using a diamond anvil cell in order to evaluate the effect of trivalent and monovalent cations on the elasticity of the orthopyroxene phase. Preliminary data (measured up to 7.12 GPa at 7 different pressures) showed that no phase transition occurs throughout the pressure range investigated and that such Li-bearing orthopyroxene results to be the softest among the *Pbca* pyroxenes studied so far. The pressure - volume data fitted using a 3rd-order Birch-Murnaghan equation of state gave a bulk modulus K_{T0} = 79(2) GPa with the first pressure derivative K' = 8(1), very anomalous values for a *Pbca* pyroxene. The evolution of the unit-cell volume and of the single unit-cell parameters with pressure is shown in Fig. A and B, respectively. Fig. B shows a significant anisotropic deformation with **a** being the most rigid direction and **b** the softest one. The evolution of the crystal structure with pressure indicates that the M2 polyhedron is the most deformed with a volume decrease by about 13% compared to that of about 5% for M1 polyhedron (Fig. C). For such calculation we assumed a 6-fold coordination for the M2 polyhedron: the O3B oxygen positioned at 3.014 Å from M2 site at room pressure enters in coordination between 6 and 7 GPa with a distance reduced to 2.528 Å at 7.12 GPa. The TA tetrahedron is practically uncompressible whereas TB undergoes a limited deformation compared to that of M2 and M1 polyhedra (–1.8%). The strong deformation of M2 is accompanied by a strong kinking (O3–O3–O3 angle) of the B tetrahedral chain with a contraction rate of 1.97 °/GPa against an extension rate of 0.68 °/GPa for the A tetrahedral chain. An analysis of the individual M2–O distances clearly shows that the main deformation for the M2 site is represented by the strong reduction of M2–O3B (–19%) and M2–O3A (–7%) distances (Fig. D) whereas the other M2–O distances as well as M1–O distances show only minor deformations.

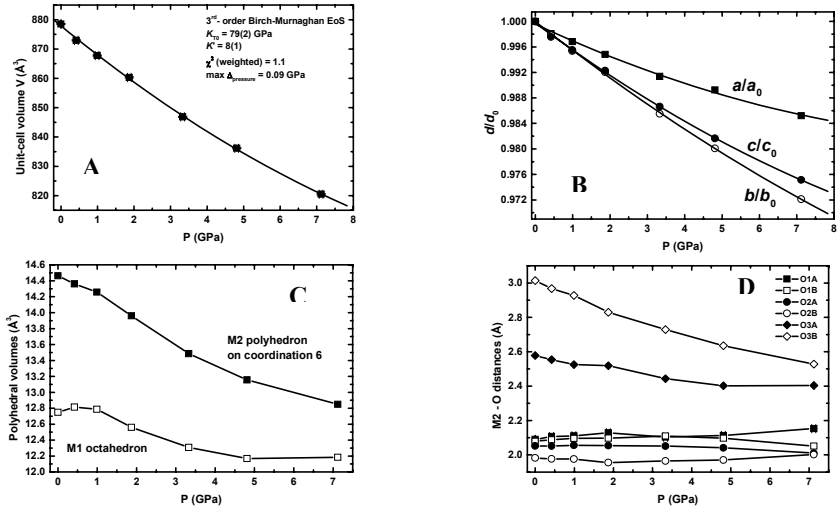

STRUCTURAL AND OPTICAL CHARACTERIZATION OF BLUE AND YELLOW ZOISITE FROM MERELANI ARUSHA (TANZANIA): A STUDY OF THE CHANGES INDUCED BY HEATING

E. Rodeghero[1], A. Martucci[1], M. Sacerdoti[1], F. De Zuane[1], D. Ajò[2]

[1]*Dipartimento di Scienze della Terra, Università di Ferrara, Italy*
[2]*Istituto di Chimica Inorganica e delle Superfici, CNR, Padova, Italy*
mrs@unife.it

Zoisite is a sorosilicate with idealized formula $Ca_2Al_3[Si_2O_7][SiO_4]O(OH)$, which is orthorhombic, space group *Pnma*. The crystal structure was determined by Ito [1] and Fesenko *et al*. [2], and later refined by Dollase [3]. It consists of one type of endless octahedral chains parallel to *b* with two distinct octahedral sites M1,2 and M3. These chains are crossed by isolated tetrahedral SiO_4 (T3) and Si_2O_7 groups (T1 and T2) in the *a* and *c* directions. When zoisite is heated between 370-650°C, it becomes an intense sapphire-blue colour (variety tanzanite) [4]; this behaviour was explained in terms of change of the oxidation state of transition metal ions, such as V and [5-6]. The aim of this work is to assess the dependence of the colour changes in yellow and blue heated varieties of zoisite when heated, not only on the concentration of metal ions and their oxidation states, but also on the possible structural changes in bond lengths and bond angles, or distortion of coordination polyhedra. Yellow and blue crystals of zoisite from Merelani Hill, in the Arusha Region, were preliminarily characterized by XRF analysis to verify their chemical composition. XRF reveals that the same trace elements (in particular V, Sr and Cr) are present in both samples, but their amount shows differences which can play a fundamental role in the change colour. TG and DTA measurements performed in air up to 900°C (heating rate 5°C/min) reveal that in both cases the weight loss is very low (~ 0.3%) and no deprotonation occurs. The XRD data were collected on a Bruker-AXS D8 advanced diffractometer equipped with a Sol-X detector, in the 4-120° 2θ range. XRD diffraction patterns were analysed by the Rietveld method. Structural refinements of yellow and blue samples at room temperature reveal differences in the unit cell parameters, as well as in the orientation of coordination polyhedra. After heating at 520°C, these differences disappear and the structures become quite similar. It is noteworthy that the heating process induces a strengthening of the H bond, directed along the **c** axis, resulting in a shortening of the *c* parameter. The UV-VIS spectra, recorded by using a Xenon lamp and an integrating sphere, are in line with the previously reported ones by Faye and Nickel [6] in spite of different experimental conditions, even though their interpretation will require a wider discussion, as regards also the separation between natural and treated blue materials. Finally, the photoluminescence spectra excited by a 532 nm LASER and recorded by a custom-made apparatus are very similar for natural and treated, yellow and blue materials, so providing a reliable method to identify the gemmological species zoisite, independently of the colour of the sample under investigation.

References. [1] T. Ito, N. Morimoto, R. Sadanga, *Acta Crystallogr*., **7**, 53-59, 1954; [2] E.G. Fesenko, I.M. Rumanova, N.V. Belov, *Structure Rep.*, **19**, 464-465, 1955; [3] W.A. Dollase, *Am. Mineral.*, **53**, 1882-1898, 1968; [4] R.G. Burns, Cambridge University Press, 114-115, 1970; [5] D.R. Hutton, *J. Phys. C Solid State*, **4**, 1251-1257, 1971; [6] G.H. Faye, E.H. Nickel, *Can. Mineral*., **10**, 812-821, 1971.

ELECTRON SPIN ECHO INVESTIGATION OF Mn(II)-As INTERACTION IN CALCITE, $CaCO_3$: TOWARDS A QUANTITATIVE MODEL

M. Romanelli[1], M. Benvenuti[2], P. Costagliola[2], F. Di Benedetto[1,2], P. Lattanzi[3]

[1]*Dipartimento di Chimica, Università di Firenze, Italy*
[2]*Dipartimento di Scienze della Terra, Università di Firenze, Italy*
[3]*Dipartimento di Scienze della Terra, Università di Cagliari, Italy*
pilarc@geo.unifi.it

The arsenic cycle is strictly related to health and environment safety, because of the toxicity of this semimetal for both animal and human life. The knowledge of this cycle, however, still presents qualitative and quantitative uncertainties, mainly related to the interface steps, among different compartments of the geosphere, which determine transition times for As. Minerals represent the main natural As-sink and an important interface between, in particular, the litho- and hydrosphere. Among them, the role of calcite, one of the most diffused minerals in the Earth's crust, in trapping As is still unclear and debated, in particular concerning the role that calcite could play as host, trap and releaser of arsenic.

The present study is focussed on the relationships between arsenic and calcite in a natural geogenic occurrence, the middle part of Pecora River Valley in Southern Tuscany (Italy), where a fossil lacustrine travertine deposit presents As-contents ranging up to 257 ppm.

Arsenic crystal chemistry was investigated by using the Electron Spin Echo (ESE) spectroscopy. As arsenic does not present naturally-occurring paramagnetic valence states, nor stable radical species, it is in principle undetectable by paramagnetic resonance techniques. We thus decided to trace it by using a paramagnetic homogeneous tool, *i.e.* Mn(II) substituting for Ca in calcite.

The preliminary experiments revealed an intense decaying echo signal behaviour due to Mn(II) electron spins, modulated by the ^{75}As nuclear superhyperfine interaction. The refinement of the experimental data revealed the decay to be explainable in terms of exponential relaxation and a axial symmetry for the coordination of As [1].

The successive step of interpretation concerns the quantitative esteem of the Mn(II)-As clusters. This step is necessary in order to describe how and how much the mechanism of As incorporation in calcite is effective in trapping the semimetal This, in principle, can be devised establishing the Mn(II)-content from the modelling of the ESE decay and the number of interacting As nuclei from the superimposed modulation. Whereas the ESEEM theory has been deeply developed, so that this second parameter can be determined as greater than 4, currently the theoretical framework necessary to give a quantitative interpretation of ESE decays is provided only for simple magnetic systems. In the present case, the complex magnetic system (five unpaired electrons) requires the development of a dedicate theoretical substrate; indeed one has to take into account the number of electronic transitions excited by the pulses and, in particular, the possibility of multiple transitions occurring in the excitation window. This is presently under study.

As a conclusive remark, As is found to substitute for C in calcite, maintaining the three coordination and potentially clustering in the proximity of Mn. These results possibly indicate that calcite may behave as a natural As-trap.

References. [1] F. Di Benedetto, P. Costagliola, M. Benvenuti, P. Lattanzi, M. Romanelli, G. Tanelli, *Earth Planet. Sc. Lett.*, **246**, 458-465, 2006.

HIGH-PRESSURE STRUCTURAL BEHAVIOUR OF MANGANITE SINGLE CRYSTAL $La_{0.815}Ba_{0.185}MnO_3$

N. Rotiroti[1], F. Nestola[2], S. van Smaalen[3]

[1]*Dipartimento di Scienze della Terra, Università di Milano, Italy*
[2]*Dipartimento di Geoscienze, Università di Padova, Italy*
[3]*Laboratory of Crystallography, University of Bayreuth, Germany*
nicola.rotiroti@unimi.it

La-manganites have recently attracted considerable interest as they show colossal magnetoresistance (CMR) and then several studies have been devoted to the investigation of their crystal structure and its relationship with the magnetic and electronic properties [1]. In particular, several studies were focused on the structural evolution of manganites at low temperature but little attention has been paid to their behaviour under high pressure conditions. Previous high-pressure studies indicate that only $La_{0.7}Sr_{0.3}MnO_3$ is reported to have $R\bar{3}c$ symmetry and no phase transition is detected under pressure for this composition using a polycrystalline material. Powder diffraction data from this work allow to determine a bulk modulus K_{T0} = 167(5) GPa [2]. To be remarked that manganites at high pressure were investigated only by powder diffraction measurements, which are very often insufficient to determine small structural details like those typical of distorted perovskite structures (*e.g.* tilting angles, accurate bond lengths, compressibilities) and then single-crystal studies are necessary to better investigate the crystal structure evolution as a function of pressure.

In this light we performed a study on the $La_{0.815}Ba_{0.185}MnO_3$ sample by single-crystal X-ray diffraction at high-pressure *in situ* using a diamond anvil cell. Recently, experiments by single-crystal X-ray diffraction clarified that for a sample with the latter composition a symmetry change occurs from $R\bar{3}c$ to $I2/c$ at about 190 K with a limited deformation of the unit-cell [3]. In the present work we analyze the structural evolution of $La_{0.815}Ba_{0.185}MnO_3$ manganite up to 7.86 GPa. For this purpose, complete intensity data were collected at 9 different pressure and relative structure refinements converge to a R value of about 4%. We observe no phase transitions as well as no anomalies for the unit cell volume against pressure.

The *y* coordinate of oxygen atom increases throughout the investigated pressure range. As a consequence, the tilting system becomes more regular as the Mn-O-Mn angle associated to the tilting angle approaches 180 degrees. By contrast, in the low temperature experiment the y_{Ox} do not show significant variations down to the transition. We observe an almost isotropic compression of both *a* and *c* parameters of the hexagonal lattice that in the low temperature studies were found to be anisotropic.

The bulk modulus of about 178(6) GPa is consistent with other $R\bar{3}c$ perovskitic structures with different compositions [4].

$La_{0.815}Ba_{0.185}MnO_3$ is the first La-manganite studied either at high pressure or at low temperature by single-crystal X-ray diffraction. The different mechanisms of deformation and elastic properties are accurately described.

References. [1] G.H. Jonker, J.H. van Santen, *Physica (Amsterdam)*, **16**, 337-349, 1950; [2] D.P. Kozlenko, I.N. Goncharenko, B.N. Savenko, V.I. Voronin, *J. Phys. Condens. Matter*, **16,** 6755-6762, 2004; [3] N. Rotiroti, R. Tamazyan, S. van Smaalen, Ya. Mukovskii, *Acta Crystallogr. C***61**, i83-i85, 2005; [4] R.J. Angel, J. Zhao, N.L. Ross, C. Jakeways, S.A.T. Redfern, M. Berkowski, *J. Solid State Chem.*, **180**, 3408-3424, 2007.

Au PRESENCE IN THE MINERALIZATIONS OF THE PELORITANI MOUNTAINS (NORTH-EASTERN SICILY, ITALY)

C. Saccà, D. Saccà, P. Nucera, A. De Fazio

Dipartimento di Scienze della Terra, Università di Messina, Italy
pnucera@unime.it

Numerous historical sources [1-3] report on the presence of gold, of the order of ppm, in some mineralizations outcropping in the Peloritani Mountains, the southernmost part of the Calabrian Peloritani Arc (North-Eastern Sicily).

Only during the second half of the last century has the Au presence in mineralized areas been confirmed by chemical analyses [4]. A further confirmation has been the identification of an "auriferous belt" of about 6 Km in extension, from Alì Terme in the eastern area to Brolo in the western area [5], on the basis of diffuse Au anomalies found in stream sediments.

Recent chemical analyses carried out by Saccà *et al*. [6-10] have allowed us to underline that the Au presence is a common element to many mineralizations belonging to different Units.

As regards the Mandanici Unit, a significant Au presence was signalled in the jamesonite mineralization found in the metamorphic rocks of this Unit cropping out in *Sciglio* (Alì area) [10]. The association is mainly formed by jamesonite followed by tetrahedrite, antimonite, sphalerite, pyrite and galena. Au content reaches a value of 45 ppm in tetrahedrite. Interesting Au contents have also been ascertained in the *S. Carlo Mine* [8]. Metalliferous mineral association is mainly composed of tetrahedrite, chalcopyrite, scheelite, galena, sphalerite and pyrite. Au value varies on average from 0.3 ppm in chalcopyrite to 1 ppm in sphalerite.

An Au-mineralization has also been recognised in the Variscan medium-grade metamorphic rocks of the *Pomia Valley* [6] belonging to the Mela Unit. The mineralization is mainly composed of chalcopyrite, arsenopyrite, pyrite, sphalerite, galena, pyrrhotite, marcasite, tetrahedrite, quartz and calcite. Au appears to be concentrated predominantly in chalcopyrite (3 ppm) and arsenopyrite (6 ppm).

The presence of Au has been found in the barite, siderite and galena mineralizations of *Linata* too [11], belonging to the medium-high grade metamorphics Aspromonte Unit. The content found varies from 2.46 ppm to 9.60 ppm.

The presence of this noble metal in all minerals is important and shows that the mineralizing event is late and widespread. The gold deposit appears to be related to Alpine deposits and to late hydrothermal processes [12,13].

References. [1] G. La Valle, *Tip. F.lli Fugazzotto*, Messina, 1-83, 1899; [2] R. Meli, *Tip. D'Angelo*, Messina, 1909; [3] L.A. Pagano, *Boll. Mens. Osserv. Econ. Banco di Sicilia,* 1939; [4] B. Baldanza, G. Cimino, F. Oteri, *Atti Acc. Pelor. Pericolanti, Cl. Sc. Mat. Fis. Nat*., **61,** 1983; [5] B. De Vivo, A. Lima, G. Catalano, A. Chersicla, *J. Geochem. Explor*., **46,** 309-324, 1993; [6] C. Saccà, D. Saccà, P. Nucera, R. Somma, *Boll. Soc. Geol. It*., **122**, 503-509, 2003; [7] C. Saccà, D. Saccà, P. Nucera, *Atti Acc. Pelor. Pericolanti*, *Cl. Sc. Mat. Fis. Nat*., **LXXXI-LXXXII,** C1A0401011, 2004; [8] C. Saccà, D. Saccà, P. Nucera, A. De Fazio, G. Pisacane, *Atti Acc. Pelor. Pericolanti*, *Cl. Sc. Mat. Fis. Nat*., **LXXXIV**, C1A0601002, 2006; [9] C. Saccà, D. Saccà, P. Nucera, A. De Fazio, D. D'Urso, *Atti Acc. Pelor. Pericolanti*, *Cl. Sc. Mat. Fis. Nat*., **LXXXV**, C1A0701008, 2007a; [10] C. Saccà, D. Saccà, P. Nucera, A. De Fazio, *Geoitalia, 6° Forum FIST*, 2007b; [11] C. Saccà, *Atti Acc. Pelor. Pericolanti*, *Cl. Sc. Mat. Fis. Nat*., **61**, 383-402, 1983; [12] A. Messina, C. Saccà, *Geoitalia, 3° Forum FIST*, 530-531, 2001; [13] P. Ferla, P. Omenetto, *Mem. Soc. Geol. It*., **55**, 293-297, 2000.

HEAVY METAL DISTRIBUTION IN MARINE SEDIMENTS OF PATTI GULF (TYRRHENIAN SEA, SOUTHERN ITALY)

C. Saccà[1], D. Saccà[1], P. Nucera[1], A. De Fazio[1], S. Giacobbe[2]

[1]*Dipartimento di Scienze della Terra, Università di Messina, Italy*
[2]*Dipartimento di Biologia Animale ed Ecologia Marina, Università di Messina, Italy*
adefazio@unime.it

The area under investigation is the Patti Gulf, a basin in the Southern Tyrrhenian (Southern Italy), extending off the northern Sicilian coast, between the island of Vulcano to the north and the area from the Milazzo Cape to the Calavà Cape to the south. The aim of this study is to determine the heavy metal distribution in sediments to assess pollution in this area of the Mediterranean Sea.

Metal concentrations (Fe, Cr, P, Hg, Pb, Ni, Zn and Cu) have been determined in the < 4 μm sediment fraction by the ICP-MS technique (Inductively Coupled Plasma-Mass Spectrometry).

According to Shepard's classification [1] samples can be classified as clayey silts except shallow sample, in which silt-size fraction appears to be clearly predominant over clay.

Among the analyzed metals in sediments from Patti Gulf, the mean concentrations of Fe (5.6 %) and P (1207 ppm) are generally higher when compared with the others. Metal concentration varies with depth: samples collected at lower 70 m depth show high values of Fe and Pb; Cr concentrations vary constantly with depth except for samples U19 (338 m) and U26 (705 m) showing, respectively, the maximum (205 ppm) and minimum value (68 ppm); P values are also constant, reaching a peak value in deeper sample; Ni and Zn concentrations exhibit a narrow range of variation, except for sample U02.

In order to evaluate metal pollution levels in this area of the Mediterranean Sea, the analyzed values in samples were compared with Preter & Anderson's [2] concentration for unpolluted and strongly polluted sediments. By comparing, it was observed that samples of the Patti Gulf can be considered such only for Fe, Cr, P and Cu levels.

The contamination index (CI; Agenzia di Bacino del Rodano), that is the ratio between the observed concentration and the concentration considered normal for unpolluted sediments, has also been calculated. The CI used to classify sediments has allowed us to consider the Patti Gulf sediments polluted by Fe and Ni. According to the interpretation proposed by the "Agenzia del Rodano", in fact, sediments can be classified as normal (CI < 3), polluted (3 < CI < 10) and at risk (CI > 10).

Besides, in order to assess if each metal concentration represents contamination level or can be considered as background level, the geoaccumulation index (I_{geo}) [3] has also been calculated, comparing the concentration of the respective elements to that of unpolluted sediments (background value). The results were calculated by using three different background values [4-6]. According to Müller's classification [3] and using Donazzolo's *et al*. background values [6], sediments of the Patti Gulf can be characterized as unpolluted to moderately polluted in Cu, Ni, Fe, Zn and moderately polluted to strongly polluted in Cr. According to Karageorgis *et al*. [5] and Turekian & Wedepohl [4] the same sediments can be considered unpolluted to moderately polluted respectively in Fe and in Cr, Pb, Zn.

References. [1] F.P. Shepard, *J. Sediment. Petrol*., **24**, 151-158, 1954; [2] MAV, CVN, Final Report, 1999 [3] G. Müller, *Umschan*, **105**, 157-164, 1981; [4] K.K. Turekian, K.H. Wedepohl, *Bull. Geol. Soc. Am*., **72**, 175-192, 1961; [5] A. Karageorgis, Ch. Anagnostou, A. Sioulas , G. Chronis, E. Papathanassiou, *J. Marine Syst.*, **16**, 269-281, 1998; [6] R. Donazzolo, O.H. Merlin, L. Menegazzo Vitturi, A.A. Orio, B. Pavoni, G. Perin, S. Rabitti, *Mar. Pollut. Bull.*, **12**, 417-425, 1981.

PURE AND Fe^{3+} DOPED HYDROXYAPATITES: ROLE OF Ca AND P PRECURSORS, SYNTHESIS ROUTE AND THERMAL TREATMENT IN THEIR PRODUCTION

G. Salviulo[1], M. Bettinelli[2], L. Nodari[2], U. Russo[3], A. Speghini[4]

[1]*Dipartimento di Geoscienze, Università di Padova, Italy*
[2]*Dipartimento Scientifico e Tecnologico, Università di Verona, Italy*
[3]*Dipartimento di Scienze Chimiche, Università di Padova, Italy*
[4]*Dipartimento di Scienze, Tecnologie e Mercati della vite e del vino, Università di Verona, Italy*
gabriella.salviulo@unipd.it

Calcium phosphate apatites form a wide class of inorganic crystalline compounds with formula $Ca_{10}(PO_4)_6(OH,F,Cl)_2$. The mineral apatite is of great importance in a large variety of fields such as Earth science, life science and materials science because of its atomic arrangement which allows numerous chemical substitutions for both Ca and (PO_4) groups. Synthetic hydroxyapatite (HA) is used as an environmental absorber of metal ions due to its cation-exchange property and as a catalytic support for heterogeneous catalysis. In addition HA presents high biocompatibility with natural bone tissues and can be easily incorporated in biological tissues, therefore it finds various applications as a bioceramic material. Numerous synthetic methodologies for the preparation of HA are known, such as solid state synthesis, hydrolysis, hydrothermal and sol-gel methods. Previous studies have noted that, different synthesis routes can lead to different product compositions as a consequence of starting materials type and concentration, reaction temperature and heat treatment. However previous results are not in full agreement with each other. In addition, numerous cations can substitute for calcium in HA affecting morphology, solubility, lattice parameters and consequently the stability of the obtained material. To our knowledge, no papers have been published reporting the highest amount of Fe^{3+} substituting for Ca in the HA structure. According to Mössbauer spectroscopy, the dissolution of Fe(III) into the apatite structure is very complex and the phases that are formed depend on the synthesis procedure, on the Fe/P and Fe/Ca ratios, and, in the case of the ceramic synthesis, on the thermal treatment. Under this perspective, the aims of this work are: 1) to evaluate the role of Ca and P precursors in HA synthesis by both solid state and hydrothermal routes; 2) to optimise the experimental conditions of three different methodologies (solid state, coprecipitation and hydrothermal synthesis) for producing HA even in presence of Fe^{3+}. A further interest is to control the crystal size of the powder as related to synthesis route; 3) to achieve the direct formation of HA using Fe^{3+} as dopant, in order to study the role of Fe^{3+} in the HA synthesis and test the solubility limit of Fe^{3+} in HA itself. Samples were characterized using X-Ray powder diffraction, Mössbauer and infrared spectroscopies. Results indicate that solid state synthesis performed at 800°C produces mixtures of HA and other phosphates depending on the Ca and P precursors. The obtained HA actually is a B-Type carbossiapatite. It is noteworthy that the use of $CaCl_2$ produces chloroapatite instead of HA. The hydrothermal route proved to be more efficient that solid state and the obtained percentage of HA is strictly controlled by pH and the used additive. The wet syntheses lead to samples with very similar diffraction patterns. They present broad peaks indicating a low degree of crystallinity, characteristic of calcium phosphate synthesized by the wet precipitation method. The X-ray diffraction pattern of all samples revealed that they are a mixture of HA and an amorphous component. As the role of Fe^{3+} in the HA synthesis and the solubility limit of Fe^{3+} in HA itself are concerned, further studies are needed, because the presence of various phases and of more than one site available to iron in each phase makes the interpretation of the Mössbauer spectra in any case very difficult.

FURTHER DATA ON THE CRYSTAL CHEMISTRY OF Ti-GARNETS

E. Schingaro[1], F. Scordari[1], S. Matarrese[1], E. Mesto[1], G. Pedrazzi[2]

[1]*Dipartimento Geomineralogico, Università di Bari, Italy*
[2]*Dipartimento di Sanità Pubblica, Sezione di Fisica e CNISM, Università di Parma, Italy*
schingaro@geomin.uniba.it

The crystal chemistry of Ti-bearing garnets of different origin and geological provenance has been revised on the basis of the results presented in [1].

Natural garnets with TiO_2 from 5 to 17 wt.% underwent multiple technique investigation, which consisted of the combination of chemical (EMPA), structural (SC-XRD) and spectroscopic techniques (Mössbauer, XPS). Specifically, the iron oxidation state was determined via: electron microprobe analysis - the flank method procedure as devised in [2], Mössbauer spectroscopy, and XPS analysis [3,4]. The first and the latter methods were used on single crystals, whereas for Mössbauer spectroscopy was employed on powders. Data from single crystals generally correlate well with those from powders. More specifically, Mössbauer analysis provided spectra with different complexity, which could be fitted with a number of components variable from one ($^{VI}Fe^{3+}$(Y)) to five ($^{VIII}Fe^{2+}$(X), $^{VI}Fe^{2+}$(Y), $^{IV}Fe^{2+}$(Z), $^{VI}Fe^{3+}$(Y), $^{IV}Fe^{3+}$(Z)). However, the $^{IV}Fe^{2+}$(Z) component has been reinterpreted by some authors [1] as due to $^{VI}Fe^{2+}(Y) \leftrightarrow {}^{IV}Fe^{3+}(Z)$ electron transfer.

Anisotropic structure refinements converged to $2.00 \leq R \leq 2.02$ %, $2.56 \leq R_w \leq 3.01$ %.

The main structural parameters are a = 12.030-12.180 Å; <X-O> (Å) = 2.423-2.453; Y-O (Å) = 1.989-2.014, Z-O (Å) = 1.652-1.690. Mean atomic numbers (electrons, e^-) are in the range 59.3-60.9 for the X site; 42.3-48.9 for the Y site; 41.4-49.1 for the Z site.

In many cases, the combination of $^{VI}Ti^{4+VI}M^{3+IV}Fe^{3+}_{-1}{}^{IV}Si_{-1}$ (schorlomite substitution) and $^{VI}M^{2+VI}Ti^{4+VI}Fe^{3+}_{-2}$ (morimotoite-like substitution), with $M^{3+} = Fe^{3+}$, Al^{3+}, and $M^{2+} = Fe^{2+}$, Mg^{2+}, Mn^{2+}, can explain the chemical variation of tetrahedral and octahedral site. In other cases an accurate evaluation of the hydrogarnet component is necessary for a complete and unambiguous assessment of the substitution mechanisms.

The data of the present investigations are also compared with those obtained from natural garnets with low TiO_2 concentration (2-5 wt.%, [3-4,6]) and from kimzeyite [5].

References. [1] A.R. Chamouradian, C.A. McCammon, *Phys. Chem. Minerals*, **32**, 277-289, 2005; [2] H.E. Höfer, G.P. Brey, *Am. Mineral.*, **92**, 873-885, 2007; [3] C. Malitesta , I. Losito, F. Scordari, E. Schingaro, *Eur. J. Mineral.*, **7**, 847-858, 1995; [4] F. Scordari, E. Schingaro, G. Pedrazzi, *Eur. J. Mineral.*, **11**, 855-869, 1999; [5] E. Schingaro, F. Scordari, F. Capitanio, G. Parodi, D.C. Smith, A. Mottana, *Eur. J. Mineral.*, **13**, 749-759, 2001; [6] E. Schingaro, F. Scordari, G.Pedrazzi, C. Malitesta, *Ann. Chim-Rome*, **94**, 185-196, 2004.

SC-XRD, MICRO-XANES AND SIMS INVESTIGATION ON PHLOGOPITES FROM MT. VULTURE

F. Scordari[1], M.D. Dyar[2], E. Schingaro[1], S. Matarrese[1], L. Ottolini[3]

[1]*Dipartimento Geomineralogico, Università di Bari, Italy*
[2]*Department of Earth and Environment, Mount Holoyoke College, MA, USA*
[3]*CNR-IGG, Pavia, Italy*
schingaro@geomin.uniba.it

Single crystals of selected phlogopites from the Mt. Vulture suite were studied using a combination of chemical (EMPA and SIMS), structural (SC-XRD) and spectroscopic (micro-XANES) techniques. Micro-XANES was employed to analyze the Fe-K edge and determine Fe^{3+}/Fe_{tot} values following a procedure described in [1].

The annite component, Fe/(Mg+Fe), of the samples studied ranged from 0.18-0.31. SIMS analysis showed H_2O = 2.07-3.77 wt.%, F = 0.43-1.29 wt.%, and Li_2O = 0.001-0.027 wt.%. Microbeam XANES investigation yielded Fe^{3+}/Fe_{tot} from 50-93%. The results generally show good agreement with Mössbauer data from powdered samples, with Fe^{3+}/Fe_{tot} = 50-87% [2-4].

All of the analyzed micas belong to the 1*M* polytype. Structural parameters were a = 5.326-5.338 Å, b = 9.221-9.243 Å, c = 10.181-10.256 Å, and β = 99.97-100.10°. Structure refinements using anisotropic displacement parameters were performed in space group *C*2/*m* and converged at $1.89 \le R \le 3.83$ %, $2.09 \le R_w \le 4.39$ %

Structural and distortional parameters are not all consistent with the prevalence of oxy-type substitutions. In particular, it is here confirmed that multiple substitution mechanisms involving M^{3+} and Ti, as well as the anionic site, are responsible for the variation of mica geometrical features. Specifically, (at least) a bimodal behaviour of Mt. Vulture phlogopites can be recognized in structural *vs*. chemical trends (*e.g*. $shift_{M2}$ *vs*. Ti, $<K\text{-}O>_{outer}$ *vs*. Ti, etc.). The two groups have crystal chemical characteristics consistent with different relative amounts of M^{3+}-oxy ($^{VI}M^{2+} + (OH)^- \leftrightarrow {}^{VI}M^{3+} + O^{2-} + ½\ H_2\uparrow$), Ti-oxy substitutions ($^{VI}M^{2+} + 2(OH)^- \leftrightarrow {}^{VI}Ti^{4+} + 2O^{2-} + H_2\uparrow$) and Ti-vacancy substitution, $2\ ^{[VI]}M^{2+} \leftrightarrow {}^{[VI]}Ti^{4+} + {}^{[VI]}[]$.

It is also shown that combination of single crystals techniques, such as those adopted here, is best suited to cope with cases of crystal-to-crystal heterogeneity that frequently occur in volcanic micas .

References. [1] M.D. Dyar, J.S. Delaney, S.R. Sutton., *Eur. J. Mineral.*, **13**, 1079-1098, 2001; [2] S. Matarrese, *Ph.D. thesis*, University of Bari, 2007; [3] E. Schingaro, F. Scordari, S. Matarrese, E. Mesto, F. Stoppa, G. Rosatelli, G. Pedrazzi, *Mineral. Mag*., **71**, 519-537, 2007; [4] S. Matarrese, E. Schingaro, F. Scordari, F. Stoppa, G. Rosatelli, G. Pedrazzi, L. Ottolini, *Am. Mineral*., **93**, 426-437, 2008.

HIGH-PRESSURE SINGLE-CRYSTAL STUDY OF PYROXMANGITE

P.F. Zanazzi[1], F. Nestola[2], S. Nazzareni[1], P. Comodi[1]

[1]*Dipartimento di Scienze della Terra, Università di Perugia, Italy*
[2]*Dipartimento di Geoscienze, Università di Padova, Italy*
zanazzi@unipg.it

Pyroxmangite, nominally $MnSiO_3$, is a single-chain silicate belonging to the pyroxenoid polysomatic series, *i.e.* the series formed by a combination of layers of the two end-member structures, wollastonite (W, Si_3O_9 chains) and clinopyroxene (P, Si_2O_6 chains). Pyroxmangite is the WPP term, with a tetrahedral chain of seven Si-O tetrahedra, and is related to rhodonite, which represents the WP term, with five-fold chains of Si tetrahedra. The mineral is triclinic centrosymmetric, and several orientations have been chosen to describe the lattice. The choice of a *C*-centered cell with the chain direction parallel to the *c* axis and the oxygen-closest packing layer parallel to (100), although not canonical, allows better comparisons with clinopyroxene and other pyroxenoids.

S5

We present the results of a single-crystal X-ray diffraction structural study on pyroxmangite in a diamond anvil cell up to 5.6 GPa. The sample with composition $(Mn_{0.576(2)}Fe_{0.284(5)}Ca_{0.044(3)}Mg_{0.089(2)})Si_{1.003(4)}O_3$ comes from Yokone-Yama, Awano Town, Tochigi Prefecture, Japan. Structure refinements were performed with intensity data collected at 1.24 and 3.57 GPa on a CCD diffractometer. Lattice parameters were accurately measured with the point-detector mounted on the same instrument.

The bulk modulus of pyroxmangite, fitting data to a second-order Birch-Murnaghan equation of state, is K_0 = 109.6(7) GPa. Axial compressibility values are β_a = 2.2(1), β_b = 3.3(1) and β_c = 2.6(1) 10^{-3} GPa^{-1} showing slightly anisotropic behavior, with the most compressible direction along the **b** axis, as commonly found in the related family of pyroxene.

Si tetrahedra are almost incompressible in the pressure range investigated. M polyhedra are more compressible: the volume change is smaller in the more regular octahedra M1-M4 (-3.3%) and greater in the more irregular polyhedra M5-M7 (-5.2%). Owing to the different contraction of Si tetrahedra and cation polyhedra, the 7-fold tetrahedral chains in pyroxmangite must kink to avoid misfit between chains and octahedral bands. This results in a shortening of 1.2% of the **c** axis and a decrease in both O_{br}-O_{br}-O_{br} and Si-O_{br}-Si angles.

The behaviour of pyroxmangite at high *P* is approximately specular and inverse to that observed at high *T* [1]. Compressibility data may be combined with those on thermal expansion to formulate the approximate equation of state: $V = V_0 (1 - 9.12\ 10^{-3}\ \Delta P + 3.26\ 10^{-5}\ \Delta T)$, where *P* is in GPa and *T* in degrees Celsius. This equation describes structural evolution at various *P/T* gradients. For pyroxmangite, the isochoric *P*-*T* path, leaving the structure about equal to that observed at room conditions, is given by the ratio β/α and corresponds to 28°C/kbar, *i.e.* to a geothermal gradient of 10.4°C/km, which fits field observations, showing that pyroxmangite structure is stabilized by high-*P*, low-*T* environments.

References. [1] L.R. Pinkney, C.W. Burnham, *Am. Mineral.*, **73**, 809-817, 1988.

GEOMATERIALS

Session 6
Applications and models for
Mineralogy, Petrology and Geochemistry

THE EFFECT OF NON-STOICHIOMETRY AT HIGH-PRESSURE AND HIGH-TEMPERATURE: IMPLICATIONS FOR THE EARTH'S MANTLE MINERALOGY

F. Nestola[1], J.R. Smyth[2], M. Parisatto[1], L. Secco[1],
F. Princivalle[3], M. Bruno[4], M. Prencipe[4], A. Dal Negro[1]

[1]*Dipartimento di Geoscienze, Università di Padova, Italy*
[2]*Department of Geological Sciences, University of Colorado, USA*
[3]*Dipartimento di Scienze della Terra, Università di Trieste, Italy*
[4]*Dipartimento di Scienze Mineralogiche e Petrologiche, Università di Torino, Italy*
fabrizio.nestola@unipd.it

Several works have been dedicated to the determination and interpretation of the evolution of the thermodynamic properties as a function of pressure, temperature and composition for mantle minerals. This is clearly due to their importance in constraining all the geological processes in which such minerals are involved. $MgAl_2O_4$ spinel not only is one of the most studied mineral being a common phase of several geological environment but at the same time can be used as a model for an analogue structure stable at the transition zone (between 410-660 km) like ringwoodite (Mg_2SiO_4, γ-olivine). In this work we have investigated a non-stoichiometric spinel with composition $Mg_{0.4}Al_{2.4}O_4$, with 0.2 p.f.u. cation vacancies, at high-pressure and high-temperature in two separated *in situ* experiments in order to determine which is the effect of a significant excess of Al on compressibility and thermal expansion. In fact, as reliable geodynamic models predict for mantle an amount of 4-5% by weight of Al_2O_3, this means that Al can be incorporated in phases like wadsleyite, ringwoodite, majoritic garnet, Mg-perovskite and therefore our results could provide new insights on the effect of composition on the determination of thermodynamic properties.

The *in situ* high-pressure and high-temperature studies were performed by single-crystal X-ray diffraction using a diamond anvil cell (P_{max} = 10 GPa) and a micro-furnace capable to reach temperatures higher than 1400 K. The pressure - volume data (Fig. 1) collected on our non-stoichiometric sample up to 9 GPa gave a bulk modulus K_{T0} = 172(2) GPa, whereas the temperature - volume data (Fig. 2) collected up to 1273 K gave a room temperature thermal expansion $\alpha = 1.86(0.37)\times10^{-5}$ K^{-1}. Our results compared with stoichiometric $MgAl_2O_4$ spinel clearly indicate that both the compressibility and the thermal expansion are strongly affected by the excess of Al of the non-stoichiometric sample. In particular, the excess of Al causes a strong increase in compressibility and a significant decrease in thermal expansion with respect to the stoichiometric spinels.

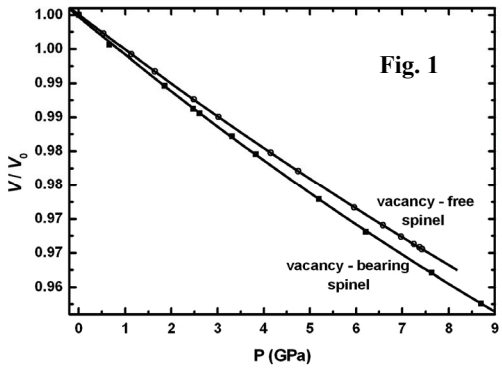

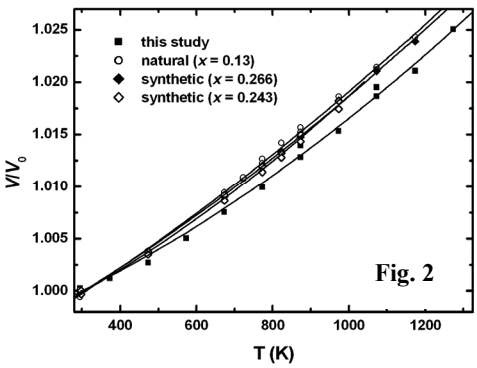

HIGH-TEMPERATURE $P2_1/c$ – $C2/c$ PHASE TRANSITION OF $LiFe^{3+}Ge_2O_6$

G.J. Redhammer[1], F. Cámara[2], M. Alvaro[3], F. Nestola[4], H. Ohashi[5]

[1]*Department of Materials Engineering & Physics, Division of Mineralogy, University of Salzburg, Austria;* [2]*CNR - IGG, Unità di Pavia, Italy*
[3]*Dipartimento di Scienze della Terra, Università di Pavia, Italy*
[4]*Dipartimento di Geoscienze, Università di Padova, Italy*
[5]*Hashi Institute for Silicate Science, Tokyo, Japan*
matteo_alvaro@manhattan.unipv.it

A synthetic clinopyroxene with composition $LiFe^{3+}Ge_2O_6$, monoclinic s.g. $P2_1/c$, a = 9.8792(7), b = 8.8095(5), c = 5.3754(3) Å, β = 108.844(6)°, V = 442.75(16) Å^3, has been studied by *in situ* high-temperature single crystal X-ray diffraction. The evolution of the lattice parameters with temperature has been recorded at steps of ca. 27°C up to 860°C. A sharp and strong variation in all the lattice parameters corresponding to a first order phase transition is observed at T_{tr} = 516°C, with a corresponding to a sudden volume increase of 1.44%. This spontaneous dilatation is reversible, shows a limited hysteresis of ± 10°C, and corresponds to the vanishing of reflections with $h + k = 2n + 1$ (b-type reflections), thus indicating a symmetry increase to space group $C2/c$. The strong change in volume may lead to the breaking of the crystal into several fragments, as it has been observed at the diffractometer. Whereas below T_{tr} an expansion is observed for all the cell parameters with β angle remaining constant, at $T > T_{tr}$ the volume increase is due to dilatation of the structure along [010] and pure shear in the (101) plane (β decreases of 1° at the transition). Lattice parameter a shows no thermal expansion at $T > T_{tr}$ whereas the expansion along c axis is very faint (<0.003 Å in 325°C). Scalar spontaneous strain prior to the transition is 0.0314.

The same transition was observed qualitatively looking at changes in birefringence using a heating stage under the polarized microscope: at the transition there is a marked increase in retardation and the crystal breaks along easy cleavage planes. A hysteresis is observed as the T_{tr} is 526°C when raising T and 509°C when decreasing T. Temperatures values are highly reproducible.

In the framework of the Landau theory, the equilibrium evolution of the order parameter (Q) was followed by integration of selected b-type reflections normalized to the intensity of adjacent reflections with $h + k = 2n$ (a-type reflections), corresponding to Q^2. Fitting the evolution of Q with T with a standard expression for a 1st order phase transition we observe that Q drops to 0 at T_{tr}, showing a jump of Q_o^2= 0.538(2) and a T_c of 208(7)°C, with a negative ratio of the Landau coefficients b/a = 2291°C. The large value of (T_{tr}-T_c) indicates that the 1st order transition is well far from being tricritical in character, while a close related composition ($LiFe^{3+}Si_2O_6$) shows a tricritical phase transition at -45°C [1].

Complete intensity data were collected at 214, 430, 537, 753 and 861°C. The evolution of the crystal structure with T indicates that the M2 polyhedron shows the major changes with a volume decrease by about 13.3% compared to that of M1 polyhedron (about 1.3%). For such calculation we assumed a 6-fold coordination for the M2 polyhedron, as no change in coordination is observed at $T > T_{tr}$: the long O3B oxygen is positioned at 3.11 Å from M2 site at 430°C (below the transition temperature), at 535°C it is positioned at 3.32 Å. The tetrahedra behave as rigid units with neither a significant change of volume at $T > T_{tr}$ (< 1 ‰), nor a change of tilting of the basal plane. The strong deformation of M2 is accompanied by a strong rotation of 51.4° at T_{tr} of the kinking angle (O3-O3-O3 angle) of the B tetrahedral chain, which switches form O-rotated to S-rotated (from 143.3(5)° to 194.7(6)°). The A chain, which is S-rotated at $T < T_{tr}$ [206.8(5)° at 430°C], extends by 12° at the transition.

References. [1] G.J. Redhammer, G. Roth, W. Paulus, G. Andre, W. Lottermoser, G. Amthauer, W. Treutmann, B. Koppelhuber-Bitschnau, *Phys. Chem. Miner.*, **28**, 337-346, 2001.

THE EFFECT OF Fe OXIDATION STATE ON THE VISCOSITY OF SILICATE MELTS: Fe STRUCTURAL ROLE IN PHONOLITIC GLASSES BY XAS

G. Giuli[1], D. Dingwell[2], K.-U. Hesse[2], P. Valenti[2], E. Paris[1]

[1]*Diparimento di Scienze della Terra, Università di Camerino, Italy*
[2]*Department of Earth and Environmental Sciences, LMU, München, Germany*
gabriele.giuli@unicam.it

Iron in silicate melts can play a variety of structural roles involving different coordination numbers and oxidation states. Common Fe species in the melt include $^{[4]}Fe^{2+}$, $^{[5]}Fe^{2+}$, $^{[4]}Fe^{3+}$, and $^{[5]}Fe^{3+}$. The relative proportions between these species can vary considerably according to bulk glass composition and oxygen fugacity conditions. However, in most natural and synthetic silicate glasses 4- and 5-fold coordinated Fe^{2+}, and 4-fold coordinated Fe^{3+} are the most common Fe species. Being a major element in silicate melts, Fe can affect considerably important physical properties like density and viscosity of a magma. Moreover, even at constant bulk composition and Fe content, also the Fe oxidation state is known to affect the melt viscosity [1].

In order to study the Fe structural role in peralkaline silicate melts and its effect on their viscosity, a set of silicate glasses with phonolitic composition have been synthesised at different oxygen fugacity conditions (ranging from air down to IW buffer). These glasses have been previously characterized by titration to get the Fe oxidation state. Moreover, the viscosity has been measured for each glass/melt at different temperatures.

XANES and EXAFS data have been collected in fluorescence mode at the ID26 beamline of the ESRF storage ring (Grenoble, F) using a Si(311) monochromator. Accurate analysis of the pre-edge peak and comparison with pre-edge peak data of Fe model compounds allowed to accurately measure $Fe^{2+}/(Fe^{2+} + Fe^{3+})$ ratios for all the glasses. EXAFS data have been analysed by the GNXAS package allowing to obtain the average <Fe-O> and <Fe-Si> distances for the most oxidized sample. Moreover, theoretical XANES spectra have been calculated and compared to the experimental XANES spectra in the aim of getting a better view of the local structure around Fe.

Pre-edge peak data clearly indicate that $Fe^{2+}/(Fe^{2+} + Fe^{3+})$ ratio varies from 7 to 56%. These values agree very well with those obtained by titration. In particular pre-edge peak data show Fe^{3+} to be in 4-fold coordination, whereas Fe^{2+} consists of both 4- and 5-fold coordination.

The <Fe-O> distance in the most oxidized samples has been found to be 1.86 Å, in agreement with that found for $^{[4]}Fe^{3+}$ in tetra-ferriphlogopite [2]. This value is considerably shorter than that typical for Fe^{2+} in silicate glasses (2.00 Å, [3]). This implies that in oxidized glasses there is a shorter and stronger bond between Fe and neighboring oxygen atoms than in more reduced glasses.

Moreover, the variation of the Fe structural role in these glasses entails a small but significant variation in the NBO/T ratio, which decreases from the most reduced to the most oxidized sample respectively.

Viscosity of the studied melts varies continuously in the oxygen fugacity range under consideration, and bears an inverse linear relationship with both the $Fe^{2+}/(Fe^{2+} + Fe^{3+})$ ratio and the NBO/T ratio.

The variations in the <Fe-O> bond lengths and in the NBO/T ratio can qualitatively explain the viscosity increase related to the Fe oxidation.

References. [1] D.B. Dingwell, *Am. Mineral.*, **76**, 1560-1562, 1991; [2] G. Giuli, E. Paris, Z. Wu, M.F. Brigatti, G. Cibin, A. Mottana, A. Marcelli, *Eur. J. Mineral.*, **13**, 1099-1108, 2001; [3] G. Giuli, G. Pratesi, C. Cipriani, E. Paris, *Geochim. Cosmochim. Ac.*, **66**, 4347-4353, 2002.

WATER CONTENT OF PYROXENES FROM ETNA AND AEOLIAN VOLCANOES: IMPLICATIONS FOR THE HAZARD OF ACTIVE ITALIAN VOLCANOES

S. Nazzareni[1], H. Skogby[2], M. Pompilio[3], P.F. Zanazzi[1]

[1]*Dipartimento di Scienze della Terra, Università di Perugia, Italy*
[2]*Department of Mineralogy, Swedish Museum of Natural History, Stockholm, Sweden*
[3]*INGV sezione di Pisa, Italy*
sabrina.nazzareni@unipg.it

The Aeolian arc and Etna are among the main active volcanic areas in Europe. Moreover, this area is densely populated leading the volcanic hazard to a high level. Both Aeolian arc and Etna have been extensively studied from geological-geophysical viewpoints suggesting complex evolutionary processes and several volcanological models have been proposed. In volcanic environments, volatiles (*i.e.* water) play a fundamental role by influencing the physical-chemical properties of magmas, and they are extremely useful in understanding the mechanisms of explosive eruptions, and thus to forecast volcanic events. The volatile activity is a clue for volcanic hazard, especially where classical precursors used for forecasting explosive eruptions seem not to work, like in Vulcano.

Nominally anhydrous minerals (NAMs), have frequently been discovered to incorporate water in the form of structurally bound OH [1], and can become a new tool to better understand magma volatile contents. Since pyroxenes are very common in volcanic rocks, they can be used to add new data on the magmas volatiles budget. We selected clinopyroxene (Cpx) crystals from Etna (3930 BP picritic eruption, Cono del Piano - 2001 and 2002 eruptions) and from different volcanic stages of Vulcano, Salina and Alicudi. Crystals no less than some hundred microns in size were handpicked and oriented by single-crystal XRD methods. Polarized IR spectra were measured in the 2000-5000cm^{-1} region on (100) and (010) Cpx sections to obtain the three main α, β, γ optical directions. Nearly all samples showed the presence of vibrational OH bands at 3630 cm^{-1}, 3530 cm^{-1} and 3460 cm^{-1} in the IR spectra, and we used the Libowitzky & Rossman calibration [2] to calculate their water contents. On the same crystals used for FTIR measurements, the structural models by single-crystal XRD and EPM analysis were performed. Mössbauer spectra were measured on selected samples to account for the possible loss of hydrogen by iron oxidation during ascent and eruption.

Vulcano Cpx showed a large variation in water content, from 22 to 345 ppm H_2O by weight, among samples belonging to the same volcanic stage: primordial Vulcano 23-236 ppm H_2O; Lentia complex 22-345 ppm H_2O; Vulcanello: 40-101 ppm H_2O. To evaluate if this variation might be ascribed to H loss during the late stage of eruption or due to variation in the reservoir, we selected 5 samples on which Mössbauer analyses and re-hydrogenation experiments were carried out. Two heat treatments were performed under hydrogen gas flow at 700°C for 6 hours each, and after each experiment the IR spectra were collected again. The most "dry" samples take up H (*i.e.* Pl7 from 23 to 136 ppm H_2O, Lt2 from 36 to 187 ppm H_2O), while the most H_2O-rich ones remain almost unchanged suggesting H loss for the former while the latter may be representative of original crystallisation conditions. The water content of the Etna Cpxs is quite high suggesting a water rich magmatic system and showed only minor variations from the different eruptions: 254 ppm H_2O for 3930 BP picritic eruption; 214 ppm H_2O for 2001 eruption; 161-254 ppm H_2O for 2002 eruption. The H_2O content of Cpxs from the Aeolian volcanoes (up to 390 ppm H_2O by weight in Salina, up to 345 ppm H_2O by weight in Vulcano and up to 270 ppm H_2O by weight in Alicudi) and in Etna samples reaches values that have so far mainly been reported for H*P* mantle Cpxs.

References. [1] E.A. Johnson, *Rev. Mineral. Geochem.*, **62**, 291-320, 2006; [2] E. Libowitzky, G. Rossman, *Am. Mineral.*, **82**, 1111, 1997.

CAN CLINOPYROXENE BE A LEADING HOST OF POTASSIUM IN THE EARTH'S UPPER MANTLE? EVIDENCES FROM CRYSTAL CHEMISTRY AND THERMODYNAMIC MODELLING

L. Bindi

Museo di Storia Naturale, Sezione di Mineralogia, Università di Firenze, Italy
luca.bindi@unifi.it

Clinopyroxenes (Cpxs) of typical crustal rocks contain only trace amounts of potassium since large K cation is much more easily accommodated by the lattices of framework and sheet silicates. However, Cpxs from rocks that crystallized at high pressures show notable K_2O concentrations. K-bearing Cpxs have been described as inclusions in kimberlitic diamonds, in eclogitic and peridotitic xenoliths in kimberlites and lamproites, and in garnet-clinopyroxene rocks of the Kokchetav ultra-high-pressure complex in Northern Kazakhstan. Usually, the concentration of K_2O in high pressure Cpxs does not exceed 1.7 wt.%. However, the discovery of samples with 2.34 and 3.61 wt.% of K_2O shows that the structure of Cpx is able to accommodate much higher concentrations of potassium. Experimental studies showed that Cpxs from potassium-rich silicate and carbonate-silicate systems at pressures of 6-11 GPa may contain up to 4.0-5.7 wt.% of K_2O. The experiments along the join $CaMgSi_2O_6$-$KAlSi_2O_6$ evidenced that the maximal content of KJd in the KCpx solid solution at 7 GPa is about 26 mol.%. At higher $KAlSi_2O_6$ contents, the KCpx solid solution decomposes to garnet and Si-wadeite *via* the reaction 4KJd + 3Di = Grs + Prp + 2SWd. It has been also shown that at 7 GPa and 1273 K a Cpx of $KAlSi_2O_6$ composition is unstable, while the stable assemblage is SWd + Ks + Ky.

A positive correlation of the concentration of K with that of Al and a negative correlation with the Mg content in Cpxs along the $CaMgSi_2O_6$-$KAlSi_2O_6$ join shows that the major substitution scheme in Di-KJd solid solution is Mg + Ca ⇔ Al + K, which is analogous to that in the Di-Jd solid solution. X-ray single-crystal diffraction data for crystals containing 7 and 23 mol.% of KJd suggest that the increase of the KJd content results in an increase in the KCpx unit-cell volume (446.29 $Å^3$ *vs*. 438.53 $Å^3$ at 23 and 0 mol.% of KJd, respectively). An opposite effect, however, was measured for a Cpx with 12 mol.% of KJd. An *in situ* X-ray diffraction study of a synthetic Cpx with 12 mol.% of KJd at pressures up to 9.72 GPa showed that the bulk modulus of the studied sample is about 129 GPa, which is higher than that of pure diopside (112 GPa).

The available experimental and crystal chemical data show that the K_2O content of Cpxs is sensitive to the pressure of equilibration and thus can be used for barometry of the host mineral assemblages. Successful applications of a geobarometric technique, based on empirically calibrated partitioning of $KAlSi_2O_6$ between KCpx and potassic aluminosilicate melt, suggest that phase equilibria of KCpx with $KAlSi_3O_8$ polymorphs could also be useful as geobarometers. To obtain theoretically the relevant geobarometric equations, the standard thermodynamic properties of the K-jadeite end-member ($KAlSi_2O_6$) and its thermodynamic activity in the clinopyroxene solid solution have been also derived. We have evaluated the standard enthalpy, volume and bulk modulus of $KAlSi_2O_6$ pyroxene from quantum-mechanical calculations, and estimated its standard entropy and thermal expansion coefficient using a force-field model based on lattice dynamics. This approach is based on the calculation of static lattice energies of a set of basis configurations, the development of an approximation for the excess energy of any possible configuration using the energies of the basis set, and Monte Carlo simulations based on the approximate equation for the excess energy.

STUDY OF THE GROWTH RATE IN DECOMPRESSION-INDUCED CRYSTALLIZATION EXPERIMENTS OF ALKALI FELDPSARS IN THE TRACHITIC MELT OF THE PHLEGRAEAN FIELDS (NAPOLI, ITALY)

M. Calzolaio, F. Arzilli, M.R. Carroll

Dipartimento di Scienze della Terra, Università di Camerino, Italy
marta.calzolaio@unicam.it

The aim of this work is to acquire experimental knowledge about growth kinetics of alkali feldspar in Phlegraean Fields trachytic melts, erupted in the Monte Nuovo event of 1538. Once combined with observation on natural samples, the experimental data will allow us to better constrain the residence, ascent and eruption times for Phlegraean eruptions.

Crystallization kinetics can be studied through hydrothermal experiments. Undercooling (dT) can be induced by decompression - exsolution of water, simulating the decompression the system undergoes during magma ascent towards the surface. In our experiments, the samples were maintained at a temperature (T) and pressure (P) higher than the liquidus T and P and then rapidly depressurized to a given final P, maintaining T constant. Changing final P, we obtain different conditions of undercooling, because with P variations water solubility in the melt varies and liquidus temperature increases. After decompression the sample remains in these conditions for a given time (t), needed for crystallization. Studying the dimensional variation of the crystals with t, we can calculate the growth rate for every final P and for every studied dT. Recent studies have shown that this may be an important process to induce crystallization in many volcanic systems, including Etna [1], Mt Saint Helens [2], Pinatubo [3] and Montserrat [4]. This crystallization can greatly influence magma physical properties (viscosity) and ultimately eruption behaviour because the timescales of such processes are similar to eruption timescale (hours to month, depending on eruptive styles), resulting in a strong non-linear feedback between ascent-rate, degassing, magma crystallization kinetics and effusion rates.

The experiments performed in this work have been carried out at P between 30 and 200 MPa, T between 750 e 860°C, t between 7200 and 57600 seconds and fO_2 = NNO + 0.8 [5]. For every series of decompression experiment with constant dT, we always performed a non-decompressed experiment, to allow a comparison with growth rates at constant P_{H2O} conditions.

To obtain alkali feldspar crystals dimensions, backscattered images were collected at the Scanning Electron Microscope (SEM). The photos were used to measure the length and the width of the crystals with Adobe Photoshop 7.0. A reasonable approximation for growth rate is to average the half-length of the ten longest alkali feldspar crystals in any experiment, as employed by Fenn [6], Hammer & Rutherford [7] and Couch [8]. The ratio between half-length and crystallisation time is used to calculate the growth rate G. Calculated crystal growth rate varies from $1.39 \cdot 10^{-8}$ to $1.57 \cdot 10^{-7}$ cm/s and is higher in experiments with lower duration, higher dT and higher dissolved water percentage. These values of G are the same (10^{-8} cm/s) or differ at the most of an order of magnitude (10^{-7} cm/s) from the G values used by Piochi *et al.* [9], so the rising time that will be calculated will surely be similar or lower than those estimated by Piochi *et al.* [9].

References. [1] N. Metrich, M.J. Rutherford, *Geoch. Cosmoch. Ac.*, **62**, 1195-1205, 1998; [2] J. Blundy, K.V. Cashman, *Contrib. Mineral. Petr.*, **140**, 631-650, 2001; [3] J.E. Hammer, K.V. Cashman, R.P. Hoblit, S. Newman, *B. Volcanol.*, **60**, 355-380, 1999; [4] S. Couch, R.S.J. Sparks, R.M. Carroll, *J. Petrol.*, **44**, 1477-1502, 2003; [5] V. Di Matteo, M.R. Carroll, H. Berhens, F. Vetere, R.A. Brooker, *Chem. Geol.*, **213,** 187-196, 2004; [6] P.M. Fenn , *Can. Mineral.*, **15**, 135-161, 1977; [7] J.E. Hammer, M.J. Rutherford, *J. Geophys. Res.*, **107**, 2002; [8] S. Couch, PhD Thesis, 2002; [9] M. Piochi, G. Mastrolorenzo, L. Pappalardo, *B. Volcanol.*, **67**, 663-678, 2005.

Eu AND Ce STRUCTURAL ROLE IN SILICATE GLASSES BY XAS

M.R. Cicconi[1], G. Giuli[1], E. Paris[1], W. Ertel-Ingrisch[2], D.B. Dingwell[2]

[1]*Dipartimento di Scienze della Terra, Università di Camerino, Italy*
[2]*Department of Earth and Environmental Science, LMU München, Germany*
mariarita.cicconi@unicam.it

Accurate knowledge of europium (Eu) and cerium (Ce) structural role in silicate glasses/melts is of key importance in Earth sciences for a better understanding of the trace elements geochemical behaviour during the crystallization of a magma. However, despite their importance as a petrogenetic indicator, no studies have been published yet on their structural role in silicate glasses.

As part of a PhD project aimed at studying Eu and Ce structural role in a suite of silicate glasses with granitic and basaltic compositions, this study shows preliminary data about the valences and the local environment of europium and cerium in silicate glasses of different composition, all synthesized in air. Also, two samples were synthesised at very low oxygen fugacity (IW buffer). All the glasses studied in this work have been produced at the Earth and Environmental Sciences Department, LMU München (D).

The samples have been characterized by X-ray Absorption Spectroscopy (XAS) to obtain the oxidation states, coordination numbers, and the <Eu-O> and <Ce-O> bond distances.

XAS measurements have been performed in fluorescence mode at the ID26 beamline (ESRF, Grenoble, F) using a Si(311) double-crystal monochromator and a Ge multi-elements detector.

EXAFS data analysis has been performed by means of the GNXAS package, calculating a theoretical signal according to a model structure, which has been iteratively modified by adjusting bond distances and coordination numbers and by adding further contributions in the second and third coordination shells respectively.

Ce in the analyzed glasses, all synthesized in air, is mostly in the trivalent state, with a minor contribution from Ce^{4+}. Furthermore, preliminary EXAFS data analysis for Ce spectra indicates Ce-O distances and coordination number compatible with a trivalent Ce [1].

Small, but significant changes, in the shape of Eu L_{III} edge of the XANES spectra can be observed when passing from basaltic to granitic glass compositions and all the changes suggest the strong effect of bulk glass composition on the $Eu^{2+}/(Eu^{2+} + Eu^{3+})$ ratio.

Preliminary XANES data analysis of the Eu-bearing glasses of haplogranitic and basaltic composition, synthesised at very low oxygen fugacity, shows an obvious increase in the $Eu^{2+}/(Eu^{2+} + Eu^{3+})$ ratio notifying this change more pronounced for basaltic composition than for the granitic one. This indicate the strong effect of bulk composition on the Eu oxidation state and consequently on the Eu partition coefficient.

In a peralkaline granitic glass (NS2) synthesised in air, the EXAFS data analysis indicates the Eu to be bonded to six oxygen atoms (<Eu–O> = 2,26 Å ±0.01) arranged as the corners of a regular octahedron; therefore, the distances confirms the trivalent state of element. Any attempt to distort this geometry by allowing a distribution of different distances resulted in a worsening of the fit.

References. [1] P.L. Roulhac, G.J. Palenik, *Inorg. Chem.*, **42**, 118-121, 2003.

APPLICATION OF GEOCHEMICAL AND CHEMICAL MODELS TO WORD FREQUENCY DATA FROM WEB INFORMATION FLOW

G.I. Lampronti[1,2,3], M. Zandi[3], P. Brunori[3,4], R. Govoni[3], A. Bonazzi[3,5]

[1]*Dipartimento di Geoscienze, Università di Padova Italy*
[2]*Dipartimento di Scienze della Terra, Università di Firenze Italy*
[3]*Associazione BayesFor, Firenze, Italy*
[4]*Dipartimento di Scienze Economiche e Metodi Matematici, Università di Bari, Italy*
[5]*Istituto Nazionale di Geofisica e Vulcanologia, Università di Bologna, Italy*
info@bayesfor.eu

In the present work we applied geochemical concepts and the normalization method from Secondary Ion Mass Spectrometry (SIMS) to analyze word frequency data from web information sources.

Bayes-Swarm is a research project that aims at designing and building an engine to extract information from internet sources (news portals, newspapers and news agencies websites, blogs, etc.), mainly homepages and economical and political pages. Once a day every page passes through a working process whose main steps are: (i) formatting tags and punctuation removal, (ii) "empty words" (*i.e.*, conjunctions, articles and function words) removal, (iii) word roots extraction. Subsequently the number of appearances of every word ("word frequency") is saved and stored in a database, as well as the webpages analyzed by the software.

Fig. 1 shows the frequency curves of the empty word "che" and ("che"/"emptysum")*525, where "emptysum" = "per" + "con" + "del" + "della", all of which are empty words. The curves extend over 80 days. During the first 40 days, half of the web pages were manually excluded from the word count procedure - this explains the "che" frequency sudden increase around January 24th. The ratio "che"/"emptysum" is constant and independent on the artificially created word flow volume variation. This shows that empty words behave as conservative elements in the web information flow: ratios between empty words are constant and independent on time or word flow volume. Thus empty words can yield a computationally convenient way to normalize word frequency data. Some examples of how this normalization procedure works are shown and discussed.

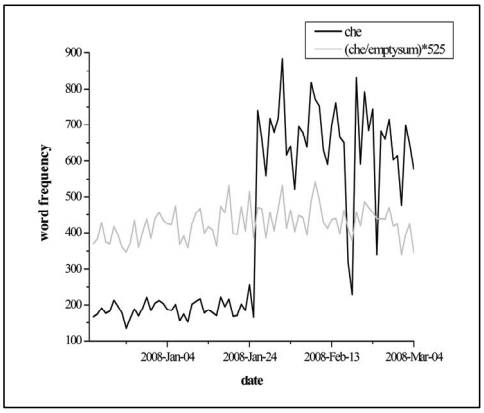

Figure 1

References. [1] P. Brunori, M. Zandi, R. Govoni A. Bonazzi, G.I. Lampronti, *Il Politico*, **217**, Gennaio-Aprile, 2008.

ARSENIC MOBILIZATION DRIVEN BY SEAWATER INTRUSION IN THE PECORA VALLEY (SOUTHERN TUSCANY, ITALY)

L. Livi[1], M. Benvenuti[1], P. Costagliola[1], F. Di Benedetto[1], M. Gasparon[2], P. Lattanzi[3], S. Vettori[1], O. Vaselli[1]

[1]*Dipartimento di Scienze della Terra, Università di Firenze, Italy*
[2]*Department of Earth Sciences, University of Queensland, Australia*
[3]*Dipartimento di Scienze della Terra, Università di Cagliari, Italy*
pilario.costagliola@unifi.it

Arsenic in soils and rocks may be distributed among various components in different physicochemical forms, and its mobility, bioavailability and toxicity are strongly dependent on speciation. The extractability of arsenic from polluted soil matrices by various salts has been evaluated by [1]. In particular, PO_4^{3-} has the highest capability in extracting As adsorbed onto silicates and Fe-oxides, although Cl^- and SO_4^{2-} may contribute significantly to the As mobilization. Accordingly, both anion- and ligand-exchange mechanisms play a major role in As mobilization.

An extensive As-anomaly (up to about 1000 ppm) has recently been assessed in the up to 60 m thick Quaternary alluvial sediments that fill the median portion of the Pecora River Valley (Southern Tuscany, Italy) [2]. Like many other coastal areas of Tuscany, excessive withdrawals of ground water from aquifers for domestic and industrial purposes have caused also in this area a severe seawater intrusion. The interaction between saline, Cl-rich waters and As-rich sediments could therefore promote scavenging and mobilization of As into groundwater [1]. As a consequence, experimental runs involving waters at different salinities and powdered < 2 mm sieved As-rich sediments have been performed to assess the extractability of As by Cl^-. Quartz, K-feldspars, phyllosilicates and minor amounts of Fe-oxyhydroxides are the main mineralogical phases, whereas SiO_2 (range 60.1-61.4 wt.%), Al_2O_3 (range 17.5-17.8 wt.%) and Fe_2O_3 (range 8.9-9.6 wt.%) are by far the main constituents of the sediments. Permeability, calculated on the basis of grain size distributions by the (empirical) Hazen formula, has low to moderate ($K = 9.61\ 10^{-6}$ to $1.96\ 10^{-8}$ m/s) values.

A sequential extraction procedure [3] has been carried out to evaluate the speciation of As in three sediment samples, whose As contents was between 473 to 737 ppm (aqua regia leaching). The analytical results indicate that most arsenic (about 60% on average) is bound to the residual fraction (presumably oxides with minor sulphides), whereas almost 20% is preferentially adsorbed onto well-crystallized Fe and Al oxyhydroxides. The amount of As adsorbed onto non-identified phases is systematically < 1% of total As.

Solutions with increasing chlorinity (0, 250, 2000, 18,500 ppm Cl) were used to leach the As-rich sediments, and different aliquots were collected and analyzed at defined time intervals. Arsenic contents in the leachates are relatively low (15-161 ppb As) even after prolonged interaction with the sediments. Nevertheless, these values exceed the maximum admissible concentrations established by the Italian low for drinkable water (10 ppb). Arsenic extraction capability by Cl^- in our experiments is lower compared to that reported in literature. This can be explained by considering that in the present study only minor amounts of As are non-specifically adsorbed, likely due to the long exposure of the Pecora Valley sediments to leaching phenomena by natural solutions.

References. [1] K.H. Goh, T.-T Lim, *Appl. Geochem.*, **20**, 229-239, 2005; [2] P. Costagliola, A. Donati, C. Rossim, C.A. Brebbia (Eds.), WIT Press Southampton, UK, 201-219, 2004; [3] W.W. Wenzel, N. Kirchbaumer, T. Prohaska, G. Stingeder, E. Lombi, D.C. Adriano, *Anal. Chim. Acta*, **436**, 309-323, 2001.

IRON OXIDATION STATE IN (Mg,Fe)O: CALIBRATION OF THE FLANK METHOD BY ELECTRON MICROPROBE AS A NEW TECHNIQUE FOR *in situ* DIAMOND INCLUSION STUDIES

M. Longo[1,2], C. McCammon[1]

[1]*Bayerisches Geoinstitut, University of Bayreuth, Germany*
[2]*Dipartimento di Scienze della Terra, Università di Roma La Sapienza, Italy*
Micaela.Longo@uni-bayreuth.de

The lower mantle, which represents more than half the Earth by volume, is constituted predominantly of $(Mg,Fe)(Si,Al)O_3$ perovskite and ferropericlase (Mg,Fe)O. Studying these phases is therefore critical to determining redox conditions and their consequences for mantle properties and dynamics. Studies have shown that the Fe^{3+} concentration in $(Mg,Fe)(Si,Al)O_3$ perovskite is essentially insensitive to oxygen fugacity; hence our attention is turned to (Mg,Fe)O. Our goal is to calibrate the "flank method" by electron microprobe using synthetic (Mg,Fe)O, and then apply the method to determine *in situ* $Fe^{3+}/\Sigma Fe$ in ferropericlase inclusions from lower mantle diamonds. Up to now a calibration of the flank method is available only for garnets [1].

A set of (Mg,Fe)O crystals over a wide range of composition (X_{Fe} = 2 to 60 at.%) and $Fe^{3+}/\Sigma Fe$ (1 to 12%) were synthesized at 11-15 GPa and 1800-2000°C in a multianvil apparatus. (Mg,Fe)O polycrystalline powders were reduced in a gas mixing furnace at 1300°C under controlled oxygen fugacity, then loaded and compressed up to 15 GPa. Subsequently the crystals were analyzed using the flank method by electron microprobe at 15 kV and 80 nA. Mössbauer spectroscopy was used to determine $Fe^{3+}/\Sigma Fe$. A linear relationship between ΣFe and Lβ/Lα measurements was observed, with a Lβ/Lα ratio ranging from 0.70 to 1.2 counts per second (cps). A positive correlation can also be observed for Lβ/Lα ratios as a function of Fe^{2+}, which is slightly non-linear.

Flank method measurements show an accuracy of 1σ which is comparable to Mössbauer data with the advantage of a spatial resolution limit of about 10 μm. Therefore, the flank method may be a promising technique for determining $Fe^{3+}/\Sigma Fe$ in natural ferropericlase from diamond inclusions.

Moreover, a set of (Mg,Fe)O single crystals synthesized by interdiffusion of Fe and Mg between single-crystal MgO and (Mg,Fe)O prereacted powders [2] was included in the flank method measurements. Fe compositional range is between 6-75 at.%, with a $Fe^{3+}/\Sigma Fe$ content of 1-13 at.%. For those samples, the presence of magnetite was detected by Mössbauer spectroscopy (0.2-11 vol.%) and confirmed by TEM analysis. Thus, it was possible to study the effect of a second phase on the Lβ/Lα. In fact, Lβ/Lα ratios seem to be affected by the chemical composition and data do not follow the trend line observed for pure (Mg,Fe)O.

Future work will focus on synthesis of further samples to extend the range of chemical composition from 0.2 to 50 at.%. This will help to understand the behavior of the trend line, and fitting procedures will be used to find the best data regression line for Fe^{2+} as a function of ΣFe and Lβ/Lα ratio, in preparation to apply the calibration to natural samples. Furthermore, (Mg,Fe)O with coexisting magnetite impurities will be characterized and investigated in order to better understanding exsolution phenomena.

References. [1] H. Höfer, G. Brey, *Am. Mineral.*, **92**, 873-885, 2007; [2] S. Jacobsen H.J. Reichmann, H.A. Spetzler, S.J. Mackwell, J.R. Smyth, R.J. Angel, C.A. McCammon, *J. Geophys. Res.*, **107**, B2, 2002.

FLUID-ROCK INTERACTION IN THE GEOTHERMAL RESERVOIR OF MT. AMIATA: AN EXPERIMENTAL APPROACH

A. Orlando[1], A.M. Conte[2], D. Borrini[3], C. Perinelli[4], A. Caprai[5], G. Ruggieri[1], C. Boschi[5], G. Gianelli[5]

[1]*C.N.R.-I.G.G., Firenze, Italy*
[2]*C.N.R.-I.G.G., Roma, Italy*
[3]*Dipartimento di Scienze della Terra, Università di Firenze, Italy*
[4] *Dipartimento di Scienze della Terra, Università di Pisa, Italy*
[5]*C.N.R.-I.G.G., Pisa, Italy*
orlando@igg,cnr.it

In order to tackle the problem of CO_2 emission into the atmosphere, and fulfill the Kyoto protocol, research efforts have recently been undertaken worldwide with special focus on carbon geo-sequestration. Different approaches are being used such as pilot-projects in which CO_2 is injected underground, laboratory experiments, numerical simulations and detailed investigations on minerals that could form as a result of CO_2 consuming reactions (*e.g.*, magnesite, dolomite, calcite, dawsonite).

It is in this context that we focused on the geothermal system of Mt. Amiata (Tuscany, Italy), which represents a natural analogue to CO_2 mineral sequestration, since self-generating CO_2-rich fluids interacted with surrounding rocks (dolostone, graphite-schist, calc-schist) precipitating CO_2 consuming minerals (*i.e.* carbonates).

In this stage of the research, attention is mainly focused on the processes and reactions responsible for the genesis of the CO_2-rich gas phase. Some preliminary laboratory experiments have therefore been designed to test if, at the P-T conditions of the deep reservoir, the interaction between a graphite-bearing rock and a coexisting fluid phase may produce a CO_2-rich gas, such those of the Mt. Amiata geothermal field. Thus, experimental runs were performed at 300°C and 0.35 MPa in an externally heated pressure vessel apparatus, on Au capsules containing a mixture of rock powder and aqueous solution. The rock selected for the runs is a metapelite (graphite-schist) sampled at a depth of 1115 m below the surface in the PC-26 well sited at Piancastagnaio and thought to be representative of the deep reservoir of the Mt. Amiata geothermal field. This rock is formed mainly by quartz, muscovite, chlorite and graphite, and the granulometric analysis proved it to be mainly (94 wt.%) composed by the silt and clay terms. In order to estimate the possible influence of salinity of the aqueous solutions on the fluid-rock interaction, two different salinities were used in the experiments: 0 and 0.05 molal (NaCl equivalent). The latter salinity is thought to be representative of the actual fluids present in the deep reservoir. Moreover, three different solid/liquid ratios (6, 1, 0.2) were chosen, in order to gain an insight on the influence of this parameter on the solid-liquid equilibria. Tentatively, in addition to the rock powder and liquid, some pre-fractured natural quartz crystals were loaded into the capsules to obtain synthetic fluid inclusions capable to provide an “in situ” fluid sampling.

At the end of experiments gas phase was analyzed by means of gas cromatography revealing a CO_2 predominance (> 80 vol%) ascribable to reactions involving graphite and/or organic carbon of the metapelite. Further analyses on the solid and liquid fractions of the charges are currently in progress in order to estimate the reactivity of the system metapelite-liquid and to constrain the complex reactions occurring during the experiments.

FIRST PRINCIPLES HF/DFT CALCULATIONS OF STRUCTURE AND COMPRESSIBILITY OF AN Al-DEFECTIVE SPINEL [$Mg_2Al_3\square O_8$]

M. Prencipe[1], R. Belousov[1], F. Nestola[2]

[1]*Dipartimento di Scienze Mineralogiche e Petrologiche, Università di Torino, Italy*
[2]*Dipartimento di Geoscienze, Università di Padova, Italy*
mauro.prencipe@unito.it

Spinel structure (*e.g.* $MgAl_2O_4$, γ-Mg_2SiO_4) is involved in several geodynamic models from low-crust to deep mantle and thus its thermodynamic properties can be used in interpreting several deep geological processes. However, recent investigations [1] demonstrated that non-stoichiometry can strongly influence its compressibility and such observation can provide new explanations in interpreting geophysical and seismological profiles.

A model for the Al-defective normal spinel structure has been created by eliminating one Al neutral atom, out of four, from the primitive cell of the (normal) ideal spinel $Mg_2Al_4O_8$, to get an ordered rhombohedral phase $Mg_2Al_3\square O_8$ having the $R\bar{3}m$ space group. The elimination of one Al atom creates three holes in the electronic band structure; such holes can be delocalized over the six symmetry equivalent oxygen atoms surrounding the vacant site, or can be localized over three oxygen atoms only, with a further reduction of the crystal symmetry to the $R3m$ space group. By using the CRYSTAL06 program [2], *ab initio* calculations were performed at the Unrestricted Hartree-Fock (UHF) and Density Funtional (DFT) levels; in the latter case, some mixing of the DFT exchange with the exact non-local HF exchange has been used, in the proportion 80% DFT - 20% HF (in a standard B3LYP Hamiltonian formulation) and 40% DFT - 60% HF (F60 Hamiltonian, [3]). Symmetry, electronic and geometrical structures appeared to strongly depend by the employed Hamiltonian and, in particular, by the percentage of HF exchange used in the formulation. In particular, B3LYP delocalized the three holes over six oxygen atoms, whereas in the UHF and F60 cases, complete localization over three atoms only was observed. Such exchange dependence of hole localization is in line with theoretical results previously obtained for a similar system [4].

EPR spectra of *V-centers* bearing spinels [5] suggest complete holes localization, similarly to what had been found in MgO [6], and thus the Hamiltonians to be preferred for the calculation should be those which are able to predict such behaviour; for this reason, the F60 Hamiltonian was chosen for the subsequent calculations of the structure at high pressures and of compressibility. Consistently with the experimental data so far obtained [1], our results indicate a strongly reduced compressibility of the defective phase with respect to the ideal one.

By using the F60 Hamiltonian only, a calculation of the compressibility of an ordered partial inverse spinel having an Al vacancy in a tetrahedron [$^t(Mg\square)^o(Al_3Mg)O_8$; s.g. $R3m$] has also been performed: such phase resulted to be slightly more stable than the (normal) one having the octahedral Al vacancy (though the stability order is reversed with respect to the stoichiometric phases), and its compressibility is the same as that calculated for the Al-defective normal phase.

References. [1] F. Nestola, J.R. Smyth, M. Parisatto, L. Secco, F. Princivalle, M. Bruno, M. Prencipe, A. Dal Negro, *Nature* (submitted); [2] R. Dovesi, V.R. Saunders, C. Roetti, R. Orlando, C.M. Zicovich-Wilson, F. Pascale, B. Civalleri, K. Doll, N.M. Harrison, I.J. Bush, Ph. D'Arco, M. Llunell, *Crystal User Manual*, 2006; [3] M. Prencipe, F. Nestola, *Phys. Chem. Minerals*, **32**, 471-479, 2005; [4] P. Baranek, G. Pinarello, C. Pisani, R. Dovesi, *Phys. Chem. Chem. Phys.*, **2,** 3893-3901, 2000; [5] A. Ibarra, F.J. López, M. Jiménez de Castro, *Phys. Rev. B*, **44**, 7256-7262, 1991; [6] B.H. Rose, L.E. Halliburton, *J. Phys. C. Solid State Phys.*, **7**, 3981-3987, 1974.

GEOMATERIALS

Session 7
Cultural Heritages

SHAFT-HOLED AXES FROM SLOVENIA AND NORTH WESTERN CROATIA: AN ARCHAEOMETRIC STUDY ON ARTEFACTS MANUFACTURED FROM DOLERITIC BASALTS

F. Bernardini[1], A. De Min[2], G. Demarchi[2], F. Princivalle[2], E. Montagnari Kokelj[1]

[1]*Dipartimento di Scienze dell'Antichità, Università di Trieste, Italy*
[2]*Dipartimento di Scienze della Terra, Università di Trieste, Italy*
bernardinifederico@hotmail.com

Among the Prehistoric stone axes, which represent a class of material common in the European Neolithic and Copper Age, the shaft-holed ones are generally manufactured using several raw materials (sedimentary, magmatic and metamorphic rock types) and usually testify to small-medium scale exchange systems. These notably differ from the long distance contacts proved by the circulation of some classes of axe blades as those made from HP metaophiolites having their origin in North Western Italy and found across Europe [1,2].

A group of Copper Age shaft-holed axes from *Caput Adriae* (North Eastern Italy, Central Western Slovenia and North Western Croatia), manufactured with variably recrystallized doleritic basalts, have been studied through petrographical observations and analysed (ICP-MS) for major and 54 trace elements. It is to notice that this is the first occurrence of this class of artefacts in the Northern Balkans.

Despite the slight recrystallization, the magmatic textures, as well as relicts of primary mineralogical phases (labradoritic-plagioclase, clinopyroxenes and opaque), are well preserved. Geochemical data suggest that the lithoid materials have been generated during a fore-arc or pre-arc tectonic setting and show chemical behaviours which identify them as high-Mg andesites and boninites [3].

A comparison of petrographical and geochemical data indicates the existence of a strong similitude with some lithotypes from the Banja Ophiolite Complex (Northernmost edge of the Central Dinaric Ophiolitic Belt; Croatia), here considered the most probable source area [4-6].

These results open a new perspective in the study of the exchange systems between the North Eastern Adriatic and the Balkans during the Copper Age. Considering all the available archaeometric data about the shaft-hole axes found in Northern Italy and *Caput Adriae* in comparison to the axe blades discovered in the same area, it emerges an utilization of different rock types whose source appears to be quite proximate to the finding sites. In the investigated area the shaft-holed axes are largely made from ophiolitic related rocks which are associated to copper deposits. Their provenance and distribution zones well correspond to areas that at least from the IV millennium BC function as important metallurgical districts.

References. [1] C. D'Amico, *Archaeometry*, **47**(2), 235-252, 2005; [2] P. Pétrequin, M. Errera, A.M. Pétrequin, P. Allard, *J. Eur. Archaeol.*, **9**, 7-30, 2007; [3] A.J. Crawford (ed.), *Boninites and related rocks*, University press, Cambridge, 1989; [4] B. Lugović, R. Altherr, I. Raczek, A.W. Hofmann, V. Majer, *Contrib. Mineral. Petrol.,* **106**, 201-216, 1991; [5] F. Trubelja, V. Marchig, K.P. Burgath, Ž. Vujović, *Geol. Croat.*, **48**, 49-66, 1995; [6] V. Garašić, M. Vrkljan, M. Vladimir, *Rudarsko geološko naftni zbornik*, **16**, 1-19, 2004.

CHEMICAL AND ISOTOPIC TRACERS IN COPPER DEPOSITS AND ANCIENT ARTEFACTS : A GEOCHEMICAL DATABASE OF COPPER MINES TO ESTABILISH THE PROVENANCE OF MATERIALS

I. Giunti[1], B. Giussani[2], G. Artioli[1], M. Marelli[2], S. Recchia[2], B. Baumgarten[3], P. Nimis[1], I. Angelini[1], P. Omenetto[1]

[1]*Dipartimento di Geoscienze, Università di Padova, Italy*
[2]*Dipartimento di Scienze Chimiche e Ambientali, Università dell'Insubria, Como, Italy*
[3]*Museo di Scienze Naturali dell'Alto Adige, Bolzano, Italy*
ilaria.giunti@unipd.it

The provenance of ore minerals used in prehistoric and historic times for copper smelting and extraction is one of the basic questions that archaeologists pose to modern analytical archaeometry [1]. To aid metal provenance studies, a database of fully characterized Alpine copper mineralization is being developed as the fundamental reference frame for metal extraction and diffusion in the past. In the early stages of the project, some of the most well known copper deposits in the Western Alps were selected and compared with very different minerogenetic deposits from the French Queiras (Saint Veran) and the Ligurian Apennines (Libiola, Monte Loreto).

The fully characterized samples were then analysed by ICP-QMS (inductively coupled plasma-quadrupolar mass spectrometry). Besides the commonly used Pb-isotope ratios ($^{204}Pb/^{206}Pb$, $^{207}Pb/^{206}Pb$, $^{208}Pb/^{206}Pb$), the abundances of about 60 minor and trace elements, including most transition metals and chalcophile elements, and the rare earths were measured in all samples. Furthermore, the feasibility of the routine for reliable measurement of the $^{65}Cu/^{63}Cu$ isotope ratio [2] and its eventual use as a possible ore tracer was tested.

Advanced strategies based on multivariate analysis were then used to discriminate the ore mineral provenance. Data were treated with the chemometric software "The Unscrambler Version 9.5" (CAMO AS, Trondheim, Norway). Data pre-treatment, PCA [3] and PLS-DA [4,5] models were performed as implemented in the software. The availability of such unprecedented and complete amount of data of Alpine copper deposits may also yield interesting information concerning the geochemical and minerogenetic interpretation of the deposits themselves. The discriminating power of the database was tentatively applied also to the provenancing of copper metal from the Agordo, Veneto area and the recently found prehistoric slags from Millan, Alto Adige.

Application of PCA and PLS-DA to the geochemical and isotopic data proved to be a very powerful tool to discriminate the ore source areas and geochemical character. The presented preliminary applications to copper metal samples seem to indicate that the analysis can be successfully performed on archaeometallurgical specimens for provenance and diffusion investigations. Future efforts are directed towards (1) completion of the mine database, (2) investigation of archaeological copper slags, (3) deeper interpretation of the geochemical tracers and their behaviour during the smelting processes.

References. [1] C. Renfrew , P. Bahn, *Archaeology: Theories, methods and practice*. Thames & Hudson, London, 2000; [2] E. Ciceri, C. Dossi, S. Recchia, I. Angelini, G. Artioli, F. Colpani, *Atti del XIX Congresso di Chimica Analitica*, Università degli Studi di Cagliari, 2005; [3] S. Wold, K. Esbensen, P. Geladi, *Chemometrics Intell. Lab. Syst.* 2, 37, 1987; [4] K. Esbensen, *Multivariate Data Analysis* - In Practice ISBN 82-993330-3-2, CAMO Process AS, Oslo, 5th Edition, 2002; [5] P. Geladi, B.R. Kowalski, *Anal. Chim. Ac.*, **185**, 1-17, 1986.

CRYSTAL STRUCTURE REFINEMENT OF SEPIOLITE/INDIGO PIGMENT USING SYNCHROTRON RADIATION

R. Giustetto, D. Levy, O. Wahyudi

Dipartimento di Scienze Mineralogiche e Petrologiche, Università di Torino, Italy
roberto.giustetto@unito.it

Sepiolite clay $Mg_8Si_{12}O_{30}(OH)_4(OH_2)_4 \cdot nH_2O$, together with palygorskite and kalifersite, belongs to the so-called palysepioles polysomatic series. Its structure can be described as a framework of zigzagged TOT ribbons, in which a discontinuous O layer is bonded to a continuous T one, whose apical oxygen atoms alternately point up and down (Fig. 1) [1].

The framework is crossed by *z*-axis elongated channels usually filled by weakly-bound zeolitic H_2O. Tightly-bound structural H_2O completes the cations coordinations at the borders of the O ribbons.

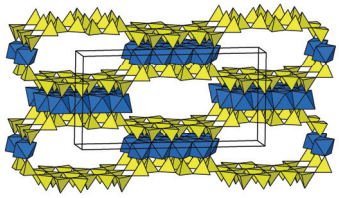

Fig. 1 - The crystal structure of sepiolite.

Although it is well known that palygorskite was used by the ancient Mayas to prepare their famous Maya Blue pigment, several archaeological specimens were found to contain sepiolite too [2]. By moderately heating (120-180°C) a clay-indigo mixture, a partial loss of the zeolitic water occurs allowing the consequent encapsulation of indigo inside the clay micropores. Dye molecules are kept *in situ* by H-bonds formed between their carbonyl groups and the clay structural water, responsible for the pigment stability. Following recent works, aimed at outlining the crystal structure of Maya Blue and the interaction between the guest indigo dye molecule and the host palygorskite framework [3,4], a research was planned in order to study the very same features when sepiolite is the host structure.

A blue pigment was obtained by mixing sepiolite and indigo (2 wt.%) and heating up to 190°C for 20 hours. Although similar in aspect to Maya Blue, such pigment showed a less remarkable stability (4-days attack with HNO_3 destroyed both the colour and the structure and a contextual NaOH attack slightly altered the structure not affecting the colour), presumably ascribable to the larger maximal effective channel width of sepiolite (10.6 Å) compared to palygorskite (6.4 Å).

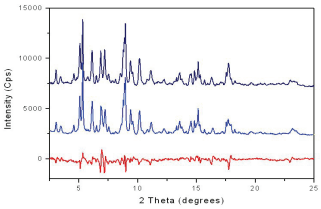

Fig. 2 - Synchrotron XRPD patterns of sepiolite (black), sepiolite+indigo (blue) and related difference (red).

The structural features of both sepiolite and sepiolite+indigo pigment were studied through Rietveld refinement, using GSAS [5], on XRPD patterns collected with synchrotron radiation (ESRF, ID31 beamline, Grènoble, France). Noteworthy differences were remarked between the observed intensities of the collected XRPD profiles, accounting for the indigo interaction with the clay framework (Fig. 2). The refinement of the pigment structure suggested that indigo – treated as a *rigid body* inside the clay channels, in competition with zeolitic water – shows an extremely disordered disposition, occupying only 1 out of 12 possible sites. The measured O…O distances between the indigo C=O and the clay structural water are compatible with the existence of H-bonds. The dye molecule slightly tilts from its ideal position on the (100) plane, presumably in order to favour the H-bond formation, thus inducing a partial loss of its planarity.

References. [1] G. Ferraris, E. Makovicky, S. Merlino, *Crystallography of Modular Materials*. IUCr/Oxford University Press, 2008; [2] C. Reyes-Valerio, *De Bonampak al Templo Mayor: el Azul Maya en Mesoamerica*. Siglo XXI Ed., 1993; [3] R. Giustetto, D. Levy, G. Chiari, *Eur. J. Mineral.*, **18**, 629-640, 2006 [4] R. Giustetto, F.L.I. Xamena, G. Ricchiardi, S. Bordiga, A. Damin, M. Chierotti, R. Gobetto, *J. Phys. Chem. B*, **109** (41), 19360-19368, 2005; [5] A.C. Larson, R.B. Von Dreele, *Los Alamos Nat. Lab. Rep. LAUR*, 86-748, 2007.

GOLD *TESSERAE* FROM THE PALEO-CHRISTIAN GLASS MOSAIC OF ST. PROSDOCIMUS (PADUA, ITALY): AN ARCHEOMETRIC STUDY

S. Tonietto[1], A. Silvestri[1], G. Molin[1], M. Brustolon[2], A. Zoleo[2]

[1]*Dipartimento di Geoscienze, Università di Padova, Italy*
[2]*Dipartimento di Scienze Chimiche,Università di Padova, Italy*
serena.tonietto@unipd.it

In 1958, during restoration of the paleo-Christian votive chapel of St. Prosdocimus (VI Century), inside the Basilica of St. Justine in Padua, many mosaic fragments and more than three thousand glass polychrome *tesserae* were found under the paved floor.

This study focuses both on loose *tesserae* with a gold thin metal layer and *tesserae* with transparent glass which had lost their metal layer and *cartelline* (about 1000 samples). In addition, about 60 *cartelline* were found without their supporting *tesserae*.

Eighty samples, selected among *tesserae* with gold layers, transparent *tesserae* and *cartelline* with colourless and pale-green glass, were analysed in order to define the chemical composition of the glass by means electron microprobe for major and minor elements and LA-ICP-MS for trace ones.

This is probably the first case that allows us to study so many glass *tesserae* from mosaics and to apply statistical analysis to these kinds of materials, in order to identify compositional groups and possible correspondence with historical glasses. Hierarchical cluster analysis was applied to all chemical data and three compositional groups were identified.

The first group of samples is the most numerous (about 70% of samples). Their chemical similarity to Roman glass [1,2] and the presence of antimony indicate that these *tesserae* were produced by using recycled Roman glass.

The second group is mainly composed by samples with pale-green glass. The elevated content of iron, magnesium, manganese and titanium allows the samples of this group to be compared with HITM glass recognized by Freestone in 1994 [3]. The glass of this group was produced in the VI century to realize the *tesserae* for the St. Prosdocimus mosaic.

The third group (that contains only 4% of samples) is composed by *tesserae* characterized by ash used as flux. Their chemical composition is similar to that of late Medieval glass [4] and they are ascribable to ancient restorations.

Trace analysis were realized in order to identify the provenience of the raw materials. The results confirm the deeper differentiation between glass groups due to the similar trend of trace elements. This supports the hypothesis that the *tesserae* of each group were realized using the same raw materials.

Some *tesserae* were analysed also by means of Electron Paramagnetic Resonance spectroscopy (EPR): strong Mn(II) and Fe(III) signals were detected. Differences in intensity and shape of the spectral profile were qualitatively related to the different Mn(II) and Fe(III) content. Currently, simulations are being performed to quantify Mn(II) and Fe(III) and to get some information useful to characterize the *tesserae*.

References. [1] D. Foy, M. Picon, M. Vichy, V. Thirion-Merle, In: Echanges et commerce du verre dans le monde antique, *Actes du colloque de l'Association Francaise pour l'Archeologie du Verre*, Aix en Provence et Marseille, 7-9 juin 2001 (D. Foy and M.D. Nenna eds.), Editions Monique Mergoil, Montagnac, 41-85, 2003; [2] C.M. Jackson, *Archaeometry*, **47**, 763-780, 2005; [3] I.C. Freestone, In: *Excavation at Carthage*, vol. II, the Circular Harbour, North Side (ed. H.R. Hurst), Oxford University Press for the British Academy, Oxford, 1994; [4] A. Silvestri, G. Molin, G. Salviulo, *Archaeometry*, **47**, 797-816, 2005.

ELEVENTH CENTURY BYZANTINE MOSAIC TESSERAE FROM THE GREEK MONASTERIES OF DAPHNI AND HOSIOS LOUKAS

R. Arletti[1], M. Vandini[2], C. Fiori[2], G. Vezzalini[1]

[1]*Dipartimento di Scienze della Terra, Università di Modena e Reggio Emilia, Modena, Italy*
[2]*Dipartimento di Storie e Metodi per la Conservazione dei Beni Culturali, Università di Bologna, Sede di Ravenna, Italy*
rossella.arletti@unimore.it

At the end of the first millennium AD several changes occurred in glass manufacturing processes. In this period the natron trade came to an end [1] and plant ashes began to be used as fluxing agent for the production of glass. Even if in the Mediterranean regions Na-rich coastal plant ashes were used, the levels of K_2O and MgO in the glass (usually below 1% in natron based glass) noticeably increased. As a consequence, the concentration of these two oxides is a common marker for the identification of the alkali source in glass.

The study of 11th century Byzantine mosaic tesserae represents a useful approach for understanding the changes in opaque glass production, since this glass was produced some time after the change in the fluxing agent.

Along with the changes recorded in the fluxing agent, other changes typically connected with the production of opaque glass accompanied the evolution of mosaic glass production, in particular changes in the materials used as opacifiers or colouring elements.

In this work fifty-one glass mosaic tesserae of well dated Byzantine wall mosaics from the Daphni and Hosios Loukas monasteries in Greece were analysed by Electron Microprobe and X-ray Powder Diffraction. The choice of the samples to be analyzed was performed on the basis of their colours: most of the colour shades present in the decorations were sampled and studied.

The tesserae used for the study could belong to the original decorations of the mosaics, but could also be reused tesserae belonging to previously existing mosaics or the results of restorations executed in subsequent times. This issue represents a crucial point in the investigation: before outlining the distinctive traits of Byzantine mosaic tesserae, it is fundamental to discriminate between the original tesserae and those from other periods.

The aims of this work are: i) to provide a chemical characterization of the mosaic tesserae from the two Greek monasteries; ii) to identify the groups of "original" tesserae for each mosaic; iii) to determine the origin of the opacifiers and colouring elements; iv) to compare the chemical data of the Daphni and Hosios Loukas mosaics in order to understand whether the glass from the two decorations could come from the same atelier.

On the basis of the chemical analyses, it has been possible to outline the distinctive traits of Byzantine Daphni and Hosios Loukas mosaic tesserae. For both the monasteries, the original mosaics were decorated with tesserae produced with plant ash based glass. The samples coming from Hosios Loukas decorations show a more homogenous composition respect to those coming from Daphni. The slight differences found in the amounts of Mg and Na between the two sample sets could indicate the use of different alkali sources.

References. [1] D. Whitehouse, *J. Glass Studies*, **44**, 193-196, 2002.

SIENESE "ARCHAIC" MAJOLICA: CHARACTERIZATION OF COATINGS BY ANALYTICAL ELECTRON TRANSMISSION MICROSCOPY

G. Giorgetti[1], C. Fortina[2], A. Santagostino Barbone[1], I. Turbanti Memmi[1]

[1]*Dipartimento di Scienze della Terra, Università di Siena, Italy*
[2]*Dipartimento di Scienze della Terra, Università di Pavia, Italy*
memmi@unisi.it

Three types of coated ceramics representative of Sienese "archaic" majolica have been studied by analytical electron-transmission microscopy (AEM-TEM) in order to characterize the mineralogy of glazes and enamels at the nanometer scale. Based on textural and mineralogical features of the coatings (both enamels and glazes), the ceramics can be grouped as follows: 1) post-firing wastes and 2) technological wastes were produced by the same coarser SiO_2-rich mixture, but the second group underwent higher firing temperatures; 3) wastes of uncertain classification were produced by a finer and lead-richer initial mixture [1].

Newly-formed minerals in enamels of groups 1 and 3 include Ca-Mg pyroxene, wollastonite, K-feldspar, cassiterite, and rare plagioclase. Newly-formed minerals in glazes include Ca-Mg pyroxenes, wollastonite, K-Pb feldspar, Fe-oxides. Newly-formed minerals in enamels of group 2 include Ca-Mg pyroxene, cristobalite, cassiterite. Glazes comprise Ca-plagioclase and Ca-rich pyroxene. TEM techniques allowed to better determine the mineralogy of coatings: the occurrence of Ca-Mg pyroxenes (previously defined as Ca-Mg silicates) and of K-Pb feldspars has been recognized by chemical analyses at the nanometer scale (AEM) and by structural determination of minerals through electron diffraction.

The high Pb content of glazes (30-60 wt.% PbO) joined to the high Al_2O_3/alkali ratio led to the crystallization of K-Pb feldspars; only K-feldspar crystallized in high-Pb enamels showing a lower Al_2O_3/alkali ratio. The poor conrol of firing temperature of technological wastes caused the formation of peculiar mineralogy and textures in both enamels and glazes.

References: [1] C. Fortina, A. Santagostino Barbone, I. Turbanti Memmi, *Archaeometry*, **47**, 535-555, 2008.

HISTORICAL GLASS FROM THE SVEVIAN CASTLE OF COSENZA ITALY: CHEMICAL CHARACTERIZATION BY LA-ICP-MS AND SEM-EDS METHODOLOGIES

M. Abate[1], D. Barca[1], G.M. Crisci[1], D. De Presbiteris[2]

[1]*Dipartimento di Scienze della Terra, Università della Calabria, Rende (CS), Italy*
[2]*Dipartimento di Archeologia e Storia delle Arti, Università della Calabria, Rende (CS), Italy*
d.barca@unical.it

This work shows the preliminary results obtained from a chemical characterization study of twenty-six samples of variously coloured historical glass fragments found during the cleaning activity around the external walls of the Svevian Castle of Cosenza (Calabria, Italy).

All the vitreous fragments are not stratigrafically correlated but, on the basis of the different associated ceramics classes, they can be chronologically attributed to a period of time between the 16th - 17th and 19th centuries.

The twenty-six vitreous finds are extremely fragmentary and very badly preserved; nevertheless two fragments of goblets, probably correlated to a fragment of stem, five variously coloured and shaped necks of bottle and two fragments of ink-pot are noteworthy.

All vitreous fragments, actually kept in the Civic Museum of Cosenza, were investigated by means of scanning electron microscopy with energy dispersive X-ray spectroscopy (SEM/EDS) for major elements and by applying the Laser Ablation inductively coupled plasma mass spectrometry (LA-ICP-MS) method to determine trace elements and REE concentrations.

The LA-ICP-MS method complements the electron microprobe analysis, typically measuring a great number of trace elements at a lower concentration range (10 ppb - 100 ppm) with very low detection limits; it allowed us to analyze a great number of trace and RE elements on very little vitreous fragments and to chemically characterize the historical artificial glass.

Before the analytical phase, a little portion (approximately 0.3 cm wide and 0.3 cm long with millimetric thickness) of each glass object was cut and, in order to remove any trace of soil, each shard was cleaned by ultrasound in Millipore water, embedded in a resin block and successively polished to expose the internal fresh portion.

All analysed samples are essentially composed of SiO_2 (61-73 wt.%), Na_2O (7.5-17 wt.%) and CaO (5.5-14.5 wt.%). Potassium and magnesium contents are extremely variable (MgO = 0.5-5.5 wt.% and K_2O = 0.3-9 wt.%) and allowed us to subdivide the fragments essentially into two groups and several fragments outlier. Also trace and RE elements show a very interesting correspondence between the colour of glass fragments and the geochemical features and confirm the clear distinction between the two large compositional groups. In particular, Pb and Cu contents allowed us to characterize the single outlier fragments and to individuate the fragments which belong to the same objects.

THE ARCHAEOMETALLURGICAL SITES OF MONTE STREGA AND MAGAZZINI AT ELBA ISLAND, TUSCANY, ITALY: THE FIRST STEPS OF THE *AITHALE* RESEARCH PROJECT

M. Benvenuti[1], G. Giuntoli[1], M. Naldini[1], F. Cambi[2], A. Corretti[3], S. Ducci[4], L. Chiarantini[1], P. Costagliola[1]

[1]*Dipartimento di Scienze della Terra, Università di Firenze, Italy*
[2]*Dipartimento di Archeologia e Storia delle Arti, Università di Siena, Italy*
[3]*Scuola Normale Superiore di Pisa, Laboratorio di Storia, Archeologia e Topografia del Mondo Antico, Università di Pisa, Italy*
[4]*Soprintendenza per i Beni Archeologici della Toscana, Firenze, Italy*
chiarantini@geo.unifi.it

In 2007 a comprehensive research programme concerning the exploitation and metallurgical processing of iron and base metal deposits of Elba Island and the whole Tuscan Archipelago has been started by archaeologists and geoscientists with long experience in this field of research. Scientific, archaeological and historical aspects of exploitation of iron and copper deposits of Elba Island are the main focus of the research project.

Several large heaps of metallurgical wastes, heavily damaged by slag recovery during the XX century, are spread mainly along the shorelines (Roman metalworking sites) and close to inner water tributaries (Medieval sites) of Elba Island. Preliminary archaeological field surveys have been carried out on two of these metalworking sites: the Roman site of Magazzini-La Chiusa (Portoferraio) and the Medieval site of Monte Strega (Rio Elba).

A selected number of metallurgical materials have been collected from both sites and analysed for macroscopic features (colour, streak, texture and porosity), mineralogical composition (OM and XRD) and chemical composition (XRF).

The original stratigraphy of the Magazzini site has been deeply upset by intense agricultural activities, and only a small area may be suitable for future archaeological excavations. Preliminary fieldwork and surface recognition led to the discovery of abundant fragments of tapped smelting slag, and of hematite-rich charge which show mineralogical and textural features typical of the Rio Albano- Rio Marina iron ores. Only fragmentary materials may be attributed to furnaces built with clayey materials; no fragments of tuyeres have been so far identified.

The Monte Strega metallurgical site is rather well preserved. Unlikely the Magazzini site, here the metallurgical debris is confined within small heaps discharged over a confined area (100 m^2). Total tonnage of slags may be estimated in the order of 1 tonne. Here both smelting and smithing activities have been apparently carried out in the same place. Most smelting slags are tapped slags and a relevant amount of fragments from clayey tuyeres have been found. Ore charge fragments seem to come, also in this case, from iron ores of northern Elba mines. Several fragments of plano-convex smithing slags have been found suggesting mostly activities of iron bloom deputation.

THE FAÇADE OF HUNGARIA HOTEL (LIDO, VENICE): SYSTEMATIC STUDY OF MATERIALS AND DECAY MECHANISM

R. Bertoncello[1,2], B. Dal Bianco[1,2], V. Donà[1], L. Nodari[1,2], G. Salviulo[3], U. Russo[1,2], S. Voltolina[1,2]

[1]*Dipartimento di Scienze Chimiche, Università di Padova, Italy*
[2]*INSTM, Unità Operativa di Padova, Italy*
[3]*Dipartimento di Geoscienze, Università di Padova, Italy*
gabriella.salviulo@unipd.it

The use of ceramic tiles as wall facing in historical buildings is quite uncommon in Italy, one of the most impressing artwork being the façade of the Hungaria Hotel, placed in Lido Venice. In fact the 800 m^2 of the façade are completely covered by several types of ceramic tiles, such as polychromes "basso-rilievo", allegories and floral motifs. This hotel was built in 1905, with the aim of making an "a la page" summer residence, and in the 1914 the façade was embellished by the ceramic tiles. The façade, in typical Liberty and Neo-Renaissance style, was realized by famous artist Luigi Fabris (Bassano del Grappa, 1883-1952). By 2006 the façade was almost completely damaged by environmental deterioration. Together with the restoration program, a diagnostic project was planned with the aim of a complete and detailed analysis of all the materials employed. By means of mineralogical, chemical and physical investigations it was possible to obtain a characterization not only of the materials (ceramics and mortars) and of the firing technology, but also of degradation process. All the materials were studied by a combination of spectroscopic (infrared spectroscopy, FT-IR, XPS), diffractometric (XRPD) techniques and scanning electron microscopy (SEM). Moreover a conservation monitoring program was projected and realized.

From the technological point of view, the tiles are painted kaolinitic earthenware entirely covered by a lead glaze. Their manufacturing has implicated many productive steps: a first firing, at high temperature, of the ceramic body, a pigments application by different artistic techniques, an application of a lead glaze on the entire tile, and finally a second firing at low temperature. As first observed in macroscopic scale and then by using optical and electronic microscopy, several deterioration processes involved the glaze, the mortar used to fix the tiles to the wall, and the ceramic body. These processes are mainly due to physico-chemical and biological factors, some of which are typical of the location of the hotel between the Adriatic sea and the Venice lagoon, that generate mechanical deteriorations as craquelers and tiles detachment. In the mortar - inner glaze interface, an alkali and lead leaching is present, and lead salts were detected inside the mortar grains. The lead leaking from the glaze can be due to the basic environment of the fresh mortar during the fixing of the tiles. The crystallization of the lead salts, together with the breaking of the outer glaze by thermal effect and the subsequent growth of biological species in the interface with the ceramic body, contributed to the detachment of entire tiles, or part of them, from the façade.

ARCHAEOMETRIC STUDY ON LOCAL PRODUCTIONS AND MEDITERRANEAN IMPORTS OF 13TH-16TH CENTURY GLAZED TILES (AZULEJOS) FOUND IN LIGURIA (NW ITALY)

R. Cabella[1], C. Capelli[1], A. García Porras[2], P. Ramagli[3], M.P. Riccardi[4]

[1]*Dip.Te.Ris., Università di Genova, Italy*
[2]*Departamento de Historia Medieval y CC. y TT. Historiográficas, Universidad de Granada, Spain*
[3]*Istituto Internazionale di Studi Liguri, Savona, Italy*
[4]*Dipartimento di Scienze della Terra, Università di Pavia, Italy*
cabella@dipteris.unige.it

The peculiar use of glazed tiles (azulejos) for the decoration of floors and walls of religious or other important buildings started in Liguria (particularly in Genoa and Savona) in the 14th century, under the influence of the Islamic taste. Until the 16th century, with the beginning of the local production of polichrome Renaissance tiles, the majority of the azulejos were characterised by monochrome white, green, blue, yellow or black glazes and homogeneous shapes and dimensions.

These simple typological characteristics favoured the traditional hypothesis that all the 14th-16th century monochrome tiles were of local (Savona) production. However, recent archaeometric investigations based on thin section analyses and the comparative study with reference materials [1,2] found out that all the earlier tiles were imported from Spain (Malaga) or, in one context (San Fruttuoso di Camogli Abbey), probably from the Maghreb-Sicily area, whereas the Savona production started only at the end of the 14th century.

While the San Fruttuoso tiles are distinguished by typical Islamic geometric shapes (8-pointed star, cross), the monochrome products of Savona exactly copy those of Malaga in shape (squared), dimensions and colours, and are not distinguishable from them with the naked eye.

This study was aimed at better characterising each production from a compositional and technical point of view and finding out its distinctive features. Thin section analyses have been carried out on an extended number of tiles, while representative samples have been investigated by XRD (ceramic body) and SEM-EDS (body and glaze).

The three productions can be distinguished from each other by the body inclusions: Savona fabrics are characterised by gneiss and amphibolite fragments attributable to the local Palaeozoic basement, associated with both siliceous and calcareous microfossils derived from Pliocene marine clays; Malaga fabrics are rich in phyllite and quartz-micaschists fragments related to the Baetic Cordillera, associated with only calcareous microfossils; the San Fruttuoso group is characterised only by sedimentary inclusions. There is the textural evidence that both Savona and Malaga fabrics result from the mixing of Ca-rich marine and Fe-rich alluvial clays.

In terms of chemical composition (by SEM-EDS), Savona pastes are distinguishable by higher Mg and Na values.

SEM-EDS analyses of glazes showed in all cases a Pb, Si-rich composition, with subordinate alkali, Ca, and Al contents. The compositional range is relatively wide and the productions cannot be clearly differenciated from each other. Fe, Cu, Mn and Co are responsible for the yellow, green, black and blue colours respectively. White, green and blue glazes are tin-opacified, while yellow and black glazes are transparent. Yellow Savona tiles are characterised by a white slip layer.

References. [1] C. Capelli, A. Gardini, P. Ramagli, In *Atti del III Congresso di Archeologia Medievale (Salerno 2003)*, R. Fiorillo, P. Peduto (eds), 649-658, 2003; [2] C. Capelli, A. Garcia Porras, P. Ramagli, In *Arqueometría y Arqueología Medieval*, R. Carta (ed.), Colección de Arqueología y Patrimonio, 117-169, 2005.

ARCHAEOMETRIC ANALYSES OF ISLAMIC GLAZED CERAMICS FROM FUSTAT (CAIRO, EGYPT)

R. Cabella[1], C. Capelli[1], S.Y. Waksman[2], R.-P. Gayraud[3], L. Tilliard[4], J.-C. Treglia[3], L. Vallauri[3]

[1]*Dip.Te.Ris., Università di Genova, Italy*
[2]*MOM-CNRS, Lyon, France*
[3]*LAMM-CNRS, Aix-en-Provence, France*
[4]*Musée National de Ceramique de Sevres, France*
cabella@dipteris.unige.it

Several samples of Islamic (10^{th}-15^{th} C.) glazed ceramics found in the excavations of Fustat (Cairo, Egypt) and preserved in the Fine Arts Museum of Lyon (France) have been analysed by WD-XRF, optical microscopy, and SEM-EDS. The archaeometric investigations have been carried out on pastes and glazes of decorated ceramics (Fustat Fatimid Sgraffito, Lustreware, and Painted ware), whose provenance from Fustat is considered probable for archaeological/typological reasons, and of kiln wasters of monochrome deep blue or turquoise glazed wares. The study was aimed at characterising the Fustat production from a compositional and technical point of view and obtaining one or several reference group(s) for provenance studies on the consumption sites. This point is particularly important as the products of Fustat, the artisanal district of Cairo, were widely exported in a large part of the Mediterranean area during the Middle Ages.

Several categories of pastes were distinguished by XRF: different kind of synthetic pastes (with dominant Si, but varying amounts of Na, Ca and Al), high-Ca, very high-Ca and kaolinitic clayey pastes. Most of the samples however belong to two categories of pastes only: siliceous (Group 1, including wasters) and calcareous (Group 2).

Thin section and SEM-EDS analyses showed that Group 1 pastes are characterised by ground quartz cemented by alkaline- and alkaline-earth-based glass fragments (stonepaste or fritware), while Group 2 fabrics are composed of a calcareous clay matrix ± Fe-oxides and numerous fine-grained aplastic inclusions: basaltic and acid metamorphic rock fragments, quartz, feldspar, mica, and several heavy mineral grains.

Non-modified raw materials (probably the Nile sediments) were probably used for Group 2.

Group 1 pastes characterise the monochrome wares, the Fustat Fatimid Sgraffito and a part of the Lustreware samples. Group 2 pastes characterise the Painted ware and a part of the Lustreware samples.

Two homogeneous chemical groups have been found out by SEM-EDS analyses of glazes: alkali glazes and Pb-alkali glazes, characterising the monochrome wares and the remaining types respectively. The high Na values (12-16 and up to 8 of Na_2O wt.% respectively) point to the use of natron as flux in most cases. Relics of quartz and feldspar grains, related to the use of impure alluvial silicate sands as raw materials, are frequent in the glazes of the Painted ware and Lustreware samples with natural clay body.

As for the colouring agents, Fe is responsible for the yellow, Cu (associated with alkali) for the turquoise, and Co (+ Cu, Fe, and Mn) for the deep blue colours. Only Lustreware and Painted ware glazes are opacified with SnO_2 (cassiterite).

THE "MAESTÀ" OF AMBROGIO LORENZETTI IN ST. AUGUSTINE'S CHURCH IN SIENA (ITALY): PAINTING MATERIALS CHARACTERISATION AND EVALUATION OF THE STATE OF CONSERVATION

D. Damiani, I. Memmi Turbanti

Dipartimento di Scienze della Terra, Università di Siena, Italy
memmi@unisi.it

The fresco paintings by Ambrogio Lorenzetti in St. Augustine's Church were discovered by chance only in the 1944, behind a sixteenth-century marble altar. This study aims to acquire detailed information about pigments and painting techniques and to evaluate the alteration processes, in order to provide technical support for restoration.

Microfragments of the painting layers have been studied by means of optical and electron (SEM-EDS) microscopy and micro-Raman spectroscopy.

Twelve pigments have been identified: yellow and red ochre, burnt sienna, cinnabar, red lead, azurite, terre-verte, verdigris, chalk, lead white and carbon black. Their combination (overlapping layers and pigment mixture) produced a wider range of chromatic tonalities. The colours were applied by the classic fresco technique and by two dry techniques: lime painting and tempera.

The majority of the pigments appear chemically unaltered; only azurite shows limited chromatic alteration phenomena due to malachite (green), paratacamite (green) and tenorite (black) formation.

The overall state of conservation of the wall painting is critical. Physico-chemical processes produced strong salt crystallisation phenomena; sulphates, oxalates, nitrates and chlorides have been detected. The whitening and the darkening of the wall painting surface are mainly due to gypsum and oxalates (weddellite and whewellite) formation, respectively. Finally, lacunae, detachments and pulverizations of the paint film are due both to salt crystallisations and to intrinsic features of the painting techniques.

GLASS SLABS OF THE FARAGOLA (SOUTHERN ITALY) *SECTILIA* PANELS: X-RAY ABSORPTION SPECTROSCOPY (XAS) INVESTIGATION AT THE Cu-K, Fe-K AND Mn-K EDGES

E. Gliozzo[1], F. D'Acapito[2], A. Santagostino Barbone[1], M. Turchiano[3], I. Turbanti Memmi[1], G. Volpe[3]

[1]*Dipartimento di Scienze della Terra, Università di Siena, Italy*
[2]*European Synchrotron Radiation Facility (ESRF), BM08-GILDA, Grenoble, France*
[3]*Dipartimento di Scienze Umane, Università di Foggia, Italy*
memmi@unisi.it

At the foot of the hill presently occupied by the town of Ascoli Satriano (Foggia, Italy), the archaeological excavations at Faragola brought to light a huge and long-lasting rural settlement.

In the complex of the Late Antique *villa*, the *sectilia* panels were found along the central axis of the *cenatio*. The panels are made of red, orange, yellow, green, marbled, blue and blackish glass slabs, cut following a precise decorative motif. SEM-EDS, EMP, ICP-MS, ICP-OES were applied to the study of the slabs, in order to investigate production technology and formulate provenance hypotheses.

Moreover, an X-ray Absorption Spectroscopy (XAS) investigation (ESRF synchrotron, GILDA beamline) were carried out at the Cu-K, Fe-K and Mn-K edges in order to determine the local structure and valence states of the metals.

For what concern the technological issues, results indicate that all slabs were made by mixing a siliceous sand with natron, with the sole exception of red slabs which seem to testify the use of coastal plant ashes as a source of alkali. No indications concerning the introduction of stabilisers are recoverable. Red, light orange and blackish slabs show higher CaO contents that could suggest the voluntary addiction of this component to the glass batch.

Red, orange and yellow slabs are coloured by metallic copper, cuprite and Pb-antimonates respectively. Copper is present predominantly as Cu^{+} as revealed by XAS. However, being this ion optically silent, it is probable that minor amounts of Cu^{2+} and Pb antimonates are responsible for the green opaque colours. Dark green and yellow portions of marbled slab are perfectly comparable to the slabs of the same colours. Cu^{2+} together with Ca antimonates were used to produce light blue slabs, while Co and Mn^{2+} occur in dark blue samples. Fe is found in the 3^{+} valence state in tetrahedral geometry in green and blue *tesserae.* The blackish slabs are coloured by octahedral Fe^{2+}, and Mn^{2+}. The blackish samples show Mn-Mn coordination absent in the blue ones.

As regards the provenance, obtained results do not allow us to attribute the panels to specific eastern, local or western workshops. The comparison between the chemical composition of Faragola samples and several glass reference groups only suggests a close similarity with numerous Roman and Early Medieval glass produced with Belus sand and found in the West.

CHROMATIC ANALYSES ON SEBASTIANO GALEOTTI FRESCOES OF PALAZZO SANVITALE, PARMA

S. Meli[1], C. Pezzani[2], G. Michiara[2]

[1]*Dipartimento di Scienze della Terra, Università di Parma, Italy*
[2]*GEODE s.c.r.l., Parma, Italy*
sandrom@unipr.it

Palazzo Sanvitale is located in the centre of the town of Parma; it was built up during the XXVII century, and in the XVIII century it was frescoed by Sebastiano Galeotti, an artist of that period. He decorated the ceilings of some rooms (*Allegoria delle nozze* and *Banchetto degli dei*). The restoration of his decorative cycle has been coupled with an analytical study on small slides of chromatic films. Our purpose was to ascertain the employed stuff (*i.e.*, pigments and binding elements) and the techniques (*i.e.*, fresco, lime painting, distemper) used by Sebastiano Galeotti for the decorations, and to give hints for the restoration of the paintings (*e.g.*, characterize and mapping of their degradation and suggesting some techniques of intervention). We made the analytical investigations mainly on stratigraphic cross sections, employing the following techniques: reflected light optical microscope, SEM-EDS and FT-IR spectrophotometry. We found that Galeotti employed mainly pigments made of earths for the yellow hues and of green earths for the green hues. Then, we focussed our analyses on blue pigments. We hypothesize that the realization of the decorations was diachronous, as the analyses highlighted the employment of two different blue synthetic pigments: lime with *smaltino* and *blu di Prussia*, $Fe_4[Fe(CN)_6]_3$, whose use began during the second half of the XIX century. *Blu di Prussia* is not stable in frescoes, because such an alkaline environment tends to shift its colour to brown. The "smaltino" has an artificial origin, too (potassic glass with cobalt, obtained mixing cobaltite and smaltite, heated to obtain oxides; this stuff was mixed again with silica and melted, to obtain a blue glass which was crushed to obtain the pigment), and it has been used since the second half of the XV century. It was used until the XIX century, when it was replaced by cobalt-blue. Other yellow/orange hues were made employing also lead pigments (red lead). SEM images showed us that also organic films have been employed to complete some decorative drawings. FT-IR spectrophotometry confirmed that the distemper technique was somewhere employed: animal glue was used as binding elements. So, the chromatic pigments were realized using both natural (earths, green earths) and artificial (*smaltino*, *blu di Prussia*, red lead) stuff. Presently, the lime paintings do not show degradation processes, whereas distemper decorations, probably due to the high content of binding elements, show that they underwent detachments and lifting.

AN ANALYTICAL NON-DESTRUCTIVE STUDY OF THE "RUGGERO II" VOTIVE CROWN (S. NICHOLAS BASILICA, BARI, ITALY)

A. Monno, J.M. N'Saka, M. Santigliano, E. Scandale, G. Tempesta

Dipartimento Geomineralogico, Università di Bari, Italy
a.monno@geomin.uniba.it

The Ruggero II votive crown, the most ancient art object of the Saint Nicholas treasure, is held in the Basilica dedicated to the Saint in Bari. The manufacture locates the work as originating from Limoges, at the end of the 12th century. It is made of a copper alloy, adorned by champlevé enamels, glass stones and gemstones and it has a diameter of 26.5 cm. A subtle decoration engraved with foliage motifs characterize the outer face, decorated at intervals by twelve mountings each bearing gemstones and by three overlaying plaques in aedicule on which, with the champlevé enamelling technique, three angelic figures are found. The faces of the angels are applied with a characteristic relief technique, which locates the work as originating from Limoges between 1180 and 1190. The stereomicroscope observations, the μ-Raman and X-Ray Fluorescence analyses performed on the seven gems that at present adorn the votive crown, allows to establish that only one is a natural gemstone, a quartz amethyst, whereas the other six are glass stones of different colours and compositions. The glass stones show the characteristic elongated and/or spherical internal gas inclusions while the amethyst is characterized by traces of iron oxide, partially healed fractures and small crystalline colourless inclusions. The analyses performed on different points of the metal parts of the crown reveal the copper alloy composition and allow to identify traces of gold, thus demonstrating that the crown was originally gold plated, a typical technique used by French craftsmanship.

The alterations of the metal, visible inside the incisions and on contact of the aedicule plaques to the crown, are made of green microcrystalline powders. The EDS analyses of the crystalline phases reveal the presence of copper chlorides and copper sulphides. The former are consequence of the exposition of the object to a sea aerosol micro-clime; the latter are the classical alterations of copper in presence of urban air pollution, that well match with the location of the Basilica.

The characterization of the enamels colour has been performed by means of the VIS spectrophotometer. The spot size of the instrument allows the measurement only on a surface of enamel bigger than three millimetres and this condition limits the possible observations only to the blue enamel.

The results of the study performed on the Votive Crown give new and interesting elements useful to the historical and artistic reconstruction related to the historical period of the handicraft, that is actually going on.

ARCHAEOMETRIC INVESTIGATIONS ON WALL PAINTINGS FROM THE HYPOGEUM OF S. MARCO (FASANO-BRINDISI, SOUTHERN ITALY)

D. Pinto[1,2], R. Laviano[1,2], V. Bianchi[3]

[1]*Dipartimento Geomineralogico, Università di Bari, Italy*
[2]*Centro Interdip. Lab. di Ricerca per la Diagnostica dei Beni Culturali, Università di Bari, Italy*
[3]*Docente di Archeologia, Laurea in Scienze e Tecnologie per la Diagnostica e la Conservazione dei Beni Culturali, Università di Bari, Italy*
d.pinto@geomin.uniba.it

In the Apulia Region the development of the rupestrian settlements, attested already in the Roman age (an example is the site ad Speluncas, Torre Santa Sabina - Brindisi, South Italy), has been one of the more rooted and wider of the entire Mediterranean area. It is possible to assert that, in this territory, a sort of 'rupestrian Civilization' has developed, through all the medieval age. Proof of this is to be found in the large number, widespread diffusion and grandeur of rupestrian settlements, as well as in the abundance and quality of this exquisite cultural heritage formed by holy architecture and wall paintings hosted in many rupestrian churches or basilica or simple prayer grottoes. There are many frescoes of different pictorial cycles, painted from the IX to the XVI century, which can be considered masterpieces of European medieval art. Even though the Apulian rupestrian sites represent a unique cultural and historical heritage all over the world, they are almost unknown even today and some of them have been inhabited up to few decades ago. Moreover, this important heritage is nowadays subject to a severe deterioration due to chemical, physical, mechanical, biological and human causes, often interrelated to each others.

The present study deals with the archaeometric study of wall paintings from the rupestrian hypogeum of S. Marco, in the territory of Fasano (Brindisi, South Italy). The study is focused basically on two aspects: a) identification of pigments and painting techniques aiming to relate and compare the results obtained to those attained for other sites in the same territory; b) evaluation of deterioration forms and state of conservation of wall paintings finalized to the restoration and conservation of the site.

Analysis of microfragments in thin cross-sections by means of a polarising microscope (MO) equipped for observation in transmitted and reflected light allowed the characterization of plasters and paint layers. XRD and SEM-EDS techniques allowed the identification of pigments and the determination of the main types of alterations affecting the wall paintings. The supporting plaster, lying directly on the calcarenitic stone, are characterized by an aggregates consisting of calcite grains (about 15% of the total volume) and subordinate amounts of quartz, fossils and ferrous aggregates. The binder is calcitic, with microcrystalline texture. The identified pigments are red and yellow ochre, carbon black, often combined as overlapping layers in the paint film and/or admixed within the same layer in order to produce a wider range of chromatic tonalities. MO analysis of microstratigraphies shows that the thin pictorial layer (40-200 μm thick) of lime and pigment adapt itself to the texture of the plaster, thus suggesting that pigments were spread on the plaster while wet, such as in the *fresco* or *lime fresco* techniques. The pictorial cycle of the S. Marco hypogeum appears seriously damaged by physico-chemical and biological processes, as well as by the human action. As a matter of fact, a number of paintings have been totally removed or occulted by recent structures, whereas the most of paintings are covered by a several thin layers of lime films, which are related to the recent usage of the hypogeum as shelter for animals. The extensive deterioration of the surfaces is also due to the widespread occurrence of salts such as sulphates, chlorides and nitrates (mostly gypsym, sylvite and niter) which are present either as efflorescence or sub-efflorescence, as well as to the presence of biological patinas.

MICRO-ANALYTICAL COMPARATIVE INVESTIGATION OF LATE ROMAN-PROTO BYZANTINE AGE GLASSES FROM SICILY

S. Quartieri[1], M. Triscari[1], C. Giacobbe[1], G. Sabatino[1], U. Spigo[2]

[1]*Dipartimento di Scienze della Terra, Università di Messina, Italy*
[2]*Soprintendenza ai BB.CC.AA., Serv. Beni Archeologici, Catania, Italy*
simona.quartieri@unimore.it

The glass samples analyzed in this work were recovered from the Catania Roman amphitheatre, which lies on a pre-existing republican and proto-imperial residential suburb located at the northern limit of that town. From the "X fornice" evidences of a small workshop for glass fusion and production were detected. Abundant and widespread glass fragments, mostly discarded production, were found. It was possible to recognize different types of fragments: glass from daily use objects, unshaped blocks of raw glass and, finally, fusion drops. This area was dated - based on recovered ceramic finds - to late imperial and proto-byzantine age (between the end of IV cent. A.D. and the VII cent. A.D.)

The glass finds were firstly studied by optical microscopy, focusing the attention on the diffuse alterations. Then a morphological and micro-analytical study by SEM+EDX allowed the observation of lamellar alteration bands characterized by a systematic lack of Na and by a varying Mn concentration. Major elements were analyzed by EMPA, which showed that all glasses are "silica-soda-lime" (natron based) [1] and are comprised in the European Roman and Levantine I fields of the CaO *vs*. Al_2O_3 classificative diagram [2,3]. Mn, Fe and Ti contents of Catania glasses are spread over a wide compositional range - going from "normal" to HIMT glasses [4] - hence it was not possible to group the samples in two distinct classes, as made for analogues finds coming from the site of Ganzirri (close to Messina) [5-8].

Catania fragments were also examined by LA-ICP-MS, to quantify minor and trace elements. This kind of analysis, in fact, was recently proved to be very effective in classifying HIMT glass production. The spider diagrams show, in general, a larger variability with respect to Ganzirri samples, and in particular for Zr, Hf, Cr, V and Sc. A first hypothesis to justify this chemical heterogeneity is that Catania glassware melted recycled glass with both HIMT and normal composition. This hypothesis would be confirmed by the intermediary chemical composition of the unshaped raw blocks. In the next future, Catania glasses will be compared with other samples of the same historical period and different provenience.

References. [1] C. Lilyquist, R.H. Brill, *Studies in ancient Egyptian glass*, Metropolitan Museum of Art, New York, 1995; [2] I.C. Freestone, Y. Gorin-Rosen, M.J. Hughes, *Primary glass from Israel and the production of glass in late antiquity and the early Islamic period*, In: La route du verre, M.-D. Nenna (ed.), Travaux de la Maison de l'Orient Méditerranéen, **33**, 65-83, 2000; [3] E.V. Sayre, R.W. Smith, Science, **133**, 1824-1826 1961; [4] I.C. Freestone, *Chemical analysis of "raw" glass fragments*, In: H.R Hurst ed., Excavation of Chartage, Vol II, The Circular Harbour, North Side, Oxford Univ. Press, pp. 290, 1994; [5] G. Sabatino, R. Arletti, S. Quartieri, G. Tigano, M. Triscari, G. Vezzalini, C. Giacobbe, *Atti Convegno FIST*, Epitome, I, 111, 2005; [6] C. Giacobbe, *Studi chimici e spettroscopici su vetri di interesse archeologico dal sito di Ganzirri (Me)*, Bachelor Thesis, 2006; [7] G. Sabatino, R. Arletti, M.P. Mastelloni, S. Quartieri, M. Triscari, M.G. Vezzalini, *Atti Conv. Naz. F.I.S.T. Rimini*, Epitome, **2**, 339-340, 2007; [8] R. Arletti, S. Quartieri, G. Sabatino, G. Tigano M. Triscari, G. Vezzalini, C. Giacobbe, in press, 2008.

APPLICATION OF HYPERSPECTRAL ANALYSIS TO CULTURAL HERITAGE: A NEW EVALUATION APPROACH TO THE DETERIORATION STATUS OF HYSTORICAL BUILDINGS

S. Vettori[1], M. Benvenuti[1], M. Camaiti[2], L. Chiarantini[3], P. Costagliola[1], S. Moretti[1], E. Pecchioni[1]

[1]*Dipartimento di Scienze della Terra, Università di Firenze, Italy*
[2]*ICVBC, CNR, Firenze, Italy*
[3]*Galileo Avionica S.p.A., Finmeccanica Company, Italy*
silvia.vettori@unifi.it

The effects of atmospheric pollution are the main factors responsible for the accelerating damage observed on monuments and historic buildings located in urban areas and industrial sites. Carbonate matrices exposed to atmospheric pollution are often strongly weathered and may form gypsum patinae and/or "black crusts", which represent an aesthetic, structural and surface damage of marbles and, more in general, carbonate surfaces.

The present study intends to verify whether instruments routinely used for remote sensing may be successfully applied to evaluate and characterize the deterioration status of historic monuments and buildings by mapping the distribution of gypsum, either associated with "black crusts" or present in other materials like mortar, plaster, etc. Given the distinctive spectral features of minerals and rocks, qualitative and quantitative measurements of the mineral composition in complex matrices can be obtained by airborne hyperspectral imaging. Major advantages of a such technique include its non-destructive nature and the capability of producing large areal maps at relatively low costs.

We employed the Galileo Avionica Multisensor Hyperspectral System (SIM-GA) to detect the weathered progress on facades of historical buildings. SIM-GA consists of two electro-optical heads. The first one operates in the VNIR region (0.4-1.0 microns) providing 512 spectral channels with a spectral sampling of 1.2 nm; the second head operates in the SWIR bands (1.0-2.5 microns) providing 256 spectral channels with a spectral sampling of 6.3 nm. The Instantaneous Field of View (IFOV), which determines the pixel size, is 0.7 mrad in the VNIR range and 1.3 mrad in the SWIR bands, whereas the Field Of View (FOV), which determines the swath wide, is 40° in the VNIR and 24° in the SWIR. The collected signals are digitalised respectively at 12 bit and 14 bit in the VNIR and SWIR ranges. A set of reflectance measurements were performed using a portable hyperspectral device (ASD-FieldSpec FR Pro) in the 350-2500 nm spectral range on small areas (1-4 cm in diameter), for a feasibility check of such application as well as for calibration and validation reference points in the SIM-GA field of view.

The Santa Maria Novella church in Florence has been chosen as a case study. In particular, we have investigated the marble sepulchral arches ("Avelli") aside the church facade. Preliminary spot analyses were made in different points of the "Avelli": results are encouraging, showing that the hyperspectral instrument is potentially capable of detecting gypsum contents in "complex" natural mixtures as well. We performed two sampling campaigns on October 2007 and May 2008 using SIM-GA placed at a distance of about 10 m from "Avelli" with a pixel size of about 0.7 cm in the VNIR and about 1.3 cm in the SWIR.

Data processing and calibration have been already accomplished, whereas the selection of the most suitable algorithm for the identification and estimation of gypsum abundance on the "Avelli" facade from spectral results is still in progress. We plan to compare different methods, used in literature (SAM, SFF, UNMIX, PCA, etc.) to identify the best procedure in relation to our case study and to obtain the abundances of the component(s) of interest. The validation of the map will be achieved by in situ analysis performed portable devices (*e.g.* XRF).

GEOMATERIALS

Session 8
Geomaterials at large-scale facilities

"NANO REACTORS" UNDER HIGH PRESSURE: THE INFLUENCE OF THE FRAMEWORK/EXTRAFRAMEWORK COMPOSITION IN CHA TOPOLOGY

L. Leardini[1,2], A. Martucci[1], E. Mazzucato[2], S. Quartieri[2], G. Vezzalini[3]

[1]*Dipartimento di Scienze della Terra, Sezione di Mineralogia, Petrografia e Geofisica, Università di Ferrara, Italy*
[2]*Dipartimento di Scienze della Terra, Università di Messina, Italy*
[3]*Dipartimento di Scienze della Terra, Università di Modena, Italy*
lrdlra@unife.it

The H*P* behaviour of a series of microporous materials with chabazite framework topology (CHA), largely applied as heterogeneous catalysts and characterized by a high thermal stability, was investigated by means of *in situ* synchrotron X-ray powder diffraction, with the aim to understand the role of the framework/extraframework content on the *P*-induced deformation mechanisms. The following phases were selected for this purpose:
a) natural chabazite (Vallerano, Italy): $(K_{1.36}Ca_{1.04}Na_{0.28}Sr_{0.4}Ba_{0.06}Mg_{0.02})[Si_{7.17}Al_{4.87}O_{24}]\cdot 13.16H_2O$ [s.g. $R\bar{3}m$];
b) synthetic ALPO-34 (as synthesized): $Al_6(PO_4)_6 2F^-\cdot 2C_4H_{10}NO^+$ [s.g. $P\bar{1}$];
c) synthetic ALPO-34 (calcinated and rehydrated): $Al_6(PO_4)_6\cdot nH_2O$ [s.g. $P2/m$];
d) synthetic SAPO-34: $Si_{0.9}Al_{6.00}P_{5.10}O_{24}\cdot C_4H_9ON, C_4H_{10}NO^+\cdot 2.7H_2O$ [s.g. $R\bar{3}$].

The four phases are characterized by different tetrahedral composition: Si,Al in natural chabazite; Al,P in ALPO-34 and Si,Al,P in SAPO-34, respectively. Moreover, as-synthesized ALPO-34 contains one third of the Al atoms in octahedral coordination. Concerning the extraframework content, as-synthesized ALPO-34 and SAPO-34 contain morpholinium/ morpholine as structure directing agent, while chabazite contains alkaline/earth alkaline cations and water molecules.

H*P*-XRPD experiments were performed at the Swiss-Norwegian beamline (BM01a) at ESRF (Grenoble, France) using a Merril Basset modified DAC and silicone oil as non-penetrating *P* transmitting medium. The powder patterns were collected from P_{amb} to about 6 GPa and upon decompression. No complete amorphization is observed up to the highest investigated pressure for all the samples and the *P*-induced effects on this framework topology seem to be completely reversible for each of the considered materials. Since the peak intensities of the collected patterns are not completely reliable (poor statistics and possible strong preferred orientation), only the unit cell parameters were extracted from the powder patterns by means of Rietveld or Le Bail methods.

To compare the compressibilities of the different phases, we have selected the pressure range P_{amb} - 4.5 GPa: a volume reduction of about 6.9%, 11.5%, 9.0% and 12.4% is observed for chabazite from Vallerano, SAPO-34, as synthesized and calcinated ALPO-34, respectively. As-synthesized ALPO-34 undergoes a phase transition from the triclinic $P\bar{1}$ to the monoclinic $C2/m$ s.g. between 3.4 and 3.9 GPa.

The lower compressibility of the as-synthesized ALPO-34 with respect to SAPO-34 can be interpreted as due to the octahedral coordination of part of the framework aluminium by oxygen and fluorine anions. This coordination geometry leads to a more rigid framework with respect to the conventional tetrahedral Al coordination. The higher compressibility of calcinated ALPO-34 with respect to the as-synthesized one is due to the loss of morpholine molecules upon heating, and the consequent larger free volume in the channels. Finally, natural chabazite has the lowest compressibility among the studied phases mainly because of its high extra-framework content.

SYNTHESIS, TEM CHARACTERIZATION AND HIGH TEMPERATURE BEHAVIOUR OF $LiNiSi_2O_6$ PYROXENE

M. Tribaudino[1], G. Bromiley[2], F. Nestola[3], H. Ohashi[4]

[1]*Dipartimento di Scienze della Terra, Università di Parma, Italy*
[2]*Department of Earth Sciences, University of Cambridge, UK*
[3]*Dipartimento di Geoscienze, Università di Padova, Italy*
[4]*Hashi Institute for Silicate Science, Tokyo, Japan*
mario.tribaudino@unipr.it

Li bearing pyroxenes provide a model for pyroxene crystal chemistry and phase transitions. A $P2_1/c$-$C2/c$ phase transition with temperature was found in $LiM^{3+}Si_2O_6$ end members with M^{3+} = Cr, Ga, Fe, V, Sc at T close or slightly above room temperature [1]. The transition temperature and the $P2_1/c$ stability field between Cr, Ga, Fe, V end members increases with decreasing radius of the M^{3+} cation. This does not apply for M^{3+} = Al: in $LiAlSi_2O_6$ the s.g. is $C2/c$ at any temperature. A clue to interpret this contradictory behaviour can come from the analysis of $LiNiSi_2O_6$ pyroxene: Ni^{3+} in octahedral coordination has a cation radius intermediate to that of Cr^{3+} and Al (0.56 in low spin state for Ni^{3+} *vs*. 0.615 and 0.535 for Cr^{3+} and Al), thus providing a test for the failure of the ionic radius - critical temperature model.

An investigation on $LiNiSi_2O_6$ pyroxene was then undertaken, following preliminary reports [2]. $LiNiSi_2O_6$ pyroxene was synthesized in a piston-cylinder apparatus from stoichiometric starting mix of Li_2SiO_3 + NiO + SiO_2 at 2GPa and 1200°C. The resulting material was a mixture of $LiNiSi_2O_6$ pyroxene and a spinel with composition $(Li_{0.5}Ni_{0.5})Ni_2O_4$. The crystals in both phases sized only few microns. The cell parameters for the pyroxene at room temperature are: a = 9.4174(6) Å, b = 8.4480(6) Å, c = 5.2461(3) Å, β =110.528(5), V = 390.867(10) Å^3, in good agreement with previous investigators [2]. TEM analysis of the pyroxene revealed strong $h+k$ odd reflections indicative of a P lattice and antiphase domains sized few nm. High temperature TEM *in situ* heating was done on single crystals to seek the phase transition on $LiNiSi_2O_6$, and, by comparison, on $LiCrSi_2O_6$. The disappearance of critical reflections was observed in $LiCrSi_2O_6$ at about 60°C, but no significant decrease in their intensity was observed in $LiNiSi_2O_6$ up to 330°C.

The high temperature behaviour was followed between 25 and 500°C by continuous powder diffraction of the run products (pyroxene + spinel). The high temperature runs were done exploiting synchrotron radiation at Gilda BM8 beamline. The diffraction patterns show at all temperature strong $h+k$ odd reflections, whose intensity is much higher than found in other $P2_1/c$ Li pyroxenes. The intensity of critical reflections does not decrease in the studied range and there is no evidence that the transition is approached even at the highest T reached. This point stands against the linear model for cation radius and critical temperature, which would predict the transition below 350°C for Ni^{3+} in low spin configuration and at even lower T for Ni^{3+} in the high spin configuration.

The cell parameters follow a trend with temperature that is very close to that of $LiAlSi_2O_6$ spodumene, in spite of the different space group, and different to that observed in $P2_1/c$ $LiGaSi_2O_6$ and $LiCrSi_2O_6$ before the transition. This point is confirmed by the analysis of the strain tensor with temperature.

These observations suggest that $LiNiSi_2O_6$ pyroxene is present in a structural configuration significantly different form that of other $P2_1/c$ pyroxenes, possibly in relation with the presence of Ni^{3+} in low spin state.

References. [1] G.J. Redhammer, G. Roth, *Z. Kristallogr.*, **219**, 585-605, 2004; [2] H. Ohashi, T. Osawa, *J. Jap. Ass. Mineral. Petrol. Econ. Geol.*, **83**, 308-310, 1988.

ARSENIC UPTAKE BY NATURAL CALCITE: A XAS STUDY

F. Bardelli[1], M. Benvenuti[2], P. Costagliola[2], F. Di Benedetto[2,3], P. Lattanzi[4], C. Meneghini[5], M. Romanelli[3]

[1]*ESRF, Grenoble, France*
[2]*Dipartimento di Scienze della Terra, Università di Firenze, Italy*
[3]*Dipartimento di Chimica, Università di Firenze, Italy*
[4]*Dipartimento di Scienze della Terra, Università di Cagliari, Italy*
[5]*Dipartimento di Fisica, Università Roma Tre, Italy*
pilarc@geo.unifi.it

The possible role of calcite in sequestering As has been considered, mainly focussing on the possibility that calcite may adsorb As-oxyanions onto its surface. However, recently As oxyanions resulted potential substituents of the carbonate group in the calcite structure. The possible consequences of the As uptake by calcite in natural systems are, in principle, of considerable relevance, because of the large diffusion of this mineral in the Earth's crust and its stability in a variety of geologic environments.

In this study, we examined by X-ray Absorption Spectroscopy samples from the same travertine sequence studied by Di Benedetto *et al.* [1], with the aim of investigating the formal valence of As oxyanions substituting for carbonate groups in calcite. The XAS results indicate a heterogeneous local environment for As, showing either mixed valence states, As(III) and As(V), or a As(V)-rich background. Samples where spectra reveal only As(V) lack a well defined structure for coordination shells higher than the first. On the contrary, mixed valence As spectra reveal strong As-Ca contribution to the second shell belongs to the As(III) local environment.

The present results suggest an essentially disordered long range environment, where As(V) is not incorporated in any crystalline structure, but essentially occurs as an oxyanion adsorbed onto one or more oxide/silicate phase. On the other hand, As(III) substitutes C in the CO_3 group, following preferably the As(III) ↔ C (*i.e.*, $As^{3+}O_3^{3-} \leftrightarrow CO_3^{2-}$) substitution, already suggested in both natural and synthetic calcite, with respect to the substitution $As^{5+}O_4^{3-} \leftrightarrow CO_3^{2-}$.

The present study confirms that As-oxyanions may substitute for CO_3 groups in natural calcite samples. Moreover, XAS spectroscopy reveals that As(III), rather than As(V), oxyanions are present in calcite of these travertines, as previously suggested, but not demonstrated, by Di Benedetto *et al.* [1]. The fact that evidence for such substitution was found in a single sample only out of a set of five, suggests that the process is, in general, not favoured, possibly because of the remarkably different sizes of the arsenite and carbonate anionic groups. Therefore, the amounts of As hosted in natural calcites are expected to be low, wherever there is a competition with iron/manganese oxyhydroxides.

References. [1] F. Di Benedetto, P. Costagliola, M. Benvenuti, P. Lattanzi, M. Romanelli, G. Tanelli, *Earth Planet. Sc. Lett.*, **246(3-4)**, 458-465, 2006.

NORTH-AMERICAN MICROTEKTITES ARE MORE OXIDIZED THEN TEKTITES

G. Giuli[1], S.G. Eeckhout[2], M.R. Cicconi[1], C. Koeberl[3], B.P. Glass[4], G. Pratesi[5], E. Paris[1]

[1]*Dipartimento di Scienze della Terra, Università di Camerino, Italy*
[2]*European Synchrotron Radiation Facility (ESRF), Grenoble, France*
[3]*Department of Lithospheric Research, University of Vienna, Austria*
[4]*Department of Geology, University of Delaware, Newark, USA*
[5]*Dipartimento di Scienze della Terra, Università di Firenze, Italy*
gabriele.giuli@unicam.it

Despite the availability of geochemical studies on microtektites, very few studies exist of the Fe coordination number and oxidation state in such materials. As microtektites constitute a large fraction of the glass produced by a tektite-generating impact event, such studies are of great importance for a more complete understanding of impact-generated glasses. Previous data showed a set of microtektites from the North American strewn field to be consistently more oxidized with respect to microtektites from the other strewn fields. This case is unique among tektites and microtektites and, if confirmed, may provide further constrains for a better understanding of microtektites generation processes. In order to confirm previous data, we studied a larger set of microtektites from the same strewn field from other four DSDP cores collected at different distances from the source crater and spanning a wider compositional range. For comparison, also four bediasites and two georgiaites have been studied, as well as a tektite fragment from the DSDP612 site.

The XANES data have been collected in fluorescence mode at the ID26 beamline of the ESRF storage ring (Grenoble, F) using a Si(311) monochromator and with a beam size at the sample of 55×120 μm. The energy reproducibility has been estimated to be 0.05 eV or better.

Clear differences can be detected in the shape of these pre-edge peaks related to the amount of trivalent Fe present. Comparison with pre-edge peak data of Fe model provided information on Fe oxidation state and coordination environment in the studied glasses. In the analyzed bediasites and georgiaites, as expected, Fe is essentially divalent and in a mixture of [4] and [5] coordinated sites. On the other hand, data for the North-American microtektites clearly show the presence of considerable amounts of Fe^{3+}. XANES spectra can be interpreted as a mixture of $^{[4]}Fe^{2+}$, $^{[5]}Fe^{2+}$, $^{[4]}Fe^{3+}$ and $^{[5]}Fe^{3+}$. $Fe^{3+}/(Fe^{2+}+Fe^{3+})$ ratio of the studied North American microtektites range from 0 to 45 (±5) %.

No obvious correlation has been found between Fe oxidation state and chemical composition of the studied microtektites that could suggest alteration in a marine environment. Thus, we believe that the determined oxidation states are a signature of the formation process of these microtektites, and not the product of subsequent alteration.

Such a wide range in Fe oxidation state is unique within microtektites: microtektites from the Ivory Coast and Australasian strewn fields contain almost purely divalent Fe, as do tektites from the same strewn fields. The marked difference in the $Fe^{3+}/(Fe^{2+}+Fe^{3+})$ ratio of tektites and microtektites from the North American strewn field raises the question whether or not microtektites should simply be considered as microscopic analogous of tektites.

Although no clear explanation can be provided, we note a similarity with impact glass spherules from the K/T boundary, which showed a similar trend in pre-edge peak data extending up to 100% trivalent Fe. Remarkably, both impacts were of considerable size and occurred in a shallow marine environment. As the variation in Fe oxidation state of K/T impact glass spherules may be explained by oxidation of the impact melt droplets within a CO_2- and/or H_2O-rich plume, we suggest that a similar mechanism may have worked in the case of North American microtektites. However, no chemical correlation has been found with Fe oxidation state to support this suggestion so far.

A COMBINED *in situ* X-RAY POWDER DIFFRACTION AND *in situ* NEUTRON DIFFRACTION ON $MgFe^{3+}AlO_4$ SPINEL

D. Levy[1], N. Marinoni[2], A. Pavese[2]

[1]*Dipartimento di Scienze Mineralogiche e Petrologiche, Università di Torino, Italy*
[2]*Dipartimento di Scienze della Terra, Università di Milano, Italy*
davide.levy@unito.it

Mg-Al-Fe- rich spinels are found in a wide range of geological environments and they are also important compounds in a number of technological applications. Several studies have emphasised that cation partitioning in spinel is closely related to pressure and temperature, as both the energetic and the configurational entropy are dependent on the atomic distribution over the two different crystallographic sites. Therefore, in spite of the simple crystallographic structure of spinel, the cation diffusion over the tetrahedral and octahedral sites as a function of temperature and pressure is a rather complex process. Few studies have focused on cation partitioning on spinels containing three cations, such as Mg^{2+}, Fe^{3+} and Al^{3+}. In such a light, in the present study cation partitioning in a synthetic $MgFe^{3+}AlO_4$ spinel has been investigated in function of the temperature. Due to the impossibility to determine the occupancy of three cations on three sites by using only a diffraction technique, we combined high temperature *in situ* X-ray Powder Diffraction (XRPD) and Neutron Powder Diffraction (NPD) structural refinements on a synthetic $MgAlFeO_4$ spinel.

High temperature X-ray Diffraction data were collected with a Philips X'Pert θ-θ diffractometer, equipped with a hot chamber (AHT PAP1600). The NPD measurements were performed at ISIS spallation neutron source (Rutherford Appleton Laboratory, U.K.) by using the time-of-flight (TOF) technique, on the high intensity diffractometer POLARIS. All data have been refined by GSAS. Considering that Mg and Al have quite the same X-ray scattering power, the XRPD data have been used to extract the Fe partitioning, while the neutron scattering lengths of the two sites have been determined by means of the NPD data.

The thermal expansion curve highlights a slope change between 700 and 800 K indicating cation redistribution. The tetrahedral and octahedral bond lengths curves confirm a cation partitioning from 773 K, but they highlight also another transition at 1000 K.

The presence of two different behaviours, one at about 800 K and the other at about 1000 K, is explained examining the cations presence in the tetrahedra. By examining the figure below, it can be highlighted that Mg substitute Fe^{3+} at the tetrahedral site between 700 and 800 K, while the Al^{3+} content is constant. Above 1000 K also Al^{3+} moves with Fe^{3+} from tetrahedron.

Concluding we show that with a joint experiment by using X-ray and neutron diffraction the cation partitioning of a triple cation spinel can be determined. We determine also a double mechanism of cation partitioning for this kind of spinels: it starts with a Fe-Mg exchange, at higher temperature also Al moves from tetrahedral to octahedral site.

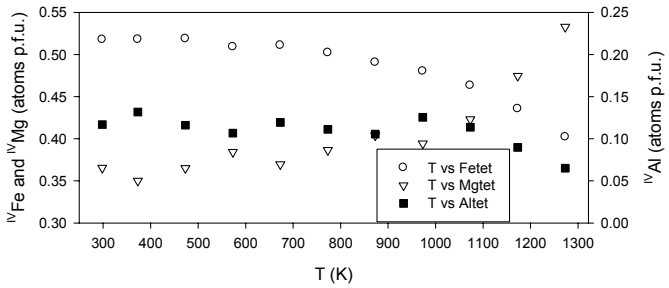

NEW INSIGHTS INTO THE CRYSTAL-CHEMISTRY OF EPIDIDYMITE AND EUDIDYMITE: A SINGLE-CRYSTAL NEUTRON DIFFRACTION STUDY

G.D. Gatta[1], N. Rotiroti[1], A. Guastoni[2], F. Nestola[2], G. McIntyre[3]

[1]*Dipartimento di Scienze della Terra, Università di Milano, Italy*
[2]*Dipartimento di Geoscienze, Università di Padova, Italy*
[3]*Institute Laue-Langevin, Grenoble, France*
diego.gatta@unimi.it

Epididymite and eudidymite are two dimorph open-framework silicates minerals, with poorly defined ideal chemical formulae (*i.e.* $Na_2Be_2Si_6O_{15}\cdot H_2O$ [1] and $NaBeSi_3O_7OH$ [2], respectively). Both of these minerals occur as late-stage minerals in the cavities of alkaline pegmatites generally associated with aegirine, Na-feldspars, zeolites and many other rare exotic minerals including Na-Be-Zr-Y silicates, Nb-Ta oxides and REE-carbonates. With bertrandite ($Be_4Si_2O_7(OH)_2$), beryl ($Al_2Be_3Si_6O_{18}$), chrysoberyl (Al_2BeO_4), and phenakite (Be_2SiO_4), epididymite and eudidymite represent some of the richest minerals in beryllium.

The crystal chemistry of two natural samples of epididymite (a = 12.7334(4), b = 13.6298(5), c = 7.3467(3) Å, V = 1275.04 Å^3, space group *Pnma*) and eudidymite (a = 12.6188(10), b = 7.3781(5), c = 13.9940(9) Å, β = 103.762(5)°, V = 1265.47 Å^3, space group $C2/c$) collected in a miarolitic granitic pegmatite hosted by A-type peralkaline granites of the Zomba-Malosa pluton in southern Malawi, has been reinvestigated by means of energy dispersive X-ray spectroscopy, thermo-gravimetric analysis, inductively coupled plasma-optical emission spectroscopy and single-crystal neutron diffraction. Two anisotropic structural refinements have been performed starting from the structural models previously published [1,2]. The final agreement index were R_1 = 0.0317 for 137 refined parameters and 2261 unique reflections with $F_o > 4\sigma(F_o)$ for epididymite and R_1 = 0.0478 for 136 refined parameters and 1732 unique reflections with $F_o > 4\sigma(F_o)$ for eudidymite. The analyses of the difference-Fourier maps of the nuclear density confirm the presence of extra-framework water molecules in both the dimorphs, and not of hydroxyl groups as wrongly reported in previous studies and in several crystal structure databases. The real chemical formula of edipidymite and eudidymite is $Na_2Be_2Si_6O_{15}\cdot H_2O$ (Z = 4). The configuration of the water molecules and the hydrogen bonds are fully described for both the dimorphs. The chemical analysis shows that a low, but significant, amount of Al and Fe (most likely substituting Si in the tetrahedral sites) and K (substituting Na as extra-framework cation) occurs in both the dimorphs. The unusually high temperature of dehydration of epididymite and eudidymite observed in the present and in previous studies [1,2] may be attributed to: 1) the peculiar configuration of the water molecule, which is bonded to two Na sites, 2) the strong hydrogen bonds to the framework oxygen atoms, and 3) the small "free diameters" of the channels in the tetrahedral framework, which hinder the migration of the water molecules toward the surface of the crystal.

References. [1] J.H. Fang, P.D. Robinson, Y. Ohya, *Am. Mineral.*, **57**, 1345-1354, 1972; [2] P.D. Robinson, J.H. Fang, *Am. Mineral.*, **55**, 1541-1549, 1970.

SULFUR SPECIATION IN MINERALS AND GLASSES BY HIGH RESOLUTION X-RAY EMISSION SPECTROSCOPY

R. Alonso Mori[1,2], P. Glatzel[2], E. Paris[1], S.G. Eeckhout[2], G. Giuli[1]

[1]*Dipartimento di Scienze della Terra, Università di Camerino, Italy*
[2]*European Synchrotron Radiation Facility (ESRF), Grenoble, France*
mori@esrf.fr

Sulfur is characteristically heterovalent, exhibiting by far the greatest range in oxidation state (from 2- to 6+) of the geochemically abundant elements. It readily forms chemical bonds with both more electropositive and more electronegative elements, hence forming a wide range of minerals.

X-ray absorption spectroscopy, and more specifically XANES probes the unoccupied density of states and thus provides information on the oxidation state and local structure of S. However, the XANES spectrum is influenced by numerous effects, such as bond distances, bond angles and ligand type, making the analysis difficult. It is thus desirable to combine XANES with alternative spectroscopic techniques.

We use S Kα and S Kβ X-ray emission spectroscopy (XES) to investigate the chemical state and local environment of sulfur in different model mineral compounds, namely sulfides (S^{2-}), sulfites (S^{4+}), and sulfates (S^{6+}). The Kα lines arise from 2*p* to 1*s* transitions and are expected to be mostly free from chemical bond effects, except for small energy shifts that reflect the valence orbital electron population via screening effects.

The quasi-independence of the Kα spectral shape on the oxidation state makes the analysis and energy shifts determination easier and more reliable as compared to XANES, and can thus be used to clearly determine the sulfur oxidation states in unknown or heterogeneous compounds. Alternatively, the Kβ lines, close to the K-edge, directly yield the p-density of occupied valence states giving valuable information on the local coordination. We further performed *ab initio* quantum-chemical calculations by means of the StoBe code, based on the density functional theory (DFT) in order to visualize the molecular orbitals and to infer how the chemical bonds are formed in these compounds.

The XES technique is now successfully applied to natural and synthetic silicate glasses. This allows us to accurately determine the sulfur oxidation states and to provide valuable information on the local chemistry, structure and thus on the geochemical role of S in these systems. More specifically we use the energy shift in the S Kα lines to make quantitative analysis of the oxidation state of sulfur in heterogeneous systems and to determine whether S is present as sulfide or sulfate.

NEUTRON DIFFRACTION APPLICATIONS TO THE STUDY OF ROMAN ARMY BRONZE ARTEFACT FROM THAMUSIDA (MOROCCO)

R. Arletti[1], L. Cartechini[2], E. Gliozzo[3], R. Rinaldi[4], S. Imberti[5], W. Kockelmann[5], I. Memmi[3]

[1]*Dipartimento di Scienze della Terra, Università di Modena e Reggio Emilia, Italy*
[2]*IST-CNR, Perugia e Centro di Eccellenza SMAArt, Università di Perugia, Italy*
[3]*Dipartimento di Scienze della Terra, Università di Siena, Italy*
[4]*Dipartimento di Scienze della Terra e Centro di Eccellenza SMAArt, Università di Perugia, Italy*
[5]*Rutherford Appleton Laboratory, ISIS Facility, Chilton, Didcot, UK*
rossella.arletti@unimore.it

The rarity and conservation state of a suite of bronze archaeological finds from the Roman army settlement of Thamusida (Rabat, Morocco) imposed the use of a non destructive analytical technique capable of providing information on the bulk metal structure and composition without any manipulation of the objects. Such is the case of Time of Flight Neutron Diffraction (ToF-ND) [1,2]. This technique offers the unique advantage of obtaining diffraction data in a totally non-invasive, non-destructive mode on samples of very variable shapes and dimensions, even in the presence of considerable surface alteration layers [3-5].

Until recently, most studies of Roman military equipment have been based on representations of soldiers in Roman art with very few studies directly performed on the objects, mainly by means of destructive techniques. The present study opens up new perspectives with an original approach as to both, analytical techniques and materials to be analyzed.

The materials include bronze objects from the 1st to the 3rd century AD, comprising horse harness fittings, buckles, scabbard fittings and also including some epigraphic material such as military diplomas and inscribed bronze appliqués.

Major aims of this study are the characterization of the alloy and the evaluation of the state of preservation (corrosion and alteration layers) of the pieces. The production technology has also been investigated.

Results allowed to reconstruct an articulated technology. Compositional, phases identification and quantization results obtained from Rietveld analyses of the diffraction profiles indicate different compositions of the alloys depending on object functionality. Ancient artisans introduced low quantities of tin for the production of sheet metal, higher quantities of tin for bell production, variable contents of copper depending on mechanical and thermal treatment, etc. The chronological parameter seems to be less relevant for the different compositions of the alloys, although archaeological typology cannot provide a precise dating of each artefact. Moreover, much information has been obtained on the alteration layers without loss of information from the bulk material of the objects. These data can also be utilized for restoration and conservation purposes.

References. [1] W. Kockelmann, E. Pantos, A. Kirfel, In *Radiation in Art and Archaeometry*, D.C. Chreagh, D.A. Bradley Eds., Elsevier Science, 347-377, 2000; [2] S. Siano, W. Kockelmann, U. Bafile, M. Celli, M. Iozzo, M. Miccio, O. Moze, R. Pini R. Salimbeni, M. Zoppi, *Appl. Phys. A*, **74**, S1139, 2002; [3] R. Arletti, L. Cartechini, S. Giovannini, R. Rinaldi, W. Kockelmann, A. Cardarelli, *Il Nuovo Cimento C*, **30**, 11-19, 2007; [4] R. Arletti, L. Cartechini, S. Giovannini, R. Rinaldi, W. Kockelmann, A. Cardarelli, *Appl. Phys. A*, **90**, 9-14, 2008; [5] L. Cartechini, R. Arletti, R. Rinaldi, W. Kockelmann, S. Giovannini, A. Cardarelli, *J. Phys. Cond. Matt.*, DOI: 10.1088/0953-8984/20/10/104253 , 2008.

FROM UNALTERED PYRITE MINERALISATIONS TO Fe-OXIDATION CRUSTS: A SYNCHROTRON MICRO-XRD, -XRF AND -XANES ANALYSES

C. Carbone[1], P. Marescotti[1], G. Lucchetti[1], E. Chalmin[2]

[1]*Dip.Te.Ris.,Università di Genova, Italy*
[2]*ESRF beamline ID21, Grenoble, France*
carbone@dipteris.unige.it

Several techniques based on synchrotron radiation have been recently applied to environmental sciences because they give the possibility for non-destructive investigations with micron spatial resolution. These studies applied a combination of different methods, such as μ-XRF; μ-XRD, μ-XANES and μ-EXAFS [1-3], to determine the mineralogy and the elemental distribution of metals in polluted soils and waste rock deposits.

We report preliminary results obtained using μ-XRF and μ-XANES analyses, performed at the ID21 beamline, on Fe-oxides and -oxyhydroxides bearing samples formed by polymetallic sulphides alteration during AMD (Acid Mine Drainage) processes at the Libiola Mine (Sestri Levante, Genova, Italy).

The samples were the same used for a previous experiment (CH-2095, ID-18F) that allowed to determine the mineralogy (by μ-XRD) and the elemental concentration (by μ-XRF; for elements with $Z > 26$) along several transects from unaltered pyrite-rich sulphide mineralisations to completely altered Fe-oxide and -oxyhydroxides oxidation crusts.

The analysed samples are representative of partially altered massive and stockwork mineralisations and of layered hardpans consisting of rhythmic alternation of submillimetric hematite-rich and goethite-rich layers.

Preliminary results evidenced that the first step of pyrite alteration is marked by sulphur oxidation to sulphate. This oxidation process starts from the crystals rims or from intragrain microfractures. Sulphate is then rapidly leached out from the systems and few μm within the outer altered layers is almost completely absent. The altered layers are composed almost exclusively by Fe-oxides (hematite) and -oxyhydroxides (goethite, ferrihydrite, lepidocrocite) that concentrically rim pyrite crystals, and fill intra- and inter-grain interstices. Elemental maps and μ-XRF transects confirmed the high affinity of the secondary minerals to adsorb or incorporate many of the elements leached from sulphides or from gangue minerals. In particular, we constantly observed significant enrichment in Cr in the hematite and goethite rich layers as well as good positive correlations between Fe and Al, Mn, Ti, and V. Conversely, μ-XANES and μ-XRF maps confirm the sulphur firstly oxidises to sulphate and than is quickly removed from the solid phase, being strongly depleted or absent in the Fe-oxide and -oxyhydroxides alteration crusts.

References. [1] A. Manceau, N. Tamura, R.S. Celestre, A.A. MacDowell, N. Geoffroy, G. Sposito, H.A. Padmore, *Environ. Sci. Technol.*, **37**, 75-80, 2003; [2] G. Morin, J.D. Ostergren, F. Juillot, P. Ildefonse, G. Calas, G.E. Brown, *Am. Mineral.*, **84**, 420-434, 1999; [3] G. Morin, F. Juillot, P. Ildefonse, G. Calas, J.C. Samama, P. Chevallier, G.E. Brown, *Am. Mineral.*, **86**, 92-104, 2001.

HIGH-PRESSURE AND HIGH-TEMPERATURE BEHAVIOUR OF BASSANITE

P. Comodi[1], S. Nazzareni[1], L. Dubrovinsky[2], M. Merlini[3]

[1]*Dipartimento di Scienze della Terra, Università di Perugia, Italy*
[2]*Bayerisches Geoinstitut Bayreuth University, Bayreuth, Germany*
[3]*ESRF, Grenoble, France*
comodip@unipg.it

Hemihydrate sulphate ($CaSO_4$ $1/2H_2O$), bassanite, is an important industrial mineral both in plaster production and dentistry (medical) products. In geological environments may have important implications in the partitioning of sea-water cations during the dehydration processes [1]. The bassanite structure [2] contains CaO_8 and CaO_9 coordination polyhedra, both held together by the SO_4^{2-} ions and forming channels where the water molecules are located forming hydrogen bonds with oxygen atoms of the sulphate tetrahedra. It is a nanoporous material and the interaction between the sulphate "host" lattice and the H_2O "guest" molecule may be important in exchange processes. Notwithstanding, there are several papers on the baric and thermal behaviour of β-anhydrite (*Amma,* insoluble anhydrite), but very few data are known on the thermal and baric behaviour of bassanite, as well as of the hexagonal form of γ-anydrite ($P6_222$, soluble anhydrite), isostructural with bassanite.

The evolution of bassanite at different pressures up to 30 GPa under room temperature was studied by X-ray diffraction at the GSECARS-BM13 beamline, Advances Photon Source (APS, Argonne Chicago, USA). A diamond anvil cell was charged with bassanite powder, obtained by dehydration of gypsum after heating at 130°C for 8h, together with ruby chip as pressure calibrant, a golden filament as image plate distance calibrant, and Neon as pressure transmitting medium. The lattice parameters were measured from 0.001 to 30 GPa by increasing and decreasing pressure at room condition. The influence of temperature on the baric behaviour was studied at ID-09 beamline, ESRF (Grenoble, France). External heated diamond anvil cell was charged with bassanite powder, ruby chip and Argon gas, as pressure transmitting medium.

Diffraction spectra were integrated by using FIT2D program, and the lattice parameters refined by Le Bail method, in the GSAS package. All the lattice parameters show a discontinuity at pressure higher than 9.2 GPa, which is manifested with the disappearance of some peaks (d = 1.25, 1.82, 2.05 Å) in the diffraction pattern. The bulk modulus of bassanite, fitting the volume cell data from 0.001 to 9.2 GPa using a second-order Birch-Murnaghan equation-of-state, was K_0 = 66 GPa. The axial compressibility values are β_a = 3.5(1), β_b = 5.2(1) and β_c = 2.7(1) 10^{-3} GPa^{-1} showing a slightly anisotropic behaviour, with the most compressible direction along the *b* axis, and the less compressibility direction along *c* axis. These values are in good agreement with those calculated for γ-anhydrite [3]. At pressure higher than 9.2 GPa, the structure becomes more rigid and the bulk modulus calculated fitting the volume data with a second-order Birch-Murnaghan equation-of-state becomes 115(9) GPa. The effect of the temperature was also evaluated along the isotherm at 109°C. The transition was completely reversible as indicated by the spectra of the recovered sample after increasing pressure up to about 30 GPa.

References. [1] J. Kushir, *Geochim. Cosmochim. Ac.*, **44**, 1471-1482, 1980; [2] C. Bezou, A. Nonat, J.C. Mutin, *J. Solid State Chem.*, **117**, 165-176, 1995; [3] H. Voigtlander, B. Winkler, W. Depmeier, K. Knorr, L. Ehm, *Host-Guest-Systems Based on Nanoporous crystal*, Wiley Ed., 2006.

ESTIMATION OF FLUCTUATIONS OF STRAINS IN POROUS MATERIALS BASED ON MATHEMATICAL MODEL OF STOCHASTIC INHOMOGENEOUS MEDIA

O. Fedoryshyn

Carpatian Branch of Subbotin Institute of Geophysics, National Academy of Ukraine, Ukraine
ofedoryshyn@mail.lviv.ua

Most of natural materials are inhomogeneous. In them, heterogeneities in the form of cracks and a pores always exist. Strains and deformations in these media will be inhomogeneous even at homogeneous external stresses. In this work the inhomogeneity of strain in a solid phase of the saturated porous medium is estimated. The stochastic inhomogeneous medium in which the physical characteristics are random functions of coordinates is considered. For such medium the theoretical method of definition of effective physical parameters is developed [1], but it can be made only if the fluctuations of fields in every phase of the inhomogeneous medium are neglected. In particular, for a finding of effective modules of elasticity it is necessary to neglect the fluctuations of strain in a solid phase.

Trying not to neglect the fluctuations of strains, and taking them into account will turn out that effective modules of elasticity essentially depend on them. This results in a possibility to estimate the fluctuations of strains in a solid phase. On the basis of the offered method, the analysis of fluctuations of elastic fields for the saturated porous medium is made. In a liquid component the pressure will be hydrostatic, whereas the fluctuations will not. In a solid component the fluctuations of strains essentially depend on the geometrical form of porous spaces. The method of definition of fluctuations of elastic fields on the basis of experimentally measured modules of elasticity is developed.

References. [1] M.A. Biot, *J. Appl. Phys*., **33**, 1482-1498, 1962.

VARIATIONS IN FE OXIDATION STATE BETWEEN DARK AND LIGHT LAYERS OF MUONG NONG-TYPE TEKTITES

G. Giuli[1], S.G. Eeckhout[2], G. Pratesi[3], C. Koeberl[4], M.R. Cicconi[1], E. Paris[1]

[1]*Dipartimento di Scienze della Terra, Università di Camerino, Italy*
[2]*European Synchrotron Radiation Facility (ESRF), Grenoble, France*
[3]*Dipartimento di Scienze della Terra, Università di Firenze, Italy*
[4]*Department of Lithospheric Research, University of Vienna, Austria*
gabriele.giuli@unicam.it

Muong Nong tektites differ in appearance from common splash form tektites by being larger, having irregular blocky shape, and a layered structure. Usually, dark layers are less abundant and, in thin section, they seem embedded in a light coloured matrix. Systematic chemical and physical variations are observable between dark and light coloured layers. In particular, light layers display a relatively higher Al and Fe content and a lower Si content with respect to dark layers. Moreover, the light layers have a higher refractive index (see [1] and references therein for a more complete description of Muong Nong type tektites from the Australasian tektite strewn field).

Previous unpublished XANES data have been collected on powder samples obtained by hand-picking separation of dark and light layers of three different Muong-Nong samples. These data showed small but detectable differences in the Fe oxidation between dark layers and light layers, the former being slightly but reproducibly more oxidized.

A new set of data has been acquired with an X-ray micro-beam on a thin section of a Muong Nong indochinite sample across the boundary between a dark layer and the light matrix in order to confirm whether or not there are systematic variations of the Fe oxidation state across Muong Nong layers.

The XANES data have been collected at the ID26 beamline of the ESRF storage ring (Grenoble, F) using a Si(311) monochromator and with a beam size at the sample of 55 x 120 μm.

XANES spectra have been collected in fluorescence mode over a 270 eV energy interval across the Fe K-edge (7112 eV) with a 0.1 eV energy step and 45 ms counting time. An average of about 20 scans for each sample allowed to obtain very good signal to noise ratios despite the small beam size. The energy reproducibility has been estimated to be 0.05 eV or better.

Background subtracted pre-edge peaks have been fitted with sums of two to three pseudo-Voigts components according to the procedure described in [2].

Experimental XANES spectra are very similar in shape to those of tektites already published. However, small and reproducible changes occur in the pre-edge peak involving the centroid energy: the pre-edge peak of the spectra collected within the dark layer is reproducibly 0.2 eV at higher energy than those of the spectra collected within the light matrix. This difference in energy position is four times the estimated energy reproducibility and, therefore, is significant.

By comparison with pre-edge peak data of Fe model compounds, we estimate the $Fe^{3+}/(Fe^{2+} + Fe^{3+})$ ratios in the light matrix and dark layer of the studied sample to be 5% and 15% (±5) respectively.

References. [1] C. Koeberl, *Geochim. Cosmochim. Ac.*, **56**, 1033-1064, 1992; [2] G. Giuli, G. Pratesi, C. Cipriani, E. Paris, *Geochim. Cosmochim. Ac.*, **66**, 4347-4353, 2002.

CATION MIGRATIONS AND BRØNSTED SITES FORMATION IN NH_4-FORM OF ZEOLITE OMEGA: AN *in situ* TIME-RESOLVED SYNCHROTRON POWDER DIFFRACTION STUDY

I. Parodi, A. Martucci, A. Alberti

Dipartimento di Scienze della Terra, Università di Ferrara, Italy
prdlri@unife.it

The aim of this work is to give an exhaustive picture of structural modifications induced by heating in the NH_4-form of zeolite omega calcinated from RT to 800°C, by an X-ray diffraction study.

Omega zeolite is the synthetic counterpart of zeolite mazzite, it is a large-pore material known for its strong Brønsted acidity [1], which is very important for various industrially reactions. Its real symmetry is $P6_3/mmc$, the same as the topological one. The alumino-silicate framework consists of gmelinite-type cages which are linked in columns parallel to the **c**-axis, sharing their 6-membered rings of tetrahedra. Two different types of channels delimited by 12- and 8-rings parallel to [001] are present. A sample of zeolite omega with chemical composition $Na_{6.6}TMA_{1.8}(H_2O)_{22.2}[Al_{8.4}Si_{27.6}O_{72}]$-MAZ was NH_4-ion exchanged three times at RT and three times at 90°C. Chemical analysis showed that after ion exchange 2.4 Na-ions remain in the structure. Rietveld structure analysis was carried out on temperature resolved powder diffraction data collected at the GILDA beamline (ESRF, Grenoble). The structure refinements by full profile Rietveld analysis were performed in the $P6_3/mmc$ space group by the GSAS package, starting from site positions of framework atoms from Martucci *et al.* [2].

Structure refinements showed that the Na cations, located in the 12-ring channel in the as-synthesized sample, are completely removed by the NH_4-ion exchange. Moreover, only half of the Na content in the 8-ring channel (in good agreement with the chemical analysis) and about 2/3 of the TMA inside the gmelinite cage were detected. Four other extraframework sites were recognized: two of these, located in the 8-ring and in the gmelinite cage, respectively, were attributed to water molecules, the residual ones located in the 12-ring, were attributed to NH_4 cations. On the bases of this assumption the chemical formula of the exchanged form was $Na_{2.4}TMA_{0.9}(H_2O)_{4.2}(NH4)_{20.0}[Al_{8.4}Si_{27.6}O_{72}]$, in good agreement with the result of the TG analysis.

Rietveld structure analysis showed the emptying of C2 site at about 200°C, and the transformation of TMA residual molecules into trimethylamine during this step. TMA degradation is complete at about 500°C. Na content in the 8-ring channel is affected by NH_4-exchange and also by the calcination process. Variations of the T-O distances and T-O-T angles indicate that charge imbalance due to the Hoffmann degradation of TMA and to calcinations of NH_4 could be compensated by Brønsted acid sites. They are located on framework oxygen atoms O2 and O5, which are bonded to T1 and T2 tetrahedra, respectively, in good agreement with the location of Brønsted sites obtained by combined X-ray and neutron diffraction study [3].

References. [1] D. McQueen, B.H. Chiche, F. Fajula, A. Auroux, C. Guimon, F. Fitoussi, P. Schulz, *J. Catal.*, **161**, 587-596, 1996; [2] A. Martucci, A. Alberti, M. de Lourdes Guzman-Castillo, F. Di Renzo, F. Fajulab, *Micropor. Mesopor. Mat.*, **63**, 33-42, 2003; [3] I. Parodi, M.C. Dalconi, G. Cruciani, A. Alberti, *VIII AIZ Congress*, 2007.

THERMAL BEHAVIOUR OF ZEOLITE GMELINITE: A COMBINED SINGLE CRYSTAL AND POWDER X-RAY DIFFRACTION STUDY

I. Parodi, A. Martucci, G. Cruciani, M.C. Dalconi, A. Alberti

Dipartimento di Scienze della Terra, Università di Ferrara, Italy
prdlri@unife.it

Zeolite gmelinite is a quite rare natural zeolite, whose crystal structure can be described as an ABAB sequence of double 6-rings of tetrahedra. The resulting framework structure consists in a two-channel system: a one-dimensional channel parallel to [001] bounded by 12-rings, interconnected by a two-dimensional channel bounded by 8-rings. The crystal structure of gmelinite was solved by Fisher [1] and refined by Galli *et al*. [2] in the -Na and -Ca natural forms and by Vezzalini *et al*. [3] in the -K natural form.

The aim of this study is to give an exhaustive description of the thermal behaviour of gmelinite, from -173°C to 800°C, by combining X-ray single crystal and powder diffraction. Thermal behaviour of zeolites is very important for industrial applications, and it depends on many parameters, such as: synthesis conditions, topology, exchangeable cations, exchange modalities, chemical composition, order-disorder in the frameworks, ion distribution and occupancies, localization of acid sites and many others.

The sample used for this study is a gmelinite-Na from Flinders, Victoria, Australia.

A first single crystal data collection was performed with a Nonius 4-Circle Diffractometer equipped with a CCD. Crystal structure refinement confirmed the structural features found by Galli *et al.* [2]. The space group was $P6_3/mmc$ and two extraframework cation sites and three water molecules were recognized. Structure refinement of a single crystal cooled to 100 K showed a lowering of gmelinite symmetry (space group $P31c$), and remarkable modifications in extraframework content. After heating at 50, 75 and 90°C single crystal refinements showed that the dehydration is completed at 75°C. The heating at 100°C caused the fragmentation of crystal. Powders of this sample were heated from 130°C till amorphization, at 880°C, and diffraction patterns collected *ex situ* showed gmelinite is stable till 300°C. Above this temperature a new phase with AlPO-5 topology, (AFI) [4], appears. This is stable up to 800°C. Moreover, *in situ* time resolved synchrotron diffraction data were collected on the GILDA beamline (ESRF, Grenoble). Rietveld refinements showed that transition from gmelinite to AFI occurs with the formation of a transient phase, whose unit cell parameters do not correspond to any structure found in the database.

References. [1] K. Fisher, *N. Jb. Miner. Mh*., 1-13, 1966; [2] E. Galli, E. Passaglia, P.F. Zanazzi, *N. Jb. Miner. Mh*., 145-155, 1982; [3] G. Vezzalini, S. Quartieri, E. Passaglia *, N. Jb. Miner. Mh*., 504-516, 1990; [4] J.M. Bennett, J.P. Cohen, E.M. Flanigen, J.J. Pluth, J.V. Smith, *ACS Symp. Series*, **218**, *Am. Chem. Soc*., 109, 1983.

MATERIALS, FROM EARTH AND LAB TO LIFE - 1

Session 10
Crystal-chemical models for minerals families

CRYSTAL-CHEMICAL MODELS TO DESCRIBE MOLECULAR STRUCTURE OF ARSENIC SULFIDES AND THEIR CHANGES INDUCED BY EXPOSURE TO LIGHT

P. Bonazzi

Dipartimento di Scienze della Terra, Università di Firenze, Italy
paola.bonazzi@unifi.it

Synthetic and natural arsenic sulfides, as well as bulk glasses and thin films in the As-S system, are widely studied for their potential or actual application in optics and optoelectronics, for their use as semiconducting component of thin devices, as well as for medical applications.Due to their vivid colours, ranging from yellow to orange or red, in the past arsenic sulfide minerals were largely used as pigments, so that the study of their light-induced alteration finds application in the examination and conservation of works of art.

In the As-S system, several compounds with different As:S ratios are known as minerals. They include duranusite, As_4S, α- and β-dimorphites, As_4S_3, realgar and pararealgar, As_4S_4, uzonite, As_4S_5, alacranite, As_8S_9, and orpiment, As_2S_3. The high-temperature polymorph β-As_4S_4 was also found as a natural phase. Non-stoichiometric sulfides with chemical composition ranging from As_4S_4 to As_8S_9 have been also reported.

Most of arsenic sulfides have a crystal structure consisting of a packing of cage-like, covalently bonded As_4S_n (n = 3, 4 and 5) molecules held together by weak interactions of van der Waals character, whereas orpiment exhibits a layered structural arrangement. The structure of wakabayashilite, ideally $[As_2S_3]_3[As_4S_5]$, consists of bundle-like units and As_4S_5 cage-like molecules.

In the context of this communication, emphasis will be put on the arsenic sulfides having molecular structures and on the effects of their exposure to visible light. Their structures will be compared in terms of molecular packing and molecular parameters which can represent useful tools to evaluate the degree of sulfur saturation in this kind of molecules.

Roberts *et al.* [1] first clarified that the yellow film commonly covering altered realgar consists of pararealgar and not orpiment as previously proposed. Since that time, many studies [2-6] have focused on the effects of the exposure of realgar or other arsenic sulfides to light. From the results of these studies it is now clear that light-induced alteration of realgar and β-phase towards pararealgar proceeds through an increase of the amount of the As_4S_5 molecules related to the following reaction: $5As_4S_4$ (realgar-type) + $3O_2 \rightarrow 4As_4S_5 + 2As_2O_3$. The additional sulfur would be then released by breaking an As-S-As linkage to form pararealgar: $As_4S_5 \rightarrow As_4S_4$ (pararealgar-type) + S. The process could cyclically continue by re-attachment of the free S to another As_4S_4 (realgar-type). When a complete conversion to pararealgar is reached, the original As/S ratio is restored by sulfur release, which was supposed to occur by SO_x emission [5]. A comparison between the effect of light exposure on different arsenic sulfides reveals that the As_4S_4 molecule is able to incorporate S to convert to As_4S_5, whereas either As_4S_3 or As_4S_5 molecules do not undergo any modification [4]. The extent of sulfur incorporation, however, appears to be strictly controlled also by the type of molecular packing.

References. [1] A.C. Roberts, H.G. Ansell, M. Bonardi, *Canad. Mineral*., **18**, 525-527, 1980; [2] D.L. Douglass, C. Shing, G. Wang, *Am. Mineral*., **77**, 1266-1274, 1992; [3] A. Kyono, M. Kimata, T. Hatta, *Am. Mineral*., **90**, 1563-1570, 2005; [4] P. Bonazzi, L. Bindi, G. Pratesi, S. Menchetti, *Am. Mineral*., **91**, 1323-1330, 2006; [5] P. Ballirano, A. Maras, *Eur. J. Mineral*., **18**, 589-599, 2006; [6] L. Bindi, P. Bonazzi, *Am. Mineral.*, **92**, 617-620, 2007.

CATION ORDERING AND MICROSTRUCTURES IN COLUMBITE

S.C. Tarantino[1], M. Zema[1], G.C. Capitani[2], M. Scavini[3], M. Brunelli[4], P. Ghigna[5]

[1]*Dipartimento di Scienze della Terra, Università di Pavia, Italy*
[2]*Dipartimento Geomineralogico, Università di Bari, Italy*
[3]*Dipartimento di Chimica Fisica ed Elettrochimica, Università di Milano, Italy*
[4]*ESRF, Grenoble, France*
[5]*Dipartimento di Chimica Fisica, Università di Pavia, Italy*
michele.zema@unipv.it

The mechanism of the intracrystalline cation exchange reaction in a natural columbite sample from Kragero, with composition $(Mn_{0.85}Fe_{0.15})(Nb_{1.8}Ta_{0.2})O_6$, has been characterised by means of TEM and HR synchrotron-radiation powder diffraction. In columbite, cations may occupy two different octahedral sites, with divalent cations preferring the A site and pentavalent cations preferring the B site. When both the octahedral sites are randomly occupied, columbite adopts the α-PbO_2-type crystal structure; ordering of divalent cations on A sites and pentavalent cations on B sites gives rise to an ...ABBABB... sequence along the *a* direction resulting in a tri-α-PbO_2-type structure in which the *Pbcn* symmetry is maintained. The completely ordered scheme represents the only thermodynamically stable state. Nevertheless, partially disordered distributions of cations among the sites are often found in natural samples. High temperature treatment of these samples leads to the completely ordered state [1,2].

Two single crystals with different degrees of order obtained by quenching experiments were prepared for TEM study. They revealed a pervasive presence of nanosized domains with rhombic shape and sides parallel to (310) planes. Diffraction contrast images and high resolution images clearly show that rhombic domains are ordered and dispersed in a disordered matrix.

In situ high temperature powder diffraction data collected at ESRF ID31 starting from untreated powders (degree of cation order $Q \sim 0.15$) and until completion of the ordering process shows that the sluggish cation ordering process in columbite is more complicated than the simple picture which is deducible from laboratory X-ray diffraction studies. The diffraction patterns show split reflections and require analysis using two distinct columbite phases with different degrees of order. The phase characterised by a higher Q value has slightly broader peak profiles. This is consistent with TEM observations of some small ordered domains in a largely disordered material. Furthermore the size of these ordered domains in the starting material, as derived by peak-profile analysis, is also consistent with TEM observations. Preliminary Rietveld analyses exclude a nucleation and growth model followed by coarsening of the domains, and indicate two stages for the cation ordering mechanism: a first stage in which the degree of order increases and the domains size remains nearly constant and a second one in which the growth of the domains accompanies the achievement of the complete cation order. PDF (Pair Distribution Function) analysis of patterns collected at different Q will allow to give further insights and a better understanding of the factors controlling the columbite ordering process.

References. [1] T.S. Ercit, M.A. Wise, P. Černý, *Am. Mineral*., **80**, 613-619, 1995; [2] S.C. Tarantino, M. Zema, *Am. Mineral*., **90**, 1291-1299, 2005.

PRESSURE-INDUCED OVER-HYDRATION OF ZEOLITES: A REVIEW AND NEW INSIGHTS FROM GISMONDINE

G. Vezzalini

Dipartimento di Scienze della Terra, Università di Modena e Reggio Emilia, Modena, Italia
giovanna@unimo.it

High-pressure (HP) structural studies on zeolites compressed in aqueous media have recently attracted great interest on the so-called pressure-induced hydration (PIH) phenomenon which is characterized by the penetration of additional water molecules into the zeolite channels. This over-hydration, and the consequent structural modifications, can in principle significantly modify the zeolite properties, opening possible new scenarios for their industrial applications.

A number of experiments performed compressing zeolites in hydrous ambient suggests the possible entry of water molecules into the porosities, only on the basis of a positive volume discontinuity, without the support of detailed structural data. Until now, certain signs of water sorption from an alcohol-based P-transmitting medium into zeolite pores were evidenced by detailed structural refinements of partially dehydrated laumontite and of the following fibrous zeolites: natrolite, tetranatrolite, synthetic potassium gallosilicate natrolite; scolecite and thomsonite.

In this contribution we review the present scenario of the HP experiments performed on zeolites using aqueous penetrating media and discuss new results on the PIH of gismondine (ideal formula $Ca_4Al_8Si_8O_{32}\cdot 16H_2O$, s.g. $P2_1/c$) obtained by a combined experimental-computational approach based on *in situ* HP synchrotron X-ray powder diffraction [1] and *ab initio* molecular dynamics simulations [2]. The study was performed from P_{amb} to 7.9 GPa, and upon decompression, using methanol:ethanol:water (16:3:1) mixture (m.e.w.) as nominally penetrating hydrostatic P-transmitting medium. From 0.6 GPa, the water content results slightly higher than the initial one, as a result of a moderate over-hydration. Moreover, at about 2 GPa, a significant water molecule system re-arrangement occurs, characterized by an ordering of part of the water molecules from four partially occupied sites to only two fully occupied ones. The over-hydration, but not the water ordering, is substantially irreversible upon pressure release. The Rietveld structural refinements of the powder patterns converged up to 2.8 GPa; above this pressure, a phase transition to triclinic symmetry was observed and only the unit cell parameters were successfully refined. The structural details of the triclinic phase have been investigated by Car-Parrinello molecular dynamics calculations, performed on the basis of the unit cell parameters derived by the refinement of the experimental data. The first results of this combined experimental-computational approach suggest that the monoclinic-triclinic phase transition is driven by the following effects: i) strong framework deformations, occurring mainly via an enhanced zigzag behaviour of the double-4-membered-ring-chains which form gismondine framework, and the consequent squashing of the channel apertures; ii) changes in the coordination polyhedra of two of the four Ca cations present in gismondine unit cell, which are compatible with the experimentally observed symmetry lowering.

A last important result derives from the comparison of the overall cell volume reductions and of the bulk modula of gismondine compressed in m.e.w. and in silicone oil: this is the unique zeolite with a higher compressibility in penetrating *vs*. non-penetrating P-transmitting media. In fact, the re-organization of the water molecule system upon compression in m.e.w., which leaves a larger free volume inside the pores with respect to the phase compressed in silicone oil.

References. [1] S. Ori, S. Quartieri, G. Vezzalini, V. Dmitriev, *Am. Mineral.*, **93**, in press; [2] S. Quartieri, E. Fois, G. Vezzalini, E. Mazzucato, G. Tabacchi, in preparation.

HP-HT PHASE STABILITY OF SULPHATES

P. Comodi[1], S. Nazzareni[1], L. Dubrovinsky[2], M. Merlini[3]

[1]*Dipartimento di Scienze della Terra, Università di Perugia, Italy*
[2]*Bayerisches Geoinstitut Bayreuth University, Bayreuth, Germany*
[3]*ESRF, Grenoble, France*
comodip@unipg.it

Sulphates are important minerals in Earth as well as in material sciences. The development of excess pore fluid pressures by their dehydration may cause a decrease in strength, thus favouring brittle failure [1] with hydrofracturing and faulting may take place due to fluid overpressure. Sulphates play a key role in regulating the hydration reaction rate during the early stages of setting and hardening of Portland cement. Notwithstanding the dehydration of gypsum under room condition was studied, its baric behaviour and the evolution with temperature, the phase transitions as well as the P/T gradient of the dehydration are almost completely unknown. We present the results of several X-ray diffraction experiments on gypsum and bassanite (single-crystal and powder samples) performed at the synchrotron sources of Chicago (APS, GSECARS-BM13 beamline) and Grenoble (ESRF ID-09 beamline). We used diamond cells charged with different pressure media: He, Ne, Ar and with external heaters. Both Raman spectra and X-ray diffraction data were collected simultaneously at ID-09. The pressure range investigated was 0.001 up to 30 GPa along four isotherms: 20, 50, 110 and 200°C.

The main results are:

- Gypsum (Gypsum I) underwent two phase transitions at about 4.5 GPa (Gypsum II) and at 8 GPa (Gypsum III) at room condition. After the first phase transition the systematic absent reflections indicated the reduction of symmetry from $C2/c$ to $P2_1/n$. In the Raman spectra the phase transition was marked with a splitting of the ν_1 sulphate mode and the appearance of additional modes. The lattice parameters measured after the phase transition showed a large discontinuity in the *b* parameter whereas the *a* and *c* parameters maintained the same compressibility. The bulk modulus of Gypsum II was 72(9) GPa, higher than that measured in Gypsum I [2]: 43(1) GPa. The pressure of the phase transition slightly increased with temperature as indicated by the data collected along the 50 and 100°C isotherms. Both phase transitions were completely reversible as showed by the diffraction pattern collected from the recovered sample. These data indicated that the dehydration of gypsum did not occur by increasing pressure only, in a confining space such as that of the diamond anvil cell.

- The equation of state of bassanite was determined by measuring the lattice parameters along the 20 and 100°C isotherms up to about 30 GPa. A phase transition was observed at 9.2 GPa and room temperature and then followed with temperature increase (for details see, Comodi *et al*., this meeting).

- The pressure dependence of the dehydration process was followed along the 2 and 5 GPa isobars, by increasing temperature up to 200°C. Bassanite appeared at 0.2 GPa at 85°C [3] from Gypsum I, at 109°C and 2.5 GPa from Gypsum II, and at 125°C and 6.1 GPa from Gypsum II, defining a slightly positive slope of the dehydration process. No rehydration occurred when temperature was decreased.

References. [1] H.C. Heard, W.W. Rubey, *Soc. Am. Bull.*, **77**, 118-126, 1966; [2] P. Comodi, S. Nazzareni, P.F. Zanazzi, S. Speziale, *Am. Mineral.*, in press, 2007; [3] P.S.R. Prasad, A. Pradhan, T.N. Gowd, *Curr. Sci. India*, **80**, 1202-1207, 2001.

OD CHARACTER AND STRUCTURAL FEATURES OF SIDERONATRITE, $Na_2Fe(SO_4)_2(OH)\cdot 3H_2O$

F. Scordari, G. Ventruti

Dipartimento Geomineralogico, Università di Bari, Italy
f.scordari@geomin.uniba.it

Sideronatrite is a secondary hydrated sulfate of sodium and ferric iron occurring in nature as a result of pyrite alteration. For this reasons it is one of the environmental indicators of soil-water processes operating in specific landscapes, and, such as, an important marker of acid mine drainage pollution. This mineral is quoted in literature as orthorhombic with space group *Pnnm* or *Pnn*2 [1]. Scordari [2], analyzing a sample from desertic sulfate deposits of Northern Chile, first recognized the OD character of the structure on the basis of its peculiar diffraction pattern (coexistence of sharp spot for $l = 2n$ and diffuse streaks along **b*** for $l = 2n+1$). The small dimensions and the extensive disorder shown by this sample hampered to date a complete structural determination.

In this work, a crystal showing very weak diffuse streaks proved to be suitable for a single crystal X-ray diffraction study. The crystal structure has been solved by direct methods and refined in the space group $P2_12_12_1$ with a = 7.265(2), b = 20.522 (6), c = 7.120 (2) Å; V = 1061.5(5) Å^3; Z = 4, by full matrix least-squares (R = 8.4% and R_w = 9.3%) using 810 reflections with $I > 3.0\ \sigma(I)$.

Sideronatrite is characterized by infinite $[Fe^{3+}(SO_4)_2(OH)]$ octahedral-tetrahedral chains of the type $[M(TO_4)_2\phi]$ running parallel to the **c** axis. The same topology is also present in guildite [2,3]. These chains are cross-linked by a chains system of corner-sharing Na distorted octahedra along **c** to form corrugated sheets parallel to the (010) plane. Adjacent sheets are hydrogen-bonded through water molecules. The weak hydrogen bonds, the easy coming in/out of two water molecules seem to be the main factors which affect the stability of the sideronatrite making easy and reversible the transformation of sideronatrite into metasideronatrite and vice versa.

The OD character will be discussed in the light of the structural results, *i.e.*, the peculiar disorder and the building layer and the possible MDO polytypes.

References. [1] H. Strunz, E.H. Nichel, *Strunz Mineralogical Tables. Chemical Structural Mineral Classification System*, 9th ed., 870 S., 226 Abb., Best.-Nr. 13-3509; [2] F. Scordari, *Tschermaks Min. Petr. Mitt.*, **28**, 315-319, 1981; [3] C. Wan, S. Ghose, G.R. Rossman, *Am. Mineral.*, **63**, 478-483, 1978.

OD-CHARACTER AND TWINNING IN THE STRUCTURE OF A NEW SYNTHETIC TITANOSILICATE: $(Ba,Sr)_4Ti_6Si_4O_{24}\cdot H_2O$

M. Cadoni[1], A. Bloise[1,2], G. Ferraris[1], S. Merlino[3]

[1]*Dipartimento di Scienze Mineralogiche e Petrologiche, Università di Torino, Italy*
[2]*Dipartimento di Scienze della Terra, Università della Calabria, Italy*
[3]*Dipartimento di Scienze della Terra, Università di Pisa, Italy*
marcella.cadoni@unito.it

As side-product of a hydrothermal run (160 h, externally heated vessel, 400°C, 1 kbar, alkaline conditions) to synthesise lamprophyllite, $Na_3(SrNa)Ti_3(Si_2O_7)_2O_2(OH)_2$, we have obtained prismatic crystals of $(Ba,Sr)_4Ti_6Si_4O_{24}\cdot H_2O$ (TR02), with length up to 100 μm, associated to matsubaraite, $Sr_4Ti_5O_8(Si_2O_7)_2$. Electron-microprobe analyses show that crystals are inhomogeneous being $4.0 < Ba/Sr < 0.7$. Single-crystal X-ray diffraction data of TR02 have been collected on a Bruker-AXS Smart Apex diffractometer (CCD, Mo*K*α radiation) according to an orthorhombic cell (a_o 5.906, b_o 20.618, c_o 16.719 Å). The structure solved by direct methods in *Cmmm* shows ordered and (Ba,Sr)-Si-disordered (001) slabs alternating along [001] (Fig. 1). The situation is quite similar to that recently observed in vurroite [1], whose real structure has been defined through the application of OD theory [2]. Although no streaking of reflections has been observed, the OD character of TR02 is revealed by the non-space-group absences of the reflections with $2h+2k+l = 2n+1$. The basic OD layer has layer-group symmetry *Cmmm*, with translation vectors $\mathbf{a} = \mathbf{a}_o$, $\mathbf{b} = \mathbf{b}_o$ and non-translation vector $\mathbf{c}_o/2$; adjacent layers are related by stacking vectors $\mathbf{t}_1 = \mathbf{c}_o/2+(\mathbf{a}+\mathbf{b})/4$ and $\mathbf{t}_2 = \mathbf{c}_o/2+(\mathbf{a}-\mathbf{b})/4$, both giving rise to pairs of geometrically equivalent layers. Among the infinite polytypes generated by different sequences of $\mathbf{t}_1$ and $\mathbf{t}_2$, the two sequences $\mathbf{t}_1\mathbf{t}_1\mathbf{t}_1\ldots$ (or $\mathbf{t}_2\mathbf{t}_2\mathbf{t}_2\ldots$) and $\mathbf{t}_1\mathbf{t}_2\mathbf{t}_1\mathbf{t}_2\ldots$correspond to the two structures with maximum degree of order: MDO1 (2*M* polytype) and MDO2 (4*O* polytype), respectively. The structure models for MDO1 (a_{2M} 5.906, b_{2M} 16.719, c_{2M} 10.735 Å, β 105.98°, *P*2/*c*, Fig. 2) and MDO2 (a_{4O} 5.906, b_{4O} 20.618, c_{4O} 33.438 Å, *Fddd*, Fig. 3) have been obtained. Refinement based on the experimental diffraction pattern, showed that only the 2*M* polytype occurs in our sample and that the measured crystal is affected by (001) twinning by merohedry (2*M* cell). In the structure (indices according to Fig. 1) infinite (010) ribbons of Ti-octahedra run along [100] and are connected by $(SiO_3)_4$ four-membered rings, thus realising a new type of heteropolyhedral framework. The ribbon represents a three-octahedron wide slice of the octahedral sheet occurring in perrierite-(Ce), $Ce_4MgFe_2Ti_2O_8(Si_2O_7)_2$ [3].

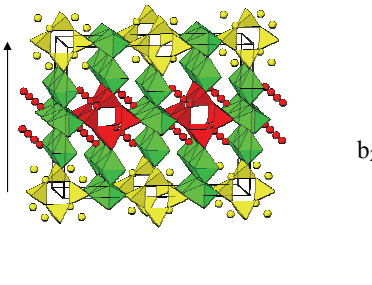

Fig. 2 – Refined structure of the ordered 2*M* polytype *P*2/*c*.

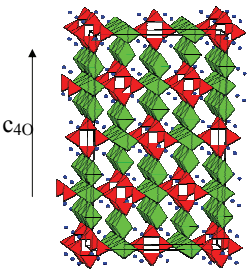

Fig. 3 – Model structure of the ordered 2*O* polytype *Fddd*.

References. [1] D. Pinto, E. Bonaccorsi, T. Balić-Žunić, E. Makovicky, *Am. Mineral*, **93**, 713-727, 2008; [2] G. Ferraris, E. Makovicky, S. Merlino, *Crystallography of Modular Materials*. IUCr/Oxford University Press (2008); [3] G. Gottardi, *Am. Mineral.*, **45**, 1-14, 1960.

THE CRYSTAL STRUCTURE AND CRYSTAL CHEMISTRY OF JINSHAJIANGITE, A GROUP-II Ti DISILICATE MINERAL

F. Cámara[1], E. Sokolova[2], F.C. Hawthorne[2], Y. Abdu[2]

[1]*CNR - Istituto di Geoscienze e Georisorse, Unità di Pavia, Italy*
[2]*Department of Geological Sciences, University of Manitoba, Winnipeg, Canada*
camara@crystal.unipv.it

Currently, the crystal structures of about 120 Ti-O compounds minerals are known, half of them Ti silicates and half of them Ti oxides. Ti disilicates constitute more than 30% of Ti silicates. Sokolova [1] considered structural hierarchy and stereochemistry for twenty-four titanium disilicate minerals. Those structures contain the TS (titanium-silicate) block, a trioctahedral central (O) sheet and two adjacent heteropolyhedral (H) sheets consisting of different polyhedra including (Si_2O_7) groups. She divided them into four groups, characterized by different topology and stereochemistry of the TS block. Each group of structures has a different linkage of H and O sheets in the TS block, and a different arrangement of Ti (= Ti + Nb) polyhedra. In a structure, the TS block can alternate with another block, an intermediate (**I**) block, so called as it is intercalated between two TS blocks. In Groups I, II III and IV, Ti equals 1, 2, 3 and 4 *apfu*, respectively. Jinshajiangite [2] was not considered by Sokolova [1] as its structure was unknown. We will report on the structure of jinshajiangite as a continuation of our work on Ti disilicate minerals with the TS block. The crystal structure of jinshajiangite, ideally $BaNaTi_2Fe^{2+}_4(Si_2O_7)_2O_2(OH)_2F$, *a* 10.6785(8), *b* 13.786(1), *c* 20.700(2) Å, β 94.937(1)°, *V* 3035.93(6) Å^3, space group *C*2/*m*, *Z* = 8, $D_{calc.}$ 3.703 g/cm^3, from Norra Kärr, Tönköping province, Sweden, has been refined to R_1 5.7% on the basis of 3193 unique reflections ($F_o > 4\sigma F$). Electron microprobe analysis gave (wt.%): SiO_2 27.56, Nb_2O_5 0.12, TiO_2 18.36, FeO 23.42, Fe_2O_3 2.89 [the Fe^{3+}/Fe_{tot} ratio of 0.10(9) was determined by Mössbauer spectroscopy], MnO 5.13, MgO 0.44, CaO 2.52, BaO 10.24, K_2O 1.95, Na_2O 2.27, Cs_2O 0.03, F 2.33, H_2O 2.00 (calc. from structure-topology requirements: OH + F = 3 *apfu*), O=F –0.98, total 98.79. The crystal structure of jinshajiangite can be described as a combination of a TS block and an **I** block. In the O sheet, there are five Fe^{2+}-dominant M^O sites which give ideally Fe^{2+}_4 *pfu*. In the H sheet, there are three [6]-coordinated M^H sites solely occupied by Ti (they give Ti = 2 *apfu*) and four *Si* sites. The M^H octahedra and (Si_2O_7) groups constitute the H sheet. Jinshajiangit is a Group-II mineral: Ti equals 2 *apfu* and it occurs in the H sheet. Linkage of H and O sheets *via* common vertices of M^H octahedra and (Si_2O_7) groups with M^O octahedra results in a TS block. The topology of the TS block is as in Group II of the Ti disilicate minerals (Ti = 2 *apfu*). There are six interstitial sites, three [10-9]-coordinated Ba-dominant A^P sites and three [10]-coordinated Na-dominant B^P sites. The total content of three A^P and three B^P sites is ideally 1 Ba and 1 Na *pfu*, respectively. Along **c**, the TS *blocks* link *via* common vertices of M^H octahedra (as in astrophyllite-group minerals) and the A^P and B^P sites which constitute the **I** block. Jinshajiangite, ideally $BaNaTi_2Fe^{2+}_4(Si_2O_7)_2O_2(OH)_2F$, is a Fe^{2+} analogue of perraultite, ideally $BaNaTi_2Mn^{2+}_4(Si_2O_7)_2O_2OH_2F$, space group *C*2 and its crystal structure is topologically identical to that of perraultite [3].The revised crystal chemistry of Group II of Ti disilicate minerals is discussed.

References. [1] E. Sokolova, *Can. Mineral*., **44**, 1273-1330, 2006; [2] W. Hong, P. Fu, *Geochemistry* (*China*), **1**, 458-464, 1982; [3] N.A. Yamnova, Yu.K. Egorov-Tismenko, I.V. Pekov, *Crystallogr. Rep.*+, **43**, 401-410, 1998.

THE MONOCLINIC POLYMORPH OF $Ba_2MgSi_2O_7$ AND ITS RELATIONSHIPS TO THE MELILITE-TYPE STRUCTURE

M. Ardit[1,2], G. Cruciani[1], M. Dondi[2]

[1]*Dipartimento di Scienze della Terra, Università di Ferrara, Italy;* [2]*CNR-ISTEC, Faenza, Italy*
cru@unife.it

Melilite-related compounds of general formula $X_2T^1T^2_2O_7$ (with X = large mono- to trivalent cations; T^1 and T^2 = small di- to tetravalent cations) are widespread over many classes of minerals and materials. Melilites are typical constituents of some ultramafic rocks (*e.g.* alnöite and melilitites) and also occur in extra-terrestrial materials (*e.g.* in carbonaceous chondrites). Their synthetic analogues have attracted considerable interest in different technological fields: ceramics, glasses, luminescent materials, low-dimensional magnets, etc. The (average) crystal structure of melilite-type compounds can be described in the $P\bar{4}2_1m$ space group. The presence of an incommensurately modulated (IC) structure in some melilite compositions (*e.g.* åkermanite) has received much attention and many studies have been devoted to its determination and to transitions from IC to normal (N) or lock-in phases as a function of temperature, pressure and chemistry. Much less attention has been paid to the occurrence of compounds having melilite stoichiometry but with reduced symmetry and, more important, different sheet topology compared to melilites [1]. $Ba_2MgSi_2O_7$ was suggested as a compound which could not crystallize with a melilite-type structure [2] but only with a $Ba_2CuSi_2O_7$-type [3] monoclinic structure. This suggestion was later confuted by a single-crystal refinement of $Ba_2MgSi_2O_7$ in the s.g. $P\bar{4}2_1m$ [4]. Nevertheless, the same dichotomy was found for $Ba_2CoSi_2O_7$ where opposing claims for $P\bar{4}2_1m$ [5] or $C2/c$ [6] structures exist. Recently, monoclinic structure refinements of Eu:$Ba_2MgSi_2O_7$ have been also reported [7,8]. However, none of the above reports attempted to solve the dichotomy, based on the different sheet topology. Aim of this contribution is to provide a better understanding of the relationships between the two polymorphs of $Ba_2MgSi_2O_7$ starting from a new Rietveld refinement of the monoclinic form.

During a systematic synthesis and characterization work of Co-doped Sr- and Ba-melilites, we obtained a nearly monophasic sample of $Ba_2MgSi_2O_7$ whose structure was successfully Rietveld refined in the $C2/c$ space group starting from the model of [6], with Mg replacing Co.

Similarly to the melilite-type polymorph the monoclinic structure consists of Si_2O_7 dimers connected by MgO_4 tetrahedra to form tetrahedral sheets parallel to the *ac* plane (*vs.* the *ab* plane in the $P\bar{4}2_1m$ structure). The first major difference between the two polymorphs is in the coordination polyhedron of Ba: a distorted square antiprism (4 ligands above + 4 below) in the tetragonal and a 3 + 5 configuration in the monoclinic form. More important is the difference in the sheet topology: only five-membered rings of tetrahedra in the tetragonal form while four- and six membered rings in the monoclinic one. This implies that the mechanism to switch between the two polymorphs must be of reconstructive nature and is not related to any IC-N or lock-in transition. We suggest that the misfit between the interlayer and tetrahedral sheets in $Ba_2MgSi_2O_7$ is reversed compared to that causing the IC structure in the tetragonal form. The monoclinic structure is the most stable form at low-T, always found in powders from solid state reactions (as in our case), while the tetragonal polymorph is a metastable form at low-T, quenched from high-T, usually found in single crystals obtained by a melt.

References. [1] T. Armbruster, F. Rothlisberger, F. Seifert, *Am. Mineral*., **75**, 847-858, 1990; [2] F. Rothlisberger, F. Seifert, M. Czank, *Eur. J. Mineral*., **2**, 585-594, 1990; [3] Yu.A. Malinovskii, *Sov. Phys. Dokl*., **29**, 706, 1984; [4] M. Shimizu, M. Kimata, I. Lida, *N. Jb. Miner. Monat.*, **1**, 39-47, 1995; [5] B. El Bali, P.Y. Zavalij, *Acta Crystallogr.*, *E***59**, i59-i61, 2003; [6] R.D. Adams, R. Layland, C. Payen, T. Datta, *Inorg. Chem.*, **35**, 3492-97, 1996; [7] A. Komeno, K. Uemastu, K. Toda, M. Sato, *J. All. Comp.*, **408-412**, 871-874, 2006; [8] T. Aitasalo J. Holsa, T. Laamanen, M. Lastusaari, L. Lehto, J. Niittykoski, F. Pelle, *Z. Kristallogr.,* Suppl., **23**, 481-486, 2006.

RIETVELD REFINEMENTS OF SIZE-STABILIZED NANO-CRYSTALLINE TETRAGONAL ZIRCONIA

G. Borghini[1], M. Dapiaggi[1], F. Maglia[2], E.S. Ferrari[1]

[1]*Dipartimento di Scienze della Terra, Università di Milano, Italy*
[2]*Dipartimento di Chimica Fisica, Università di Pavia, Italy*
giulio.borghini@unige.it

Zirconia (ZrO_2) primarily exists in three different polymorphs at ambient pressure: monoclinic (room temperature - 1175°C), tetragonal (1175 - 2370°C), and cubic (2370 - 2680°C). The high-temperature ZrO_2 phases are suitable for various industrial applications such as solid electrolytes in solid oxide fuel cells and sensors, as a catalyst/catalyst support, and as membranes and dispersed phase in composite materials. Traditionally, high temperature ZrO_2 phases have been stabilized at room temperature by doping trivalent cations, such as Y, in the ZrO_2 lattice. The high-temperature phases (cubic or tetragonal) can also be stabilized at room temperature without doping, provided ZrO_2 is synthesized in its nanocrystalline form with size less than a critical nanosize (about 20-30 nm). Five different ZrO_2 samples were studied, with the following compositions: sample 1 (pure ZrO_2, no doping), sample 2 (0.5% Y), sample 3 (1% Y), sample 4 (2% Y) and sample 5 (4% Y).

Data were collected at the European Synchrotron Radiation Facility in Grenoble, at beamline ID31 with a wavelength of about 0.4 Å, up to d = 0.23 Å for a high resolution in the reciprocal space. Only samples with the higher doping degree (2-4 wt.%) were monophasic, while the others showed the presence of various (though small) amounts of monoclinic zirconia. Even though sample 5 (Y = 4 wt.%) could have been easily refined with the cubic cell, all the datasets were refined using the tetragonal cell for an easier comparison of the results. The tetragonal distortion is small for all the samples and it has been measured by the tetragonality degree ($c_{tetr} / a_{tetr}\sqrt{2}$), which decreases with increasing Y content, and is almost 1 for the sample with Y = 4 wt.%. Particular attention was applied for the evaluation of the microstructural features of the various samples: volume weighted crystallite size and RMS microstrain were estimated. The samples resulted to be truly nano-crystalline: crystallite size were around 15 nm for Y ranging from 1 to 4 wt.% and fairly larger for the other two samples (about 40 nm). An interesting effect could be noticed when correlating the microstrain values with the dopant content: RMS microstrain increases with dopant content reaching high values in the sample with 4 wt.% yttrium. This effect can be explained with local deformations of the structure around Y atoms: for a better understanding of the local behavior, however, the samples were also studied using total scattering techniques [1].

References. [1] M. Dapiaggi, G. Borghini, F. Maglia, E.S. Ferrari*, This meeting*.

As-Nb SOLID SOLUTION IN β-FERGUSONITE-(Y) FROM MOUNT CERVANDONE

F. Cámara[1], A. Guastoni[2], F. Nestola[2]

[1]*C.N.R. - IGG, Unità di Pavia, Italy*
[2]*Dipartimento di Geoscienze, Università di Padova, Italy*
camara@crystal.unipv.it

An arsenic-rich β-fergusonite has been collected at Mount Cervandone (Verbano-Cusio-Ossola, Devero valley, Western Alps, Italy). Its crystal structure has been determined by single crystal X-ray diffraction using a Bruker-AXS diffractometer equipped with a CCD detector: it is monoclinic *I*2/*a*, *a* = 5.1794(14) Å, *b* = 11.089(3) Å, *c* = 5.1176(14) Å, β = 91.282(8)°, *V* = 293.87(14) Å^3. The chemical composition has been analyzed on the same crystal studied by X-ray diffraction giving $(Y_{0.70}Dy_{0.07}Er_{0.05}Ca^{2+}_{0.05}Gd_{0.02}Tb_{0.01}Yb_{0.01}Th^{4+}_{0.01}U^{4+}_{0.02})_{\Sigma=0.94}(Nb^{5+}_{0.68}As^{5+}_{0.27}W^{6+}_{0.06}Ta^{5+}_{0.01}Si^{4+}_{0.01})_{\Sigma=1.03}O_4$. β-fergusonite occurs as pseudo-bipyramidal crystals up to 1 mm length (Fig. 1), green-yellow in colour under incandescent light. The mineral is associated with orange-yellow barrel-shape hexagonal synchysite-(Ce) [Ca(Ce,La)$(CO_3)_2$F] crystals, up to 2 mm in length. Both are found in a cavity of Alpine type quartz veins which intersect pegmatite dikes, in the two-mica fine grained leucocratic gneisses of Mount Cervandone, which can be described as metamorphosed leucogranitic-aplitic rocks. The pegmatites show a unequivocal strong NYF (niobium-yttrium-fluorine) geochemical signature represented by the occurrence of an unique mineralogy that includes aeschynite-(Y), agardite-(Y), Nb-rich anatase, cervandonite-(Ce), chernovite-(Y), crichtonite-senaite group minerals, fergusonite-(Y), fluorite, gadolinite-(Y), monazite-(Ce), paraniite-(Y), Nb-rich rutile, synchysite-(Ce), and xenotime-(Y). Isovalent substitution of Nb by As occurs in the 4-fold coordinated site, which decreases mean bond length from 1.894 Å in pure β-fergusonite [1] to 1.807 Å in the sample studied, corresponding to a 10% reduction of the polyhedral volume and a significant reduction of polyhedral distortion (TAV decreases from 121.8 to 46.9). The changes observed in the tetrahedron are not paralleled in the large 8-fold coordinated polyhedron hosting Y in β-fergusonite, which shows a limited 3% increase of polyhedral volume, mostly due to the solution of Ca and Dy in this site. Although infrequent, there seems that there is not a structural limitation in As solid solution in β-fergusonite. However, chernovite-(Y) [(AsO_4)Y] structure is tetragonal *I*4$_1$/*amd*, and thus at a certain degree of As substitution a structural phase transition may be expected to tetragonal fergusonite/chernovite-(Y).

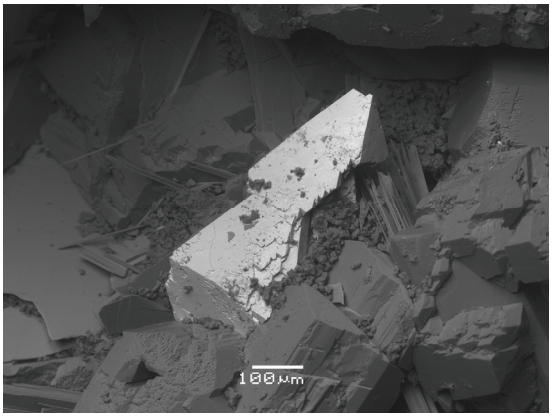

Fig. 1

References. [1] H. Weitzel, H. Schrocke, *Z. Kristallogr.*, **152**, 69-82, 1980.

EXPLORING THE CENTRAL PORTION OF THE R-Li-Ge SYSTEMS (R = rare earths)

M.L. Fornasini, A. Palenzona, M. Pani

Dipartimento di Chimica e Chimica Industriale,Università di Genova, Italy
cfmet@chimica.unige.it

The ternary systems R-Li-Ge (R = rare earths, scandium, yttrium) have been widely investigated [1] and for most of them the isothermal section at 470 K of the corresponding phase diagram is known. Similarly to the binary systems Li-Ge and R-Ge, both showing a large number of intermediate phases, also in the ternary systems numerous phases occur with different stoichiometries. While the RLiGe equiatomic phase (ZrNiAl type) occurs for the whole series of rare earths, other phases have been observed only either for the light or the heavy rare earths: $Ce_2Ni_2Si_3$-type $R_2Li_2Ge_3$ with R = La-Sm; $AlCr_2C$-type RLi_2Ge with R = La-Nd; $CaLiSi_2$-type $RLiGe_2$ with R = La-Gd; $Hf_3Ni_2Si_3$-type $R_3Li_2Ge_3$ with R = Tb-Lu,Y; Tm_4LiGe_4-type R_4LiGe_4 with R = Gd-Lu,Y.

Following our preceding work on the lithium compounds [2], we explored the central portion of the phase diagrams in the ternary systems formed by La, Ce, Pr, Nd, Sm, Ho [20-50 at.% R, 10-55 at.% Li, 20-70 at.% Ge]. The main results are here summarized:

- The R_4LiGe_4 compounds are formed also for R = La-Sm. The structure, confirmed on Nd_4LiGe_4 and Ho_4LiGe_4 single crystals, represents a ternary ordered variant of the Gd_5Si_4 type. It is worth noting that all the known binary R_5Ge_4 phases crystallize in the Sm_5Ge_4 type, a variant of the Gd_5Si_4 structure.
- The new compounds $R_3Li_4Ge_4$ (R = La-Sm) are found to crystallize with the $Gd_3Cu_4Ge_4$ structure.
- The new phases $R_7Li_8Ge_{10}$ are identified and characterized for R = La-Sm. They belong to a new structure type, determined for $Pr_7Li_8Ge_{10}$ (Fig. 1).

The structures of $R_3Li_4Ge_4$, $R_2Li_2Ge_3$ and $R_7Li_8Ge_{10}$ belong to the same structural series and can be described on the basis of similar structural fragments.

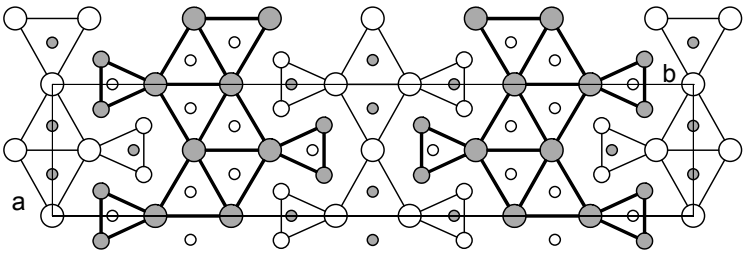

Fig. 1 - Projection along **c** of the structure of $Pr_7Li_8Ge_{10}$. Large, medium and small circles represent Pr, Li and Ge atoms. Full circles: z = 1/2; open circles: z = 0.

References. [1] P.S. Salamakha, O.L. Sologub, O.I. Bodak, *Handbook on the Physics and Chemistry of Rare Earths, Vol.* **27**, p. 1. K.A. Gschneidner Jr., L. Eyring Eds.; [2] F. Merlo, A. Palenzona, M. Pani, S.K. Dhar, R. Kulkarni, *J. Alloy. Compd.*, **394**, 101-106, 2005.

MATERIALS, FROM EARTH AND LAB TO LIFE - 1

Session 11a
The polarity in mineral surfaces: fundamental and applied aspects

THE ENERGIES OF RECONSTRUCTED SURFACES: AN *ab initio* QUANTUM-MECHANICAL AND THERMODYNAMICAL STUDY ON NaCl, LiF AND $CaCO_3$

M. Bruno

Dipartimento di Scienze Mineralogiche e Petrologiche, Università di Torino, Italy
marco.bruno@unito.it

We obtained detailed information on the structure of the i) (100) and (111) surfaces of halite (NaCl), ii) (100) surface of LiF, and iii) (01.2) surface of calcite ($CaCO_3$). We performed a quantum mechanical study of these surfaces, whose geometries were optimized at DFT (Density Functional Theory) level.

The surface energies were also calculated by taking into account the structure relaxation, the vibrational motion of atoms (vibrational entropy) in the bulk and at its surface, and the surface configurational entropy.

HYDROZINCITE CRYSTAL GROWTH UNDER CYANOBACTERIA CONTROL: AN INVESTIGATION ON LATTICE MICROSTRUCTURAL PROPERTIES

G. De Giudici[1], F. Podda[1], R. Sanna[2], E. Musu[1], R. Tombolini[3], C. Cannas[2], A. Musinu[2], M. Casu[2]

[1]*Dipartimento di Scienze della Terra, Università di Cagliari, Italy*
[2]*Dipartimento di Scienze Chimiche, Università di Cagliari, Italy*
[3]*Dipartimento di Scienze e Tecnologie Biomediche Sez. Microbiologia Applicata, Università di Cagliari, Italy*
gbgiudic@unica.it

The occurrence of hydrozincite [$Zn_5(CO_3)_2(OH)_6$] biomineralization at Naracauli creek (Sardinia, Italy) has been previously shown to be effective in the abatement of heavy metals in polluted stream waters [1]. In this work, crystallinity and microscopic properties of hydrozincite samples from Naracauli and reference standards of hydrozincite were investigated by using X-ray diffraction, Infra Red and Nuclear Magnetic Resonance spectroscopy, Scanning and High Resolution Transmission Electron Microscopy.

Overall, measurements indicate that crystallites of museum samples are larger than those of synthetic and biomineral samples. ^{13}C MAS and CPMAS NMR spectra show for all the samples investigated more than one peak, despite the carbon atoms have only one crystallographic position in the pristine hydrozincite structure. The additional peaks reflect the presence of lattice defects typical of nanocrystals as indicated by the HR-TEM images where high concentration of linear, planar and surface defects can be observed, especially in the nanocrystals from both natural and synthesized samples. This work provides new insight on microscopic properties of biologically controlled hydrozincite that will be useful in predicting its reactivity and stability.

References. [1] F. Podda, P. Zuddas, A. Minacci, M. Pepi, F. Baldi, *Appl. Environ. Microb.*, **66**, 5092-5098, 2000.

EXPERIMENTAL OBSERVATION OF CRYSTALLINE ORGANIC SEMICONDUCTORS: FROM THE STRUCTURE TO THE THEORETICAL MORPHOLOGY

M. Moret

Dipartimento di Scienza dei Materiali, Università di Milano Bicocca, Italy
massimo.moret@mater.unimib.it

Organic semiconductors represent at the same time a big hope and a hard challenge to organic materials scientists. The possibility to exploit in the next future devices based on crystalline organic active components relies upon the strong assumption of being able to grow high quality thin films or single crystals. However, for several of the most interesting and promising organic materials, the worst bottleneck is the reproducible production of top-quality crystalline materials. During this lecture a brief description of the modelling tools available for studying the theoretical crystal morphology of organic semiconductors will be presented. Comparison with experimental morphology of single crystals and thin films will be discussed to gain a better understanding of the processes involved during production of prototypical organic materials.

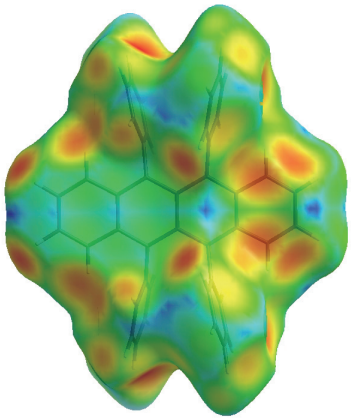

FROM MOLECULAR STRUCTURE TO CRYSTAL POLYMORPHISM: "POLYMORPH", A PREDICTIVE MODEL USING GENETIC ALGORITHM

G. Pèpe

Département de Chimie, CINaM UPR-CNRS 3118, Marseille, France
pepe@univmed.fr

Many physical and chemical properties of materials, such as propellants or explosives, depend on compound molecular packing. Consequently, in view of obtaining a desired property, predicting crystal polymorphs of a given molecule appears fundamental. This goal can be reached by the original software POLYMORPH. Starting from a molecular structure with different possible conformations, the conformational space is explored by a genetic algorithm, delivering finally the most probable packing(s) (cell parameters, associated crystal energies and space group). Selecting solutions as well as results will be presented on 50 energetic compounds.

MATERIALS, FROM EARTH AND LAB TO LIFE - 1

Session 11b
From surface interactions to bulk crystal growth

EFFECT OF TEMPERATURE ON Hg- AND Hg-CYSTEINE COMPLEXES IN VERMICULITE AND MONTMORILLONITE INTERLAYER

D. Malferrari[1], M.F. Brigatti[1], C. Elmi[1], A. Marcelli[2], W. Chu[3], Z. Wu[2,3]

[1]*Dipartimento di Scienze della Terra, Università di Modena e Reggio Emilia, Italy*
[2]*Istituto Nazionale di Fisica Nucleare, Laboratori Nazionali di Frascati, Roma, Italy*
[3]*Beijing Synchrotron Radiation Facility (BSRF), Institute of High Energy Physics, Chinese Academy of Sciences, Beijing, P.R. China*
dmalf@unimore.it

This work will address the thermal evolution (variation in oxidation state, disproportionation reactions) of Hg(II) and Hg(II)-cysteine complexes adsorbed by two different layer silicates (montmorillonite and vermiculite) via Thermo Gravimetric and Evolved Gasses Mass Spectrometry Analysis (TGA-MSEGA) and X-ray Absorption Spectroscopy (XAS) at increasing temperature. From the analysis of the near-edge region of the XAS spectra we could recognize significant structural differences between Hg treated montmorillonite and vermiculite even at room temperature. At increasing temperature Hg is not easily removed from the silicate layer and it could be identified in layer structure up to 400°C in montmorillonite and up to 700°C in vermiculite. Besides, starting from 150°C the spectrum significantly changes at the absorption edge, due to a different Hg local topology promoted by a decrease of the empty DOS of *d* character hybridized with *s* and *p* empty states. At 400°C the spectrum shows a further weak decrease at the edge, probably related to a different oxidation state for Hg (from Hg^{2+} to Hg^{0}), without showing any significant variation in the MS region. Afterward, the extremely limited residual Hg amount accounts for the noise exhibited by the higher temperature spectra (~ 700°C) almost represents an atomic cross section. From the analyses of the Extended X-ray Absorption Fine Structure (EXAFS) of spectra collected at room temperature, it is evident that Hg-H_2O complexes are present in both montmorillonite and vermiculite, whereas the HgO-like molecules appears only in vermiculite.

When considering the Hg(II)-cysteine and, in particular, bonds between metal and amino acid, Hg was observed to bind cysteine via the thiol group. Hg-SH bond lengths are similar for both clay minerals, thus suggesting independence from layer charge. On the contrary, the role of layer charge is well evident, when considering the thermal behavior of the organo-metallic complex. The spectra collected at increasing temperature of the amino acid treated montmorillonite and vermiculite are both comparable, at the edge, to the one of HgS reference compound. Besides, typical features of HgS-like compound are maintained up to 400°C indicating that the local structure of Hg does not change with temperature. At $T \geq 150$°C, the spectra indicate a short range order rearrangement with temperature and an increase in bond distances in Hg(II)-cysteine complexes adsorbed from vermiculite respect to ones adsorbed from montmorillonite. XAS data suggest major differences of Hg removal *vs*. temperature between the two substrates and enhance that at about 800°C Hg is completely removed from montmorillonite, whereas it is still present in vermiculite.

GROWTH OF DEFECTIVE YBCO WHISKERS

A. Agostino[1], S. Cagliero[1], M.M. Rahman Khan[1,2], M. Truccato[2], L. Pastero[3]

[1]*Centro di Eccellenza NIS, Dipartimento di Chimica Generale e Inorganica, Università di Torino, Italy*
[2]*Centro di Eccellenza NIS, Dipartimento di Fisica Sperimentale, Università di Torino, Italy*
[3]*Dipartimento di Mineralogia e Petrografia, Università di Torino, Italy*
angelo.agostino@unito.it

New trends in the research of Teraherz devices based on the Intrinsic Josephson Effect (IJE) [1,2] bring in the foreground the use of high Tc superconducting micro-crystals as good candidates to cover this role. In particular, the YBCO whiskers with their anisotropic shape and characteristic stacked junction structure show interesting application properties. Unfortunately, no repeatable results, probably due to the changing of the boundary conditions, were observed.

In order to understand the reasons of this low reproducibility during the whisker growth, a systematic exploration of synthesis parameters involved in the growth process [3-5], was performed.

During the whiskers growth experiments a large number of defective (twinned) crystals were obtained. Furthermore, epitaxial growth and 2D/3D nucleation on YBCO whiskers are recurrent in all experiments seemingly due to the local supersaturation gradients and the overall lack of homogeneity of the growth environment.

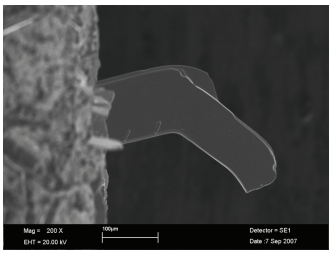

Fig. 1 - Defective YBCO crystal showing twinning and auto- epitaxy

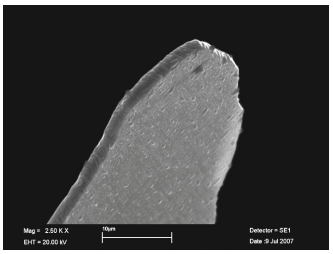

Fig. 2 - Crystal surface showing oriented overgrowth.

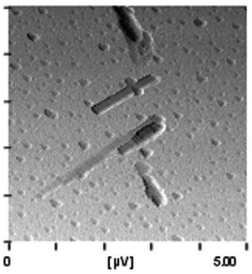

Fig. 3 - AFM (amplitude) imaging of the oriented overgrowth.

In order to determine the growth mechanisms ruling the crystallographic and morphological defectiveness of YBCO whiskers, a PBC (Periodic Bond Chain) analysis was carried out.

Preliminary crystal orientation was obtained by XRPD analysis and an optical characterization of crystals (polarized light - optical microscope) was realized. Then, the whole crystal morphologies and surface features were observed by optical microscope (parallel / polarized light), SEM and AFM.

Auto-epitaxies, oriented overgrowths and twins show a close relationship between the growth mechanisms and the discontinuities of the growth medium.

References. [1] S.-J. Kim, Yu. I. Latyshev, T. Yamashita, *Appl. Phys. Lett.*, **74**, 1156, 1999; [2] Yu. I. Latyshev, S.-J Kim., T. Yamashita, *IEEE Trans. Appl. Supercond.*, **9**, 4312, 1999; [3] T. Izumi, Y. Shiohara, *J. Phys. Chem. Solids*, **66**, 535-545, 2005; [5] M. Nagao, M. Sato, H. Maeda, K.S. Yun, Y. Takano, T. Hatano, *Appl. Phys. Lett.*, **82**, 1899, 2003; [6] I. Matsubara, H. Kageyama, H. Tanigwa, T. Ogura, H. Yamashita, T. Kawai, *Jpn. J. Appl. Phys*., Part 1, **28**, 1121, 1989.

BORON OXIDE ENCAPSULATED VERTICAL BRIDGMAN CdZnTe CRYSTALS FOR X-RAY DETECTOR APPLICATIONS

A. Zappettini[1], M. Zha[1], D. Calestani[1], L. Marchini[1], L. Zanotti[1], C. Paorici[1,2]

[1]*IMEM-CNR, Parma, Italy*
[2]*Dipartimento di Fisica, Università di Parma, Italy*
zapp@imem.cnr.it

CdZnTe crystals are employed for the production of room temperature X-ray detectors and as substrates for infrared detectors. However, the exploitation of CdZnTe crystals for such applications is still limited by the low single-crystalline device-grade yield of the growth process.

The authors had previously shown that it is possible to grow CdZnTe crystals in a vertical Bridgman configuration by means of boron oxide encapsulation. Actually, the crystals are fully encapsulated by boron oxide, thus preventing any contact between the growing crystal and the ampoule wall.

In this work, it is shown that 2-inches crystals with very large single grains can reproducibly be obtained in this way (Fig. 1a). The dislocation density (EPD) is studied both axially and radially showing values in the 1E-3-1E-4 cm^{-2} range (Fig. 1b), with a distribution that basically follows the Jordan model.

The axial zinc distribution basically follows the normal freezing law, and good homogeneity is found on the wafers obtained cutting the crystals perpendicularly with respect to the growth axis.

By means of the Optical Monitoring of Partial Vapour Pressure technique, the authors have carefully studied for the first time the anion/cation stoichiometric variation along the crystal.

In order to prepare X-ray detectors, CdZnTe crystals were doped with Indium and resistivities larger than 1E10 Ω·cm were reached.

X-ray detectors based on the grown crystals shows spectroscopic characteristics with excellent energy resolution (Fig. 2), demonstrating for the first time the possibility to obtain device-grade material with the boron oxide encapsulated vertical Bridgman technique.

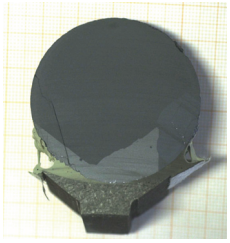

Fig. 1a - 2-inches CdZnTe wafer with a large single grain.

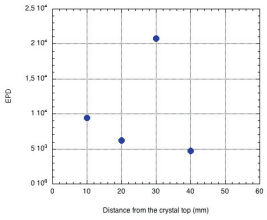

Fig. 1b - Radial EPD distribution.

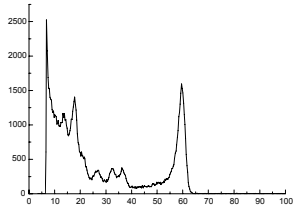

Fig. 2 - Response of a CdZnTe based detector obtained with the B_2O_3 encapsulated vertical Bridgman technique.

GROWTH AND CHARACTERIZATION OF ZnO NANOSTRUCTURES BY A SELF-CATALYTHIC CVD PROCESS

D. Calestani, M. Zha, A. Zappettini, R. Mosca, L. Lazzarini, G. Salviati, L. Zanotti

IMEM-C.N.R., Parma, Italy
calle@imem.cnr.it

In the last years, many papers have dealt with the topic of metal oxide nanowire growth and characterization. In particular, it is widely reported that Zinc Oxide (ZnO) can be obtained in a large variety of nanostructures with different morphologies, namely nanowires, nanorods, nanotetrapods (or simply "tetrapods"), nanotapes or nanoribbons, etc. The possibility to obtain this material in different nanosized crystalline structures is particularly interesting in view of several application fields, *e.g.* chemical sensors, solar-cells, optoelectronics. However, different nanostructures often appear mixed on the same substrate, thus limiting the possibility of exploitation for applications.

In this work, we report on the growth of ZnO nanostructures on large-scale by a combination of vapor transport and controlled oxidation in a CVD reactor with a typical bottom-up self-catalytic process. This kind of synthesis process is generally cheaper than the typical top-down ones used for common electronics and so they are suitable for "low-cost" device fabrication.

Using pure metallic Zn (5N) as source material, different growth conditions has been studied and tuned for the large-scale and reproducible preparation of selected nanostructures, like nanowires (Fig. 1a), nanotetrapods (Fig. 1b), and nanorods (Fig. 1c). In particular, no catalyst or organic precursor has been used in the synthesis process to avoid unwanted contaminations, often affecting the properties of these nanostructures.

Crystallographic phase, morphology and defects of the nanostructures were studied at the aid of transmission electron microscopy.

The strong luminescence of the different nanostructures at room and liquid helium temperatures was compared.

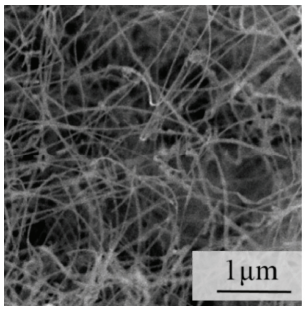

Fig. 1a

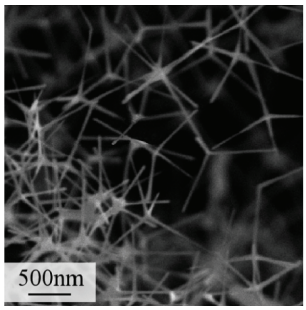

Fig. 1b

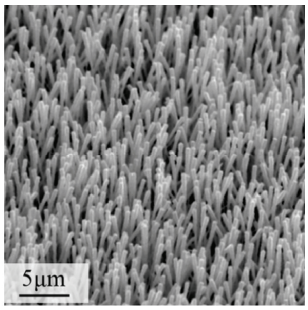

Fig. 1c

S11.P1

GROWTH AND CHARACTERISATION OF 3C-SiC NANOWIRES

G. Attolini, F. Rossi, M. Bosi, B.E. Watts, G. Salviati

IMEM-CNR Parma, Italy
giovanni@imem.cnr.it

Recently, many reports have been focused on the preparation and characterisation of one-dimensional nanostructures such as nanowires of oxides, nitrides, carbides, III-V's, metals and silicon.

They present chemical, physical, electrical, optical, and mechanical properties better than their bulk materials, thus offering opportunities for fundamental research and for the fabrication of optoelectronic, electro-mechanic and sensor devices on a nanometer scale.

Cubic silicon carbide (β-SiC or 3C-SiC) is a wide-bandgap semiconductor with high hardness, electron mobility, thermal conductivity and resistance to the chemical attack.

3C-SiC nanowires (SiC-NWs) are interesting because their good physical and chemical properties make them a promising material for devices operating in harsh environment.

Functionalized 3C-silicon carbide nanowires have the potential to act as highly sensitive detector elements in bio-chemical field and, since elasticity and strength are greater than bulk, they are also attractive for nanostructured composite materials.

Here, we report a study on the properties of cubic SiC-NWs. They have been prepared with carbon monoxide and nickel as the catalyst in nitrogen or argon atmosphere at temperatures between 1050 and 1100°C in an open tube reaction. This method is based on carbothermal reduction of silica present on silicon substrate surface as native oxide.

Nanowires were characterised by X-ray diffraction (XRD), Scanning Electron Microscopy (SEM), Cathodoluminescence (CL) and Transmission Electron Microscopy (TEM).

Structural studies using SEM and TEM reveal that the growth varies as the temperature is raised from 1050 to 1100°C. At lower temperatures long thin wires grow, while if the temperature is raised the wires tend to align but their diameters vary considerably. A core shell structure consisting of a silicon carbide core enveloped by amorphous oxide is evidenced. Stacking faults and twins are observed, mainly in the (111) basal plane.

FIRST FINDING OF "BIOMIMETIC" ARAGONITE POLYCRYSTALLINE STRUCTURES

E. Bittarello, D. Aquilano

Dipartimento di Scienze Mineralogiche e Petrologiche, Università di Torino, Italy
erica.bittarello@unito.it

Biomimetic synthesis of minerals with complex morphology, structured through the self-assembly of nano-building blocks have attracted a considerable attention in recent years. Different organic additives have been used for controlled growth of carbonate minerals [1]. In non-biological solutions containing poly(acrylic), poly(glutamic) and poly(aspartic) acids, calcium carbonate grew as a film on various surfaces [2-6]. In recent years, double hydrophilic block copolymers (DHBCs) have been developed as crystal growth modifiers [7-9]. This polyelectrolyte has a remarkable influence on the morphology of a huge number of inorganic materials [10-12]. So biomimetic morphologies are not attributable to only organic and complex molecules. Indeed, the precipitation of $BaCO_3$ and $SrCO_3$ phases in basic silica-rich environment results in the formation of peculiar polycrystalline structures, termed "Silica Biomorphs" [13-14]. The behaviour common to all biomorphs are their curved surface. Until now, the precipitation of calcium carbonate in this crystallization environment has not produced the characteristic biomimetic forms.

An important development has been done by Voinescu *et al*. [15]. They report the formation of silica-calcium carbonate biomorphs, which show a "coralline" self assembled shape. These structures are constituted by aragonite nano-crystals and an amorphous silica matrix. The experimental preparations are different with respect to the "classic" technique used to obtain the silica biomorphs [16], since the authors operate at elevated temperature (80°C) to promote the aragonite formation and with different solutions or gel concentrations compared to the experiments with $BaCO_3$ and $SrCO_3$. Here we described, within the classic method of crystallization, new polycrystalline and curved structures of aragonite, associate to sheaf aggregates and single crystals of calcite. There is a close resemblance between the planar aggregates of $BaCO_3$ and those made of aragonite (Fig. 1). But, the classical biomorphs are bigger in size, their dimensions ranging between 250 to 500 μm, while the aragonite structures do not exceed 100-120 μm in diameter. These complex arrangements display structural and morphologic features that are similar to previously reported barium [16], strontium [14] and calcium [15] biomimetic shapes.

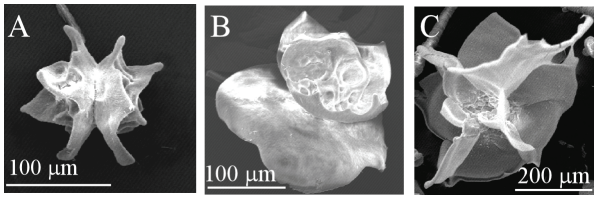

Fig. 1 - Similarity between planar aggregates of aragonite (A, B) and witherite (C) grown under the same crystallization conditions.

References. [1] H. Cölfen, *Curr. Opin. Colloid Interface Sci*., **8**, 23, 2003; [2] L.A. Gower, D.A. Tirrell, *J. Cryst. Growth*, **191**, 153, 1998; [3] L.B. Gower, D.J Odom, *J. Cryst. Growth*, **210**, 719, 2000; [4] T. Kato, T. Amamiya, *Chem. Lett*., 199, 1999; [5] A. Sugawara, T. Kato, *Chem. Commun*., 487, 2000; [6] A. Sugawara, T. Ishii, T. Kato, *Angew. Chem*, Int. Ed., **42**, 5299, 2003; [7] M. Sedla´k, M. Antonietti, H. Cölfen, *Macromol. Chem. Phys.*, **199**, 247, 1998; [8] H. Cölfen, M. Antonietti, *Langmuir*, **14**, 582, 1998; [9] H. Cölfen, *Macromol. Rapid Commun*., **22**, 219, 2001; [10] S.H. Yu, H. Cölfen, K. Tauer, M. Antonietti, *Nat. Mater*., **4**, 51, 2005; [11] S.F. Chen, S.H. Yu, T.X. Wang, J. Jiang, H. Cölfen, B. Yu, *AdV. Mater*., **17**, 1461, 2005; [12] T.X. Wang, A.W. Xu, H. Cölfen, *Angew. Chem*., Int. Ed., **45**, 4451, 2006; [13] J.M. García-Ruiz, J.L. Amorós, *Boll. Real Soc. Esp. de Hist. Nat., Sec. Geo.*, **77**, 101-119, 1979; [14] T. Terada, S. Yamabi, H. Imai, *J. Cryst. Growth*, **253**, 435-444, 2003; [15] A.E. Voinescu, M. Kellermeier, B. Bartel, A.M. Carnerup, A.K. Larsson, D. Touraud, W. Kunz, L. Kienle, A. Pfitzner, S.T. Hyde, *C. Gr. & Des*., **8**, 1515-1521, 2008; [16] J.L. Amorós, J.M. García-Ruiz, *Inv. y Ciencia*, **71**, 6-15, 1982.

QUARTZ/WITHERITE ($BaCO_3$) EPITAXY. EXPERIMENTAL FINDING AND THEORETICAL IMPLICATIONS ON BIOMINERALIZATION

E. Bittarello, F.R. Massaro, D. Aquilano

Dipartimento di Scienze Mineralogiche e Petrologiche, Università di Torino, Italy
erica.bittarello@unito.it

Despite barium carbonate (witherite) is an important raw material in several industrial applications [1] and is the main constituent of silica biomorphs [2-6], its theoretic growth morphology has been had minor attention in this kind of studies. On one hand, our work is devoted to the study of witherite to give a contribution to the knowledge of its theoretical equilibrium and growth morphology through PBC (periodic bond chain) analysis [7] based on a previous study on aragonite [8]. On the other hand, this paper describes the interactions between $BaCO_3$ (witherite) and quartz crystals. This is to find experimental proves about our hypothesis on the epitaxial interaction between growing witherite crystal and silica groups present in the sodium metasilicate (NaMTS) rich solution. Barium carbonate crystals are synthesized at constant temperature and ambient pressure by mixing two solutions of $BaCl_2 \cdot 2H_2O$ (0.02 M) and $NaHCO_3$ (0.002 M). Then, we tried to crystallize witherite on single crystals quartz seeds in the growth solution. The concentrations of the reagent solutions are the same of those employed in the previous experiments. In this way, we could observe the main differences between these two kinds of crystallization environments and outline the influence of quartz on the $BaCO_3$. Generally, witherite grows in the form of pseudo-hexagonal prismatic crystals (Fig. 1). But, when quartz is introduced in the system, pseudo-hexagonal plates (40-50 μm in size), form onto quartz faces, one week after the crystallization began (Fig. 2).

Finally, geometrical and physical epitaxial relationships are investigated to explain these new peculiar findings.

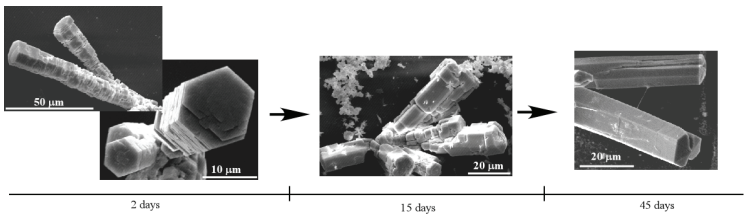

Fig. 1 - Morphological change with time of witherite without crystal quartz in solution.

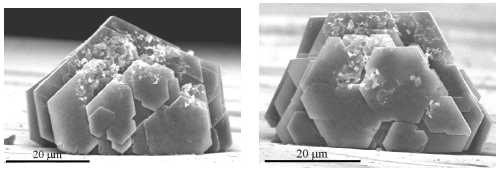

Fig. 2 - Pseudo-hexagonal laminae of witherite on the quartz surfaces.

References. [1] J.J. MacKetta, Marcel Dekker Inc., New York, 1977, p. 51; [2] J.M. García-Ruiz, J.L. Amorós, *Boll. Real Soc. Esp. de Hist. Nat., Sec. Geol.*, **77**, 101-119, 1979; [3] J.M. García-Ruiz, *Orig. Life Evol. Biosph.*, **24**, 451-467, 1993; [4] J.M. García-Ruiz, A. Carnerup, A.G. Christy, N.J. Welham, S.T. Hyde, *Astrobiology* **2** (**3**), 353-369, 2002; [5] J.M. García-Ruiz, S.T. Hyde, A. Carnerup, A.G. Christy, M.J. Kranendonk, N.J. Welham, *Science*, **302**, 1194-1197, 2003; [6] S.T. Hyde, A. Carnerup, A.K. Larsson, A.G. Christy, J.M. García-Ruiz, *Physica A*, **339**, 24-33, 2004; [7] P. Hartman, W.G. Perdok, *Acta Cryst.*, **8**, 49, 1955; [8] D. Aquilano, M. Rubbo, M. Catti, A. Pavese, *J. Cryst. Growth*, **182**, 168-184, 1997.

THE EPITAXIAL ROLE OF SILICA GROUPS IN PROMOTING THE SILICA BIOMORPH FORMATION. A FIRST HYPOTHESIS

E. Bittarello, F.R. Massaro, D. Aquilano

Dipartimento di Scienze Mineralogiche e Petrologiche, Università di Torino, Italy
erica.bittarello@unito.it

The aim of this work is to understand the influence of sodium metasilicate (NaMTS hereinafter) on the morphogenesis of $BaCO_3$, one of the main polycrystalline component of "Silica Biomorphs". These peculiar nano-aggregates form from the precipitation of $BaCO_3$ (or $SrCO_3$ [1]) in basic-silica rich environment [2-5]. In general, these morphologies form either in NaMTS gel or in a stagnant solution, exhibiting regular shapes like helicoidal filaments and cardioidal sheets.

Non-crystallographic aggregates made by nanosized $BaCO_3$ individuals were synthesized using different concentrations of sodium metasilicate in solution. The size of nucleated barium carbonate crystals change significantly with the amount of silicate anion. When the NaMTS amount was lower than 500 ppm, single well-shaped micrometric crystals grew in solution (Fig. 1a-2a). Higher concentrations of NaMTS (4000-5000 ppm) produced polycrystalline structures built by pseudo-hexagonal nano-rods (Fig. 1c-d). XRPD diagrams show the changes of crystal size with NaMTS concentration and point out as well that silicate groups cannot be incorporated into the barium carbonate lattice (Fig. 3).

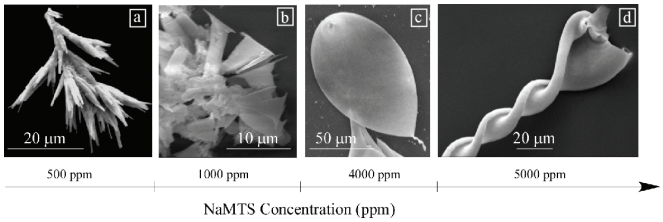

Fig. 1 - Morphological evolution of aggregates as a function of sodium metasilicate concentration in solution.

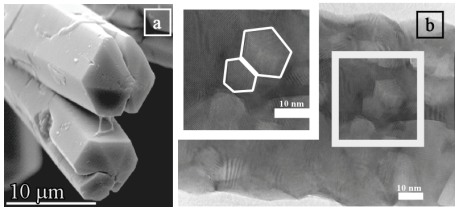

Fig. 2 - (a) Single crystal of $BaCO_3$ growth from pure aqueous solution (micrometer in size) and (b) TEM image of the hexagonal shaped nanocrystals that form the helicoidal filaments grown in presence of NaMTS 5000 ppm.

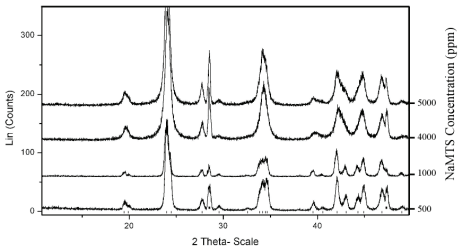

Fig. 3 - XRPD patterns of precipitates obtained from solution with different concentrations of NaMTS.

References. [1] T. Terada, S. Yamabi, H. Imai, *J. Cryst. Growth*, **253**, 435-444, 2003; [2] J.M. García-Ruiz, *Orig. Life Evol. Biosph.*, **24**, 451-467, 1993; [3] J.M. García-Ruiz, A. Carnerup, A.G. Christy, N.J. Welham, S.T. Hyde, *Astrobiology*, 2 (**3**), 353-369, 2002; [4] J.M. García-Ruiz, S.T. Hyde, A. Carnerup, A.G. Christy, M.J. Kranendonk, N.J. Welham, *Science*, **302**, 1194-1197, 2003; [5] S.T. Hyde, A. Carnerup, A.K. Larsson, A.G. Christy, J.M. García-Ruiz, *Physica A*, **339**, 24-33, 2004.

AB INITIO QUANTUM-MECHANICAL AND THERMODYNAMICAL STUDY ON NaCl, LiF AND $CaCO_3$ RECONSTRUCTED SURFACES

M. Bruno, M. Prencipe, M. Rubbo

Dipartimento di Scienze Mineralogiche e Petrologiche, Università di Torino, Italy
marco.bruno@unito.it

In the past, particular attention had been paid to the study of the polar {111} faces of crystals with rocksalt-type structure, which are expected to be not stable. Along the ⟨111⟩ directions, the crystals with NaCl structure consist of alternating layers of cations and anions. Therefore, the (111) surface must have a highly divergent electrostatic energy, which makes this surface theoretically unstable and not present in the equilibrium morphology of NaCl-type crystals. Then, to explain the presence of the {111} form in ionic crystals with rocksalt-type structures grown from aqueous solution, the adsorption of impurities, H_2O molecules and/or H^+ and OH^- ions was invoked. Instead, when no impurities are present, theoretical calculation suggests two possibilities to stabilize the {111} surfaces: (a) the bulk terminated {111} surfaces break up into neutral {100} facets upon annealing or (b) the surfaces reconstruct [1,2].

We obtained detailed information on the structure of the (i) (100) and (111) surfaces of halite (NaCl), (ii) (100) surface of LiF, and (iii) (01.2) surface of calcite ($CaCO_3$). We performed a quantum mechanical study of these surfaces, whose geometries were optimized at DFT (Density Functional Theory) level. The surface energies were also calculated by taking into account the structure relaxation, the vibrational motion of atoms (vibrational entropy) in the bulk and at its surface, and the surface configurational entropy.

References. [1] M. Bruno, D. Aquilano, L. Pastero, M. Prencipe, *Cryst. Growth & Design*, in press; [2] M. Bruno, F.R. Massaro, M. Prencipe, *Surface Science*, submitted.

HYDROZINCITE CRYSTAL GROWTH IN PRESENCE OF PHTHALATE: A FIRST INVESTIGATION ON THE ADSORPTION REACTION

G. De Giudici[1], F. Podda[1], R. Sanna[3], R. Tombolini[2], M. Casu[3]

[1]*Dipartimento di Scienza della Terra, Università di Cagliari, Italy*
[2]*Dipartimento di Scienze e Tecnologie Biomediche, Sez. Microbiologia Applicata, Cagliari, Italy*
[3]*Dipartimento di Scienze Chimiche, Università di Cagliari, Italy*
gbgiudic@unica.it

In this work, crystallinity and microscopic properties of hydrozincite [$Zn_5(CO_3)_2OH_6$] synthesised *in vitro* were investigated by using X-ray diffraction, Infra Red spectroscopy, Nuclear Magnetic Resonance spectroscopy, Scanning Electron Microscopy and High Resolution Transmission Electron Microscopy. An organic molecule, DEHP (di-2-ethyl exhylphthalate), was added to the *in vitro* experiments. DEHP is a plasticizer commonly used in polivynilchloride resin, that is released to the environment through volatilization and leaching from PVC products during their useful lifetime and after disposal in landfills. DEHP and other plasticizers have been detected in soils, water, sediments, human and animal tissues [1].

Several *in vitro* experiments were driven adding cyanobacteria inocula to synthetic solution in presence of DEHP. Solid samples and water samples from the *in vitro* experiments were then analysed to assess the quality of hydrozincite nanocrystals and, eventually, the presence of DEHP in the solid samples.

Infrared spectra and ^{13}C MAS and CPMAS NMR spectra show that DEHP can be found in the precipitated hydrozincite. In some of the samples, DEHP is present as absorbate onto the hydrozincite surface.

This work provides new insight on microscopic properties of biologically controlled hydrozincite that will be useful in predicting its reactivity and stability. The consortium between bacteria, water and precipitating biomineral could be effective in DEHP removal from waters.

References. [1] D.L. DeFoe, G.W. Holcombe, D.E. Hammermeister, K.E. Biesinger, *Env. Toxicol. Chem*., **9**, 623-636, 1990.

CLINOCHLORE STRUCTURE AND ITS SURFACE INTERACTIONS WITH ORGANIC MOLECULES

C. Elmi[1], M.F. Brigatti[1], D. Malferrari[1], G. Valdrè[2], G.R. Castro[3], J. Rubio-Zuazo[3]

[1]*Dipartimento di Scienze della Terra, Università di Modena e Reggio Emilia, Italy*
[2]*Dipartimento di Scienze della Terra e Geologico-Ambientali, Università di Bologna, Italy*
[3]*SpLine at ESRF, Grenoble, France*
chiara.elmi@unimore.it

This study is focused on clinochlore crystal chemistry and on its surface interactions with biomolecules. Clinochlore, which is a chlorite, is formed by two different polyhedral units: (i) two tetrahedral sheets (T) sandwiching a Mg-rich octahedral sheet (O) and (ii) an octahedral Mg-, Al-rich, brucite-like, interlayer (B). The excess of negative charge of the TOT layer is neutralized by the positively charged B interlayer. Extensive hydrogen bonding provides structural cohesion between the TOT layer and the B interlayer.

The clinoclhore studied is triclinic IIb-4 polytype, with symmetry $C\bar{1}$ and unit cell parameters a = 5.3301(4) b = 9.2511(6) c = 14.348(1) Å, α = 90.42(1) β = 97.51(1) γ = 90.00(2)°. The chemical composition is $^{[VI]}(Mg_{9.6}Fe^{2+}_{0.27}Al_{2.01}Cr_{0.09})^{[IV]}(Si_{5.86}Al_{2.14})O_{20}(OH)_{16}$.

Measurements of surface reflectivity carried out at ESRF, Spanish beam line, suggest that biological molecules, such as nucleotides, can be adsorbed as (001) organized layer on the mineral surface. Furthermore AFM (Atomic Force Microscopy) and EFM (Electric Force Microscopy) studies suggest that clinochlore presents at the nanoscale negative regions of exposed oxygens (tetrahedral sheets, lower layer) and positive regions of exposed hydroxyl groups belonging to the brucite-like which is about 0.5 nm thick [1]: the brucite-like layer is more effective in assembling the biological molecules rather than the exposed oxygen surface.

References. [1] G. Valdrè, *Eur. J. Mineral.*, **19**, 309-319, 2007.

THEORETICAL EQUILIBRIUM AND GROWTH MORPHOLOGY OF GYPSUM

F.R. Massaro, M. Rubbo, D. Aquilano

Dipartimento di Scienze Mineralogiche e Petrologiche, Università di Torino, Italy
francesco.massaro@unito.it

In this work, the theoretical equilibrium and growth morphologies of gypsum have been calculated by means of the General Lattice Utility Program (GULP) simulation code [1], which is based on force field methods and allows to calculate structures and properties of minerals from a given set of empirical potentials.

Starting from the $CaSO_4 \cdot 2H_2O$ structural refinement by Boeyens and Ichharam [2] (space group *C*2/*c*, *a* = 6.284, *b* = 15.200, *c* = 6.523 Å, β = 127.41°) and making use of the inter-atomic potential for gypsum developed by Adam [3], we have performed caculations on the most probable F forms resulting from literature, namely the {010}, {021}, $\{\bar{1}10\}$ and $\{\bar{1}11\}$. In addition, we have considered some vicinal S forms belonging to the x-axis zone ({031}, {041}, {051}, {061}) we believe to compete with the previous ones in the crystal morphology.

The surfaces (γ) and attachment (E_{att}) energies in vacuum at 0 K, for the relaxed and unrelaxed forms have been determined. For this purpose, we have chosen to consider the surface structures following two different strategies:

- the first one involves to build surfaces by adopting the PBC method, in terms of Hartman-Perdok theory;
- the second strategy consists in building different profiles, cutting systematically gypsum structure parallel to the considered plane. An average value of both γ and E_{att} for each form was obtained.

It follows that, after relaxation, unusual forms can enter the equilibrium morphology: we are referring to the {031} and {061} forms obtained by means of the PBC method (Fig. 1a), and the {041} form by using the other strategy (Fig. 1b). The same no longer holds for the growth morphology (Fig. 1c, d).

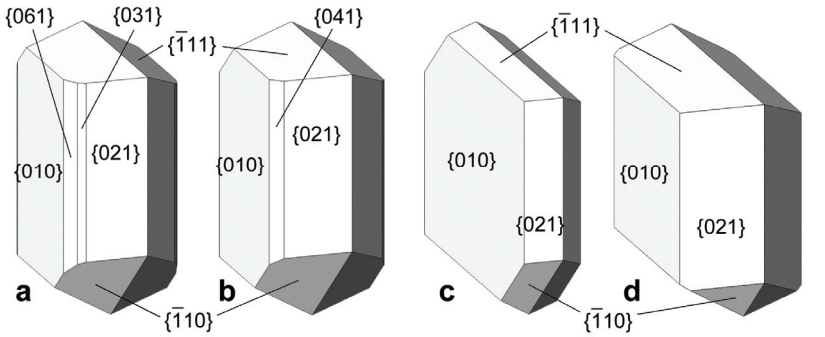

Fig. 1 – Calculated equilibrium (a, b) and growth (c, d) relaxed morphologies according to the PBC method (a, c) and the systematic cuts strategy (b, d).

References. [1] J.D. Gale, *J. Chem. Soc. Faraday T.*, **93**, 629, 1997; [2] J.C.A. Boeyens, V.V.H. Ichharam, *Z. Kristallogr.*, **217**, 9, 2002; [3] C.D. Adam, *J. Solid State Chem.*, **174**, 141, 2003.

GROWTH MORPHOLOGY OF GYPSUM IN THE PRESENCE OF ORGANIC HABIT MODIFIERS

D. Montagnino[1], G. Artioli[2], E. Costa[1]

[1]*Dipartimento di Scienze Mineralogiche e Metrologiche, Università di Torino, Italy*
[2]*Dipartimento di Mineralogia e Petrologia, Università di Padova, Italy*
daniela.montagnino@unito.it

Gypsum is the most abundant sulphate mineral and it's widely used in industrial processes. From both theoretical and practical points of view it is interesting to understand the growth mechanisms of the different crystal forms because of their competing rates determining the final crystal shape. Natural gypsum crystals primarily show three forms: the {010} pynacoid along with the {120} and {11$\bar{1}$} prisms. Moreover, the structural analysis based on the PBC theory indicates that the {011} form should be more stable than the {11$\bar{1}$}, at variance with observations. Natural crystals also occur as {010} platy, while synthetic crystals are usually acicular and [001] elongated. The crystallization process of gypsum is dramatically influenced by additives and impurities, which exert their specific action upon the crystal surface. Not only the crystallization kinetics, but also the habit and morphology of the gypsum crystals as well as their dispersive properties can thus be modified [1,2].

We performed experiments to investigate the growth mechanism and the effects of growth inhibitors (phosphonates and co-polymers) on the (010) and (120) surfaces. The mother phase, obtained by mixing two equimolar $CaCl_2 \cdot 2H_2O$ and Na_2SO_4 solutions, was kept in contact with the growing face at 35°C.

The aim of this paper is at studying the inhibiting effects of phosphonates and copolymers at different concentrations. New generations of organic superplasticizers nowadays find a widespread use in the organic molecules (sulphonates, phosphonates, acrylates and other polymers) with the clinker phases. We have tested as well the inhibiting modifying effects of the phosphonic ethylenediamine-tetra (methylene phosphonic acid) EDTMP and diethylene-triammino-pentamethylene-phosphonic acid (DTPMP) and copolymers SP1, SP3, SR3.

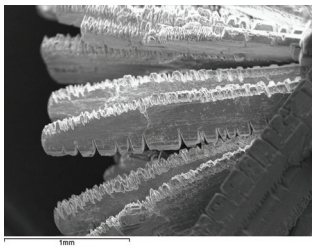

Fig. 1 - Gypsum growth in the presence of DTPMP (10^{-4} M with respect to [Ca^{2+}]).

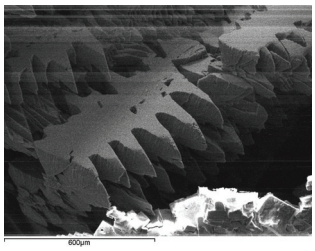

Fig. 2 - Gypsum growth in the presence of EDTMP (10^{-4} M with respect to [Ca^{2+}]).

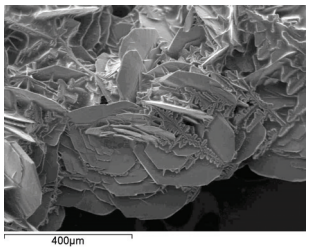

Fig. 3 - Gypsum growth in the presence of SR3 (0.4% with respect to dry cement powder).

References. [1] M.P.C. Weijnen, G.M. Van Rosmalen, P. Bennema, J.J.M. Rijpkema, *J. Cryst. Growth*, **82**, 509-527, 1987; [2] M.P.C. Weijnen, G.M. Van Rosmalen, P. Bennema, *J. Cryst. Growth*, **82**, 528-542, 1987.

INTERPLAY BETWEEN CRYSTAL STRUCTURE AND CRYSTAL MORPHOLOGY: THE CASE OF ORGANIC SEMICONDUCTORS

M. Moret[1], D. Aquilano[2]

[1]*Dipartimento di Scienza dei Materiali and CNISM, Università di Milano-Bicocca, Italy*
[2]*Dipartimento di Scienze Mineralogiche e Petrologiche, Università di Torino, Italy*
massimo.moret@mater.unimib.it

During the last years organic semiconductors have become a hot topic for solid state physics and technology. Among many parameters and intrinsic properties that can influence the final outcome of a research in this field, growth morphology of crystalline materials has a fundamental role. Therefore, an a priori analysis of the equilibrium and growth morphology should be mandatory in order to unravel the intrinsic behaviour of the selected systems. Subsequent comparison with experimental morphologies obtained when macroscopic crystals or thin films are grown under very different ambient conditions can shed new light upon the best routes to produce the desired crystalline materials.

In order to select optimum semiconducting or optical properties, good candidates organic materials have been chosen among the class of large polycyclic aromatic molecules, mainly oligothiophenes, polyphenyls and oligoacenes [1,2]. However, since for several of these promising materials the reproducible production of top-quality crystals is still quite uncertain, a thorough analysis of the interplay between their crystal structures and the predicted and observed morphologies under different experimental conditions can be very fruitful.

In this respect, modelling with the well consolidated method of Periodic Bond Chains [3] of crystals of quaterthiophene, sexithiophene and rubrene allowed us to classify and study the crystal forms that should reasonably dominate the crystal morphology. Common features of the crystal packing are shown to lead to recurrent features of the equilibrium and growth morphologies which well compare with crystalline materials grown by us or appearing in the scientific literature.

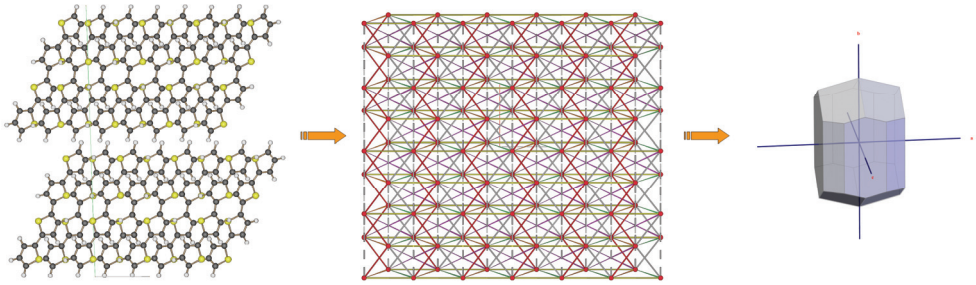

Crystal structure PBC net Crystal morphology

References. [1] M. Bendikov, F. Wudl, D.F. Perepichka, *Chem. Rev.,* **104**, 4891-4945, 2004; [2] J.-L. Brédas, D. Beljonne, V. Coropceanu, J. Cornil, *Chem. Rev.*, **104**, 4971-5003, 2004; [3] P. Hartman, W.G. Perdok, *Acta Crystallogr.*, **8**, 49-52, 1955; ibid, 521-524; 525-529.

STUDY OF EPITAXIAL RELATIONS BETWEEN SEXIPHENYL CRYSTALS AND KAP(010) SURFACE

M. Moret[1], M. Campione[1], T. Haber[2], R. Resel[2], A. Sassella[1], A. Thierry[3]

[1]*Dipartimento di Scienza dei Materiali e CNISM, Università di Milano-Bicocca, Italy*
[2]*Institute of Solid State Physics, Graz University of Technology, Austria*
[3]*Institut Charles Sadron, Centre National de la Recherche Scientifique, Strasbourg, France*
massimo.moret@mater.unimib.it

Fundamental research on mechanisms of aggregation of organic molecular materials is an important step for the understanding of film growth mechanisms and for controlling their growth. Efforts in this field are motivated by the potential of organic semiconductors in electronic devices. Device performance is strictly dependent on molecular orientation due to the anisotropy of the molecules in the crystals and the correlated electronic and optical properties. Therefore, the ability to control molecular orientation and crystallographic order of molecular materials is highly beneficial for improving device performances.

Para-sexiphenyl (p6P) is a blue light emitting organic semiconductor with an outstanding high quantum yield. Moreover, p6P is a wave guiding crystal in the plane of the herringbone layers. The waveguide effect abruptly ends at grain boundaries and hence ordered, single crystalline structures are of particular interest for future applications.

Recently, the field of organic molecular films moved beyond the growth on metallic, semiconducting or insulating surfaces to organic hetero-epitaxy [1-4]. p6P nanostructures were grown on the (010) cleavage plane of potassium hydrogen phthalate (KAP). This surface exposes exclusively phenyl rings with two distinct surface corrugations along <101> and [001]. Elongated p6P crystallites grow epitaxially ordered with the $(30\bar{2})$ plane parallel to KAP(010) with the long axis of p6P molecules aligned to the KAP<101> surface corrugations (Fig. 1). To rationalize these findings, empirical force field calculations were performed which confirm the experimentally observed preferential epitaxial alignment of the p6P crystallites (Fig. 2).

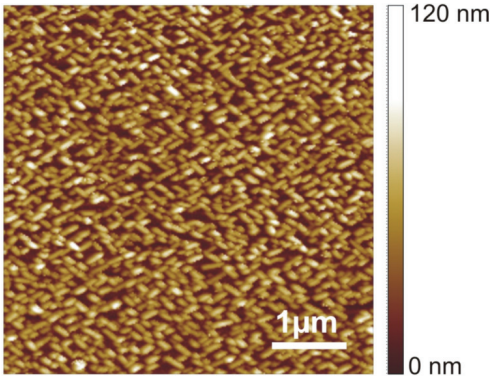

Fig. 1

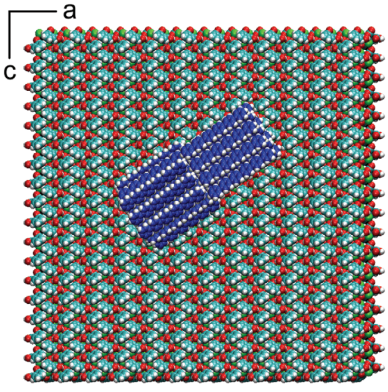

Fig. 2

References. [1] M. Campione, A. Sassella, M. Moret, A. Papagni, S. Trabattoni, R. Resel, O. Lengyel, V. Marcon, G. Raos, *J. Am. Chem. Soc.*, **128**, 13378, 2006; [2] A. Sassella, A. Borghesi, M. Campione, S. Tavazzi, C. Goletti, G. Bussetti, P. Chiaradia, *Appl. Phys. Lett.*, **89**, 261905, 2006; [3] G. Koller, G. Koller, S. Berkebile, J.R. Krenn, F.P. Netzer, M. Oehzelt, T. Haber, R. Resel, M.G. Ramsey, *Nanoletters*, **6**, 1207, 2006; [4] M. Oehzelt, M. Oehzelt, G. Koller, J. Ivanco, S. Berkebile, T. Haber, R. Resel, F.P. Netzer, M.G. Ramsey, *Adv. Mater.*, **18**, 2466, 2006.

CALCITE ($CaCO_3$) / ZABUYELITE (Li_2CO_3) EPITAXIES. SECTOR ZONING OF CALCITE AND ANOMALOUS MIXED CRYSTALS

L. Pastero, D. Aquilano

Dipartimento di Scienze Mineralogiche e Petrologiche, Università di Torino, Italy
linda.pastero@unito.it

Many papers dealing with the stabilization of the {0001} form of calcite due to the Li^+ presence in the growth solution have been published in the last 20 years [1,2]. Recently it has been proved that lithium adsorption modifies the {0001} pinacoid surface structure, turning its character from kinked (K, no PBC in the slice) to flat (F, at least 2 PBC in the slice) [3]. A detailed PBC study and a growth model of {0001} form bearing calcite have been proposed in our previous papers [3,4]. The pinacoid stabilization involves a 2D epitaxial growth mechanism between calcium and lithium carbonate, the model being supported by parametric fit between crystal phases.

An integrated study involving spectroscopic and imaging characterization techniques as ICP-OES, SEM, AFM, XRPD, CL and EPR on calcite crystals grown both from gel and solution allowed to identify two growth sectors characterized by the formation of calcite/zabuyelite anomalous [5,6] mixed crystals.

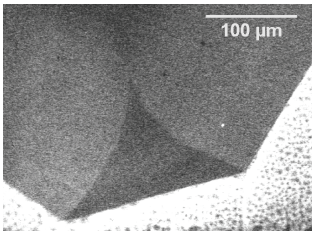

Fig. 1 - Panchromatic image of the {0001} growth sector of calcite (cathodoluminescence).

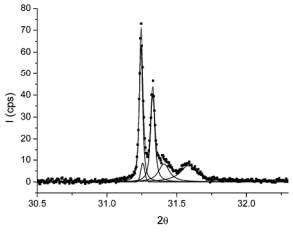

Fig. 2 - Decomposed XRPD (0006) peak clearly showing at least two crystal populations.

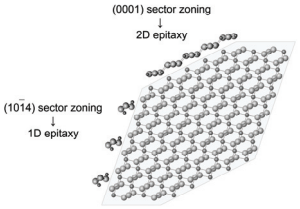

Fig. 3 - Epitaxies between calcite and zabuyelite related to (00.1) and (10.4) growth sectors of calcite.

Experiments and theoretical considerations confirm that lithium enters the calcite crystals during their growth, according to strongly differentiated sector absorption mediated by 2D and 1D epitaxy on the corresponding {0001} and {10$\bar{1}$4} crystal forms (Fig. 3).

References. [1] S. Rajam, S. Mann, *J. Chem. Soc., Chem. Comm*., 1789-1791, 1990; [2] I.V. Nefyodova, V.I. Lyutin, V.L. Borodin, P.P. Chvanski, N.I. Leonyuk, *J. Cryst. Growth*, **211**, 458-460, 2000; [3] L. Pastero, E. Costa, M. Bruno, G. Sgualdino, D. Aquilano, *Cryst. Growth Des.*, **4**, 485-490, 2004; [4] L. Pastero, D. Aquilano, E. Costa, M. Rubbo, *J. Crystal Growth*, **275**, e1625-e1630, 2005; [5] A. Johnsen, *Neues Jb. Miner.*, Bd.II, 93-138, 1903; [6] A. Neuhaus, *Z. Kristallogr.* **105**, 161-220, 1944.

MORPHOLOGY OF HALITE GROWING FROM PURE AQUEOUS SOLUTION. EXPERIMENTS AND PRELIMINAR THEORETICAL CONSIDERATIONS

L. Pastero, D. Aquilano, M. Bruno, M. Rubbo

Dipartimento di Scienze Mineralogiche e Petrologiche, Università di Torino, Italy
linda.pastero@unito.it

Many papers dealing with the NaCl morphology have been published since the sixties [1,2]. It's commonly recognized that solution grown halite crystals usually show a richer morphology compared with those obtained from vapor growth. Beside the cube, the {111} octahedron occurs both in the presence of surface specific impurities (formamide [3]) and, in pure aqueous solution, under well defined supersaturation conditions ($\beta > 1.1$) [2].

Here we worked with pure NaCl aqueous solutions, initially saturated at 90°C. Supersaturation have been reached trough different T/t paths corresponding to temperature gradients starting from 1°C/h to 50°C/h, the last one being practically considered as a quenching.

According to the supersaturation range, the growth morphology of halite crystals is determined by the growth rate competition between the {100} cube and the {111} octahedron. The SEM images we obtained show, unambiguously and for the first time, that the {111} octahedron becomes stable in solution, and confirm the pioneering findings of the Kern' School obtained by means of optical microscopy [2].

A preliminary morphodrome is shown in Fig. 1.

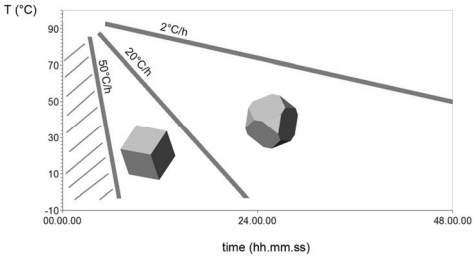

Fig. 1 - Preliminary morphodrome of {100} and {111} NaCl forms occurring in pure aqueous solution.

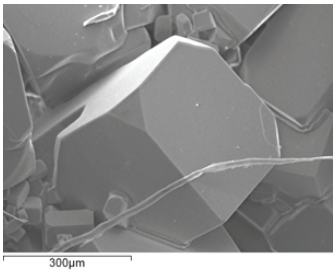

Fig. 2 - NaCl cube truncated by the {111} octahedron, grown from pure aqueous solution.

Calculated surface energies for rigid and relaxed {100} and {111} surfaces [4,5] confirm that the octahedron obtained from pure aqueous solution cannot belong to the equilibrium morphology of halite crystals. Then, it is reasonable assuming that cube/octahedron rate ratio is kinetically controlled. Further, no crystals were found at very high concentration gradients: this could be related to the nucleation kinetics dominating on growth during quenching.

References. [1] A. Johnsen, *Neues Jb. Miner.*, Bd.II, 93-138, 1903; [2] M. Bienfait, R. Boistelle, R. Kern, *"Adsorption et Croissance Cristalline" Coll. Intern. CNRS*, **152**, 515- 535, 1965; [3] N. Radenovic, W. van Enckevort, P. Verwer, E. Vlieg, *Surf. Sci.*, **523**, 307-315, 2003; [4] D. Aquilano, L. Pastero, M. Rubbo, in preparation; [5] M. Bruno, D. Aquilano, L. Pastero, M. Prencipe, *Cryst. Growth Des*., 2008, in press.

A NEW DRUG DELIVERY SYSTEM: β-CYCLODESTRIN BASED NANOSPONGES

L. Pastero[1], R. Cavalli[2], F. Trotta[3], D. Aquilano[1]

[1]*Dipartimento di Scienze Mineralogiche e Petrologiche, Università di Torino, Italy*
[2]*Dipartimento di Scienza e Tecnologia del Farmaco, Università di Torino, Italy*
[3]*Dipartimento di Chimica IFM, Università di Torino, Italy*
linda.pastero@unito.it

Cyclodextrin (CD) inclusion compounds [1-3] have been widely used in pharmaceutics, especially to improve solubility, dissolution rate and bioavailability of hydrophobic drugs. Nanosponges are hyper-cross-linked cyclodextrins forming solid nanoparticles insoluble in water.

However, drug supply through nanosponges could bring to a reduction of toxicity, an enhancement of therapeutic activity, a prolonged release and, not a negligible detail, a reduction of costs. Moreover, cyclodextrins as nanosponges show an excellent encapsulation capacity for drugs and can act as protecting agents for encapsulated molecules.

We started studying cyclodextrin nanosponges mainly through XRPD and DSC techniques.

From XRPD data we can establish a direct dependence between crystallinity degree of these nanosponges and β-CD/reticulating agent ratio. Comparing the XRPD peak intensity and the intensity/FWHM ratio of the diffraction peaks the crystallinity decreases from low to high β-CD/reticulating agent ratio (Fig. 1).

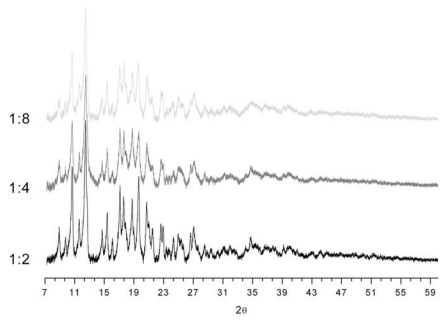

Fig. 1 - Comparison between three reticulation degrees of β-CD nanosponges.

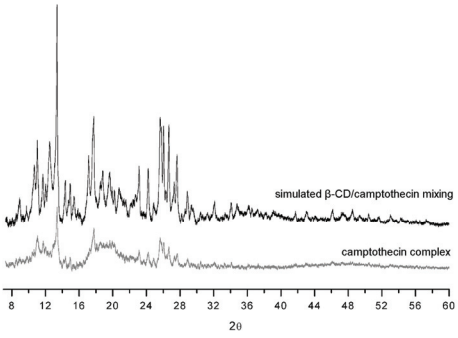

Fig. 2 - Comparison between the simulated XRPD pattern of a mechanical mixture between β-CD nanosponge, camptothecin drug and the true complex.

XRPD runs were also carried out on complexes obtained freeze-drying the β-CD nanosponges (1:4 reticulation ratio) in the presence of three different drugs previously studied by XRPD (camptothecin, dexamethasone and flurbiprofen), to deeply understand the behaviour of the complexes. A comparison between experimental and simulated XRPD data of such complexes was made in order to evaluate if the obtained the interaction was merely mechanical rather than chemical (Fig. 2): different drugs show different behaviours and only the camptothecin - β-CD complex can be undoubtedly considered a new crystalline phase.

References. [1] D. Duchêne, *Cyclodextrins and their industrial uses*, Ed. De Santè Paris, 1987; [2] K. Uekama, F. Hirayama, T. Irie, *Chem. Rev.*, **98**, 2045-2076, 1998; [3] R. Cavalli, F. Trotta, M. Trotta, L. Pastero, D. Aquilano, *Int. J. Pharm.*, **339**, 197-204, 2007.

CRYSTALLIZATION KINETICS OF CALCIUM CARBONATE AT 25, 30 AND 37°C

S. Rosa[1], H.E. Lundager Madsen[2]

[1]*Dipartimento di Scienze Mineralogiche e Petrologiche, Università di Torino, Italy*
[2]*IGV, Faculty of Life Sciences, University of Copenhagen, Denmark*
silvia.rosa@unito.it

The crystal growth kinetics of calcium carbonates ($CaCO_3$) was determined by mass crystallization experiments at 25°C, 30°C and 37°C, recording pH at selected time intervals during 4 hours, by mixing $CaCl_2$, Na_2CO_3 and HCl solutions in test tubes, the total volume being 10 ml. The data from recording pH *vs.* time were analyzed using the Ion Equilibrium Program IONICS, a general computer program for equilibrium in aqueous electrolyte solutions, applicable to a system for which the relevant equilibrium constants are known [1,2]. From data of each experiment, kinetics calculations were done. At the first approach, calculating the crystal growth rates as a function of supersaturation, the data obtained show that the growth curves agree with the surface nucleation mechanism only in part, because the growth rate does not tend to zero with decreasing supersaturation as fast as it should if this were the only mechanism operative. This points to the spiral growth mechanism as a competing mechanism. All the rate contributions related to the mechanisms of growth were calculated using:

- classical BCF theory [3] for the spiral growth contribution at low supersaturation;
- Gilmer's equation [4] for the combination of spiral growth and surface nucleation operating at higher supersaturation ;
- the equation for the rate of polynuclear growth, based on the theory of Christoffersen *et al.* [5] in order to calculate the edge free energy related to the (10.4) form of calcite.

The results obtained are:

- 30°C experiments: all the edge free energy λ values obtained arrange reasonably to a value of 39±1.5 pJ/m.
- 25°C experiments: two mechanisms of crystallization were found: 1. homogenous nucleation at the beginning of the precipitation experiments witnessed by γ surface free energy values of 43±3 mJ/m^2, the analysis based on the classical theory of Becker, Döring, Zel'dovich and Frenkel (BDZF) [6]; 2. surface nucleation with an edge free energy λ (pJ/m) value of 36.5±1.5 pJ/m.
- 37°C experiments: the situation was more complex than at lower temperatures, because not only calcite, but aragonite as well crystallized. This caused the otherwise linear kinetic plots to become curved, the growth rate tending to 0 earlier than expected. Aragonite crystals were, in fact, detected by microscopy.

References. [1] H.E. Lundager Madsen, *Néphrologie*, **5**, 151, 1984; [2] Y. Berland, M. Olmer, M. Grandvuillemin, H.E. Lundager Madsen, R. Boistelle, *J. Cryst. Growth*, **87**, 494, 1988; [3] W.K. Burton, N. Cabrera, F.C. Frank, *Philos. Trans. Roy. Soc*., **243**, 299, 1961; [4] G.H. Gilmer, *J. Cryst. Growth*, **35**, 15, 1976; [5] M.R. Christoffersen, J. Dohrup, J. Christoffersen, *J. Cryst. Growth*, **186**, 283, 1998; [6] S. Thoschev, In: Crystal Growth, An Introduction, P. Hartman, Ed., North-Holland, Amsterdam, Ch. 1, 1993.

INFLUENCE OF MAGNESIUM, BARIUM AND LEAD(II) IONS ON CRYSTAL GROWTH OF BRUSHITE

S. Rosa[1], H.E.Lundager Madsen[2]

[1]*Dipartimento di Scienze Mineralogiche e Petrologiche, Università di Torino, Italy*
[2]*IGV, Faculty of Life Sciences, University of Copenhagen, Denmark*
silvia.rosa@unito.it

Calcium hydrogen phosphate dihydrate, $CaHPO_4 \cdot 2H_2O$, known as the rare mineral brushite, has been precipitated at 25°C in pure solution and in the presence of foreign di-valent metal ions as Mg^{2+}, Ba^{2+}, Pb^{2+}, recording pH at selected time intervals during 6 hours. $Ca(NO_3)_2$, KH_2PO_4 and K_2HPO_4 (all solutions 0.1M) were used as the pure system and $Mg(NO_3)_2$, $Ba(NO_3)_2$ and $Pb(NO_3)_2$ as additives (all solutions 0.1M). The experiments were done as series with decreasing amount of the additives.

The data from recording pH *vs.* time were analyzed using the Ion Equilibrium Program IONICS, a general computer program for equilibrium in aqueous electrolyte solutions, applicable to a system for which the relevant equilibrium constants are known [1,2]. From data of each experiment, all the rate contributions related to the mechanisms of growth were calculated using:

- classical BCF theory [3] for the spiral growth contribution at low supersaturation;
- Gilmer's equation [4] for the combination of spiral growth and surface nucleation operating at higher supersaturation ;

The results obtained are:

- "Mg^{2+}" experiments: the values of edge free energy λ obtained increase with decreasing the amount of additive, until a value close to that of pure brushite was reached. All the values arrange reasonably to a linear trend, following the Gibbs' adsorption isotherm [5] adapted to adsorption along a step;
- "Ba^{2+}" experiments: we obtained the same linear trend of the edge free energy values, showing that the theory of Gibbs' adsorption along a step may be valid for this case as well;
- "Pb^{2+}" experiments": the system with $Pb(NO_3)_2$ additive is more difficult and complicated probably due to the precipitation of one or more lead phosphates.

References. [1] H.E. Lundager Madsen, *Néphrologie*, **5**, 151, 1984; [2] Y. Berland, M. Olmer, M. Grandvuillemin, H.E. Lundager Madsen, R. Boistelle, *J. Cryst. Growth*, **87**, 494, 1988; [3] W.K. Burton, N. Cabrera, F.C. Frank, *Philos. Trans. Roy. Soc.*, **243**, 299, 1961; [4] G.H. Gilmer, J. Cryst. Growth, **35**, 15, 1976; [5] R. Defay, I. Prigogine, A. Bellemans, D.H. Everett, *Surface Tension and Adsorption*, Longmans, London, Ch. VII, 1966.

VIBRATIONAL MODES ON (100) SURFACE OF LiF CRYSTAL

M. Rubbo, M. Bruno, M. Prencipe

Dipartimento di Scienze Mineralogiche e Petrologiche,Università di Torino, Italy
marco.rubbo@unito.it

A key factor determining the stability of a crystal face is the surface free energy. It accounts for the athermal work of separation at 0 K, the vibration and zero point surface energy, and the surface entropy. Usually the athermal work of separation at 0 K is calculated while the measured quantity (*e.g.* the reversible work to cleave a crystal [1]) includes all the mentioned contributions. Moreover, the stability of polar surfaces, such as (111) of LiF, can be assessed by calculating the surface phonon dispersion across the 2D Brillouin zone, where the presence of any imaginary phonons would indicate that a reconstruction must occur [2].

As a preliminary work toward the study of polar faces, we present the method followed to calculate the entropy associated to the (100) surface of LiF. Essentially the vibrational partition functions is calculated from the frequency spectrum of the infinite crystal and of slabs limited by (100) faces (the figure shows the frequency dispersion curves along [100]*).

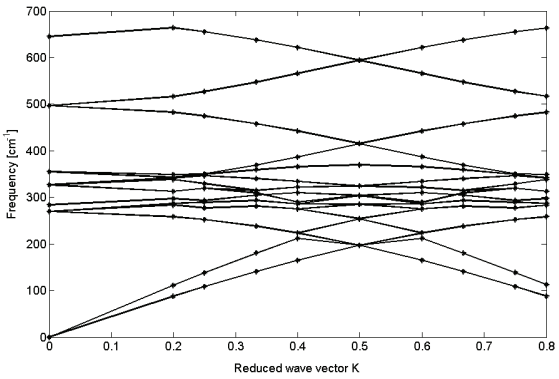

The harmonic vibrational frequencies and modes are calculated using the CRYSTAL06 [3,4] software for quantum-mechanical *ab-initio* calculations. The differences between the values of the thermodynamic functions of a macroscopic slab and of those of a bulk crystal, are ascribed to the surface.

It is calculated that the vibrational energy and entropy decrease the surface free energy of a macroscopic slab by -5.651 erg/cm^2 at 77 K, and by -47.123 erg/cm^2 at 298.15 K. By considering that the calculated value of the separation work is ≈ 350 erg/cm^2, it appears that the vibrational contribution cannot be neglected even at relatively low temperature.

References. [1] J.J. Gilman, *J. Appl. Phys.*, **31**, 2208-2218, 1960; [2] A.L. Rohl, K. Wright, J.D. Gale, *Am. Mineral.*, **88**, 921-925, 2003; [3] R. Dovesi, V.R. Saunders, C. Roetti, R. Orlando, C.M. Zicovich-Wilson, F. Pascale, B. Civalleri, K. Doll, N.M. Harrison, I.J. Bush, Ph. D'Arco, M. Llunell, *CRYSTAL06 User's Manual*, University of Torino, 2006; [4] C. Pisani, R. Dovesi, C. Roetti, *Hartree-Fock ab-initio treatment of crystalline systems, Lecture Notes in Chemistry*, Springer, 1988.

MATERIALS, FROM EARTH AND LAB TO LIFE - 2

Session 12
Building-up organic-based nanodevices

MULTIPHOTON LASER SCANNING CONFOCAL SPECTRO-MISCROSCOPY FOR ADVANCED MOLECULAR BASED OPTOELECTRONIC AND PHOTONIC NANODEVICES

M. Muccini

Dipartimento di Progettazione Molecolare, CNR-ISMN, Bologna, Italy
michele.muccini@ismn.cnr.it

During the last decade it has become clear that organic materials can be successful candidates as "basic brick" for a new class of nano devices. The development of optical nanoprobes such as Laser Scanning Confocal Microscopy (LSCM) and spectroscopy can play a key role for material science and nanotechnology enabling a direct correlation of the spectroscopic properties of materials and devices with morphological features at the nanoscale. Recent results of LSCM studies on organic thin films allowing imaging and direct correlation of molecular ordering toward optoelectronic properties of semiconduting organic thin films will be presented in view of real devices such as Organic Light Emitting Diodes (OLED), Organic Light Emitting Transistors (OLET) and ultrafast photonic switches.

FUNCTIONAL SURFACES WITH SPECIAL WETTABILITY FOR NEW MATERIALS AND DEVICES

M. Maggini

Dipartimento di Scienze Chimiche, Università di Padova, Italy
michele.maggini@unipd.it

Wettability is important in many industrial and biological processes, ranging from self-cleaning surfaces to microfluidics and biomedicine. This communication presents our results on the wetting properties of solid surfaces that have been functionalized with organic molecular structures. In particular, we describe the wettability characteristics, studied through water contact angle measurements, of crystalline and porous silicon surfaces containing grafted [60]fullerene derivatives. Also, the effect of rearrangement of chemical functionalities, such as spiropyrans present at the solid surface, on wettability will be presented and discussed.

COMPUTATIONAL MODELLING OF LAYERED MATERIALS FOR ADVANCED APPLICATIONS

M. Causà[1], V. Barone[1,2]

[1]*Dipartimento di Chimica "P. Corradini", Università di Napoli, Italy*
[2]*Istituto per i Processi Chimico-Fisici, CNR, Pisa, Italy*
mauro.causa@unina.it

Layered materials are important in many relevant fields: controlled blends between organic molecules and clays, natural or synthetic, are promising new materials, with tuneable physical and chemical properties; some heterogeneous catalysts have a dominant layered structure, that shows abundant and active reaction sites. Intercalated graphenes have remarkable electronic properties, and offer new possibilities for advanced applications. In our laboratory we are studying the structure and reactivity of layered materials using a set of *ab initio* models: from molecular clusters, that allow high accurate description of local phenomena to periodic models with cyclic boundary conditions in 2 and 3 dimensions, that allow to describe collective phenomena. The effect of the material environment can be studied introducing systematically perturbations on the molecular clusters, embedding in electrostatic fields, polarizable continuum and more complex representation of the crystal fields, like effective ion potentials. The cooperative use of different *ab initio* models offer new exciting possibilities for an accurate description of physico-chemical processes of relevance in several fields of materials sciences. Status and perspectives of new integrated strategies will be illustrated by some case studies from our own experience. The Quantum mechanical methods on crystalline materials are used for getting information, together with experiments, about the structure of artificial Aluminum-Phosphorus phyllosilacate-like materials used in composed plastic materials. The *ab initio* methods are used for answering to open questions about the polymerization catalysts based on the layered crystals [1] $TiCl_3$ and $MgCl_2$ (Ziegler-Natta catalysts). The open questions about the structural properties of elementary carbon materials, based on poly-aromatic and graphenic structures are also addressed [2], with implication in technologies and environmental problems.

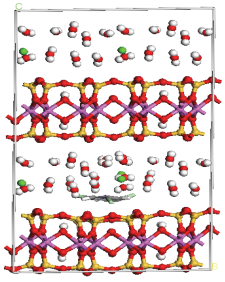

Organic dies in Ca-montmorillonite framework.

References. [1] V. Busico, M. Causà, R. Cipullo, R. Credendino, F. Cutillo, N. Friederichs, R. Lamanna, A. Segre, V.V. Castellit, *J. Phys. Chem. C*, **112**, 1082-1089, 2008; [2] A. Giordana, A. Maranzana, G. Ghigo, M. Causà, G. Tonachini, *J. Phys. Chem. A*, **112**, 973-982, 2008.

CODEPOSITION OF HYBRID NANOSTRUCTURED MATERIALS BY SUPERSONIC BEAMS FOR FOTOVOLTAIC APPLICATIONS

N. Coppedè[1], T. Toccoli[1], M. Nardi[1], R. Verucchi[1], S. Iannotta[2]

[1]*IFN-CNR, Trento, Italy*
[2]*IMEM-CNR, Parma, Italy*
coppede@science.unitn.it

Hybrid materials based on metal oxides and organic molecules have been developed using different techniques, in particular to find applications in photovoltaic systems. Typical problems in the realization of organic-inorganic interface exist: nano-crystalline metal oxides need annealing which are incompatible with organics, the deposition done after the annealing with polymers presents difficulties in matching completely the porous structures and also using small molecules the interface is not maximized, while weak bonds are typically present between the two species. We present a different approach to the synthesis of hybrid materials using Supersonic beam Codeposition, where clusters of metal oxides and organic molecules are deposited together through Supersonic Seeded Beams, promoting thermodynamical processes highly out of equilibrium. In particular, using Pulsed Supersonic Cluster Beam deposition, we are able to realize porous TiO_2 films with a nanocrystalline structure even on substrates at RT [1], allowing the codeposition with organic molecules without any annealing. Moreover by Continuous Supersonic Beam deposition we synthesize the metal oxide with organic molecules, using the high kinetic energy of the molecules in the beam to kinetically activate chemical process at the interface [2]. The contemporary deposition from supersonic beams allows the formation of a hybrid material [3] made of nanocristalline grains of metal oxide directly decorated with organic molecules. The matrix of sensitized metal oxide and organic molecules allows the maximizing of the interface between organic and inorganic, where happens the separation of the excitons. We realized prototypal solar cells by supersonic beam deposition based on TiO_2 and CuPc. To understand the role of codeposited hybrid interface we compare the performances of cells with a sharp interface between the two layers, respect to a cell with a hybrid codeposited interface layer in the active zone of the device. These last present an enhancement of the photocurrent a factor 50 and of the efficiency of a factor 30. The ability to grow metal oxides with nanocrystalline structure at RT pave the way to the realization of new hybrid solar cell, also on plastic and flexible substrates.

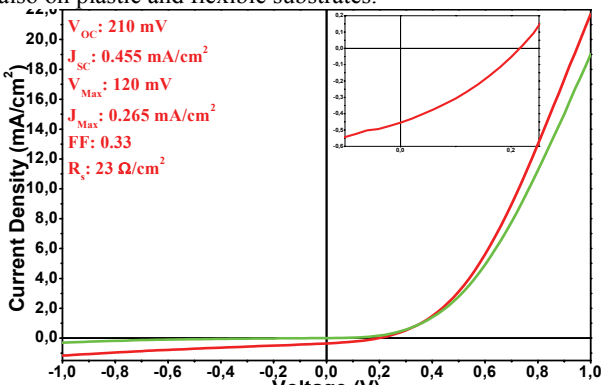

References. [1] T. Toccoli, S. Capone, L. Guerini, M. Anderle, A. Boschetti, E. Iacob, V. Micheli, P. Siciliano, S. Iannotta, *IEEE Sens. J.*, **3**, 199, 2003; [2] S. Iannotta, T. Toccoli, *J. Polym. Sci. Pol. Phys.*, **41** 2501, 2003; [3] F. Siviero, N. Coppedè, A.M. Taurino, T. Toccoli, P. Siciliano, S. Iannotta, *Sens. Actuat. B-Chem*, **130**, 405-410, 2008.

HOMO- AND HETERO- EPITAXIAL GROWTH OF THIN FILMS AND NANOSTRUCTURES BY ORGANIC MOLECULAR BEAM EPITAXY

A. Sassella[1], A. Borghesi[1], M. Campione[1], M. Moret[1],
L. Raimondo[1], C. Goletti[2], G. Bussetti[2], P. Chiaradia[2]

[1]*Dipartimento di Scienza dei Materiali e CNISM, Università di Milano-Bicocca, Italy*
[2]*Dipartimento di Fisica e CNISM, Università "Tor Vergata" di Roma, Italy*
adele.sassella@unimib.it

In the frame of research on molecular materials, particular attention is devoted to organic semiconductors in view of their application in organic devices, *e.g.* organic light emitting diodes, transistors, and solar cells. One of the main limits of such devices is the limited charge carrier mobility in organic semiconductors, which can only be improved when highly controlled structural and morphological properties of materials and interfaces will be available. In addition, the organic active materials have usually to be integrated in the device in the form of thin films, possibly within multilayered structures. Therefore, the growth of high quality crystalline organic films and multilayers is a goal of primary importance.

Here, we show how homo- and hetero- epitaxial films and multilayers can be grown by organic molecular beam epitaxy (OMBE [1]), discussing some examples of organic-organic epitaxial structures obtained choosing single crystalline organic substrates and finely tuning the growth conditions. The analysis of the grown samples is carried out *in situ* during growth by reflection anisotropy spectroscopy [2] and *ex situ* by atomic force microscopy (AFM) and clearly demonstrates the characteristics of organic epitaxy [3,4]. As an example, the figure below shows two AFM images, one (left) collected over a 6×6 μm^2 region of a submonolayer film of α-quaterthiophene (α-4T) grown on a α-sexithiophene (α-6T) single crystal and the other one (right) over a 11×11 nm^2 region of a crystalline α-4T island of the same sample. In the left image, the monomolecular α-4T islands are clearly visible as the brightest regions; close to the edge of a terrace of the original α-6T crystal surface, the step flow mode of growth of α-4T is also observed. In the right image, collected with molecular resolution, the surface unit cell can be identified and is found to match with that of the (001) lattice plane of the known low-temperature polymorph of α-4T; the α-4T film is therefore crystalline and the alignment of its crystal structure with that of the substrate demonstrates a perfect heteroepitaxial growth.

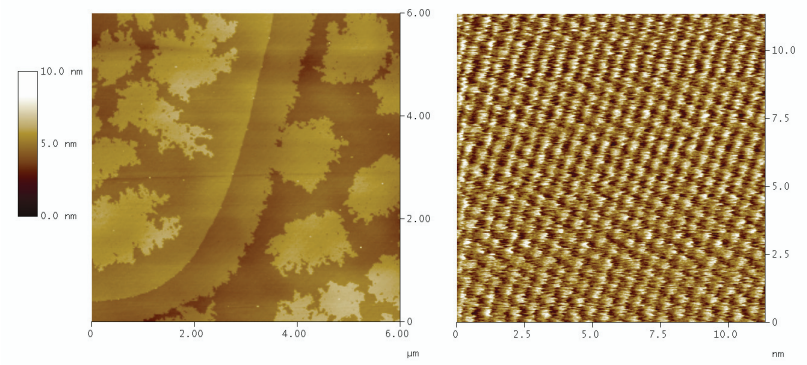

References. [1] S.R. Forrest, *Chem. Rev*., **97**, 1793-1896, 1997; [2] P. Weightman, D.S. Martin, R.J. Cole, T. Farrell, *Rep. Prog. Phys*., **68**, 1251-1341, 2005; [3] M. Campione, A. Sassella, M. Moret, A. Papagni, S. Trabattoni, R. Resel, O. Lengyel, V. Marcon, G. Raos, *J. Am. Chem. Soc*., **128**, 13378-13387, 2006; [4] A. Sassella, M. Campione, A. Papagni, C. Goletti, G. Bussetti, P. Chiaradia, V. Marcon, G. Raos, *Chem. Phys*., **325**, 193-206, 2006.

MATERIALS, FROM EARTH AND LAB TO LIFE - 2

Session 13
Structural characterization of nano-crystalline materials

STRUCTURE SOLUTION OF A NOVEL Li-Ni-Ti OXIDE WITH PRECESSION ELECTRON DIFFRACTION DATA

M. Gemmi[1,2], H. Klein[2,3], A. Rageau[2], P. Strobel[2]

[1]*Dipartimento di Scienze della Terra, Università di Milano Italy*
[2]*Institut Néel, CNRS, Grenoble, France*
[3]*Université J. Fourier, Grenoble, France*
mauro.gemmi@unimi.it

A novel Li-Ni-Ti oxide was synthesized from a mixture of Li carbonate, Ni acetate and Ti oxide treated at 900°C in air and leading to a final composition of $LiNi_{0.5}Ti_{1.5}O_4$. The final product contains several new phases, therefore it has been impossible to index its powder X-ray diffraction pattern. Electron diffraction investigations allow to identify two new phases, having an hexagonal and a monoclinic cell respectively. X-ray diffraction indicates that the hexagonal phase should be the dominant one. Its cell has $a = b = 5.051(1)$ and $c = 32.489(2)$ Å respectively. Electron diffraction data are compatible only with two trigonal space groups $P3c1$ and $P\bar{3}c1$, due to *00l* odd extinctions and to the absence of an *mm* symmetry in the [100] zone axis. In order to solve the structure we collected precessed electron diffraction patterns [1] on 7 different zone axes, with precession angle varying between 2.5° and 3.5°. The patterns were integrated with the program QED [2] and the intensities were merged using two common rows of reflections after correction for the precession geometry [3]. The final internal R value is surprisingly low for electrons: 6.3%. A structure solution is obtained in the space group $P\bar{3}c1$ using SIR2008 program [4] and treating the electron diffraction intensities as $|F|^2$. The solution gives 1 position for Ni, 4 for Ti, and 8 weaker peaks in the Fourier map that are assigned to O and Li. From simple crystal chemical considerations 4 O positions are sorted among the weak peaks, and the rest can be assigned to Li atoms. A Rietveld refinement on synchrotron radiation diffraction data, using this model as starting point, is stable, and gives as figures of merit wRp = 14.3%, Rp = 8.6% and $R(F^2) = 12.8\%$ confirming that the structure solution is achieved and can be refined.

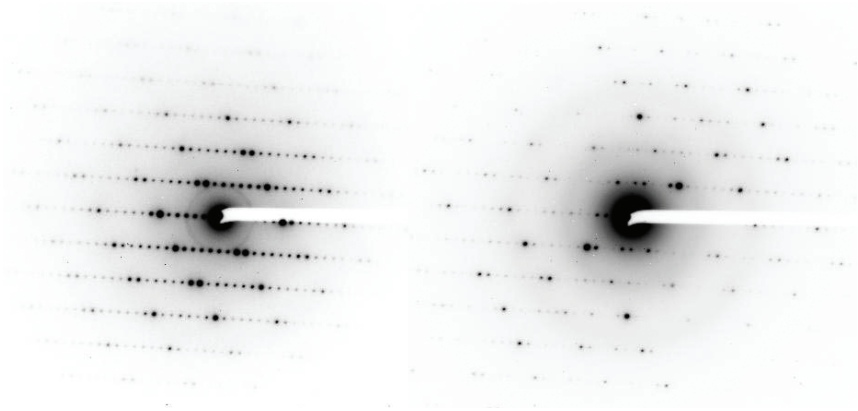

Fig. 1 - Normal selected area diffraction pattern (left) and precessed electron diffraction pattern (right) of $Li_6Ni_2Ti_8O_{21}$ taken on [100] zone axis. The precession angle is 2.5°

References. [1] R. Vincent, P.A. Midgley, *Ultramicroscopy,* **53**, 271-282, 1994; [2] D. Belletti, G. Calestani, M. Gemmi, A. Migliori, *Ultramicroscopy,* **81,** 57-65, 2000; [3] M. Gemmi, X. Zou, S. Hovmöller, A. Migliori, M. Vennström, Y. Andersson, *Acta Crystallogr. A***59**, 117-126, 2003; [4] M.C. Burla, R. Caliandro, M. Camalli, B. Carrozzini, G.L. Cascarano, L. De Caro, C. Giacovazzo, G. Polidori, D. Siliqi, R. Spagna, *J. Appl. Crystallogr.*, **40**, 609-613, 2007.

LOCAL AND AVERAGE BEHAVIOUR OF SIZE-STABILISED NANO-CRYSTALLINE ZIRCONIA BY PAIR DISTRIBUTION FUNCTION AND RIETVELD ANALYSIS

M. Dapiaggi[1], G. Borghini[1], F. Maglia[2], E.S. Ferrari[1]

[1]*Dipartimento di Scienze della Terra, Università di Milano, Italy*
[2]*Dipartimento di Chimica Fisica, Università di Pavia, Italy*
monica.dapiaggi@unimi.it

The high-temperature ZrO_2 phases (cubic and tetragonal) are suitable for various industrial applications such as solid electrolytes in solid oxide fuel cells and sensors, as a catalyst/catalyst support, and as membranes and dispersed phase in composite materials. Unfortunately they are stable above 1200 and 2300°C, respectively, and cannot be quenched at room temperature. They are usually stabilized at room temperature by doping by bi and trivalent cations, such as Y and Ca, for example, but they can also be stabilized without doping, provided that ZrO_2 is synthesised in its nanocrystalline form with a grain size lower than a critical value (about 20-30 nm). Five samples of nanocrystalline zirconia were analysed: pure ZrO_2 (no doping), and various (small) Y contents (0.5, 1, 2, and 4 wt.%).

The data were collected at room temperature at ID31 (European Synchrotron Radiation Facility) up to Q_{max} = 30 $Å^{-1}$. The Rietveld refinements were performed using the software GSAS-EXPGUI [1] and the PDF refinements with the softwares PDFgui and PDFfit2 [2].

The PDFs of the various samples showed small but well detectable differences from one another, in particular in the low R region (below about 6 Å), where local distortions due to the presence of the larger dopant cation are more likely to appear. From the PDFs, it is easier to recognize the tetragonal from the cubic structure, as the tetragonal form presents two different Zr-O distances at low R (instead of the one for the cubic structure), clearly visible for all the samples. In particular, these two peaks are present at slightly different distances, and their separation is different for all the samples studied. Moreover, the first peak presents different widths as a function of Y content, with a maximum for Y = 2 wt.% and a minimum for Y = 4 wt.%. A different peak width in a PDF might be a sign of thermal disorder as well as of static disorder (*i.e.* a distortion that leads to 4 slightly different distances in place of 4 equal ones). As the thermal effect should be roughly the same for all samples (all collected at room temperature), a larger peak width can be a sign of a structural distortion. The Zr (or Y) atoms are at the centre of a distorted cubic polyhedron, with alternate long-short Zr-O distances. The difference between these two distances is a measure of the polyhedron distortion, which changes with increasing dopant content.

References. [1] A.C. Larson, R.B. Von Dreele, *Los Alamos National Laboratory Report LAUR*, 86-748, 1994; [2] C.L. Farrow, P. Juhas, J.W. Liu, D. Bryndin, E.S. Bozin, J. Bloch, T. Proffen, S.J.L. Billinge, *J. Phys.-Condens. Mat.*, **19**, 335219, 2007.

TWIN LAMELLA CHARACTERIZATION OF 15R-SiC BY MEANS OF TRANSMISSION ELECTRON MICROSCOPY

G. Agrosì, G.C. Capitani, E. Scandale, G. Tempesta

Dipartimento Geomineralogico, Università di Bari, Italy
g.agrosi@geomin.uniba.it

The study of SiC has been recently developed significantly because of the physical and electrical properties of its basic polytypes, which make it a promising semiconductor material for electronic devices. Nevertheless, the device performance is often compromised by the grown-in structural defects such as dislocations, micropipes, grain boundaries, misoriented areas, etc. [1]. Moreover, due to the low stacking fault energy, it is difficult to obtain single polytype material during bulk crystal growth and, consequently, it is common to find the coalescence of 6H, 4H, 15R and 3C polytypes. These polytypes differ among them for different ordered stacking sequences of SiC bilayers. Different stacking of bilayers can also generate twins but, unfortunately, works that investigate on the twins of SiC are quite rare. Although several improvements have been recently obtained on the reduction of the micropipes and of the density of dislocations [2], the presence of several structural defects in the SiC crystals remains a problem that has not been solved yet.

In this contribution the results on a twin micro-lamella of 15R, embedded in a macro-lamella of 15R enclosed in 6H-SiC wafer, are reported. The wafer, grown by PVT method, shows a complex syntactic coalescence of polytypes that was previously investigated by means of X-Ray Diffraction Topography, using both White-Beam-Synchrotron-Radiation-Source and MoKα_1 conventional source and μ-Raman Spectroscopy. This earlier multi-analytical study permitted to localize and to identify the twin lamella that, subsequently, was prepared for TEM analyses.

The selected area electron diffraction patterns (SADPs) taken exactly above the interface of the micro-lamella show the presence of twinning. In order to determine the twin law, comparisons among SADPs and simulations of the diffraction pattern introducing all the possible twin operations were carried out. Moreover, taking into account also the XRDT and μ-Raman data previously obtained, it has been found that the twin law consists of π-rotation around [0001] with (0001) as composition plane. Additionally, the analysis of SADPs permits also to determine that the twin index is 3 and the obliquity is zero.

High Resolution (HRTEM) images of the twin boundaries reveal that the interpretation of the contrast is not trivial because of the presence of numerous adjoining stacking faults parallel to (0001) with interleaving (33) and (22) lamellae. The Fourier Transform calculated across the boundary (33)/(22) does not show any splitting and thus this sequence introduces no twinning within the 15R but consists of 4H and 6H like sequences. On the contrary, HRTEM images taken across the boundaries can be interpreted with reference to the primitive oblique 2D cell of the 15R polytype as a zig-zag pattern (23) that switches to (32) by a twin coherent interface or, alternatively, as zig-zag pattern (32) which passes to (23) through an isolated (33) lamella. In other words, the twin interface can be also considered as the interposition of a 6H lamella and thus the origin of the twin lamella is strictly related to the stacking faults. Consequently, it can be concluded that the low energy of stacking faults in 15R SiC [3] favours also the growth of twin lamellae.

References. [1] G. Agrosì, R.A. Fregola, A. Monno, E. Scandale, G. Tempesta, *Mater. Sci. Forum*, **483-485**, 311-314, 2005; [2] D. Nakamura, *Mater. Sci. Forum,* **527-529,** 3-7, 2006 [3] H.P. Iwata, U. Lindefelt, S. Oberg, P.R. Briddon, *Physica B*, **340-342,** 165-170, 2003.

MOLECULAR ORIENTATION IN QUATER- AND QUINQUE-THIOPHENE THIN FILMS

M. Gazzano, M. Melucci, L. Favaretto, G. Barbarella

Istituto per la Sintesi Organica e la Fotoreattività (ISOF), CNR, Bologna, Italy
gazzano@isof.cnr.it

Solution-processable organic semiconductors are potentially low-cost alternatives to amorphous-silicon materials for electronics applications. Organic thin-film transistors are particularly suitable for the fabrication of large-area devices where high switching speeds are not essential. For practical applications the organic semiconductors need to provide high field-effect transistor mobilities that could be achieved if a proper molecular order is obtained in the semiconductor. In recent years Barbarella *et al*. [1,2] reported many examples of modified quater- and quinque- thiophene based molecules that posses a high self-assembly capability (some examples are reported at the bottom). These molecules are able to get a very high degree of order, some of them even by simply casting from solution.

X-ray diffraction (XRD) directly performed on the films was used to investigate the crystal phases and the structural ordering of these molecules. The profiles obtained are affected by a severe reduction of the peak number and show an irregular intensity distribution. In this communication we show the application of Rietveld-Toraya or March-Dollase routines for the calculation of patterns from single crystal data matching very well experimental data. The results obtained allow to estimate the position of the molecules respect to an applied electrical field and hence to foresee their electrical properties in possible devices.

The limitation of these models will also be discussed.

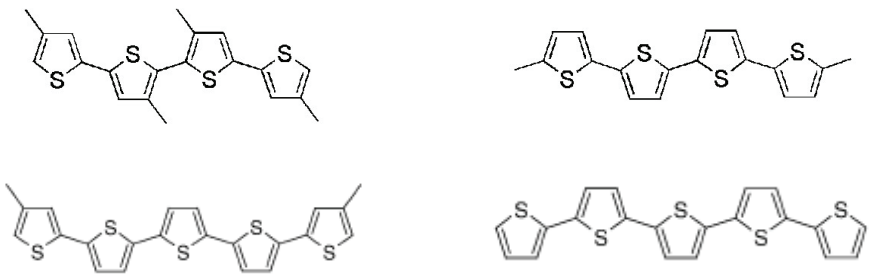

References. [1] P. Ostoja, P. Maccagnani, M. Gazzano, M. Cavallini, J.C. Kengne, R. Kshirsagar, F. Biscarini, M. Melucci, M. Zambianchi, G. Barbarella, *Synthetic Met.*, **146**, 243-250, 2004; [2] M. Melucci, M. Gazzano, G. Barbarella, M. Cavallini, F. Biscarini, P. Maccagnani, P. Ostoja, *J. Am. Chem. Soc.*, **125**, 10266-10274, 2003.

TEXTURE ANALYSIS OF AN Al-EVAPORATED THIN FILM, WITH ELECTRON DIFFRACTION DATA

M. Gemmi[1], M. Voltolini[2], H.R. Wenk[2]

[1]*Dipartimento di Scienze della Terra, Università di Milano, Italy*
[2]*Department of Earth &Planetary Science, University of California, Berkeley, USA*
mauro.gemmi@unimi.it

An Al thin film, produced by evaporation on an amorphous carbon film, has been investigated with selected area electron diffraction (SAED). The powder SAED patterns were collected with a CCD camera using the largest diaphragm in order to have complete diffraction discs with reliable statistics. The patterns were integrated using the software Fit2D, after refining the camera length, the beam center, and the tilt of the CCD detector. The resulting intensity *vs.* 2Θ spectrum, collected with the sample normal to the beam, was analyzed with the Rietveld method GSAS, after inserting the electron scattering factor for Al to check if a Rietveld refinement is possible. The fit is acceptable only if a strong preferential orientation of a [111] direction normal to the film is considered. In order to directly investigate the texture of the film, we tilted the sample along the two orthogonal axes of the sample holder, and collected electron diffraction patterns at 5° intervals. Texture analysis was carried out adapting a consolidated texture analysis procedure for synchrotron hard X-ray diffraction data [1] using the MAUD software. After importing the electron structure factors F_{hkl} for cubic Al, we proceeded with texture analysis using the EWIMV algorithm, refining experimental geometry parameters, peak profile function coefficients, backgrounds, scale factor and texture. Pole figures obtained for the aluminum film are plotted in Fig. 1, and clearly show a strong (111) fiber texture. As a check, the analysis was carried out both without sample symmetry and with axial symmetry imposed and the resulting texture data are practically identical. Even without imposing symmetry the analysis was surprisingly stable. We present here for the first time, a texture analysis based on the Rietveld method applied to electron diffraction data. This new procedure seems very suitable to study textures in nanocrystalline materials and seems mature enough to be applied to more complex systems.

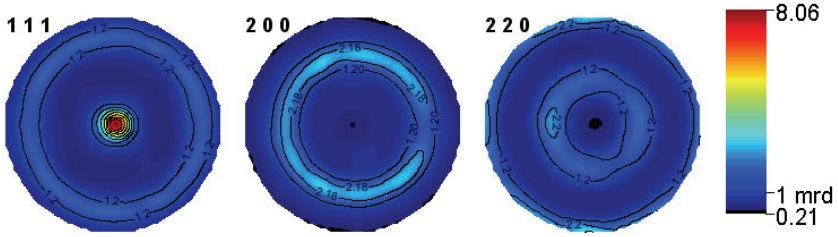

Fig.1 - (111), (200) and (220) pole figures for the aluminum film sample. No sample symmetry imposed. Equal area projection. Intensity in multiples of random distribution (m.r.d.).

References. [1] G. Ischia, H.-R. Wenk, L. Lutterotti, F. Berberich, *J. Appl. Crystallogr.*, **38**, 377-380, 2005.

NATURAL AND SYNTHETIC NANODIAMONDS: FROM STARS TO LABORATORIES

V. Guglielmotti[1], S. Orlanducci[1], E. Tamburri[1], D. Sordi[1], F. Toschi[1], M.L. Terranova[1], M. Rossi[2]

[1]*Dipartimento di Scienze e Tecnologie Chimiche, MINASlab, Università "Tor Vergata" di Roma, Italy*
[2]*Dipartimento di Energetica, Università "La Sapienza" di Roma, Italy*
valeria.guglielmotti@uniroma2.it

The methodologies recently settled for production of nanostructured forms of carbons have recently opened a new scenario in the field of innovative materials. The potential impact of nanographites, nanotubes, graphene, fullerenes and nanodiamonds on science and technology is enormous and only in the last years the consequences on our lives began to be perceived. It is intriguing, however, to note that some of these nanostructures are natural occurrences.

In particular, nanodiamonds have become a topic of great interest since they exhibit a number of remarkable features both in their structure and in their physicochemical properties.

Owing to their superior chemical and physical properties as well as biocompatibility, diamond-based nanostructures have emerged as promising alternative materials for biomedical applications such as the use of fluorescent nanodiamond particles for biological tagging and imaging applications [1,2]. Furthermore may be useful in a wide range of products because they are inert chemically, thermally and mechanically.

Natural nanodiamonds are found in: meteorites (the nanodiamonds recovered from meteorites are considered "messengers from the stars" because they carry out traces of chemical and physical processes in interstellar media [3]), as mineral inclusions in terrestrial rocks (for example in zircon minerals from Jack Hills, Western Australia) and as very old fragments of the Earth's crust.

All these materials have closely related properties and show a variety of shapes, such as nanoparticles, nanowires, needle-like, platelets [4]. The synthetic diamond nanocrystals mimic the same shapes of the natural nanodiamonds. By using synthetic processes carried out under far-from- equilibrium conditions (CVD, PECVD techniques) a variety of exciting nanostructures can be fabricated.

Some examples of diamond layers, grown by HFCVD, will be discussed and their characterizations by means of SEM, Raman Spectroscopy, Electron and X-Ray Diffraction will be presented.

References. [1] S.J. Yu, M.W. Kang, H.C. Chen, K.M. Chen, Y.C. Yu, *J. Am. Chem. Soc.*, **127**, 17604-17605, 2005; [2] C.C. Fu, H.Y. Lee, K. Chen, T.S. Lim, H.Y. Wu, P.K. Lin, P.K. Wei, P.H. Tsao, H.C. Chang, W. Fann, *Proc. Natl. Acad. Sci. U.S.A.*, **104**, 727-732, 2007; [3] I. Mann, E. Murad, A. Czechowski, *Plan. Space Sci.*, **55**, 1000-1009, 2007; [4] H.G. Chen, L. Chang, *Diamond Relat. Mater*, **13**, 590-594, 2004.

FILM DEPOSITION, X-RAY DIFFRACTION AND OPTICAL ABSORPTION OF NOVEL $(R\text{-}NH_3)_2ZnCl_4$ HYBRID PEROVSKITES

R. Mosca, P. Ferro, T. Besagni, A. Zappettini, F. Licci

IMEM - C.N.R., Parma, Italy
mosca@imem.cnr.it

Organic-inorganic $(C_nH_{2n+1}NH_3)_2MX_4$ hybrid perovskites (where M is a divalent metal and X a halide) are presently attracting much attention, due to their unique electronic properties and excellent film processability [1]. These self-assembling structures contain 2D semiconductor layers ($(MX_6)^{=}$) alternately stacked with organic ammonium layers. Excitons resulting from the low dimensionality of the semiconductor sheets have binding energy of several tenths eV, and are expected to have interesting potentialities for optoelectronic and electronic applications [2].

In this communication we report on the preparation and the basic X-ray and optical characterization of the novel $(C_nH_{2n+1}NH_3)_2ZnCl_4$ ($1 < n < 6$) compounds, deposited as thin films by spin-coating alcoholic solutions of stoichiometric precursors on glass and quartz substrates.

X-ray diffraction data prove that the as-prepared films are single phase, well crystallized and with a dominant in-plane grain orientation. The distance between the inorganic sheets, as measured through the "d" parameters, linearly increases with the amine chain length ("n" value) (Fig. 1a), thus suggesting that the organic chains are ordered perpendicularly to the film surface. The diffraction pattern refinement is presently in progress, in order to assign the appropriate space group and to determine the in-plane lattice parameters.

Room temperature optical absorption spectra exhibit a maximum at about 240 nm, which is almost independent on "n" (Fig. 1b). Such finding is consistent with the results we obtained in the homologous series of Cu-based hybrids [3] and suggests that also in the Zn-compounds the optical absorption phenomena are related to the inorganic cluster of the structure.

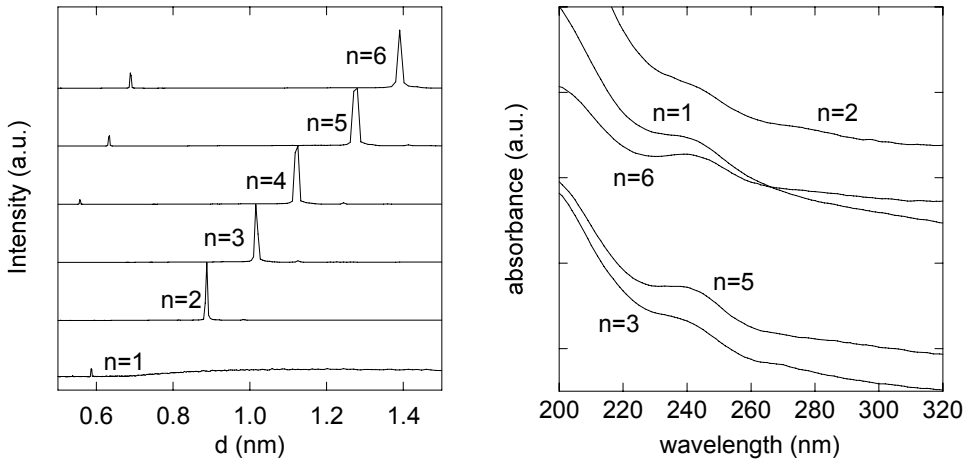

Fig. 1 - X-ray diffraction patterns *vs.* d (a) and RT optical absorption *vs.* wavelength (b) of $(C_nH_{2n+1}NH_3)_2ZnCl_4$ ($1 \le n \le 6$)

References. [1] D.B. Mitzi, K. Chondroudis, C.R. Kagan, *IBM J. Res. Dev*., **45**, 29-45, 2001; [2] M. Era, S. Morimoto, T. Tsutsui, S. Saito, *Appl. Phys. Lett*., **65,** 676-678, 1994; [3] F. Chiarella, A. Zappettini, T. Besagni, F. Licci, A. Cassinese, M. Barra, R. Vaglio, C. Aruta, *Cryst. Res. Technol*., **40**, 1028-1032, 2005.

MATERIALS, FROM EARTH AND LAB TO LIFE - 2

Session 14
Biological and synthetic supramolecular systems

S14.KN1

A MESOPOROUS PATTERN CREATED BY NATURE

G. Croce

Dipartimento di Scienze e Tecnologie Avanzate, Università del Piemonte Orientale, Italy
gianluca.croce@mfn.unipmn.it

The biological formation of skeletal structures formed by amorphous hydrated silica is called biosilicification and occurs in a wide variety of organisms. In particular siliceous sponges deposit hydrated silica in needle-like spicules and other structural patterns. Siliceous spicules are produced within specialized cells (Sclerocytes) and contain an organic axial filament, which functions as template for silica deposition. This presentation deals with the fiber diffraction structural study of the organization of the axial filaments of monoaxonic spicules from different sponges, carried out by diffraction experiments using a small angle X-ray scattering setup with synchrotron radiation.

We carried out our measurements on a number of species belonging to two different sponge families: the Demosponges *P. ficiformis*, *G. cydonium*, and *T. aurantium* and the Hexactinellid *S. joubini*. All these samples present needle-like spicules with a length of some mm. This allowed the collection of fiber diffraction patterns from a bundle of almost parallel spicules. The diffraction patterns show diffraction spots sharper than what can be expected from a regular polymeric fiber, indicating that the protein (Silicatein) units in the spicule axial filaments must form highly ordered patterns. As also suggested by TEM investigations, the protein units are packed in a compact hexagonal way. The diffraction patterns of different samples are quite different and the most relevant result, from a phylogenetic point of view, is that all Demosponges have a common hexagonal lattice period $a = 5.8$ nm, while the Hexactinellid has a longer period $a = 8.4$ nm. The analysis of the position and distribution of the spots reveals different possible bi- and tri-dimensional arrangements of protein units along the main axis of the spicules and the microdiffraction of a single spicule and of the circular section of the cut spicule confirmed the presence of an hexagonal structural order in the cavity. Moreover the analysis after thermal treatments reveals a structural ordering accompanying the thermal degradation of the organic material. This confirms our hypothesis that the protein units act as template in the formation of an inorganic mesoporous structure.

Apart from fiber diffraction, the study was carried out also by a unique combination of other techniques such as SEM, thermogravimetry, FTIR. All our results suggest the following possible mechanism for the biosilification process in spicules. The initial step consists in the formation of a very ordered disposition of the silicatein units, forming a regular mesoporous arrangement in a silica matrix, similar to that found in some synthetic materials. In a second step the biosilification process should continue with a deposition of amorphous silica on the outer walls of the mesoporous filament.

STRUCTURAL ENZYMOLOGY IN DRUG DESIGN AND CANCER GENE THERAPY

M. Degano

Unità di Biocristallografia, Fondazione Centro San Raffaele, Milano, Italy
degano.massimo@hsr.it

The catalytic activity of enzymes plays a fundamental role in the economy of living cells. Several enzymatic activities are absolutely crucial for the life cycle of microorganisms, and their functional inhibition represents a rational approach for the development of novel compounds endowed with antibiotic activity. The process of structure-based drug design relies on the determination of the three-dimensional structure of the target macromolecule, and its complexes with functional inhibitors to guide the rapid development of selective lead compounds. The identification and characterization of enzymes with nucleoside hydrolase activity will be presented as a successful example of such process. The activity of enzymes can also be exploited in the process of prodrug activation, that is the conversion of a non-toxic molecule to a compound that leads to cell death. This approach, called suicide gene therapy or enzyme-directed gene prodrug activation therapy, is highly regarded as a novel tool for the treatment of tumors. The therapeutic advantages of the use of nucleotide-metabolizing enzymes coupled to 5-fluorouracil-based prodrugs will be discussed, together with the role of structural studies in enhancing the efficiency of prodrug activation.

S14.KN3

FROM STRUCTURAL BIOLOGY TO SUPRAMOLECULAR CHEMISTRY

S. Geremia

Centro di Eccellenza in Biocristallogafia, Dipartimento di Scienze Chimiche, Università di Trieste, Italy
sgeremia@units.it

Chemical and biological supramolecular systems are governed by generally weak non-covalent interactions. The fine control of these forces is important in both materials science (sensors, conductivity, magnetism, nonlinear optics, etc.) and biology (pairing in the double helix DNA, receptor-protein binding, recognition enzyme-substrate, protein folding, etc.). In particular, the ability of molecules to form short-lived transition states and to perform easily trial-and-error corrections is important to create highly flexible systems for molecular recognition and self-assembly. On the other hand, the weakness of these single interactions makes the supramolecular architecture sometimes hard to predict. In this contest, the structural characterization of the supramolecular complexes is clearly essential to gain a deep knowledge on the chemical system. Technical and methodological aspects in small-molecule crystallography and in biocrystallography are generally quite different. However, some methods developed in one specific contest can be successfully applied to other. A series of supramolecular systems, ranging from protein to small-molecule complexes, characterized by "unconventional" crystallization, phase-problem solution and refinement methods will be discussed (Fig. 1a,b).

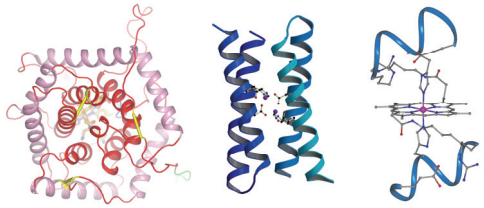

Fig. 1a - References [1-3] respectively.

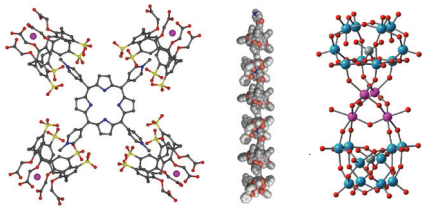

Fig. 1b - References [4-6] respectively.

References. [1] J. Wuerges, G. Garau, S. Geremia, S.N. Fedosov, T.E. Petersen, L. Randaccio, *Proc. Natl. Acad. Sci. USA,* **103**, 4386-4391, 2006; [2] A. Lombardi, C.M. Summa, S. Geremia, L. Randaccio, V. Pavone, W.F. DeGrado *Proc. Natl. Acad. Sci. USA*, **97**, 6298-6305, 2000; W.F. DeGrado, L. Di Costanzo, S. Geremia, A. Lombardi, V. Pavone, L. Randaccio, *Angew. Chem. Int. Ed. Engl.*, **42**, 417-420, 2003; L. Di Costanzo, F. Forneris, S. Geremia, L. Randaccio, *Acta Crystallogr. D. Biol. Crystallogr.*, **59**, 1435-1439, 2003; S. Geremia, L. Di Costanzo, L. Randaccio, D.E. Engel, A. Lombardi, F. Nastri, W.F. DeGrado, *J. Am. Chem. Soc.*, **127**, 17266-17276, 2005; [3] L. Di Costanzo, S. Geremia, L. Randaccio, F. Nastri, O. Maglio, A. Lombardi, V. Pavone, *J. Biol. Inorg. Chem.*, **9**, 1017-1027, 2004; [4] L. Di Costanzo, S. Geremia, L. Randaccio, R. Purrello, R. Lauceri, D. Sciotto, F.G. Gulino, V. Pavone, *Angew. Chem. Int. Ed. Engl.*, **40**, 4245-4247, 2001; F.G. Gulino, R. Lauceri, L. Frish, T. Evan-Salem, Y. Cohen, R. De Zorzi, S. Geremia, L. Di Costanzo, L. Randaccio, D. Sciotto, R. Purrello, *Chem-Eur. J.*, **12**, 2722-2729, 2006; R. De Zorzi, B. Dubessy, J.C. Mulatier, S. Geremia, L. Randaccio, J.P. Dutasta, *J. Org. Chem.*, **72**, 4528-4531, 2007; [5] L. Pirondini, A.G. Stendardo, S. Geremia, M. Campagnolo, P. Samori, J.P. Rabe, R. Fokkens, E. Dalcanale, *Angew. Chem. Int. Ed. Engl*., **42**, 1384-1387, 2003; F. Corbellini, L. Di Costanzo, M. Crego-Calama, S. Geremia, D.N. Reinhoudt, *J. Am. Chem. Soc.*, **125**, 9946-9947, 2003; R. Pinalli, V. Cristini, V. Sottili, S. Geremia, M. Campagnolo, A. Caneschi, E. Dalcanale, *J. Am. Chem. Soc.*, **126**, 6516-6517, 2004; R.M. Yebeutchou, F. Tancini, N. Demitri, S. Geremia, R. Mendichi, E. Dalcanale, *Angew. Chem. Int. Ed. Engl.*, **47**, 4504-4508, 2008; [6] A. Sartorel, M. Carraro, G. Scorrano, R. De Zorzi, S. Geremia, N.D. McDaniel, S. Bernhard, M. Bonchio, *J. Am. Chem. Soc.*, **130**, 5006-5007, 2008.

INCLUSION OF VOLATILE GUESTS IN ORGANIC-INORGANIC SYSTEMS

A. Bacchi, M. Carcelli, T. Chiodo

Dipartimento di Chimica Generale ed Inorganica, Chimica Analitica e Chimica Fisica, Università di Parma, Italy
alessia.bacchi@unipr.it

We are interested in inclusion compounds with flexible dynamic frameworks that can create pores to accomodate small guest molecules. These dynamic pores come from a sort of "bistability" of the soft apohost framework, capable to convert between a close and an open phase in response to guest molecules (G). A reversible dynamic reorganization between the apohost and the solvate phases requires two conditions: (i) a low cost structural rearrangement between the two states, (ii) an easily accessible migration path for the outcoming and incoming guest molecules. The host molecules must switch from a situation where they interact with themselves (self-mediated network) to another one where they interact with the guests (guest-mediated network). Trans-palladium complexes of triarylcarbinol ligands have shown suitable structural requisites to give reversible host-guest properties [1]. The reversibility of guest uptake/release by these crystalline frameworks has been interpreted according to a model where the host molecules may alternatively either pack in arrays held together by hydrogen bonds between the terminal –OH groups and the coordinated X anions on the axle, or use the –OH function to catch guest molecules, disentangling the –OH…X arrays [2]. The conversion between the two situations is realized by simple oscillation of the molecules around their centres of mass. In this work we first investigate the influence on inclusion properties of shape modifications induced by changing metal stereochemistry and wheel hindrance, and show that both axle linearity and wheel bulkiness are needed to establish inclusion properties. Then we analyze the structures and properties of inorganic *waad* of $Pd(L2)_2X_2$ based on iminic ligands L2 designed in order to favour the creation of bistable flexible networks on a scaffold similar to the previously described palladium complexes of triarylcarbinol ligands, modified to increase the molecular length and the hindrance and rigidity of the terminal groups [3].

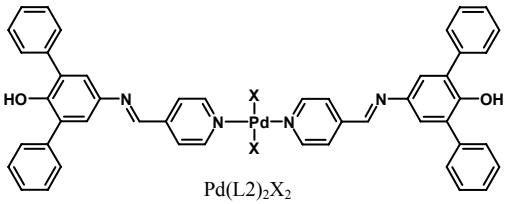

$Pd(L2)_2X_2$

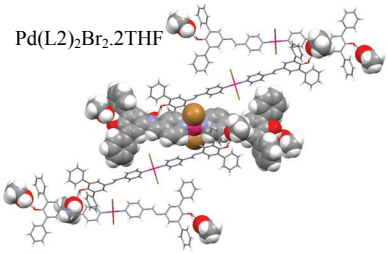

$Pd(L2)_2Br_2.2THF$

By investigating structural properties of $Pd(L2)_2Br_2$, $Pd(L2)_2Cl_2$ hosts (H) and their solvates we outline a continuous path of conversion H → H.G → H.2G of the pure host to the 1:2 inclusion compound, which takes advantage of the flexibility of the host framework capable of adapting to different compositions by slight modifications of the cell geometry and commutation between a self-mediated network based on OH…OH interactions and a guest-mediated network based on OH…G hydrogen bonds.

References. [1] A. Bacchi, E. Bosetti, M. Carcelli, *Cryst. Eng. Comm.*, **7**, 52, 2005; [2] A. Bacchi, In *Models, Mysteries and Magic of Molecules*, Ed. C.A. Boyens and J.F. Ogilvie, Springer, Ch. 4, 87-108, 2008,; [3] A. Bacchi, M. Carcelli, T. Chiodo, F. Mezzadri, *Cryst. Eng. Comm.*, submitted.

POLARIZING MICROSCOPY ANALYSIS OF METAL ORGANIC FRAMEWORKS: SOLID STATE BEHAVIOR OF Rh(0)/Rh(I) BISPHOSPHINE AND M(II) BENZENETRICARBOXYLATES POLYMERS

P. Macchi

Dipartimento di Chimica Strutturale e Stereochimica Inorganica, Università di Milano, Italy
piero.macchi@unimi.it

The rotating polarizer multi-imaging technique (METRIPOL), recently introduced by M.A. Glazer and coworkers [1], was used to investigate the structural modifications occurring to various organometallic polymers. These are prototypical of first, second and third generation type metal organic frameworks (MOF). The aim of this study was identifying the mechanisms and possible intermediate phases in the desolvation/re-solvation processes of MOFs and their high temperature amorphization/re-crystallization phenomena. The study is complemented by X-ray structural characterization of the intermediate phases and thermal analysis [2].

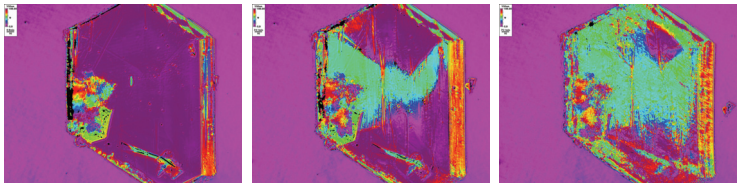

References. [1] A.M. Glazer, J.G. Lewis, W. Kaminsky, *Proc. R. Soc. London*, *Ser. A*, **452**, 2751-2765, 1996; [2] N. Janjic, G. Peli, L. Garlaschelli, A. Sironi, P. Macchi, *Cryst. Growth Des.*, **8**, 854-862, 2008.

FULL IMPLEMENTATION OF THE *in situ* SIMULTANEOUS RAMAN / X-RAY POWDER DIFFRACTION SETUP: METHODS AND APPLICATIONS

M. Milanesio[1], G. Croce[1], S. Kumar[1], L. Palin[1], D. Viterbo[1], W. van Beek[1,2]

[1]*DISTA, Università del Piemonte Orientale, Alessandria, Italy*
[2]*Swiss-Norwegian Beamlines, ESRF, Grenoble, France*
marco.milanesio@mfn.unipmn.it

Materials containing light atoms, disordered moieties and/or amorphous or liquid-like phases or showing surface- or defect-related phenomena constitute a problem for their characterization using X-ray powder diffraction (XRPD), and in many cases Raman spectroscopy can provide useful complementary information. The novel experimental set-up for simultaneous *in situ* Raman/High-resolution XRPD experiments [1] developed at SNBL was employed to study four solid-state transformations: *i)* the kinetics of the fluorene: TCNQ solid-state synthesis; *ii)* the photoinduced 2+2 cyclization of (E)-furylidenoxindole; *iii)* the thermal swelling and degradation of stearate-hydrotalcite nanocomposites; *iv)* the decarboxilation process of layered zirconium aminophosphonates. The reported experiments demonstrated that, even though the simultaneous Raman/XRPD experiment is more challenging than the separated ones, high resolution XRPD and Raman data can be collected at *in situ* conditions. The complementarities between Raman and XRPD were fully exploited by an accurate choice of the Green or Red Laser for the Raman experiment.

In the first two experiments the surface-bulk complementarities of the Raman and XRPD probes were exploited. Raman allowed to detect the reaction speed at the surface in the first step of the reactions, when no reaction is detected by XRPD. The mechanism of the reaction for the formation of the Fluorene/TCNQ complex was fully characterized and a kinetic analysis carried out, with the determination of the activation energy and the reaction order for the reaction at the surface and in the bulk. Concerning the photoinduced 2+2 cyclization of (E)-furylidenoxindole, the complex polymorph space of the product phase (one stable and two metastable crystalline phase and one amorphous phase) was fully understood and the structure of one metastable phase was also solved.

In the last two experiments the sensitivity of Raman to the structure and conformation of organic moieties (not easily detectable by XRPD alone, especially when disorder is present) was exploited. Concerning stearate-hydrotalcite experiment, a detailed description of the structural changes occurring at 365 K to both organic and inorganic moieties in the ST-HT sample was obtained. The XRPD data gave clear information on the swelling of the inorganic lamellar component of the hybrid nanocomposite. Raman spectra indicated that, up to 365 K, the all-*trans* conformation is prevalent for the organic chains, whereas above this temperature the occurrence of folded chains due to *gauche* conformations became significant. Finally the decarboxilation of layered zirconium aminophosphonates was studied. When heated this compound shows a phase transformation with a remarkable reduction of its interlayer distance (detected by XRPD), due to the loss of HF and to a change in the zirconium environment (detected by the Raman probe).

References. [1] E. Boccaleri, F. Carniato, G. Croce, D. Viterbo, W. van Beek, H. Emerich, M. Milanesio, *J. Appl. Crystallogr.*, **40**, 684, 2007.

STRONTIUM-SUBSTITUTED HYDROXYAPATITE NANOCRYSTALS

A. Bigi, E. Boanini, C. Capuccini, M. Gazzano

Dipartimento di Chimica "G. Ciamician", Università di Bologna
e Istituto per la Sintesi Organica e la Fotoreattività (ISOF), CNR, Bologna, Italy
gazzano@isof.cnr.it

Apatites are a family of inorganic crystalline compounds, of general formula $M_{10}(XO_4)_6Y_2$. M is usually a bivalent cation, distributed over two different crystal sites, XO_4 is usually PO_4^{3-}; VO_4^{3-} or AsO_4^{3-}, Y is a monovalent anion. Apatites are widely spread in nature; in particular, the inorganic phase of the hard tissues of vertebrates is assimilated to the synthetic hydroxyapatite $Ca_{10}(PO_4)_6(OH)_2$, CaHA [1].

Among the many cations that can substitute for calcium in the structure of hydroxyapatite, strontium provokes an increasing interest because of its beneficial effect on bone formation, and prevention of bone resorption.

Strontium is known to replace calcium in the HA structure in the whole range of composition. The solid solutions display a linear variation in the lattice parameters with composition, whereas different data are reported on the preferential substitution site of Sr for Ca in CaHA. A better understanding of the interaction of Sr with hydroxyapatite structure is necessary to provide useful information also for clarifying the biological role of Sr in the process of biomineralization of bone and related pathologies. With this aim, we have carried out a chemical, morphological, spectroscopic and structural analysis of calcium-strontium-hydroxyapatite solid solutions prepared by direct synthesis in aqueous medium.

The X-ray diffraction patterns of the solid products synthesized with different Sr/(Ca+Sr) molar ratios indicate that they are constituted of hydroxyapatite as a unique crystalline phase. Line profile analysis has been applied in order to investigate the line broadening variations and the peaks shifts observed in the XRD patterns of the samples. The results reveal that strontium replacement to calcium induces a decrease of the coherent length of the perfect crystalline domains and disturbs the shape of the crystals, whereas crystallinity, as well as mean dimensions of the crystals, increase again at relatively high strontium contents.

Strontium is quantitatively incorporated into hydroxyapatite where its substitution for calcium provokes a linear increase of the lattice constants and a linear shift of the infrared absorption bands of hydroxyl and phosphate groups, coherent with the greater ionic radius of strontium. The isomorphous substitution does not significantly affect the stoichiometry of hydroxyapatite, since the (Ca+Sr)/P molar ratio assumes a mean value of 1.68±0.03, independently from the Ca and Sr content. TEM investigation indicates that the products were obtained in the form of nanosized crystals whose morphology and dimensions is affected by the chemical composition and associated crystallinity.

The results of the structure refinements carried out using the Rietveld method indicate that although strontium distribution is similar in the two cationic sites, a slight Sr enrichment of M(2) site prevails in most of the range of composition, whereas a modest preference of Sr for the smaller M(1) site can be appreciated only at a very low strontium content. This result, which is opposite to what was expected on the basis of the difference in ionic radii, is of peculiar importance for it concerns a composition in the range of strontium concentration in the bone.

References. [1] J.C. Elliott, *Structure and Chemistry of the Apatites and Other Calcium Orthophosphates*, Elsevier, Amsterdam, 1994.

NANO-CRYSTALLINE BONE FORMATION AND BIOCERAMIC SCAFFOLD RESORPTION: A MICRODIFFRACTION-BASED STUDY

A. Guagliardi[1], C. Giannini[1], M. Ladisa[1], A. Cedola[2], S. Lagomarsino[2], C. Ranieri[3], M. Mastrogiacomo[3]

[1]*Istituto di Cristallografia, CNR-IC, Bari, Italy*
[2]*Istituto di Fotonica e Nanotecnologie - CNR, Roma, Italy*
[3]*Istituto Nazionale per la Ricerca sul Cancro e Dipartimento di Oncologia, Biologia e Genetica, Università di Genova, Italy*
antonella.guagliardi@ic.cnr.it

Bone damage, due to either pathologies or trauma, is a common occurrence in orthopedics and different therapeutic approaches have been proposed to repair large defects. A very promising approach relies on the association of suitable Bone Graft Substitutes (BGS) with osteogenic cells. Studies have been addressed to compare the performances of pure hydroxyapatite (HA)-based BGS and Tricalcium Phosphate (TCP)-based BGS, especially with respect to their ability to participate to the cell-mediated re-modeling process and the formation of new bony tissue[1,2]. In a recent study, the performance of implants of Skelite™, resorbable BGS based on Silicon-stabilized TCP, was evaluated in promoting the repair of a critical-sized sheep tibia defect. The study demonstrated that a progressive scaffold's resorption by osteoclasts is replaced by highly mineralized lamellar bone, suggesting that these two processes are interrelated. To further investigate the coupling of the two processes, scaffolds alone and scaffolds seeded with Bone Marrow Stromal Cells (BMSC) were subcutaneously implanted in immuno-deficient mice for 2 and 6 months and, then, analysed using high-resolution scanning X-ray micro-diffraction techniques with synchrotron radiation. Experiments were performed at the European Synchrotron Radiation Facility (ESRF, Grenoble, France). The structural investigation at the interface Bone-scaffold put in evidence that the mechanism of scaffold resorption is based on the TCP depletion. This depletion increases with the increase of implant time. A novel method of correlation analysis (Canonical Correlation Analysis, CCA) was applied to provide a quantitative classification map of the 2-dimensional investigated samples [3]. The spatial variation of phases concentration highlights that in the contact areas, between the newly deposited bone and the ceramic scaffold, the TCP component of the ceramic decreased much faster than the HA component.

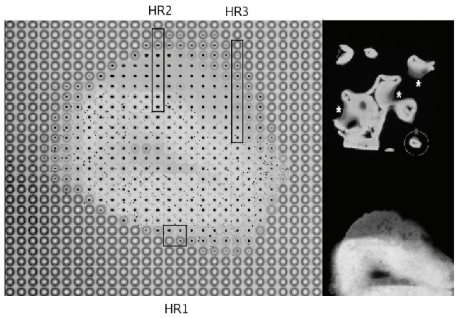

Fig. 1 - Grid of 2-D microdiffraction patterns colleted at ESRF (left); classification map provided on the same sample by the CCA technique (right).

References. [1] R. Quarto, M. Mastrogiacomo, R. Cancedda, S.M. Kutepov, V. Mukhachev, A. Lavroukov, *N. Engl. J. Med.*, **344**, 385, 2001; [2] M. Mastrogiacomo, A. Papadimitropoulos, A. Cedola, F. Peyrin, P. Giannoni, S.G. Pearce, M. Alini, C. Giannini, A. Guagliardi, R. Cancedda, *Biomaterials*, **28**, 1376-1384, 2007; [3] A. Guagliardi, G. Giannini, M. Ladisa, A. Lamura, T. Laudadio, A. Cedola, S. Lagomarsino, R. Cancedda, *J. Appl. Crystallogr.*, **40**, 865-873, 2007.

MONOFUNCTIONALIZED β-CYCLODEXTRINS: A MOLECULAR DYNAMICS STUDY OF THE SELF-INCLUSION PROCESS

M. Saviano[1], R.M. Vitale[2], P. Amodeo[2]

[1]*Istituto di Biostrutture e Biommagini, CNR, Napoli, Italy*
[2]*Istituto di Chimica Biomolecolare, CNR, Pozzuoli Napoli, Italy*
msaviano@unina.it

β-Cyclodextrins (CDs) are cyclic oligosaccharides containing seven D(+)-glucopyranosyl units linked by α-1,4 glycosidic bonds. Their hydrophobic interior hosts a wide variety of guest molecules, forming inclusion compounds. Monosubstituted derivatives are obtained by grafting the bioactive compound onto CD. In this case, the tendency of resulting derivatives to form auto-inclusion complexes depends upon the nature of both the ligand, and the covalent linkage, and the spacer eventually used.

The peculiar features of intramolecular inclusion prevent the use of those methods applied to non-covalent complexes to enhance sampling efficiency by application of external forces or by constraining molecules on a path in molecular dynamics simulations. Our approach was based on unrestrained molecular dynamics (UMD) with a generalized Born solvation model suitable to best reproduce experimental data. Different analysis tools were used or developed to characterize and compare the simulated molecules.

The experimental behavior of a series of monosubstituted β-CDs, bearing amino acids or dipeptides, differing for sizes, polarities and self-inclusion capability, was well reproduced by nanoscale UMD simulations with implicit solvent. A good agreement of theoretical *vs*. experimental results (NMR and X-ray data) was obtained, also for derivatives in which no inclusion complexes are formed. Comparative UMD simulations in explicit solvent with the same or longer timescale were also carried out but no large conformational changes were observed. Factors contributing to self-inclusion mechanism were also identified.

INVARIANT CHARACTERIZATION AND RECOGNITION OF THE POINT GROUP SYMMETRIES USING HIGH ORDER MOMENTS

S. Cerrini

Istituto di Cristallografia - CNR, Sede di Monterotondo, Roma, Italy
s.cerrini@libero.it

Previous studies pointed out that a 3D density function, continuous or piecewise continuous, can be characterized in the three-dimensional space by a series of invariant numerical parameters derived from the high order moments of the function: ${}^{n}\mu$ being n = 0, 1, 2, 3, 4, … . These invariants, which are independent upon location, orientation and scaling of the function, form a unique set of orthogonal parameters that capture all the features of the 3D shape of the function, so they can be named shape invariants.

In the present communication the attention is focused on how the shape invariants are able to fully characterize and distinguish the symmetries of the 32 point groups, and to unambiguously discriminate pairs of enantiomorphic shapes.

The constraints imposed by the point group symmetries to the moment components can be obtained by application of the Neumann principle, due to the tensor property of the components.

The main results of the investigation are summarized as follows.

i) Point group symmetries affect the moment components with systematic absences, sign reversing and linear combinations among the components, which are specific of the symmetry. The general trend is that the number of independent components of a moment decreases on the increasing of the symmetry.

ii) The set of ${}^{2}\mu$, ${}^{3}\mu$, ${}^{4}\mu$, ${}^{5}\mu$, ${}^{6}\mu$, ${}^{7}\mu$, ${}^{8}\mu$ and ${}^{9}\mu$ is the minimum set of moments that allows the unique assignment of the symmetry and the recognition of each one of the 32 point groups in any arbitrary reference system.

iii) A new type of descriptors has been found, having the pseudo-invariance property of the axial vectors, that make possible to detect the occurrence of enantiomorphism or homomorphism between similar shapes.

iv) The effects of point group symmetries on the moment invariants are double. The first one consists of a series of equalities among the singular values of the representative matrices of the moments, the second results in the partitioning of the eigenspaces into a number of orthogonal subspaces. The equality patterns and the dimensions of the partitions are specific and distinctive of each point group.

v) The complete spectral analysis of the eigenvectors/eigenvalues systems associated to the representative matrices of the eight moments ${}^{2}\mu$ ···· ${}^{9}\mu$ allows to reveal the presence of symmetries and to recognize the point group.

Theoretical, computational and practical details of the 32 point groups will be discussed.

Applications of the method, for example, to the finding of lattice type and Laue symmetry of a 3D diffraction pattern, to the determination of the point group symmetry in presence of significant anomalous scattering, and to the characterization of clusters of molecules and of the quaternary structure of macromolecules will be presented.

A CRYSTALLOGRAPHIC STUDY OF NEW Cu(II) AND Ln(III) COMPLEXES AS CONTRAST AGENTS FOR MRI

G. Bombieri[1], F. Meneghetti[1], R. Artali[1], Z. Baranyai[2], M. Botta[3], S. Aime[4]

[1]*Istituto di Chimica Farmaceutica e Tossicologica "P. Pratesi", Università di Milano, Italy*
[2]*Department of Inorganic and Analytical Chemistry, University of Debrecen, Hungary*
[3]*Dipartimento di Scienze dell'Ambiente e della Vita, Università del Piemonte Orientale "A. Avogadro", Alessandria, Italy*
[4]*Dipartimento di Chimica IFM, Università di Torino, Italy*
gabriella.bombieri@unimi.it

Many efforts have been recently devoted to the search for heptadentate ligands able to give Gd(III) complexes for *in vivo* use as CAs for MRI as they have an increased relaxivity related to the possible presence of two coordinated water molecules. An efficient heptadendate ligand is the triaminotetracarboxylic AAZTA [1]. Its coordination geometry and the mutual disposition of donors atoms may offer useful information on the behaviour of CAs. The structure of the $Na[Gd(H_2O)AAZTA]\cdot 3H_2O$ [2] is known as well as its associated magnetic properties but not those of the uncharged complexes. Here the structure of the neutral derivative $[La(H_2O)HAAZTA]\cdot 4H_2O$ is reported together with that of another complex with the acyclic polyaminocarboxylate ligand EBTA [3] in its copper complex $[Cu_2EBTA(H_2O)_3]_2$ in order to understand its role in transmetallation reaction of the $[GdEBTA]^-$ complex.

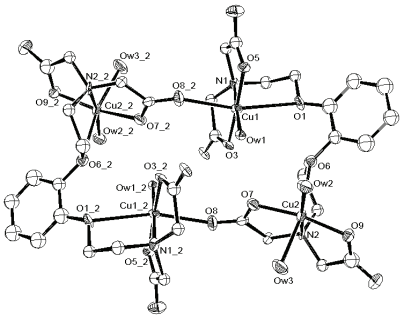

(1)

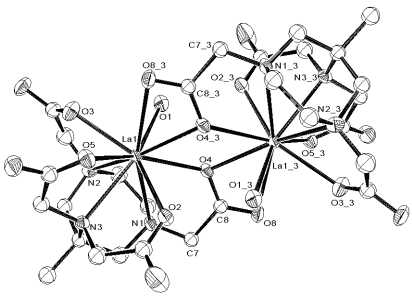

(2)

References. [1] S. Aime, L. Calabi, C. Cavallotti, E. Gianolio, G.B. Giovenzana, P. Losi, A. Maiocchi, G. Palmisano, M. Sisti, *Inorg. Chem*., 2004, **43**, 7588-7591; [2] S. Aime, G. Bombieri, C. Cavallotti, G.B. Giovenzana, D. Imperio, N. Marchini, *Inorg. Chim. Acta*, **361**, 1534-1541, 2008; [3] L. Tei, Z. Baranyai, M. Botta, L. Piscopo, S. Aime, G.B. Giovenzana, *Org. Biomol. Chem*., DOI: 10.1039/b804195d, 2008.

POROUS SYSTEMS BASED ON IMINE SUBSTITUITED PYRIDINE MOLECULE: INCLUSION COMPOUNDS, POLIMORPHISM AND DESOLVATATION KINETICS

T. Chiodo, A. Bacchi, M. Carcelli, F. Mezzadri

Dipartimento di Chimica Generale ed Inorganica, Chimica Analitica, Chimica Fisica, Università di Parma, Italy
tiziana.chiodo@nemo.unipr.it

In this work we analyse the structural properties of the *orto* imino pyridine compound L (Fig. 1). We are interested in its solid-state organization, particularly on its general self-assembly trends in the perspective of using L as a ligand for wheel-and-axle organic-inorganic molecules [1,2]. We show here that L acts as a host, including small guest molecules in the organic framework. This ability is largely dependent on its molecular size and shape and derives from the supramolecular solid-state organization. *Trans* disposition around the iminic double bond induces the formation of zig-zag supramolecular chains sustained by hydrogen bonds involving the oxydrilic groups and the pyridine nitrogen atoms. Guest species are included in channels due to the supramolecular solid state porous organization. Solvate forms were isolated by crystallization in acetone and chloroform. From toluene two solvate polymorph forms, different in the guest diposition, were characterized. The various solvates are isostructural. If the solvent is not able to template the formation of a porous phase, a non-solvate form crystallizes: in fact a non-solvate form was isolated by crystallization in the bulky tert-butylmethylether. Supramolecular zig-zag chains organization of the solvate and non-solvate L forms are compared in Fig. 2.

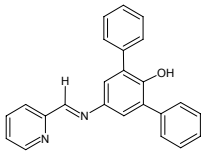

Fig. 1

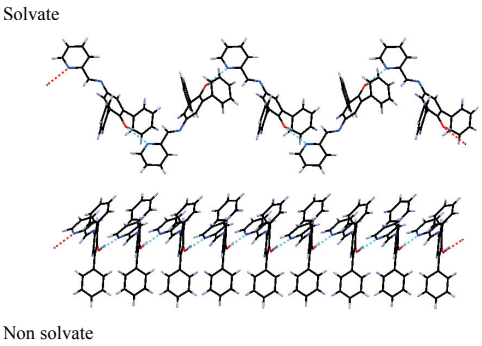

Fig. 2

X-ray diffraction was used to follow the irreversible process of desolvatation.

Kinetics of the desolvatation processes have been determined by carrying out a series of isothermal analysis [3-7].

References. [1] A. Bacchi, E. Bosetti, M. Carcelli, P. Pelagatti, D. Rogolino, G. Pelizzi, *Inorg. Chem.*, **44**, 431-442, 2005; [2] A. Bacchi, E. Bosetti, M. Carcelli, *Cryst. Eng. Comm.*, **7**, 527-537, 2005; [3] L.R. Nassimbeni, H. Su, *J. Chem. Soc,* **2**, 1246-1250, 2002; [4] L.R. Nassimbeni, *Cryst. Eng. Comm.*, **5(35)**, 200-203, 2003; [5] A. Jacobs, L.R. Nassimbeni, J.H. Taljaard, *Cryst. Eng. Comm.*, **7**, 731-734, 2006; [6] M.E. Brown, *Introduction to thermal analysis*, Kluwer Academic Publishers, 2001; [7] A.K. Galwey, M.E. Brown, *Thermal Decomposition of Ionic Solids*, Elsevier, Amsterdam, 1999.

CLATHRATING PROPERTIES AND DESOLVATATION PROCESSES IN HYBRID ORGANIC-INORGANIC WHEEL-AND-AXLE COMPLEXES

T. Chiodo[1], A. Bacchi[1], M. Carcelli[1], F. Mezzadri[1], M. Pranzo[2]

[1]*Dipartimento di Chimica Generale ed Inorganica, Chimica Analitica, Chimica Fisica, Università di Parma, Italy*
[2]*Dipartimento di Scienze Farmacologiche, Biologiche e Chimiche Applicate, Università di Parma, Italy*
tiziana.chiodo@nemo.unipr.it

We are interested in the design of hybrid organic-inorganic wheel-and-axle systems [1] with flexible dynamic frameworks that can create pores "on demand" to accommodate small guest molecules. Our purpose is the design of bistable systems capable of switching between networks based on host-host (self-mediated) and host-guest (guest-mediated) interactions [2,3].

In this perspective, the iminic ligand L (Fig. 1) acts as a building block ideally suited for the supramolecular synthesis of hybrid organic-inorganic materials. Its syntheses and solid-state organization are reported elsewhere [4]. L was coordinated with palladium salts with formation of wheel-and-axle *trans*-$[Pd(L)_2X_2]$ (X = Cl, Br) (Fig. 2). The terminal large aryl moieties and the presence of the OH groups are connected with potentially solid-state clathrating properties. These hybrid organic-inorganic crystalline matrices are able to include small guest molecules G ($CHCl_3$, THF, toluene tert-butylmethylether, ethanol).

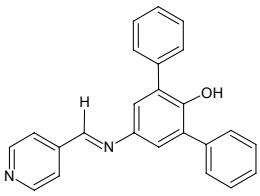

Fig. 1

Desolvatation processes were analysed by variable temperature X-ray powder diffraction and hot stage microscopy.

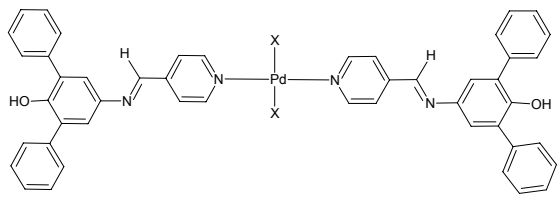

Fig. 2

Thermal behaviour of PdL_2Cl_2 and PdL_2Br_2 solvates is different. First the PdL_2Br_2 melting point is significantly higher than the PdL_2Cl_2 one. Thermal analysis of $PdL_2Cl_2 \cdot G$ shows the appearance of an amorphous phase before the melting point. Instead a crystalline sample of $PdL_2Br_2 \cdot 2G$ quantitatively converts into the apohost form without observing any transient amorphous phase during the transition; then the melting is observed. Variable temperature X-ray powder diffraction shows that solvent loss starts at ambient temperature and that two non-solvate forms are concomitant with the solvate one. By heating, the higher symmetry non-solvate is the only form existing before the melting temperature.

References. [1] M.R. Caira, A. Jacobs, L.R. Nassimbeni, F. Toda, *Cryst. Eng. Comm.*, **5**, 150, 2003; [2] A. Bacchi, E. Bosetti, M. Carcelli, *Cryst. Eng. Comm.*, **7**, 527-537, 2005; [3] A. Bacchi, E. Bosetti, M. Carcelli, P. Pelagatti, D. Rogolino, G. Pelizzi, *Inorg. Chem.*, **44**, 431-442, 2005; [4] A. Bacchi, M. Carcelli, T. Chiodo, G. Cantoni, C. De Filippo, S. Pipolo, in preparation.

IN SITU SIMULTANEOUS RAMAN / HIGH-RESOLUTION X-RAY POWDER DIFFRACTION STUDY OF STEARATE-HYDROTALCITE COMPOSITE AT NON-AMBIENT CONDITIONS

G. Croce[1], F. Carniato[1], M. Milanesio[1], D. Viterbo[1], W. van Beek[2]

[1]*DISTA, Università del Piemonte Orientale, Alessandria, Italy*
[2]*Swiss-Norwegian Beamlines, ESRF, Grenoble, France*
davide.viterbo@mfn.unipmn.it

Hydrotalcite has a sheet structure of octahedral units composed of metal hydroxides. Mixed hydroxides can be synthesized by coprecipitation from mixed metal chloride solutions with sodium hydroxide or sodium hydrogen carbonate. The hydrotalcite interlayer space includes negative anions that effectively balance the positively charged layers. Thanks to its chemical structure, hydrotalcite is able to accommodate by anionic exchange some aliphatic acids in the interlayer space, obtaining organo-modified hydrotalcite, such as the stearate-hydrotalcite (ST-HT) nanocomposite material.

This work is focused on the study of the temperature effect on the possible structural modifications of the lamellar material and on how possible conformational transitions of the organic chains of stearate molecules can influence the final structure of the inorganic hydrotalcite. The study of this complex composite material can highlight the importance of using Raman and X-Ray diffraction in simultaneous conditions [1]. X-Ray diffraction gave information on the possible swellings of the interlayer space focusing on the inorganic component of the material (structural information), while the Raman probe, sensible to the organic stearate molecule, gave information on the local mobility of the organic chains chemically inserted by ionic bonds in the interlayer space, during the heating process. The *in situ* simultaneous Raman-XRPD experiments were performed at the ESRF in Grenoble on the BM1B (SNBL) beam line employing the experimental set-up described in [1].

The rearrangement and decomposition processes induced by thermal treatment on a lamellar ST-HT sample were analyzed to shed light on the discrepancies between two previous *ex situ* studies, carried out on the same materials, reporting very different inter-layer distances (d = 48 Å in [2] and d = 31 Å in [3]). XRPD data gave clear information on the behaviour of the inorganic lamellar component of the hybrid nanocomposite. In particular a non reversible phase transition, due to the swelling of the layers, was observed at 362 K with a change of the d-spacing from 31 to 48 Å. The observed d-spacing of 31 Å at low temperature and the thickness of the inorganic layer of 4.8 Å indicate that the inter-layer space, available for the organic anion, is of about 27-28 Å. Considering that the length of the stearate "all *trans*" chains is 24 Å, only an interdigitated bilayer of stearate molecules could be accommodated. The increase of the d-spacing to 48 Å in the new phase suggested a conformational change of the stearate molecules. The Raman data and in particular, the C-H and C-C stretching modes are sensitive to the changes in the *trans-gauche* conformation of the CH_2 units and to the packing of the embedded phase. Up to 365 K the Raman spectra confirmed the presence of a significant all-trans fraction of chains, whereas above this temperature the occurrence of folded chains due to *gauche* conformations was observed. Since the non-linear chains hinder each other in their free rotation around the hanging point (the COO- anion linked to the inorganic layer) a further rearrangement to a double layer of folded chains occurs.

References. [1] E. Boccaleri, F. Carniato, G. Croce, D. Viterbo, W. van Beek, H. Emerich, M. Milanesio, *J. Appl. Crystallogr*., **40**, 684, 2007; [2] T. Itoh, M. Ohta, T. Shichi, T. Yui, K. Tagaki, *Langmuir*, **19**, 9120, 2003; [3] U. Costantino, A. Gallipoli, M. Nocchetti, G. Camino, F. Bellucci, A. Frache, *Polym. Degrad. Stabil*., **90**, 586, 2005.

X-RAY VARIABLE TEMPERATURE STUDY ON PROTON TRANSFER AND POLYMORPHISM IN 3-(*p*-CHLOROPHENYL)-1,5-DIPHENYLFORMAZAN

V. Ferretti, V. Bertolasi

Dipartimento di Chimica e Centro di Strutturistica Diffrattometrica, Università di Ferrara, Italy
frt@unife.it

Formazans are a class of compounds which have attracted our interest because of two characteristics: (i) in their 'closed' conformations they can easily form strong intramolecular N-H…N hydrogen bonds assisted by resonance (RAHBs), and (ii) they can display prototropic tautomerism (Scheme 1).

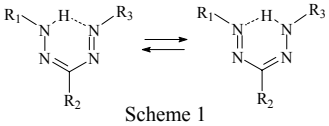

Scheme 1

In this communication we present our studies on two polymorphic forms of 3-(*p*-chlorophenyl)-1,5-diphenylformazan, monoclinic (**1)** and orthorhombic (**2)**, which display tautomerism in the solid state. The question of the N-H…N / N…H-N competition has been addressed through variable temperature (100, 150, 200, 295 K) crystal structure determinations, which have confirmed the presence in both polymorphs of an intramolecular Double-Minimum / Low Barrier H-bond.

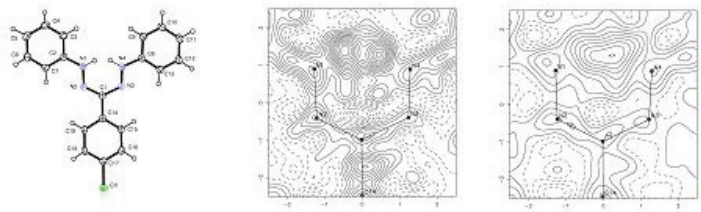

Crystal structure of polimorph 1 and Difference Fourier maps in the mean plane of the H-bond chelate ring at T = 100 and 295 K.

The energy difference between the two N-H…N ground vibrational levels has been evaluated by refining the proton population at the different temperatures, obtaining different values of –110 and –48 cal mol^{-1} for the two polymorphs **1** and **2**, respectively.

EMERGING PROTEIN TARGETS FOR ANTICANCER METALLODRUGS: INHIBITION OF THIOREDOXIN REDUCTASE AND CATHEPSIN B BY ANTITUMOR RUTHENIUM(II)-ARENE COMPOUNDS

A. Guerri[1], T.J. Geldbach[2], A. Casini[3], C. Gabbiani[3], M.P. Rigobello[4], A. Bindoli[5], P.J. Dyson[2], L. Messori[3]

[1]*Polo Scientifico, Università di Firenze, Italy*
[2]*Institut des Sciences et Ingénierie Chimiques (EPFL), Switzerland*
[3]*Dipartimento di Chimica, Università di Firenze, Italy*
[4]*Dipartimento di Chimica Biologica, Università di Padova, Italy*
[5]*Istituto di Neuroscienze, CNR, Padova, Italy*
annalisa.guerri@unifi.it

Ruthenium(II)-arene pta (pta = 1,3,5-triaza-7-phosphadamantane) compounds (RAPTA hereafter) are a family of Ru(II) compounds of interest as potential antitumor agents. Unlike the platinum-based compounds which presumably act through a direct DNA damage, RAPTA compounds work on molecular targets other than DNA [1] implying a biochemical mode of action completely different from the classical platinum anticancer drugs. In order to explore the mechanism of action, the inhibition of two specific enzymes, namely cathepsin B and thioredoxin reductase, by a panel of RAPTA compounds was studied. Some of these compounds have already shown to interact with model proteins such as cytochrome c, ubiquitin and lysozyme [2,3]. Among the thirteen compounds, **9** has been characterized by means of single crystal X-ray diffraction analysis. The structure is reported in Fig. 1.

RAPTA compounds behaved as rather potential inhibitor of cathepsin B while they are far less potent with thioredoxin reductase. Moreover the IC_{50} values are in the μM range for cathepsin B while the inhibition of thioredoxin reductase seems to be modest and scarcely relevant.

Another interesting feature implies that the value of the IC_{50} is related to the nature of the arene ligand of the RAPTA compounds under investigation. Upon binding to the enzymes, the RAPTA compounds are likely to retain the arene ligands while the chloride ions undergo facile aquation allowing the formation of adducts that inhibit the enzyme functionality.

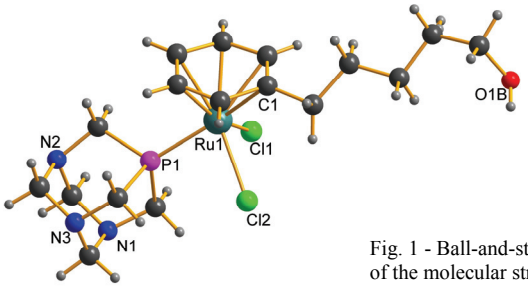

Fig. 1 - Ball-and-stick representation of the molecular structure of **9**.

References. [1] P.J. Dyson, G. Sava, *Dalton Trans*., 1929-1933, 2006; [2] C. Scolaro, A.B. Chaplin, C.G. Hartinger, A. Bergamo, M. Cocchietto, B.K. Keppler, G. Sava, P.J. Dyson, *Dalton Trans*., 5065-5072, 2007; [3] A. Casini, G. Mastrobuoni, W.H. Ang, C. Gabbiani, G. Pieraccini, G. Moneti, P.J. Dyson, L. Messori, *Chem. Med. Chem*., **2**, 631-635, 2007.

XRD AND FTIR CRYSTALLINITY INDICES IN THE CASE OF NANOCRYSTALLINE HAp PRECIPITATED IN THE PRESENCE OF CITRATE AND HYDROGEN L-GLUTAMATE IONS

G.I. Lampronti[1], M. Benvenuti[1], P. Bonazzi[1], P. Costagliola[1], E. Valsami-Jones[2], P.F. Schofield[2], D. Lammie[3], T.J. Wess[3]

[1]*Dipartimento di Scienze della Terra, Università di Firenze, Italy*
[2]*Department of Mineralogy, Natural History Museum, London, UK*
[3]*Cardiff School of Optometry & Vision Sciences, Cardiff University, UK*
giulio.lampronti@unifi.it

Nanocrystalline hydroxylapatite (HAP), $Ca_5(PO_4)_3(OH)$ (hexagonal; $P6_3/m$), was synthesized by wet method in the presence of different amounts of citrate, $C_6H_5O_7^{3-}$, and hydrogen L-glutamate, $C_5H_8NO_4^-$, at pH 7.4 and T = 25°C. The products were characterized using a range of analytical techniques including X-ray Diffraction (XRD), Fourier Transformed Infrared Spectroscopy (FTIR), Scanning Electron Microscopy (SEM), Small Angle X-ray Scattering (SAXS) and Inductively Coupled Plasma - Atomic Emission Spectrometry (ICP-AES).

Rietveld refinements on the collected X-ray patterns yielded a way to detect the microstructural parameters most affected by the organic ligands, *i.e.* the size and the strain on the *a* unit-cell dimension. FTIR spectra were analyzed by Fourier deconvolution and peak fitting and a crystallinity parameter was obtained from the undeconvoluted spectra. SAXS analyses were performed to estimate the average crystal thickness. A comparison between FTIR, XRD and SAXS analyses is reported and discussed.

α-TCP HYDROLYSIS INTO OCP IN POROUS COMPOSITE SCAFFOLDS

K. Rubini, S. Panzavolta, B. Bracci, A. Bigi

Gruppo di Biomimetica e Chimica dei Materiali, Dipartimento di Chimica "G.Ciamician", Università di Bologna, Italy
katia.rubini@unibo.it

Composites of calcium phosphates ceramics with protein-based polymers are of great interest for bone tissue repair because they display mechanical/physical and biological characteristics that are similar to human bone. Bone is a complex material composed of nanocrystals of a basic calcium phosphate deposited within an organic matrix. The inorganic phase of bone is assimilated to synthetic hydroxyapatite, $Ca_{10}(PO_4)_6(OH)_2$, (HA), whereas the organic matrix is mainly type I collagen. Bone tissue formation requires also the presence of pores, which allow migration and proliferation of osteoblasts and mesenchymal cells, as well as vascularization.

In this work porous composite scaffolds of varying compositions were prepared by freeze-drying gelatin foams containing increasing amounts of α-tricalcium phosphate (α-$Ca_3(PO_4)_2$, α-TCP), up to about 42 wt.%. Thanks to the presence of gelatin, a partial hydrolysis of α-tricalcium phosphate into octacalcium phosphate ($Ca_8H_2(PO_4)_6{\cdot}5H_2O$, OCP) occurs during foaming. As a consequence, the scaffolds contain both α-tricalcium phosphate and octacalcium phosphate (Fig. 1a). The relative amount of the two phases was evaluated using the routine QUANTO, based on the X-ray diffraction full profile analysis. It resulted that the scaffolds contain 74% α-TCP and 26% OCP, independently from the initial composition.

In physiological conditions the inorganic component of the scaffolds undergoes a further hydrolysis as shown by the finding that after immersion in phosphate buffer solution (PBS) at 37°C for 1 week the scaffolds contain poor crystalline HA together with OCP (Fig. 1b). The relative amount of the two phases is about 40% HA and 60% OCP, independently from the initial inorganic phase content.

The co-presence of OCP and α-TCP in the composite porous scaffolds, both of which easily hydrolyze to poor crystalline hydroxyapatite, should accelerate *in vivo* resorption, and as a consequence promote new bone formation.

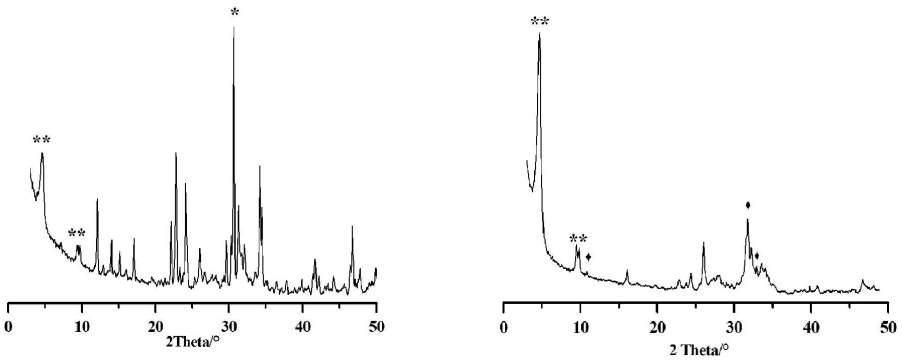

Fig. 1 - Powder X-ray diffraction pattern of the inorganic phase isolated from composite scaffold (a) just after freeze-drying. * α-TCP, ** OCP and (b) after 1 week in PBS ♦ HA, **OCP

MATERIALS, FROM EARTH AND LAB TO LIFE - 2

Session 15
Crystallographic miscellanea

INTRA RARE EARTHS PEROVSKITES: A STABILITY FIELD STUDY AND STRUCTURAL PROPERTIES

C. Artini[1], G.A. Costa[2], M.M. Carnasciali[3], R. Masini[4]

[1]*INFM-LAMIA, INSTM e DCCI, Genova, Italy*
[2]*INFM-LAMIA e DCCI,Genova, Italy*
[3]*INSTM e DCCI, Genova, Italy*
[4]*CNR- IMEM, Genova, Italy*
artini@chimica.unige.it

Interlanthanide ABO_3 perovskitic oxides constitute an important family of RE mixed oxides, but despite the technological relevance of RE oxides for optical applications [1], only few reports exist on their preparation and characterization [2,3]. The ideal perovskitic structure consists of a cubic unit cell where A is in twelvefold coordination and B in octahedral coordination with respect to the oxygen atoms. The ABO_3 general formula refers to a mixed oxide where A is a large cation and B is a small one; in particular the ratio between A and B is described by the Goldschmidt tolerance factor *t* [4], whose value can vary between 1 and 0.75.

La-RE perovskites (RE = Ho, Er, Tm, Yb, Lu, Y) were synthesized by thermal decomposition of the corresponding coprecipitated oxalates. The thermal treatments were performed at temperatures ranging between 600 and 1800°C. The samples were analyzed by X-ray powder diffraction and a correlation between the *t* value and the temperature stability range was found, as the perovskitic field stability widens when the difference between the cationic radii increases.

DTA-TG analyses allowed us to state that all the La-RE mixed oxalates decompose in a similar way at temperatures ranging from 810 to 1020°C. Magnetic measurements were also performed on the samples: $LaYO_3$ is not magnetic, while the other compounds carry a magnetic moment in good accordance with the magnetic moment of RE.

Rietveld refinements were carried out on all the $LaREO_3$ samples synthesized at 1200°C and reveal the occurrence of an orthorhombic distorted perovskitic structure. The La-La distances do not change considerably, while the misalignment of the ReO_6 octahedra increases as the RE ionic radius increases.

References. [1] J.C.G. Bünzli, S. Comby, A.-S. Chauvin, C.D.B. Vandevyver, *J. Rare Earths*, **25**, 257-274, 2007; [2] U. Berndt, D. Maier, C. Keller, *J. Solid State Chem*., **13**, 131-135, 1975; [3] K. Ito, K. Tezuka, Y. Hinatsu, *J. Solid State Chem*., **157**, 173-179, 2001; [4] V.M. Goldschmidt, *Skrifter Norske Videnskaps-Akad. Oslo, I. Mat.-Naturv. Kl.*, 8, 1926.

S15.P2

MECHANISMS OF IRON DISTRIBUTION IN TOURMALINE

F. Bosi

Dipartimento di Scienze della Terra, Università di Roma "La Sapienza", Italy
ferdinando.bosi@uniroma1.it

The partitioning of iron among octahedrally coordinated sites in tourmaline, and its stereochemical consequences, were investigated in a Fe-rich dravite from a skarn rock located in Utö, Sweden. A multi-analytical approach using structural refinement (SREF), electron microprobe analysis (EMPA) and Mössbauer Spectroscopy (MS) established the chemical and structural nature of the tourmaline. A structural formula obtained by optimization procedures indicates disordering of Al, Mg and Fe^{2+} over the *Y* and *Z* sites, and an ordering of Fe^{3+} at the *Y* site. Two Fe-rich tourmalines from the literature, re-examined with the optimizing site assignment procedure, appear to have iron partitioning comparable to that of the Utö tourmaline with Fe^{2+} disordered over the octahedral sites. This is best explained by disordered Fe^{2+} distributions that minimize the strain state of the *Y*-O bonds and provide a shielding effect reducing *Y*-*Z* repulsion. This is consistent with predictions from the bond-valence theory and Pauling's rules.

Indication on *Z*-site occupancy of Fe^{2+} in tourmaline may be signaled by a significant correlation between <*Z*-O> and *c*-lattice parameter ($r^2 = 0.96$). The *c* value for a very Fe^{2+}-rich tourmaline and an ideal end-member schorl, with Fe^{2+} and Al ordered at *Y* and *Z* (respectively), yielded <*Z*-O> values larger than 1.907 Å (the likely bond length for $<^{Z}$Al-O>). These large <*Z*-O> lengths indicate that Fe^{2+} occurs at the *Z* site. The hypothesis of a dragging effect from <*Y*-O> to explain lengthening of $<^{Z}$Al-O> is not supported by experimental evidence.

SYNTHESIS AND STRUCTURAL CHARACTERIZATION OF REE MICROPOROUS SINGLE-LAYER SILICATES BASED ON n-MEMBERED RINGS

M. Cadoni, Y.L. Cheah, G. Ferraris

Dipartimento di Scienze Mineralogiche e Petrologiche e CrisDi Centro Interdipartimentale di Ricerca per lo Sviluppo della Cristallografia Diffrattometrica, Università di Torino, Italy
marcella.cadoni@unito.it

Microporous alkali lanthanide silicates present a great potential in photonic applications, in catalysis and in fast ionic conduction [1-3]. As part of a program on synthesis and characterization of microporous layer silicates with general chemical formula $A_3REESi_6O_{15}\cdot mH_2O$ (A = Na, K, H), results for REE = La and Ce are here presented. Suitable crystals were obtained from hydrothermal experiments in Teflon-lined autoclaves, under static conditions, in ovens preheated at about 230°C and gels with, *e.g.*, composition: 1.1 SiO_2; 0.050 REE_2O_3; 1.1 NaOH; 26.5 H_2O. The structures have been solved and refined by using single-crystal data collected on an Oxford Gemini R Ultra diffractometer (CCD, MoKα radiation).

The Ce compound, $Na_{1.50}K_{0.5}CeSi_6O_{14}(OH)\cdot 2H_2O$ (TR05; *a* 7.413, *b* 30.9652, *c* 7.176 Å, *Cmm*2, Z 4), looks similar to one (CeSIO-Cj2) recently published [4]. However, we have found that TR05 shows a different distribution of Na and H_2O; besides, there are evidences that the charge balance is reached by the presence of a proton and not of Ce^{4+} as affirmed in [4]. The presence of REE^{3+} only is strengthened by the structural data on single crystal obtained for $Na_{2.5}K_{0.5}LaSi_6O_{15}\cdot 2.25H_2O$ (TR06; *a* 7.415, *b* 30.9177, *c* 7.197 Å, *Cmm*2, Z 4). Besides, powder diffraction patterns of La samples with alkalis less than 3 apfu show that they are isostructural with the two samples studied by single crystal diffraction (Fig. 1), thus suggesting that the lack of sodium is compensated by the presence of protons. New syntheses with other REE (Eu and Yb) are in progress.

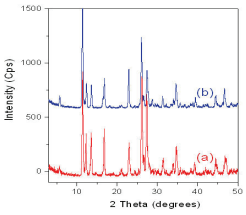

Fig. 1 - Powder diffraction patterns of $A_3LaSi_6O_{15}\cdot mH_2O$: (a) $A_3 = Na_{2.5}K_{0.5}$ (structure known), (b) $A_3 = Na_{2.5}H_{0.5}$ (structure unknown).

The structures of the studied compounds contain strongly corrugated $[Si_6O_{15}]^{6-}$ layers that are parallel to (001) and based on four-, five-, six- and eight-membered rings (Fig. 2). A similar layer is found in $Na_3NdSi_6O_{15}\cdot H_2O$ [1]. Parallel to the layers, the framework is crossed by channels that are delimited by 8-membered ellipsoidal rings formed by six tetrahedra and two 7-coordinated-REE-polyhedra. There are two types of these channels and their maximal effective channel width is about 3 Å. In the anionic framework built by Si and REE polyhedra the negative charge is (in part) balanced by alkalis located in the pores. The content of alkalis may vary from 2 to 3 apfu, depending on the lanthanide and on the synthesis conditions; the excess negative charge is compensated by protons. Electron microprobe analyses reveal that the content of K never exceeds 0.5 apfu and the structure refinements show that K is confined to a specific site. In fact, attempts to synthesize K-pure isostructural compounds resulted in the formation of crystalline $KHSi_2O_5$ plus amorphous Ce-K silicate, suggesting that the presence of Na is essential in directing the crystallization towards the desired phase.

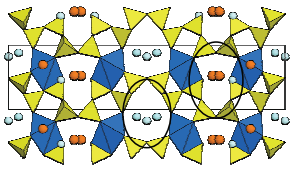

Fig. 2 - Channels delimited by heteropolyhedral 8-membered rings seen along [100] in $Na_{1.50}K_{0.5}CeSi_6O_{14}(OH)\cdot 3H_2O$.

References. [1] S.M. Haile, B.J. Wuensch, R.A. Laudisse, J. Maier, *Acta Crystallogr. B***53**, 7-17, 1997; [2] F. Càmara, L. Ottolini, B. Devouard, L.A.J. Garvie, F.C. Hawthorne, *Mineral. Mag.*, **70**, 405, 2006; [3] D. Ananias, A. Ferreira, J. Rocha, P. Ferreira, J.P. Rainho, C. Morais, L.D. Carlos, *J. Am. Chem. Soc.*, **123**, 5735-5742, 2001; [4] G. Wang, W. Yan, P. Chen, X. Wang, K. Qian, T. Su, J. Yu, *Micropor. Mesopor. Mat.*, **105**, 58-64 (2007).

ARYL BENZYL SULFOXIDES FRAMEWORKS: HALOGEN BONDING AND C-H…O INTERACTIONS

F. Capitelli[1], V. Bertolasi[2], M.A.M. Capozzi[3], C. Cardellicchio[4], F. Naso[4]

[1]*Istituto di Cristallografia - CNR, Bari, Italy*
[2]*Dipartimento di Chimica e Centro di Strutturistica Diffrattometrica, Università di Ferrara, Italy*
[3]*Dipartimento di Scienze Agro-Ambientali, Chimica e Difesa Vegetale, Università di Foggia, Italy*
[4]*Istituto di Chimica dei Composti Organometallici - CNR e Dipartimento di Chimica, Bari, Italy*
francesco.capitelli@ic.cnr.it

Ten aryl benzyl sulfoxides having the (*R*)-configuration at the sulfur atom were subjected to X-ray single crystal diffraction. The crystal structures can be divided in two main families according to the position of the aryl groups, as observed through the dihedral angle (aryl carbon)-(methylene carbon)-sulfur-(aryl' carbon). In half of them, the aryl moieties are arranged in a *gauche* position (dihedral angle values in the range 52-65°), whereas in the remaining five molecules, the aryl groups are in an *anti-periplanar* conformation (dihedral angle values in the range 166-179°). Three-dimensional frameworks, as already observed in our previous work [1], are built up from a complex balance of different interactions, the most relevant of which being hydrogen bonding between the benzyl methylene group and the sulfinyl oxygen atom. Further contributions from the other heteroatoms, such as halogen bondings [2], complete the interactions framework.

References**.** [1] F. Naso, C. Cardellicchio, M.A.M. Capozzi, F. Capitelli, V. Bertolasi, *New J. Chem.*, **30**, 1782-1789, 2006; [2] P. Metrangolo, G. Resnati, In *Encyclopedia of Supramolecular Chemistry*, J.L. Atwood & J.W. Steed, Eds., Dekker, New York, pp. 628-635, 2004.

STRUCTURE REFINEMENT OF SYNTHETIC *REE*$Al_{2.07}(B_4O_{10})O_{0.6}$ BORATES (with *REE* = Nd, Ce)

F. Capitelli[1], G. Della Ventura[2], F. Bellatreccia[2], N.I. Leonyuk[3], V. Koporulina[3]

[1]*Istituto di Cristallografia - CNR, Bari, Italy*
[2]*Dipartimento di Scienze Geologiche, Università Roma Tre, Italy*
[3]*Department of Crystallography and Crystallochemistry, Moscow State University, Russia*
francesco.capitelli@ic.cnr.it

The natural REE-borate peprossiite was discovered few years ago as a late pegmatitic to hydrothermal phase from the holocrystalline ejecta of the Vico volcanic complex [1]. The crystal structure of peprossiite [2] showed that this rare borate has a mica-like structure consisting of layers of six-membered rings of B tetrahedra alternating with layers of 5-coordinated Al and interlayer REE (± Th,U, Ca). Such atomic arrangement in fact represented the first example of a natural counterpart, from the structural point of view, of the synthesized Nd metaborate [3].

In this work we relate a crystal chemical study of a set of synthetic metaborates with composition *REE*$Al_{2.07}(B_4O_{10})O_{0.6}$ (with *REE* = Nd, Ce) done by combining single-crystal X-ray diffraction and FTIR spectroscopy. The examined samples were obtained by slow cooling (at the Dept. of Crystallography and Crystallochemistry, Moscow State University, supported by the RFBR grants ## 07-05-00680 and 08-05-90010-bel_a) from $K_2Mo_3O_{10}$ based fluxed melts in the form of transparent hexagonal sheet-like crystals 500 to 1000 μm wide and few μm thick. Single-crystal X-ray structure refinements show all crystals to be isostructural within hexagonal space group $P\bar{6}m2$, with the following unit cell parameters: a = 4.5984(3) Å; c = 9.3178(7) Å and V = 170.63(2) Å^3 (Ce phase), a = 4.5880(6) Å, c = 9.2853(7) Å and V = 169.27(3) Å^3 (Nd phase). The *REE* cations present a trigonal prismatic coordination, with *REE*-O bond distances of [6×] 2.455(8) Å (Ce) and 2.436(14) Å (Nd); next oxygen atoms are at 3.045(6) Å (Ce) and 3.040(15) Å (Nd), making up a complex network of *REE*…O interactions within VdW sphere. Al cations are surrounded by five oxygen atoms, resembling a square pyramidal coordination, with Al-O bond distances ranging from 1.794(10) up to 1.841(6) Å (Ce), and from 1.804(19) up to 1.835(10) Å (Nd). The BO_4 groups display tetrahedral arrangement, with B-O bond distances from 1.428(16) up to 1.487(6) Å (Ce), and from 1.41(3) up to 1.491(10) Å (Nd). The three-dimensional framework can be thus described as a packing of *REE*O_6, BO_4 and AlO_5 polyhedral layers perpendicularly to the crystallographic c axis, as already shown to be the case for the $NdAl_{2.07}(B_4O_{10})O_{0.6}$ [3] and the $LaAl_{2.03}(B_4O_{10})O_{0.54}$ [4] compounds and mineral peprosiite-(Ce) [2]. Single-crystal FTIR spectra collected in the OH-stretching region (4000-3000 cm^{-1}) show all synthetic phases to be anhydrous.

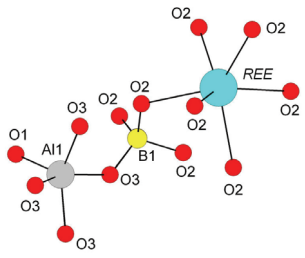

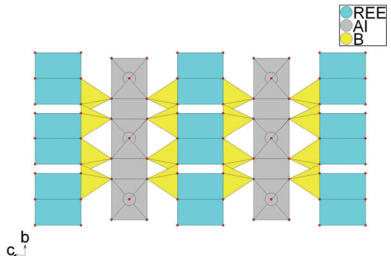

References. [1] G. Della Ventura, G.C. Parodi, A. Mottana, M. Chaussidon, *Eur. J. Mineral.*, **5**, 53-58, 1993; [2] A. Callegari, F. Caucia, F. Mazzi, R. Oberti, L. Ottolini, L. Ungaretti, *Am. Mineral.*, **85**, 586-593, 2000; [3] D.Yu. Pushcharovskii, O.G. Karpov, N.I. Leonyuk, N.V. Belov, *Dokl. Ak. Nauk SSSR*, **241**, 91-94, 1978. [4] P. Yang, W. Yu, J.Y. Wang, J.Q. Wei, Y.G. Liu, *Acta Crystallogr. C***54**, 11-12, 1998.

FRAGMENT BASED DISCOVERY OF S100B INHIBITORS: WHEN STRUCTURAL INFORMATION MEETS *in silico* PREDICTIONS

L. Cesari[1,2], M. Agamennone[3], A. Padova[1], M. Andreini[1],
P. Turano[4], R. del Conte[4], D. Lalli[4], S. Mangani[1,4]

[1]*Drug Design Technologies Unit, Siena Biotech S.p.A., Siena, Italy*
[2]*Dipartimento di Chimica, Università di Siena, Italy*
[3]*Dipartimento di Scienze del Farmaco, Università "G. d'Annunzio", Chieti, Italy*
[4]*Magnetic Resonance Center CERM, Università di Firenze, Italy*
mangani@unisi.it

S100B is an EF-hand Ca^{2+}-binding protein that belongs to the S100 family. It has been demonstrated that the binding of S100B and p53, a well known tumor-suppressor protein, prevents p53 phosphorylation and tetramerization, blocking its anticancer activity [1-3].

Few inhibitors have been identified so far by Markowitz *et al.* [4] using a NMR-based screening, but no 3D structural data of S100B complexed with small ligands are available.

Our objective is the identification of small molecules able to block the S100B-p53 interaction, combining computational and biophysical screening of fragment libraries.

Siena Biotech's fragment collection was used for a virtual screening campaign based on docking and pharmacohore approaches approach, leading to the selection of 280 molecules.

NMR-based screening (WATER-LOGSY) was performed in order to identify interacting fragments and ^{15}N-HSQC analysis confirmed the interaction of the strongest binders.

Co-crystallization trials have been set up for the most active molecules. Crystals of protein-ligand complexes grow in few days and the analysis of diffraction data provides good-quality electron density maps at about 2.0 Å resolution. The binding site of the fragments has been clearly identified. However, the ligands investigated so far display multiple binding modes within the binding pocket. Further optimization of crystallization conditions is on going, aimed at improving the resolution of electron density maps. Moreover structure-based library design has started in order to increase the potency of the fragments.

References. [1] C. Scotto, J.C. Deloulme, D. Rousseau, E. Chambaz, J. Baudier, *Mol. Cell. Biol*., **18**, 4272-4281, 1998; [2] J. Lin, M. Blake, C. Tang, D. Zimmer, R.R. Rustandi, D.J. Weber, F. Carrier,. *J. Biol. Chem.,* **276**, 35037-35041, 2001; [3] M.R. Fernandez-Fernanedez, D.B. Veprintsev, A.R. Fersht, *PNAS*, **102**, 4735-4740, 2005; [4] J. Markowitz, I. Chen, R. Gitti, D.M. Baldisseri, Y. Pan, R. Udan, F. Carrier, A.D. MacKerell, Jr., D.J. Weber. *J. Med. Chem*., **47**, 5085-5093, 2004.

A JOINT THEORETICAL AND EXPERIMENTAL APPROACH TO INVESTIGATE SYNTHETIC LAYERED MATERIALS

M. D'Amore[1,2], M. Causà[2], M. Cossi[1], M. Milanesio[1], L. Marchese[1], V. Barone[2]

[1]*Dipartimento di Scienze e Tecnologie Avanzate, Università del Piemonte Orientale "A. Avogadro", Alessandria, Italy*
[2]*Dipartimento di Chimica,"Paolo Corradini" Università di Napoli "Federico II", ,Napoli, Italy*
mauro.causa@unina.it

Layered organomodified aluminophosphates [1] and saponite materials have been recently synthesized and characterized. Layered aluminophosphates are intermediates in the synthesis of microporous molecular sieves with channels and cavities of molecular dimensions similar to well-known zeolites [2]. The interest devoted to lamellar materials lies also in the field of polymer nanocomposites or, more generally, of the intercalation chemistry. It is well reported, in fact, that layered compounds can accommodate ions or molecules to give intercalation compounds suitable to be used as additives for the preparation of polymer nanocomposites. Cheng *et al*. in their pioneering work [3] reported the synthesis of the layered aluminophosphate ALPO-kan (whose empirical formula is $ALPO_2(OH)_2[NH_2(CH_2)_xCH_3]$, x = 3, 5, 7), employing amines as structure directing agents. Synthetic saponite clays containing Na^+ and H^+ ions have been prepared and a composite materials have been obtained by the insertion of a multifunctional Ti-containing aminopropylisobutyl-POSS (Ti-NH_2POSS), within the interlayer space. These systems where tridimensional nanoparticles containing metals are intercalated between the interlayer space of saponite show potential application in the field of nanocomposite materials and heterogeneous catalysis.

Even if rich experimental information is available at now, since the preparation of a single crystal for these lamellar materials is an hard task to deal with, the structure and surface properties are still unknown and the phenomena occurring at the interface have not been fully interpreted yet. Useful (and in some cases unique) insights on the structure and surface properties of these materials can be provided by a combined theoretical and IR and powder XRD experimental study. Theoretical simulations can help the experimental interpretation by providing a reliable description of hydrogen bonds in clay minerals and zeolites since these bonds strongly affect the IR data [4]. ALPO-kan modified by intercalation of alkylamines have been investigated by us through this combined approach. At first the structure of the aluminophosphate layers, the acidity of the surface sites and the interactions with intercalated butylammonium ions in n-BA ALPO-kan have been studied by IR spectroscopy and modelled with density functional theory (DFT) calculations. The modelling allowed us the assignment of IR bands and the interpretation of the spectrum. The theoretical frequencies, including anharmonic corrections on the main stretching modes, were compared to the experimental IR spectra. The very satisfactory agreement allowed all the observed peaks to be assigned, providing for the first time a clear-cut interpretation of the broad and complex absorption at 2800-1700 cm^{-1} in terms of Fermi-type resonances. To fully resolve the structure of alkylamines ALPO-kanemite we resorted to more detailed *ab initio* 3D simulations of these materials. Many cells have been optimized within different symmetries ($Pmn2_1$, $Pca2_1$, $P2_1/c$) starting from different positions of butylammonium ions and different orientations of alkyl chains.

Starting from the experimental data, models have been proposed for saponite clays still resorting to density functional theory (DFT) calculations.

References. [1] H.O. Pastore, E.C. de Oliveira, G.B. Superti, G. Gatti, L. Marchese, *J. Phys. Chem. C*, 111, 2007; [2] H.O. Pastore, S. Coluccia, L. Marchese, *Ann. Rev. Mater. Res*., **35**, 351, 2005; [3] S. Cheng, J. Tzeng, B. Hsu, *Chem. Mater*., **9**, 1788, 1997; [4] S. Tosoni, K. Doll, P. Ugliengo, *Chem. Mater*., **18**, 2135, 2006.

IS 2.07 Å THE RECORD FOR THE SHORTEST Pt-S DISTANCE? TWO QUESTIONABLE EXPERIMENTAL STRUCTURES

A. Ienco, M. Caporali, C. Mealli

ICCOM-CNR, Sesto Fiorentino, Italy
andrea.ienco@cnr.it

The available crystal structures of the very similar compounds $(Ph_3P)_2Pt(\mu\text{-}S)_2Pt(PPh_3)_3$, **1**, [1] and $(Ph_2PyP)_2Pt(\mu\text{-}S)_2Pt(PPh_2Py)_2$, **2**, [2] raise intriguing questions about their geometrically different Pt_2S_2 cores. In particular, the independent Pt-S distances in **1** are the shortest ever reported for this kind of bond and also the trans-annular S-S separation of 2.69 Å is dramatically shorter than that in **2** (= 3.01 Å). This apparent case of structural isomerism could be in principle due to a different amount of electronic coupling between the sulfido bridges. This topic is part of our ongoing interests [3], hence it has stimulated a careful examination of the problem in question. The conclusion is that complex **1** has been incorrectly formulated and its actual nature is $[(Ph_3P)_2Pt(\mu\text{-}OH)_2Pt(PPh_3)_2](BF_4)_2$, **3**. To verify the hypothesis, the available crystal structure of the latter [4] has been examined and found to be also affected by error. Although suspiciously similar, the unit cells of **1** and **3** are not equal and, in particular, the ratio between the volumes is 2:1. Matrices transforming one cell into the other are readily devised, hence leading to the conclusion that the two compounds are the same but the structure of **3** was determined by using only one half of the collectable diffraction data. The new synthesis, crystallization and X-ray analysis of **3** fully support the working hypothesis and dismiss any further conjecture about the inconsistent Pt_2S_2 core in **1**.

References. [1] H. Li, G.B. Carpenter, D.A. Sweigart, *Organometallics*, **19**, 1823, 2000; [2] V.W.-W. Yam, P.K.-Y. Yeung, K.-K. Cheung, *Chem. Commun.*, 267, 1995; [3] C. Mealli, A. Ienco, A. Poduska, R. Hoffmann, *Angew. Chem. Int. Ed.*, **47**, 2864, 2008.

$PrMn_7O_{12}$, A NOVEL PEROVSKITIC MANGANITE: HIGH PRESSURE SYNTHESIS AND STRUCTURAL CHARACTERIZATION

F. Mezzadri[1], M. Calicchio[2], G. Calestani[1], R. Cabassi[2], F. Bolzoni[2], F. Bissoli[2], E. Gilioli[2]

[1]*Dipartimento di Chimica, Università di Parma, Italy*
[2]*Istituto IMEM-CNR, Parma, Italy*
francesco.mezzadri@nemo.unipr.it

We report the synthesis and structural characterization of $PrMn_7O_{12}$, a new member of the rich family of quadruple-perovskite manganites with general formula XMn_7O_{12} (X = Na, Ca, La, Pb, Bi, Tl). This family of materials is extremely interesting because of its structural complexity and versatility: contrary to simple perovskites, in these compounds Mn ions occupy different crystallographic sites, allowing the direct observation of the charge/orbital/spin orderings. Furthermore the Mn^{3+}/Mn^{4+} ratio, and consequently the structural and electronic properties, may be tuned through the choice of "X" cation. These features make of the whole family of compounds a model system for the study of charge, orbital and spin ordering phenomena [1].

$PrMn_7O_{12}$ is a metastable material, requiring synthesis via solid state reaction in high pressure, high temperature (HP/HT) conditions. The compound shows polymorphism, which has been never observed in this class of materials. In particular, different HP/HT synthesis conditions yield the crystallization of two structures. Low P and low T lead to the formation of a rhombohedral phase, while high P and high T promote the growth of a monoclinic one, with crystallographic cell displaying a variable distortion depending on the synthesis conditions. The approximate stability fields of the two $PrMn_7O_{12}$ phases have been defined in the P/T space and the two structures have been refined by powder (both phases) and single crystal (monoclinic only) X-ray diffraction.

Bond Valence Sum calculations suggest that manganese and praseodymium are in 3+ oxidation state both in the rhombohedral and monoclinic phases; this is confirmed in the monoclinic structure by the detection of Jahn-Teller distortion. This feature leads to the definition of an orbital ordered scheme involving an A-type magnetic structure, in which ferromagnetic *ab* planes are antiferromagnetically coupled along the *c* axis.

Although the available data on the rhombohedral structure do not allow a precise determination of the MnO_6 octahedra distortion, the simple change of symmetry from monoclinic to rhombohedral rules out the orbital ordering scheme previously proposed for the monoclinic structure, dramatically modifying the whole system of spin interactions and, reasonably, the physical properties of the compound. This hypothesis is confirmed by SQUID measurements, which evidence radically different magnetic properties, indicating different spin ordering models and thus suggesting a possible change of the other order parameters, making further study of this material worthwhile for the comprehension of the complex phenomena displayed by the whole class of compounds.

References. [1] A. Prodi, E. Gilioli, A. Gauzzi, F. Licci, M. Marezio, F. Bolzoni, Q. Huang, A. Santoro, J.W. Lynn, *Nat. Mater.*, **3**, 48-52, 2004.

A NEW METHOD TO ESTIMATE THE ATOMIC VOLUME OF TERNARY INTERMETALLIC COMPOUNDS

M. Pani, F. Merlo

Dipartimento di Chimica e Chimica Industriale, Università di Genova, Italy
marcella@chimica.unige.it

Within a binary intermetallic system, the experimental values of the average atomic volume of the intermediate phases show often large deviations from the values calculated on the basis of the elemental volumes (Vegard's rule). This is due to ionic, elastic, geometric and other effects, which must be taken into account for a correct prevision [1].

Going to ternary systems, the volume of a ternary phase can be estimated starting from those of binary phases of selected compositions. This method, employed to derive thermodynamic quantities in polynary systems following some suggested procedures (methods by Colinet, Muggianu, Kohler) [2], have been applied for the first time to the volume calculation of ternary intermetallic phases [3].

Besides the three cited procedures, a new method to calculate and weigh the contribution of the binary phases is proposed. The agreement between observed volume values and those calculated by the present formula shows the minor importance of ternary interactions as regards the volume effects occurring in the formation of binary phases. So, the total volume effect during the formation of a ternary phase can be mostly imputed to the processes of formation of the binary compounds.

References. [1] M.L. Fornasini, F. Merlo, *Z. Kristallogr*., **221**, 382, 2006; [2] H. Lukas, S.G. Fries, B. Sundman, *Computational Thermodynamics, The Calphad Method*, Cambridge University Press, Cambridge, 2007; [3] M. Pani, M.L. Fornasini, F. Merlo, *Proceedings of XXXVII National Congress of Physical Chemistry*, Camogli, 2008, p. 217.

CRYSTALLOGRAPHIC STUDIES OF NEW HUMAN THYMIDYLATE SYNTHASE INHIBITORS

C. Pozzi[1], G. Guaitoli[2], M. Benvenuti[1], M.P. Costi[2], S. Mangani[1]

[1]*Dipartimento di Chimica, Università di Siena, Italy*
[2]*Dipartimento di Scienze Farmaceutiche, Università di Modena e Reggio Emilia, Italy*
mangani@unisi.it

Thymidylate synthase is a dimeric enzyme involved in DNA biosynthesis, since it catalyzes the reductive methylation of 2'-deoxyuridine-5'-monophosphate (dUMP) to 2'-deoxythymidyne-5'-monophosphate (dTMP), using N5,N10-methylenetetraydrofolate as cofactor [1].

Human thymidylate synthase (hTS) is an important target in chemotherapy of ovarian cancer, one of the most common causes of death in women, and of some other kind of cancer.

The lack of effectiveness of available drugs is connected to the development of resistance which depends on multiple factors including DNA repair by malignant cells [2].

hTS down-regulates its cellular expression by binding its own mRNA [3] leading to inactivation of the expression. Consequently, inhibition of hTS by ligands frees the hTS-mRNA with consequent increased levels of hTS expression. The appearance of resistance could depend on the lack of this down-regulatory activity [4]. It has been found that hTS binds mRNA in two sites of interaction localized at the interface between the two monomers [5].

Our studies are aimed to the identification of small ligands designed to bind at the hTS monomer/monomer interface affecting the formation of the hTS dimer.

The first approach for the development of interface inhibitors consists in analyzing the structure of hTS. We have identified two cavities that can be used to design small molecules able to interfere with the dimerization process**.**

A second approach consists in finding small peptides that can mimic the protein-protein interactions at the dimer interface.

We have identified a library of peptides of different length and tests of inhibitory activity against hTS have provided encouraging results.

In order to provide a structural basis to explain the inhibitory activity of peptides and to support structure-based design of better inhibitors, we have crystallized complexes of the enzyme with molecules and peptides that have shown inhibitory activity towards hTS.

The identification of new molecules that prevent the dimerization of hTS by blocking the catalytic and regulatory activity can be very important for the further development of therapeutic agents with an original mechanism of action.

This work was supported by LIGHTS project (LIGand to Interfere with Human TS, LSHC-CT-2006-037852) (STREP funded by the FP6 program).

References. [1] K. Perry, E. Fraumann, J.S. Finer-Moore, W.R. Montfort, C.F. Maley, F. Maley, R.M. Stroud, *Proteins*, **8**, 315-333, 1990; [2] P.H. Sayre, J.S. Finer-Moore, T.A. Fritz, D. Biermann, S.B. Gates, W.C. MacKeller, V.F. Patel, R.M. Stroud, *J. Mol .Biol*., **313**, 813-29, 2001; [3] E. Chu, D. Voeller, D.M. Koeller, J.C. Drake, C.H. Yakimoto, G.F. Maley, F. Maley, C. Allegra, *Proc. Natl. Acad. Sci. USA*, **90**, 517-521, 1993; [4] J. Liu, J.C. Schmitz, X. Lin, N. Tai, W. Yan, M. Farrell, M. Bailly, T. Chen, E. Chu, *Biochim. Biophys. Acta*, **1587**, 174-82, 2002; [5] R. Das, D. Baker, *Proc. Natl. Acad. Sci. USA*, **104**, 14664-14669, 2007.

STRUCTURAL AND MAGNETIC PROPERTIES OF THE $RCu_{5-x}Pd_x$ PHASES (R = La, Ce; x = 1; 2)

A. Provino[1,2], K.V. Shah[3], S.K. Dhar[3], M.L. Fornasini[1], P. Manfrinetti[1,2]

[1]*Dipartimento di Chimica e Chimica Industriale, Università di Genova, Italy*
[2]*Laboratorio LAMIA, CNR-INFM, Genova, Italy*
[3]*DCMPMS, T.I.F.R., Mumbai, India*
alessia.sting@hotmail.it

The binary compounds RCu_5 (R = rare earth) crystallize with the hexagonal $CaCu_5$-type structure [1,2]. We have studied the Cu substitution by Pd atoms for the lighter rare earths (from La to Nd, Sm and Gd). The results obtained on the La and Ce homologous, along with some physical properties of the occurring phases, will be presented. We find that, in both La and Ce compounds, Cu can be replaced by Pd up to at least RCu_3Pd_2. In the La phases the hexagonal structure is retained up to $LaCu_3Pd_2$; on the other hand, $CeCu_4Pd$ retains the hexagonal symmetry of the parent $CeCu_5$, but $CeCu_3Pd_2$ crystallizes in the cubic $AuBe_5$-type structure (Fig.). In particular, $CeCu_5$ is known to order antiferromagnetically near 4 K [3]; our heat capacity data indicate that both $CeCu_4Pd$ and $CeCu_3Pd_2$ order magnetically below 1.8 K. Moreover, while the resistivity of $CeCu_4Pd$ shows normal metallic behavior, the measurements show that $CeCu_3Pd_2$ is a dense Kondo lattice.

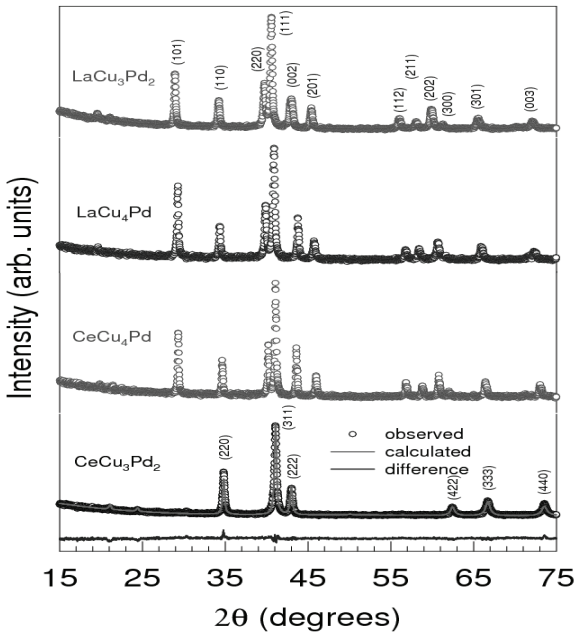

References. [1] Pearson's Handbook of Crystallographic Data for Intermetallic Phases, American Society for Metals, Metals Park, Oh 44073, **3**, 1985; [2] Crystmet - The Metals Database, v. 3.9.0. Toth Information System Inc., 2008; [3] J.O. Willis, R.H. Aiken, Z. Fisk, E. Zirngiebl, J.D. Thompson, H.R. Ott, B. Batlogg, In *Theoretical and experimental aspects of valence fluctuations and heavy fermions,* eds. L.C. Gupta and S.K. Malik, Plenum Press, New York, **57**, 1987.

GAS STORAGE PROPERTIES OF A SUPRAMOLECULAR ORGANIC ZEOLITE

C. Tedesco[1], L. Erra[1], V. Cipolletti[1], M. Brunelli[2], C. Gaeta[1], P. Neri[1], A.N. Fitch[2]

[1]*Dipartimento di Chimica, Università di Salerno, Italy*
[2]*ESRF, Grenoble, France*
ctedesco@unisa.it

At the Dept. of Chemistry of the University of Salerno we prepared and characterized a new crystalline solid based on *p*-Bu^t-calix[4]dihydroquinone **1** revealing the simultaneous existence of water channels and very large hydrophobic cavities (988 Å^3). The compound has a cubic structure [a = 36.412(4) Å] with 48 calixarene molecules and 155 water molecules in the unit cell.

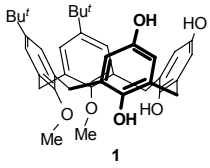

1

Interestingly, the supramolecular framework is preserved also after the removal of channel water molecules, as shown by thermogravimetric and X-ray powder diffraction (XRPD) measurements [1]. The simultaneous presence of networked channels, filled with easily removable water, and isolated hydrophobic cavities may prelude to potential applications of nanotechnological interest [2].

High resolution XRPD measurements have been devised to characterize the guest uptake and release properties of this new material using several gases under different temperature and pressure conditions. To probe the size and molecular affinity of the host channels, gases with different size and polarity have been used. High resolution XRPD measurements have been performed at ID31 beamline using a rotating glass capillary cell with gas handling system to allow *in situ* studies by powder X-ray diffraction. The cell can be used to follow solid-state chemical reactions under vacuum or at gas pressures up to around 7·10^5 Pa [3].

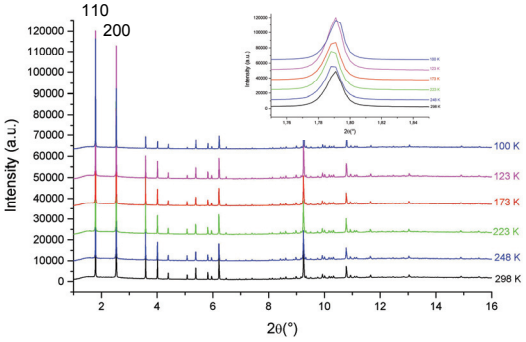

Fig. 1 - X-ray diffraction patterns for CH_4 loaded sample.

Most promising results have been obtained for samples loaded with CH_4, the corresponding X-ray diffraction patterns are reported in Fig. 1. As it is evident from the inset of Fig. 1, peak positions do not shift as the temperature is decreased.

For comparison, measurements have been also performed on an evacuated sample. While the evacuated sample shows a progressive decreasing of the lattice parameter with decreasing temperature, the methane loaded sample shows an increase down to 248 K and then a decrease. This probably indicates that methane is able to enter into the channels and this process is favoured by decreasing the temperature down to 248 K.

References. [1] C. Tedesco, I. Immediata, L. Gregoli, L. Vitagliano, A. Immirzi, P. Neri, *Cryst. Eng. Comm.*, **7**, 449-453; 2005; [2] P.K. Thallapally, B.P. McGrail, J.L. Atwood, C. Gaeta, C. Tedesco, P. Neri, *Chem. Mater.*, **19**, 3355-57, 2007; [3] M. Brunelli, A. Fitch, *J. Synchrotron Radiat.*, 10, 337-339, 2003.

$CeMgSi_2$, A NEW EXAMPLE OF LINEAR INTERGROWTH STRUCTURE

F. Wrubl[1], M. Pani[1], P. Manfrinetti[1,2], P. Rogl[3]

[1]*Dipartimento di Chimica e Chimica Industriale, Università di Genova, Italy*
[2]*Laboratorio LAMIA, CNR-INFM, Genova, Italy*
[3]*Institut für Physikalische Chemie, Universität Wien, Austria*
marcella@chimica.unige.it

Few literature data exist on the R-Mg-Si phases (R = rare earths) [1,2]. In particular, while the R_2MgSi_2 compounds (Mo_2FeB_2 type) occur for the whole series of rare earths, the 1:1:1 phase only occurs with the divalent Eu and Yb metals, and $CeMg_2Si_2$ (its own type) only with cerium. During our investigation on the physical properties of compounds in the Ce-Mg-Si system, we synthesized a new phase with $CeMgSi_2$ stoichiometry, which melts congruently at 1200°C.

The single crystal X-ray analysis showed that the $CeMgSi_2$ phase crystallizes in a new tetragonal structure type [$I4_1/amd$, $tI32$, with lattice constants a = 4.2652(4) Å and c = 36.830(4) Å]. The crystal structure of $CeMgSi_2$ can be formally built up by alternating along the z direction four slabs of AlB_2-type $CeSi_2$ with four $CeMg_2Si_2$ cells, one after the other (Fig. 1). It is well known that, besides the $CeSi_{2-x}$ with the defect AlB_2-type, stoichiometric $CeSi_2$ adopts the α-$ThSi_2$ type, formed by slabs of AlB_2-type, differently oriented along the c axis of its tetragonal cell, to form a three dimensional Si-framework. Only few examples of $CeMg_2Si_2$-AlB_2 slabs intergrowth phases are available in the literature [3,4]; among these, the orthorhombic $NdNiGa_2$ structure type can be cited (2+2 slabs) [4].

The single crystal results obtained for $CeMgSi_2$ have been confirmed on the homologues compounds of La, Pr and Nd by means of Rietveld refinements. The trend of the unit-cell mean atomic volumes, plotted *versus* the R^{3+} ionic radius, shows a linear behaviour which strongly suggests a trivalent state for the Ce atoms.

To study the main physical properties of these four compounds, detailed heat capacity, electrical resistivity and magnetization measurements are now under investigation.

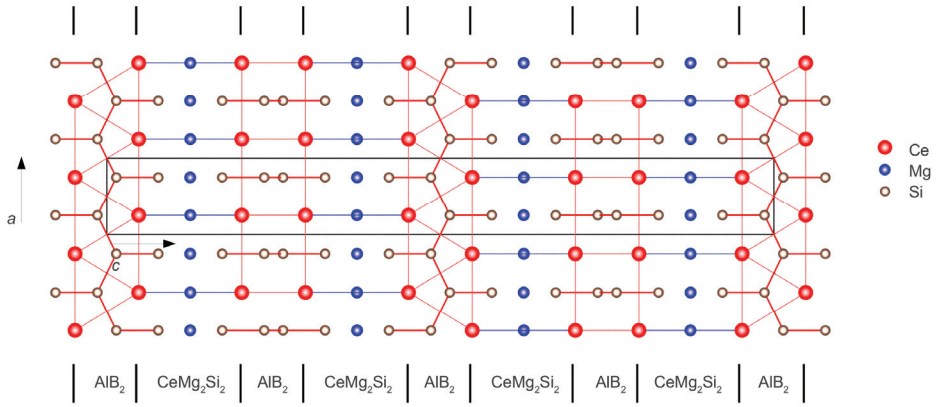

Fig. 1 - The $CeMgSi_2$ structure viewed along [010].

References. [1] CRYSTMET - The Metals Database, V.3.9.0. Tooth Information System Inc. (2008); [2] S.K. Dhar, P. Manfrinetti, A. Palenzona, *J. Alloys Comp.*, **252**, 24-27, 1997; [3] D. Johrendt, A. Mewis, *Z. Anorg. Allg. Chem.*, **621**, 57-62, 1995; [4] E. Parthé, B. Chabot, In: K. Gschneidner, L. Eyring, Eds., *Handbook on the Physics and Chemistry of Rare Earths*, Vol. 6, Elsevier. Ch. 48, 113-334, 1984.

DESCRIPTION OF THE CUBIC AND ICOSAHEDRAL FORMS BY THE PLATONIC SOLIDS AND THE CATALAN POLYHEDRA, DUALS OF THE ARCHIMEDEAN POLYHEDRA

L. Zefiro, M.R. Ardigò

Dip.Te.Ris., Università di Genova, Italy
zefiro@dipteris.unige.it

It is common knowledge that the two 235 and $m\bar{3}5$ icosahedral point groups share each of the six special forms, whereas the relative *{hkl}* general forms are necessarily different: then the total forms present in every point group are seven, as many as the forms belonging to each of the five cubic point groups, in general more familiar than the icosahedral ones.

In particular, both $m\bar{3}5$ icosahedral point group and $m\bar{3}m$ cubic point group include, in addition to two forms, each dual of the other, that correspond to Platonic solids (*dodecahedron* and *icosahedron* in $m\bar{3}5$, *cube* and *octahedron* in $m\bar{3}m$), another form with fixed Miller's indices, this time corresponding to a Catalan polyhedron, dual of a semi-regular Archimedean polyhedron: in $m\bar{3}5$ point group it is the *rhomb-triacontahedron*, dual of *icosi-dodecahedron,* whereas in $m\bar{3}m$ it is the *rhomb-dodecahedron*, dual of *cuboctahedron.*

By the attribution of appropriate values to the indices, each of the other four forms:

- *triakis-icosahedron, deltoidal hexecontahedron, pentakis-dodecahedron, hexakis-icosahedron* relatively to $m\bar{3}5$ point group
- *triakis-octahedron, deltoidal icositetrahedron, tetrakis-hexahedron, hexakis-octahedron* relatively to $m\bar{3}m$ point group

can be led to coincide with an isomorphic Catalan polyhedron.

It is conceivable that whichever form belonging to $m\bar{3}5$ or $m\bar{3}m$ point groups derives from the intersection of single forms, in turn obtained by proper variations of both the central distances, concerning all the seven forms, and the indices, concerning only the four forms previously listed.

Analogously to what happens in case of icosahedral symmetry, it must be pointed out that the ratios of the indices of the faces generally do not take on rational values also in case of the peculiar forms, belonging to $m\bar{3}m$ cubic point group, that correspond to Catalan polyhedra.

Ten of the thirteen isohedral Catalan polyhedra (dual of isogonal Archimedean polyhedra having the same symmetry) are hence equally distributed between $m\bar{3}5$ and $m\bar{3}m$ point groups.

Concerning the three other Catalan polyhedra, *triakis-tetrahedron* is ascribable to the $\bar{4}3m$ cubic point group (as well as *truncated tetrahedron*, its Archimedean dual, and *tetrahedron*, the further fifth Platonic solid), *pentagonal icositetrahedron* (dual of *snub cube*) to the 432 cubic point group and *pentagonal hexecontahedron* (dual of *snub dodecahedron*) to the 235 icosahedral point group.

One can note that, in crystals belonging to $\bar{4}3m$, 432 and 235 point groups, polarity can be detected in every direction except the perpendiculars to mirrors and even-*fold* axes, whereas polar axes lack in $m\bar{3}5$ and $m\bar{3}m$ point groups, due to the presence of the centre of symmetry.

After the complete characterization of the thirteen Catalan polyhedra, even an isomer of *rhomb-cuboctahedron* is introduced, the controversial pseudo14*th* Archimedean polyhedron named *Miller solid* or *elongated square gyrobicupola* (according to Johnson's nomenclature): it belongs to the $\bar{8}2m$ non crystallographic point group since it includes, in addition to four mirrors and four 2-*fold* axes, a 8-*fold* rotoinversion (or rotoreflection) axis. Also its pseudo-Catalan dual is examined and compared with *deltoid-icositetrahedron*, the Catalan dual of *rhomb-cuboctahedron.*

INDEX OF AUTHORS

D

E

F

G

NOTES

Editing a cura di Lorenza Fascio

Si ringraziano Elena Bonaccorsi e Michele Zema
per la collaborazione nella realizzazione della copertina

Finito di stampare nel mese di Luglio 2008
presso Mediaprint Srl
Via Gozzano, 7 – Livorno
Italy